L O N G I T U D I N A L W A V E S

T H R O U G H

T H E E A R T H ' S C O R E

Thesis by

Mayette Elner Denson, Jr.

In Partial Fulfillment of the Requirements

For the Degree of

Doctor of Philosophy

California Institute of Technology

Pasadena, California

1950

ACKNOWLEDGMENTS

In following this investigation the writer has been supervised by Dr. Beno Gutenberg, Director of the Pasadena Seismological Laboratory, and by Dr. Charles F. Richter, both of the California Institute of Technology. The help and the suggestions received from these scientists are gratefully acknowledged. The writer has benefited also from discussion of certain aspects of the problem with Dr. Hugo Benioff. The cooperation extended by Mr. John Nordquist and all other personnel of the Seismological Laboratory is greatly appreciated.

This study has been materially aided by the Stanolind Oil and Gas Company Fellowship which was awarded to the writer by the California Institute of Technology for the school years 1948-49 and 1949-50.

ABSTRACT

The amplitudes, periods, and travel times of PKP or P' and PP have been investigated. Results indicate that the epicentral distance of the main P' focal point varies with period. Amplitude considerations indicate that the focal point for short period waves is near 147 degrees; for longer period waves the position is believed to lie between 147 and 143 degrees. The position of the end of the reversed segment for wavesthrough the outer core is believed to be near 157 degrees.

Travel times show that the P' core waves are recorded as three groups separated by intervals of about 10 and 20 seconds. Each group evidences separate focal phenomena. This variation suggests dispersion as an explanation.

Variations in energy and period of the P'' phase with distance are reasonably interpreted as a consequence of rapid velocity increase with increasing depth approaching the inner core transition zone. Anomalous energy ratios for all P' phases indicate complexities which are not yet fully understood.

TABLE OF CONTENTS

FIGURES

Figures cont'd

$A_T(PP)-A_T(P'',P_1',P_2')$

$A_o(PP)-A_o(P'',P_1')$

$A_o(PP)-A_o(P_2')$

PLATES

INTRODUCTION

Purpose and Scope of Investigation

The present stage of scientific investigation of the internal constitution of the earth has not yet progressed beyond the stage of inference and extrapolation from observed physical phenomena. Following this pattern of endeavor the following data are presented to add to the array upon which our logical deductions are based. It is hoped that from these particular data some additional inferences may be made, some current divergences of opinion further clarified.

This investigation has been directed to shed more light upon the properties of the core of the earth. To this end observations of amplitude, period, and arrival time of particular core phases have been recorded from a number of earthquake seismograms. In modified form these properties have been analyzed and variances are discussed.

Particular phases to which this study applies are collectively referred to as PKP or P' which consist of P", P_1', P_2', and associated unnamed phases. These are longitudinal waves which are recorded as the first distinct arrivals at stations whose epicentral distances are between 110° and 180° of the earth's circumference. Generalized paths of these phases and their time distance relations are shown diagrammatically in

Fig. 1; path relationships as shown in Fig. 1, b, are taken in modified form from Gutenberg and Richter (1939, p 123). Data on the phase PP have been recorded to provide a base with which the P' data may be compared.

Historical Summary

The first documented seismological evidence which indicated the existence of the core of the earth was furnished by Oldham (1906). While the theories of dilatational and distortional wave forms were not yet wholly accepted, Oldham expressed his belief that the innermost four-tenths of the earth (by radius) was characterized by some form of fluid state. However, Oldham misinterpreted reflected waves and consequently his figure for the radius of the core of the earth was too small. Gutenberg (1914) from consideration of wave velocities and time-distance relations presented further evidence which indicated the radius of the core to be 3470 kilometers, a figure still retained. Independently of Gutenberg, Knott (1919) presented his third paper on energy and velocity relations of elastic waves; he expressed views on the earth's interior largely similar to those expressed by Oldham in 1906.

In 1925 Macelwane (1925) announced seismological evidence for shear or distortional waves through the core. (Gutenberg in 1914 had presented calculations in prediction of the travel times of these phases, which, then, had not been observed.) However, Jeffreys (1926) showed that the rigidity of the earth

must be confined largely to the mantle to be compatible with lunar tides observed in the earth; the implication from Jeffreys' work as to a"fluid"core possessing little or no rigidity has been variously accepted. Results of further investigations by Macelwane (1930) have given this author pause. However, researches by various others have led some seismologists to the belief that rigidity within the core may be a function of the period of vibration. To date, no generally accepted evidence has been presented which indicates that shear waves are propagated through the core of the earth.

Large amplitudes observed at angular distances around 143° were interpreted as indicating a focal point; two branches of the P' travel time curve beyond that point suggested a velocity variation with depth inside the core. The observations have led to amplifications of the original theory, notably by Gutenberg (1925).

Observations of P" phases at distances between 110°and 143° were initially interpreted as being the result of some obscure diffraction process within the core. Consideration of the characteristics of the P" phases led Lehmann (1937) to the belief that these waves could be better explained as phases refracted or reflected from a high velocity "inner" core; Miss Lehmann presented qualitative calculations in support of her

hypothesis. Gutenberg and Richter (1938) accepted Lehmann's hypothesis and presented quantitative calculations on velocity distribution and travel times within the core; these ideas and figures were amplified by Gutenberg and Richter (1939). Jeffreys (1939 a,b) presented two papers on velocity and time-distance relations within the core; these data were later amplified and published in collaboration with Bullen as the Jeffreys-Bullen (or "J-B") Seismological Tables (1940).

The Gutenberg-Richter and the Jeffreys hypotheses have divergent concepts. The main point from whence this divergence arises is the velocity distribution at the contact of the inner and outer core: Gutenberg and Richter have made their interpretations in light of a rapid increase of velocity with depth; Jeffreys has carried out his investigations in light of a rapid decrease of velocity with depth followed by an abrupt increase (see Fig. 2).

The velocity distribution just outside the boundary of the inner core relates to the epicentral distance of the point C in Fig. 1 and to the existence of the reversed segment (C D). According to Jeffreys' hypothesis of a decrease in velocity at the inner core boundary, the reversed segment, if it exists, is probably a reflected phase (Jeffreys, 1939b, p 600) while the point C, according to Bullen (1947, p 175), occurs at around

147°. According to the Gutenberg-Richter hypothesis the reversed segment does exist by reason of refraction, while the point C occurs at 169° (Gutenberg and Richter, 1939, table 23).

THEORETICAL CONSIDERATIONS

Energy Relations

The study of seismic waves is better integrated by consideration of energy-distance relations. Results of the original investigations of Knott (1899), and Zoeppritz (1919), have had wide application. An example, is the study of the "20° discontinuity"; more recent applications have been made by Gutenberg and Richter in the study of mantle structure, and by Mooney (1950) and Martner (1948) in studies of mantle phases. Indeed, amplitude considerations of the P" group by Lehmann first led to the search for new hypotheses to explain these waves. Hence, energy relations have been considered in this study of core waves.

Gutenberg (1945 a, p 58) gives a method of comparing theoretical and observed energies by establishing a parameter from consideration of theoretical ground displacements and observed amplitudes. The basic formula for a displacement at the earth's surface is given as

$$1. \quad u,w = Q_{H,Z}\, K\, T\, \sqrt{E_1} \sqrt{\frac{(F_1,F_2....)a \sin i_h \, di_h/d\Delta}{\sin \Delta \cos i_o}}$$

from whence

$$2. \quad \frac{u,w}{T} \cdot \frac{1}{K\sqrt{E}} = Q_{H,Z} \sqrt{\frac{(F_1, F_2 \ldots) a \sin i_h \, di_h/d\Delta}{\sin \Delta \cos i_o}}$$

The derivation of this equation, based upon the original theory of Zoeppritz, may be found in the original paper of Zoeppritz, Geiger, and Gutenberg (1912); Gutenberg (1944, 1945 a) discusses its application. The quantity under the radical on the right hand side of equation 2 is directly proportional to the energy which arrives at the earth's surface per unit area at arc distance Δ, from a wave front with surface angle of incidence i_o; the derivation may be followed in Bullen (1947, p 123). In the quantity $K\sqrt{E_1}$, K depends on the fraction of total energy E_1 which goes into compressional or distortional motion at the source. The parameters established from these relations are:

$$3. \quad A_T = C - \log K\sqrt{E} - \log \frac{u,w}{T} = C - \log Q_{HZ} \sqrt{\frac{(F_1, F_2 \ldots) a \sin i_h \, di_h/d\Delta}{\sin \Delta \cos i_o}}$$

$$4. \quad A_o = M - \log \frac{u,w}{T} - G(M-7) \; *$$

where A_T is the theoretically determined parameter and A_o is the observational parameter. Definition of A_T by equation 3 assumes plane motion in media which are isotropic between discontinuities; we infer from isotropy that motion may be purely compressional and purely shear. A further assumption is that from a point

* Evaluation of A_o is discussed on pages 11 and 12.

source energy is propagated equally in all directions. These assumptions known to be invalid have been incorporated in nearly all treatments of this subject; their use can be reconciled only upon their sufficiency in providing a first approximation. Variances which may be found to exist between theory and observation must be partly considered in this light. Evaluation of A_T in equation 3 has been carried out in this study as follows:

C ---this quantity is dependent on energy distribution at the source; it has been determined by Gutenberg (1945 a) to have a value close to 6.3 for both longitudinal and distortional waves. This figure, herein used, was determined statistically from observations and is subject to the aforementioned assumptions.

$di_h/d\Delta$ --this factor is taken equal to $di_o/d\Delta$ since core wave rays follow nearly symmetrical paths for normal depth (25 km) earthquakes. In taking the logarithim of this quantity any difference between $di_h/d\Delta$ and $di_o/d\Delta$ becomes insignificant compared to the accuracy with which either may be determined. If we assume that i_h, the angle at which a ray leaves the source, is equal to i_o, the surface angle of incidence of this ray at an angular distance Δ, A_T may then be expressed as:

5. $$A_T = C - \log Q_{H,Z} \sqrt{\frac{(F_1F_2) \, a \tan i_o \, di_o/d\Delta}{\sin \Delta}}$$

$di_o/d\Delta$ --from geometrical considerations the sin i_o is approximated to the ratio of $V_o/\overline{V}$ where V_o is the true surface longitudinal velocity. $\overline{V}$, the apparent velocity along the surface, is equal to the inverted slope of the travel time curve.

$$\overline{V} = (d\Delta/dt)\ (110)\ \text{km/sec.}$$

By computing $V_o/\overline{V}$ at a given distance the corresponding i_o may be determined. From a plot of i_o versus Δ the $di_o/d\Delta$ slope is taken.

In this investigation the apparent velocity becomes a critical factor since small variations in $\overline{V}$ lead to appreciable changes in i_o; small errors in $\overline{V}$ are magnified in $di_o/d\Delta$. To minimize discrepancies from this factor, apparent velocities were determined by mechanical differentiation of travel times and by measurement of travel time slopes. "J-B" travel time data and Gutenberg-Richter travel time data have been used to evaluate $di_o/d\Delta$. Gutenberg-Richter travel time data may hereafter be referred to in this paper as "G-R" travel time data. Modified values of $di_o/d\Delta$ from "G-R" travel time data determined by Dana (1944) have been used in this study.

a -- this factor may be expressed as e^{-kD} where k is the absorption coeffecient per unit of ray path D. As determined statistically by Gutenberg (1945 a), k has a value of 0.00012/km for longitudinal core waves. Absorption thus

produces an additive amount of about 0.33 in the parameter A_T for the core phases; for PP the effect is of course more variable.

F -- This factor is proportional to the amount of incident energy which is reflected or refracted at a discontinuity. Determination of this factor is based upon the equations of Knott (1899) and Zoeppritz (1919). A discussion of the Knott equations in modified form and their application is given by Gutenberg (1944). In this study only the core into mantle and the mantle into core refractions contribute significantly to the theoretical parameter for core phases. Values of F for core refractions have been determined by Dana (1944) following the method and formulae established by Knott (1899). F for surface reflections enters into the theoretical parameter for PP phases; this F has been calculated by Gutenberg (1944). At a discontinuity between materials of given properties, the value of F is dependent upon the angle of incidence. The angle of incidence at a discontinuity is determined from the ray parameter, p, which is constant for each particular ray throughout its path.

$$6. \qquad p = (r \sin i)/V = (r_o \sin i_o)\, V_o$$

where the subscript , o, refers to values at the surface of the earth; no subscripts refer to values at a radius r. The angle of refraction is readily determined by use of Snell's Law.

The following velocity distribution from Bullen (1947, p 209) was used in this calculation:

depth-km	P velocity km/sec
above 33	6.0
just below 33	7.75
just above 2900 km	13.64
just below 2900 km	8.10

Q -- the incident amplitude of a wave motion impinging on the earth's surface, is registered by vertical (Z) and horizontal (H) seismographs. In order that the displacements registered by these components may be properly related to the actual ground motion under different angles of incidence, the factor $Q_{H,Z}$ has been determined; results of this work have been presented by Gutenberg (1944) for various values of Poisson's ratio, upon which factor Q is dependent.

It will be noted that A_T has been determined for PP between 100° and 165° by Gutenberg (1945 b). It has been independently recalculated here for consistency in results. The table below shows the variances between the two sets of data. Residuals are A_T (Gutenberg, 1945 b) minus A_T (here calculated) for horizontal (H) and vertical (Z) data.

	H	Z		H	Z
100	-0.01	-0.03	135	-0.04	-0.06
105	+0.09	+0.08	140	+0.04	+0.03
110	+0.17	+0.17	145	+0.09	+0.06
115	+0.08	+0.14	150	-0.30	-0.27
120	+0.01	+0.05	155	-0.34	-0.30
125	-0.08	-0.03	160	-0.03	-0.06
130	-0.10	-0.14	165	-0.02	-0.04

These data are seen to be in good accord excepting at a distance of 150° to 155°. For these distances the writer has used a value of $di_o/d\Delta$ which is smaller than that used by Gutenberg, whose values are based on empirically adjusted data for P. Calculated values of A_T for horizontal and vertical components are shown in Figs. 3 and 4 for phase PP, in Figs. 9 and 10 for phases P'' and P_1', and in Fig. 15 for phase P_2'.

The observed parameter, A_o, defined by equation 4, page 6, is evaluted by measuring phase motions on seismograms written by seismic disturbances of known magnitude and location. Amplitudes (A) and periods (T) were measured from seismograms of horizontal and vertical instruments. The absolute instrumental magnification factors determined by Martner (1948) were applied to amplitude/period ratios (A/T) in calculating displacements. (w is vertical displacement; u, horizontal displacement, is the vector sum of the NS and EW displacements.) For instruments, absolute magnifications of which have not been determined, relative magnifications V were calculated from a formula given by Benioff (1932, p 164).

$$7. \qquad V = \frac{1/T^3}{(1/T_o^2 - 1/T^2)\,(1/T_g^2 - 1/T^2)}$$

where T_o is the seismometer period, T_g is the galvanometer period, and T is the period of the applied motion.

Magnitudes (M) used in this study have been determined by Gutenberg from consideration of trace amplitudes or displacements reported by international seismological stations. Earthquake magnitude was defined empirically by Richter (1935) in terms of trace amplitude; in later investigations Gutenberg and Richter (1942) estimated source energy in terms of magnitude. The quantity--G(M-7)--is a consequence of the energy to magnitude relation; variation in the duration of a phase with variation in magnitude necessitates this term. The factor G equals 0.1 for earthquakes of 6.5 to 7.5 magnitude; G equals 0.25 for earthquakes of magnitude greater than 7.5. Empirical correction factors for seismological stations considered in this study have been determined by Gutenberg (1945 b); these have been included in A_o calculations.

In order that the effect of the G(M-7) term may be observed results of the observational parameter computations are plotted as A_o and as A_o'; the primed parameter denotes that the G(M-7) term has not been included. It may be seen that this term has the effect of reducing scatter of values.

data
A_o and A_o'/from horizontal and vertical instruments are shown in Figs. 5, 6, 7 for PP, in Figs. 11, 12, 13, for P" and P_1', and in Figs. 16, 17 for P_2'.

Velocity Relations

Depth-velocity distributions within the core have been determined by Gutenberg and Richter (1938) and by Jeffreys (1939 b). Results of their calculations are reproduced in Fig. 2. The approach used by these authors is one which has been attributed to Wadati and Masuda. This method will be described briefly since Jeffreys and Gutenberg-Richter have both followed this calculation and it has been partially followed in the present study.

The procedure is to subtract from the travel-time and distance of the P' (and S') core phase the travel time and distance of the PcP (and ScS) phase having the same apparent velocity--hence, the same angle of incidence at the earth's surface. The resulting figures represent the time and angular distance of wave travel between points on the earth's core. This method requires that the travel times be accurate.

To travel-time data for the core Gutenberg and Richter (1938) have applied the method of Wiechert, Herglotz, and Bateman to determine the velocity-depth relation. Macelwane (1936, p 216) discusses the limitations and procedures of this method; the limiting factor is the rate of change of velocity with depth in relation to the velocity at a given depth. This

requires that no shadow zone exist in the core travel time curve.

From considerations of the ray parameter, p, equation 6 page 9, and core travel time data Jeffreys (1939 b) finds that a decrease in velocity is necessary about 1400 km below the surface of the core; this decrease is followed by an abrupt increase. For agreement with the surface observations of P" at 110°, a velocity decrease with depth is necessitated to produce a desirable variation in the parameter p. By such procedure Jeffreys' calculations show agreement with observed P' travel time data. The validity of this velocity decrease existence theorem is based upon probability that the branch CD, Fig. 1, is a reflected phase.

PROCEDURES

Materials Used

Seismograms from several stations have been included in this study. Stations and instrumental characteristics of the components from which data were taken are given below.

Station	Component	Period of galvanometer	Period of seismometer	Peak magnification
Pasadena	Z	0.23	1.0	short
	Z	90.0	1.0	long
	NS	0.2	1.0	short
	NS	90.0	1.0	long
	EW	0.2	1.0	short
	EW	90.0	1.0	long
Tucson	Z	0.2	1.0	short
Huancayo	NS	——	6.5--5.5	long
	EW	——	6.5--5.5	long
Victoria	Z	0.2	1.0	short

In addition to the above sources of data, readings of amplitude, period, and time were taken from the station bulletins of:

La Paz	Z	11.7	10.0	long
Jena	Z	____	4.5 to 3.6	long

Peak magnification is arbitrarily designated as short if less that 1 sec, as long if equal to or greater than 1 sec. Correspondingly, instruments with these peak magnifications are referred to as being long period or short period instruments.

In making travel time curves of the core phases from particular shocks at epicentral distance of about 145°, the seismograms were used from La Jolla, Tinemeha, Santa Barbara, Haiwee, Riverside, Mount Wilson, and Pasadena. These stations all have short period vertical instruments from which arrival times may be accurately obtained.

Data from earthquake recordings from 1932 to 1945 are included in this study. During earlier years most of the Pasadena instruments had constants different from those now used; as no absolute magnification curves exist for these instruments, only those readingswere taken which could be used with relative magnifications for comparison of amplitude/period (A/T) ratios.

In this study data from about 561 station-earthquakes were inspected. These data are proportioned as follows:

Pasadena	300
La Paz	124
Huancayo	71
Tucson	50
Jena	15
Victoria	1

From these station-earthquakes about 741 readings were accepted from seismograms on which absolute magnifications were known. These are proportioned as follows:

P" and P_1'	302
P_2'	119
PP	320

About 50 readings used for ratio comparisons are not included above.

An insufficient number of short period horizontal P' readings and readings of PKKP, SKS, and SKP which were measured have not been entered in this study. P' data from about 100 station-earthquakes of greater than normal depth have not been analyzed.

Methods of Comparison of Data

Using the previously discussed A_T and A_o parameters three types of comparison have been made on data of P" and P_1', P_2', and PP. These comparisons, which have been carried out for both horizontal and vertical components, are:

a. $(A_o - A_T)PP, P'$

b. $A_T(PP) - A_T(P')$

c. $A_o(PP) - A_o(P')$

The first of these quantities, a., relates the observed amplitude/period (A/T) ratios for a phase to the theoretical ratios for that phase. The quantities which define this function are:

$$(A_o-A_T) = \log \frac{(u,w/T)_T}{(u,w/T)_o} - M \text{ ---} G(M-7)-C-\log k\sqrt{E_1}$$

where $\log(u,w/T)_T$ is defined by equation 3, page 6; $(u,w/T)_o$ is evaluated from seismogram measurements. The quantity

$$M-G(M-7)-C-\log k\sqrt{E}$$

should be equal to zero; this follows from definition of magnitude (M) by Richter (1935), from relation of magnitude to energy by Gutenberg and Richter (1942) and from evaluation of constant C by Gutenberg (1945 a). Errors to which (A_o-A_T) is subject are $di/d\Delta$, F, and measuring errors; in the (A_o-A_T) calculations the averaged value of the "J-B" A_T and the "G-R" A_T has been used for all phases excepting P_2'. For P_2' appreciable discrepancies between the two A_T's have warranted separate residual computations.

A residual (A_o-A_T) equal to zero means that the theoretical and observed amplitude/period ratios are equal; a positive residual indicates that observed ratios are smaller than expected from theory; a negative residual indicates the observed ratios are larger than expected from theory. (A_o-A_T) residuals are plotted for all components and all phases in Figs. 8, 14, and 18.

The second quantity, b., gives the comparison of theoretical amplitude/period ratios of a P' phase to theoretical ratios of the standard phase PP. This calculation furnishes a base to which the corresponding quantity from observed values (c.) may be referred. Theoretical ratios are calculated from considerations of travel time data; factors which evaluate this ratio are given by:

$$A_T(PP)-A_T(P') = \log \frac{(u,w/T)P'}{(u,w/T)PP}$$

where u,w/T is defined by equation 3, page 6. The factors which may introduce errors are $di/d\Delta$ and F. These ratio comparisons are plotted in Figs. 19 and 20; in these figures the antilogs of $A_T(PP)-A_T(P') = \log \frac{(u,w/T)P'}{(u,w/T)PP}$ are plotted on logarithmic paper.

The last quantity, c., represents the comparison of observed amplitude/period ratios of the P' phases to ratios of PP. Direct measurement of amplitudes and periods on seismograms evaluates this function which is defined as:

$$A_o(PP)-A_o(P') = \log \frac{(u,w/T)P'}{(u,w/T)PP}$$

Errors to which this calculation are subject are measuring errors; these arise in view of the character of the motion which is recorded. It is often difficult to determine the period related to maximum amplitudes. Superpositions occur which can produce erroneous results if not recognized.

Discrepancies arising from epicenter location and origin time are believed to be of an appreciable extent; earthquakes to which this study refers are chiefly those listed in Gutenberg and Richter (1949). Instrumental response curves are assumed to have an accuracy within the limits imposed by assumptions of the theory upon which this study is based. Observed ratios of P' to PP are plotted in Figs. 21 to 26 inc. for horizontal and vertical instruments; in these figures the actual ratio values are plotted on logarithmic paper.

OBSERVATIONAL AND THEORETICAL RELATIONSHIPS

Time-distance-energy relations

In the process of recording P' data, evidence accumulated which indicated that no coherent picture could obtain from energy relationships unless the amplitude/period data could be properly related to time. Beyond 145° a multiplicity of phases was noted; in many cases the short and long period instruments responded differently to incident motion. This suggested that different phases might contain different energy carrying periods. To resolve this complexity phase travel times were determined and plotted; origin times given by Gutenberg and Richter (1949) were used in this determination. In ascertaining arrival times greater reliability was placed upon short period vertical recordings than upon long period recordings for two reasons. First, the short period recordings which were available are written with a larger time scale than

are the long period recordings which were available. Second, short period instruments by virtue of their characteristics are more sensitive to first motion than are longer period displacement meters.

Results of the travel time analysis are shown in Fig. 27. Three identifiable groups of P' waves were found to exist; each of these has its own focal point and associated P", P_1', and P_2' phases. All of these groups are generally registered on both short and long period instruments; however, the square root of the amount of energy which is registered for a phase, as evidenced by amplitude/period ratios, varies depending upon instrumental characteristics.

The No. 2 and No. 3 P_2' phases (which are often not recorded on short period instruments) represent a wide scatter of values throughout their extent and many very late arrivals (or later phases) are noted; however, No. 1 P_2' is fairly well represented by aligned arrival times on short period recordings from 150° to 165°. At distances near the focal zone, extreme complexity of phases from well recorded earthquakes renders phase identification impossible. P_1' and P" phases are well documented for all groups. No. 2 and No. 3 P_1' phases are not recorded prominently beyond 157° to 160°; an unexplained segment, E, fades out beyond 160°. Group 3 P" motions are noted with varying amplitudes at distances shorter than 130°; amplitude/period ratios for this phase at shorter distances

have not been entered in this study.

The No. 1 group P" consists of a number of impulses. An average time value of these impulses has been plotted; it is not impossible that the impulses may actually represent a series of overlapping segments. In traversing the travel time curve in Fig. 1, a, from A to B to C to D to E, theoretical considerations require that on the ascending branches the angle of incidence must decrease with the increasing distance. Therefore, branches BC and DE should be concave toward the distance axis. Since the No. 1 curve as plotted is convex toward the distance axis around 135°, at least two separate segments are implied.

The outstanding feature associated with the travel time curves is that the groups vary as to principal energy carrying periods. No. 1 group is generally registered most significantly by short period instruments with the following exception: from 147° to about 157° long period instruments recorded No. 1 P_1' motion with magnitudes comparable to the recorded motion from No. 3 P_1'. At distances greater than 157° long period instruments recorded comparable amplitudes from phases No. 2 P_1' and E. No. 3 group phases are generally most significant on long period recordings; these phases are generally recorded as low energy emergents on short period instruments. No. 2 motion is generally registered more significantly by short period than by long period instruments but on short period recordings group

2 motion is frequently clouded by interference from group 1. The earliest arrivals between 130° and 160° are most often noted on short period recordings. From amplitude considerations of the materials which were inspected the position of the focal point is qualified thus:

For motions of period around 1 to 2 sec. 147°

For motions of period around (2 to 3.5 sec.) 145°-146°

For motions of period around 3.5 to 10 sec. 143½°-147°

For long period instruments the 145° focal point is the most prominent. The extension to 143½° as will be shown later is based upon very few available observations. Arrival times have been ascertained as closely as possible from amplitude considerations. Emergent phases on long period recordings cause uncertainty as to the time and distance of the No. 3 focal point. The arrival times which have been associated with the focal zones are as follows:

147°	± 19m 45s
145°-146°	± 19m 50s
143½°-147°	up to 20m 5s

It is indeed possible that the focal distances and times as given may be subject to modification from consideration of diffraction phenomena. Airy's theory of diffraction at a caustic has been interpreted by Jeffreys (1939 a, p 553) to be sufficient to produce appreciable long period (10 sec) amplitudes at distances up to 14° from the position of the

caustic; however, for shorter period motion (1-2 sec) this effect is not believed by Jeffreys to be appreciable beyond a few degrees.

Examples of reception to groups 1, 2, and 3 phase motions by instruments with different constants are shown in Plates I, II, III.

Energy parameters by phases

Phase PP

All data for the PP phase are shown in Figs. 3 to 8 inc. Theoretical data, Figs. 3 and 4, indicate that for vertical components energy should remain essentially constant from 100° to 180° epicentral distance; horizontal components should show a slight decrease in energy (increase in A_T) with increasing distance. Factors which account in the main for variations noted are:

$di_o/d\Delta$ --accounts for minor fluctuations.

F (at surface reflection), Q, and a increase with increasing distance while sin Δ and angle of incidence terms decrease with increasing distance in such amounts that the effect is nearly constant; for horizontal components decreasing terms produce the dominant effect. Observational data on PP are shown in Figs. 5, 6, and 7. The wide scatter of points at shorter distances will be discussed shortly; this scatter may be related to angle of incidence i_o.

$(A_o - A_T)$ residuals of Fig. 8 indicate that theory and observation are in excellent agreement for the long period

horizontal component of the PP phase. The slight upswing at 160° may be due to an insufficient number of observations or to variations in $di_o/d\Delta$.

Short period vertical residuals shown in Fig. 8, indicate fair agreement between theory and observation up to 145°; the low at 135° (positive residuals) indicates observed ratios are too small, compared to theory, by a factor of about 1.5. Similarly, the decided increase in observed values past 145° indicates that observed ratios, compared to theory, are too high by factors up to 2.5.

From the longer period nature of the PP phase, we might expect our long period instrumental data to approach theoretical values more closely than do shorter component data. For long period horizontal data, as opposed to short period vertical data this is so. However, observational data for long period vertical instruments, shown in Fig. 5, show poor agreement with theory. Values of A_T determined by Gutenberg, page 11, would reduce long period vertical residuals in Fig. 8 by an average amount of 0.1 from 105° to 120° and would increase residuals about 0.1 from 120° to 135°. The net effect, in any event, would be that the long period vertical observed PP ratios from 100° to 135° are too small by a factor of 2, or that theoretical ratios are correspondingly large.

The residuals of Fig. 8 appear to be qualifiedly related to components and their responses; this relation can affect

horizontal components but slightly. Certainly, the only factor in our theory to which this partiality to components and responses could be attributed is $di_o/d\Delta$. This factor is dependent on velocity and is, a priori, a function of the recorded period and wave length. In light of this it seems reasonable that components of wave motion are differently affected by the path over which they travel, depending on period and wave length. Recent studies by Gutenberg and Richter have indicated complexities in the mantle structure, effects of which are not yet fully known. The present results indicate that the apparent velocities of long period motions are affected at shorter distances while the short period motions are affected at longer distances. It seems reasonable that this may be related to a dispersion effect in the mantle; very conceivably this effect could be dependent on the angle of incidence of an incoming wave train. If dispersion is the cause of these effects, at shorter distances (and larger angles of incidence) longer period components of incident motion should arrive at the surface more steeply, hence, at smaller angles of incidence. Thus, at shorter distances $di_o/d\Delta$ would decrease, while at longer distances $di_o/d\Delta$ would increase. It seems reasonable that layering with velocity variations in the uppermost mantle could cause dispersion as described; if so, theory and observation for the PP phase may be brought into more reasonable agreement.

Phases P" and P_1'

Data for these phases which will be further discussed later are shown in Figs. 9 to 14 inc. Factors which largely control the theoretical values (Figs. 9, 10) are:

$di_0/d\Delta$ --this factor increases with increasing distance. At around 143° $di_0/d\Delta$ becomes infinite (point B, Fig. 1, a); following the Gutenberg-Richter interpretation $di_0/d\Delta$ becomes infinite at 110° and 169° also. (The 169° focal point refers to point C, Fig. 1, a; in view of variance of opinion as to the travel time and distance of point C, focusing effects are not shown here in the theoretical parameters.) Effects of the focusing in relation to energy distribution are not precisely known. Large amplitudes are here shown to persist only a short distance (3°) from the caustic.

Q ---- varies little for vertical components; for horizontal components Q decreases with increasing distance (and decreasing angle of incidence). At 180° A_T for horizontal components should show zero energy from consideration of Q.

Observational data for P" and P_1' are shown in Figs. 11, 12, and 13. These data have been taken from phases in groups 1 and 2. Long period data, except for infrequent observations are taken from group 2 phases; short period data with scattered exceptions are taken from group 1 phases.

Significant features which these observational data display are:

1. Greater scattering of energy is noted between 110° and 145° than between 145° and 175°.

2. Long period vertical instruments show an abrupt rise in energy at 145°, while short period vertical instruments show an abrupt rise between 145° and 147° (no readings were obtained at 146° from instruments whose absolute magnifications are sufficiently known).

3. Long period vertical data show an abrupt drop in energy at 160°; short period vertical data show a gradual decrease from 147° to about 160° but short period observations over the larger part of this distance are too few and scattered for conclusions. Both of the long period components have A_o values of higher average (lower energy) beyond 157°.

4. Vertical instruments show a gradual rise in energy past 160° and approaching 175°; horizontal data here indicate this rise poorly.

5. Vertical data for P" suggest that energies occur in overlapping levels. Since data are relatively abundant over some intervals of distance and relatively sparse over other intervals this overlapping of levels may well be only a pseudo-effect caused by insufficient data. As portrayed, however, these data are suggestive. Widely scattered A_o data of high average (low energy) value between 110° and about 120° followed

by relatively well grouped data of lower average value at greater distances might suggest a shadow zone at distances shorter than 120°. Long period vertical data at 133° suggest an overlap zone with energy levels on each side differing by a logarithmic factor of 0.5. Sparse horizontal data do not indicate these variations. Variations in energy as suggested by A_o could not be connected to arrival times with any degree of certainty; however, it seems reasonable that scattering of energy between 110° and 145° may be a consequence of segmentation of the P" travel time curve. A further suggestion for this relationship may be inferred from period--distance data shown in Fig. 28; in this figure are plotted the periods of the P" and P_1' phases which carry the maximum energies. An increase of period with increasing distance is displayed for P". Singularly enough, the 110° to 120° interval is characterized by an average of 1.5 seconds for long period instruments; beyond the apparent threshold at 120° widely scattered, higher periods are common. Inferences which these data imply may warrant further investigation.

Residuals, (A_o-A_T), for P" and P_1' are shown in Fig. 14. Variances between observational data and theoretical data have been calculated from smoothed averages of the observational data. It is apparent that the long period vertical data are

q uantitatively most nearly in agreement with theory. Short period vertical data and horizontal data show large negative residuals which indicate that observational ratios of P^* and P_1' are too large compared to theoretical ratios by factors varying between 10 and 3. Interestingly enough, horizontal component data which are very closely in agreement with theory for the PP phase, here show the largest average discrepancy.

Phase P_2'

Data for P_2' are shown in Figs. 15 to 18 inc. Theoretical ratio curves in Fig. 15 show appreciable difference between those determined using Gutenberg-Richter travel time data and those determined using Jeffreys-Bullen data. Factors to which differences may largely be attributed are:

$di/d\Delta$ --this factor decreases in value from 145° to about 160° and fluctuates in value from 160° to 175°.

F --P_2' phases within the core have the largest angles of refraction and incidence. Small variations of the angle of incidence or refraction inside the core cause large variations in the amount of energy refracted into longitudinal waves. Hence, travel time slopes for P_2' are a critical factor. The surface angle of incidence, i_0, which is determined from travel time slope, is dependent upon angles of

incidence on and within the core. Small variations in i_o thus produce disproportionate variations in F.

Observational data for P_2' are shown in Figs. 16 and 17. Scarcity of short period readings at distances shorter than 150° is occasioned by the complexity of phase motion from 145° to 150°; hence, only one reading was taken in this interval and that was registered as P_1'. It will be noted that several P_2' readings are shown in the long period component data of Fig. 16 at distances between 145° and 150°; these observations which were recorded as weak emergents or not at all on short period instruments, represent focal point observations of the No. 3 group. Reference to Fig. 11 will show that from long period vertical recordings the average A_o of the No. 3 focal point is smaller (larger energy) than the average A_o of the No. 1 and No. 2 focal points by an amount 0.5 or by a factor of 3. Another significant feature of the P_2' observational data is that energy highs, which might indicate a focal point, are not evidenced (except of course that at 145°).

(A_o-A_T) residuals in Fig. 18 show that short period vertical observed ratios are too large compared to theory by an average factor of about 4. Long period data appear too large from 150° up to about 160°. Based upon the Gutenberg-Richter travel time data, theory and observation are in fair agreement from about 160° to 175°. The Jeffreys-Bullen data, if correct,

indicate that at 175° observed horizontal and vertical amplitudes are too large by factors varying from 6 to 14. We might reasonably expect our P_2' motion in the neighborhood of 175° to have observed amplitude/period ratios which are about twice that indicated from theory. This arises from the fact that at distances near 180° P_2' from one side of the earth is believed to coincide with the P_2' arriving from the opposite side of the earth. However, we would not expect this reinforcement to produce anomolies by factors of 6 to 14.

Relationships of P' to PP

Features and discrepancies of the data for P' may be further evaluated by comparison to data for PP. Theoretical and observational comparisons are shown by Figs. 19 to 26 inc. It will be noted that in these figures actual values or antilogs are plotted on logarithmic paper. Factors which affect the theoretical comparisons, shown in Figs. 19 and 20, are those which have been previously discused individually for A_T of P' and PP.

Observational data are shown in Figs. 21, 22, and 23. For points on observational curves clear identification of both PP and P' from each seismogram is necessary; such is most frequently not the case. However, readings from Benioff instruments on which the absolute magnification is not known may also be used in this comparison; relative magnifications

in these cases are calculated by use of formula 7, page 12. Observed ratios while relatively few in number are of definite weight. The only sources of error to which observational data are subject are measuring errors.

Comparison of Fig. 19 with Figs. 21, 22, and 23 shows that amplitude/period ratios for P"/PP are greater than theoretical values by an average factor of about 5. From previously discussed relationships of PP this variance may be attributed in the main to P". The rapid increase in value of observed ratios from 110° to 125° may indicate that existing travel time slopes over this distance interval are in need of slight modification.

Data from vertical instruments (Figs. 21 and 22) indicate that between 120° and 145° amplitude/period ratios vary greatly depending on instrumental characteristics. Peculiarities in these ratio comparisons add to the peculiarities that exist in the A_0 parameter, in period variations, and in time-distance relations. All sources of data imply complexities in the P" phase, causes of which are not clearly understood.

Figs. 21 and 22, in addition to Figs. 11 and 12 constitute the evidence which can be presented to show variation in the distance of the focal point with period of recorded motion. The combination of Figs. 22 and 12 affix the short period focal point at 147°. Long period data in Fig. 21 while less

abundant indicate that the focal point for longer period motions is registered at distances shorter than 145°.

The inconclusive, scattered low values of A_o past 157° in Figs. 11, 12, and 13 are clearly evidenced in Figs. 21, 22, and 23. From the two sets of comparison, either a focal point or an energy drop is indicated at 157° or 158°. Short period data suggest a drop in energy between 147° and 157° and hence a focal point at 157°; long period data in this distance interval suggest a level of energy between 145° and 157° and, hence, the end of a phase at 157°. The data which have been discussed are believed to indicate that the point C, Fig. 1, is located near 157°.

At distances just beyond 157° all instruments (Figs 21, 22,23) evidence a rapid drop in energy reception which appears similar to a shadow zone effect. At distances approaching to 175°, all instrumental data indicate an abrupt rise in energy. It is worth noting that the horizontal instruments at distances near 175° show a ratio level equal to one-half or one -third that shown by vertical instruments. While this relationship may lie within limits of error/it is further substantiated qualitatively by Figs. 11, 12, and 13; these data near 170° show an average of horizontal A_o values less than vertical averages by logarithmic amounts of 0.6 to 1.0 which correspond to factors of one-fourth to one-tenth. We would expect

horizontal instruments located at 175° to register very little motion from rays of the P' longitudinal wave which have traveled nearly directly through the earth and which reach the surface with an angle of incidence less than one degree. However, horizontal observational data of Fig. 23 indicate that the rays of the wave arriving near 175° have an appreciable apparent angle of incidence. Yet, our simplified theory as shown in Figs. 9 and 10 indicates that the magnitude of horizontal ratios near 175° should be only one-fiftieth or one-sixtieth the magnitude of vertical ratios. This discrepancy in data from horizontal instruments may suggest the following; 1, that the true angle of incidence of P_1' near 175° is actually much greater than supposed; or 2, that the wave does not arrive at the surface with pure longitudinal motion; or 3, that wave energy in the P_1' longitudinal wave distributes itself or migrates within the wave front and thus gives rise to a component of horizontal motion; or 4, that small inaccuracies in instrument installations result in disproportionately large amplitudes from motion of small incident angle. Of these suggestions we may immediately discount No. 1 from considerations of travel time data; No. 2 and No. 3 will require extensive consideration of elastic wave propagation theory before they may be evaluated; No. 4 may well explain part of the discrepancies noted.

Comparison of observed amplitude/period ratios of P_2' to those of PP are shown in Figs. 24, 25, and 26. These data, compared to theoretical values of Figs. 19 and 20, further substantiate A_o data in that P_2' ratios appear too high by

factors of 2. The rise in ratio values by factors of 2 to 3 from 170° to 176° is of such magnitude as to suggest a reinforcement of phases as previously mentioned. Data at these distances are too scant for conclusions; nonetheless, it is odd that the sparse observations near 175° should indicate a horizontal component in P_2' less than or equal to that of P_1'. This is contrary to theory as evidenced by Figs. 9, 10, and 15. P_2' arrives near 175° with 12° angle of incidence; at 175°, P_1' with less than 1° angle of incidence should have a nearly unobservable horizontal component. This suggests that the discrepancies evidenced by horizontal instruments are related to the angles of incidence.

POSSIBLE EXPLANATIONS OF VARIANCES

Multiple P' Groups and Focal Points

The existence of multiple phases in the P' waves has long been known. Gutenberg and Richter (1934, p 86-92) have discussed multiplicity and listed travel times for multiple phases of P'. Availability of additional data has made possible the relation of period and multiplicity.

The P' travel time data which have been discussed suggest dispersion; this is the dependency of velocity on wave length or frequency. In a dispersive medium a single harmonic train can be propagated without distortion of wave form; any wave motion containing different harmonic components will undergo distortion which increases with time. Solutions of

the wave equation for the seismic case lead to expressions for velocity of propagation which are dependent upon physical constants; if these constants are such that frequency of vibration is not proportional to wave number, dispersion can result. Constants which determine velocity may vary spatially or they may vary with the frequency of applied motion. For the case in which frequency to wave length proportionality is preserved, a harmonic motion containing n components is propagated with a velocity v defined in terms of frequency ν and wave number k as

$$v = \frac{1}{n} \sum_{i=1}^{n} \nu_i / k_i \qquad \text{and} \quad d\nu/dk = \text{constant}$$

For the case in which proportionality is not preserved

$$v \neq \frac{1}{n} \sum_{i=1}^{n} \nu_i / k_i \qquad \text{and} \quad \frac{d\nu}{dk} = f(v)$$

f(v), the variation of frequency with wave number, is called group velocity; if we express frequency ν in terms of wave length λ and velocity v

$$\nu = kv = v/\lambda$$

then

$$f(v) = d\nu/dk = v + k\, dv/dk = v - \lambda\, dv/d\lambda$$

which is the well known equation for group velocity associated with dispersion. Jeffreys (1946, p 479) has shown that periods, wave lengths, and wave velocities are propagated with the group velocity in dispersive media, while individual components change their periods, wave lengths, and velocities as they travel. This result may be realized by assuming that component amplitudes are a function of wave number and further that there exists an optimum wave number which propagates the maximum disturbance.

We may reasonably expect dispersion within the earth to occur under different sets of conditions. One of these refers to the case of a harmonic motion traveling along layered media; the individual layers may be isotropic, yet if each layer possesses different properties, dispersion effects can result. Those components of the motion which have larger wave lengths are subject to propagation with velocities proportional to the average velocity of all transmitting layers, while components of smaller wave length are subject to propagation with the average velocity of a fewer number of layers. Thus, depending upon velocity distribution within the layers an instantaneous disturbance may be dispersed into a wave train in which the observed period, as registered by suitably chosen instruments, is seen to increase or decrease with increasing time and distance. An example of this type of dispersion is observed in seismic surface waves. This case has been discussed by Munk

(1947); from empirical evidence he has shown that surface w wave period variations are of the same order of magnitude as indicated by theory. Period variations with distance are shown to be of the order 1.4×10^{-8} sec/cm.

The second set of conditions which may lead to dispersion are exemplified by motion traveling through an anisotropic medium, the anisotropism of which varies with path of travel. Anisotropism may be in the form of spatial velocity variation or may relate variations in the reaction of elastic constants depending upon frequency of applied motion; either of these may be a function of absorption. We may imagine media to be composed of an infinite number of layers of nearly dimensionless thickness; thus, this set of conditions may become partially analogous to the first case. If we require that the wave front of the motion travels oblique to the layers, dispersion effects may result which are different from those discussed above. The problem of refraction in such case becomes very complex. Refraction at a discontinuity between two dispersive media of different properties is discussed briefly by Jeffreys (1946). By equations 3 and 5 (loc. cit., p 487), the travel time of the dominant period or predominant disturbance is seen to be determined by group velocities.

It is believed that the aforediscussed period relations associated with the travel time data may be inter-

preted as a consequence of some form of dispersion--a form which may be analogous to the above. The theory for this case might best be approximated by empirical relationships as has been done for surface waves. Unfortunately, data on the phase SKS (which is propagated to and from the core as distortional motion) is necessary before empirical extrapolations may be positively established. This arises in view of the fact that core travel times for shorter distances can not be determined from P' data alone.

The core travel times have here been calculated from Fig. 27 by the method described on page 13. The results of this procedure offer a means of evaluating, insofar as is possible, the variations in time, period and distance of the P' phases. An assumption in all core travel time calculations is that no noticeable dispersion effects exist for the PcP (or ScS) phases. Thus, the effects which appear to be confined to the core, may be more properly viewed as the result of dispersion from passage throughout the earth. Results of the travel time calculations for all phases are shown in Fig. 29. These results are not to be construed as being quantitatively correct. Apparent velocities for PcP and P' were determined by unsmoothed slope measurements and are thus subject to appreciable errors. The relations portrayed by Fig. 29 are more clearly visualized in Fig. 30. In view of the uncertainties attached

to the calculation of Fig. 29, path relationships as shown in Fig. 30 can only be qualitative. An assumption in the Fig. 30 portrayal is that the rays travel a symmetrical path through the earth; points of entry into and exit out of the core are determined graphically from core travel time data. Path relationships which are shown within the core are interpolated between the points of entry and exit. These interpolated paths, while speculative, seem most reasonable. Variations in distance and path depending on the character of motion are evident. This is particularly clearly shown by the long period P_1' motion (which from 145° to 157° arrives with group 1 travel times) and the short period P'' motion; these phases may arrive at the surface of the earth at widely different distances, yet they both enter the core in the same vicinity. These variations may be interpreted in light of either or both of the two following phenomena:

1. Dispersion of elastic waves takes place within the mantle. In this case under simplified conditions the initial disturbance during its outward propagation tends to sort itself into individual groups which travel with individual group velocities as determined by their respective wave lengths. We may reasonably expect that dispersion varies with direction of propagation in which event the individual groups may arrive at different locations on the core. On refraction into the

core the individual groups are refracted differently by reason of their differing wave lengths; the dispersed train is thus more widely spread by the core.

2. Dispersion of elastic waves taken place within the core. In this case, for simplified conditions, the incident motion is assumed to be dispersed at the core contact. The individual components travel different paths with different velocities. In this case the core of the earth may exhibit properties more like those of a viscous medium for long period waves. Elements of volume in the core may react quite differently to the short period components of an incident motion.

Both of these cases are subject to further complexities arising from diffraction--or the scattering which results when a plane wave is reflected or refracted at a surface with small radius of curvature. Certainly the assumption of plane motion can no longer be tenable for propagation in the vicinity of the inner core.

At best it can as yet only be stated that effects of dispersion are evidenced by the P' phases. No means are available by which period, velocity, and distance variables may be differentiated. Whether the type of dispersion may be normal or abnormal cannot be stated without additional data.

The Point C, Fig. 1

Data which have been discussed indicate that the point C, Fig. 1, is located at or near 157° epicentral distance. Observed parameter relationships, Figs. 11, 21, 22, and 23 indicate that an abrupt drop in energy occurs at slightly larger distances. Only the short period, Fig. 12, data indicate a gradual decline in energy level over the distance interval at which longer period instruments record an abrupt drop. This variation suggests that the point C for long and short period motions may be determined by different conditions.

For long period motion, Fig. 30 indicates that the point C at 157° may be determined by the size of the inner core. Energy in that portion of the wave which grazes the inner core arrives at or near 157°; that portion of the wave which is incident with large angle upon the highly curved surface of the inner core may be so diffracted or dissipated as to account for the abrupt drop in the amount of energy (Fig. 14) received at slightly larger epicentral distances. The phase E (Fig. 27) may represent that portion of the wave which is diffracted around the inner core. Those portions of the wave incident with smaller angle upon the inner core are more easily visualized as being refracted or reflected.

On the other hand it does not necessarily follow that the path of propagation of short period motion would be the

same as that of longer period motion. In a region characterized by a rapid increase of velocity with depth shorter period motions, depending on the angle of incidence, would tend to follow more readily the path of refraction dictated by the velocity variation. The gradual decline in energy from 147° to 165° (Fig. 14) may indicate that shorter period components of motion are refracted to shorter distances. This is strengthened by the increase of period with distance as shown in Fig. 28. Thus, from the current data, the focal point C for short period motions appears to be determined by velocity distribution within the core. This is the result which Gutenberg and Richter (1939, p 123) have shown. For long period motions the point C appears to be influenced by the size of the inner core.

Anomalous Energies of P' Phases

Discrepancies between theoretical and observational data for phases affected by the core of the earth have been noted by Martner (1948). Results from Martner's investigation, and also the present one, indicate that horizontal components exist in those longitudinal phases whose path of travel is determined by the core of the earth dependent on the angles of incidence at the outer core contact and the characteristics of the recording instruments. This discrepancy is not evidenced to any degree beyond limits of error in data from those

phases such as PP and P. Martner (op cit. p 37) has discussed possible causes for the variations noted; he has concluded that the causes do not appear reasonably related to the theoretical equation for displacement (equation 1, page 5) or to any reasonable error in physical constants.

In view of the near agreement between observational and theoretical data for the phase PP (Fig. 8), the conclusion seems warranted that the P' discrepancies of Figs. 14 and 18 arise largely from passage in the core. Effects which may be present, but unobservable, for PP, may be magnified by reflection and refraction phenomena at the core boundary. Considering the uniformly smaller residuals for longer period vertical instruments, the discrepancies may be related further to the period or wave length of motion. Still further restrictions may enter from consideration of P_2' residuals (Fig. 18) in relation to P" and P_1' residuals (Fig. 14). Variation in quantities here concerned are small when viewed in light of possible limits of error imposed by theory and methods of evaluation. However, this comparison suggests that for horizontal instruments the discrepancy is larger for smaller angles of incidence since P_2' angles of incidence vary from about 13° to about 9° (at the 145° focus), while P_1' angles of incidence vary from 0° at 180° epicentral distance to about 6° at shorter distances. Data from vertical instruments while variable do not indicate similar relations.

As has been indicated on page 40, dispersion within the mantle is possible. A suggested cause or related factor for such dispersion may be anisotropism. If anisotropism is present and is related to dispersion, the discrepancies which have been discussed may conceivably be explained as a consequence of both. The relation of anisotropism to elastic wave propagation has been discussed by Stoneley (1949); his results indicate that under given conditions, elastic motion in anisotropic media may be neither purely compressional nor purely rotational. Considerations of anisotropism and dispersion combined with resulting selective reflection and refraction at the core boundary may lead to the explanation of the discrepancies noted.

Variations in Phase P'

Results of this study indicate that P' observational data are characterized by anomolies which include travel time irregularities, period variations, and amplitude/period ratio discrepancies. It is believed that many of the anomolies which have been discussed from Figs. 11, 12, 21, 22, and 28 may arise from the reaction of dispersed components to velocity distribution. This is suggested by period variations with distance and by the extreme variations shown in Fig. 21. No adequate theory has been applied to the various ramifications of dispersion and insufficient data are at hand to analyze the discrepancies or anomalies which have been discussed. It can only be stated

that the discrepancies do not appear to be wholly unrelated and thus they may be found to result from the effects of related phenomena. Adding to any complexities which may arise from dispersion is the probability of energy loss at the inner core contact. If the inner core has rigidity of sufficient amount, appreciable energy loss to distortional S phases should occur. Depending upon the angle and period of incident motion and the nature of the velocity distribution at the inner core contact widely varying effects may result.

SUMMARY AND CONCLUSIONS

Study of the P' longitudinal waves from seismic records has revealed characteristics of such nature that dispersion is indicated. Three different groups of P' waves have been disclosed by travel time analysis. The individual groups of waves are recorded differently depending upon epicentral distance and upon the recording seismometers.

The first, and earliest arriving group is recorded from 110° to 176° with large amplitude/period ratios by short period instruments; from 145° to about 157° the P_1' phase of this group is also prominently recorded by long period instruments. From energy considerations the focal point of this group for short period instruments occurs near 147°; no prominent focal point is recorded in this group by long period instruments.

The second P' group is well observed between 130° and 160° for P" and P_1' phases. At distances shorter than 130° scattered observations may belong to motion of this group. P_2' phases for this group are more predominant for long period recordings but are scattered in arrival time. For this group large energies are recorded near 145° by long period instruments.

The third and latest arriving P' group is also well observed between 130° and 160° for P" and P_1' phases. The P_2' phase of this group is generally recorded only by long period instruments and with widely scattered arrival times. P' and P" phases are here generally recorded prominently by long period instruments. The position of the focal point of this group is not definitely known. In the neighborhood of the focal point only long period recordings indicate large energy receptions. The shortest distance at which large amplitudes were noted was about 143°, the longest distance 147°. These observations varied in time by a span of about 15 seconds.

Insufficient data are at hand to evaluate the dispersion indicated. Variations in path of travel with period within the core are suggested from qualitative considerations of travel time data. Either abnormal or normal dispersion may be present. It seems reasonable that the distortion of wave motion may take place within the core, at the core boundary, or within the mantle. If dispersion takes place in the mantle

the effects are possibly magnified upon reflection and refraction at the core boundary.

Consideration of P" energy relations and period variations with distance are reasonably interpreted to indicate that a rapid increase in velocity with depth marks the zone of approach to the inner core. Complexities existing in the P" phase are not fully understood; these may relate both to velocity distribution and to possible S phase generation at the inner core contact.

Amplitude/period ratios and energy parameters indicate that C, the point of reversal of waves through the outer core, is located near 157°. Qualitative relationships suggest that this is an end point for long period motion, a focal point for shorter period motion. For short period motion, results of this study are reasonably viewed in light of path relationships determined by Gutenberg-Richter (1939, p 123).

Observed amplitude/period ratios and energy parameters of PP conform with limits dictated by classical theory. Abnormally high ratios and energy parameters for the P", P_1', and P_2' phases cannot be reconciled with the classical theory. Variations in degree of discrepancy with different instrumental components and perhaps with angle of incidence suggest that the discrepancies may be related to anisotropism and an associated dispersion caused by absorption or by variation of physical constants with the period of incident motion.

SUGGESTIONS FOR FURTHER STUDY

Results of this study may be further clarified by investigation of the phase SKS. Completion of core travel time in relation to period may permit determination of velocity variation with period and depth. Whether dispersion arises in the mantle or the core or both should evolve from this investigation. Additional information should result from study of the phase PKKP. Less phase interference by reason of greater intervals of time and distance between focal points should permit evaluation and refinement of time, distance, and period variables.

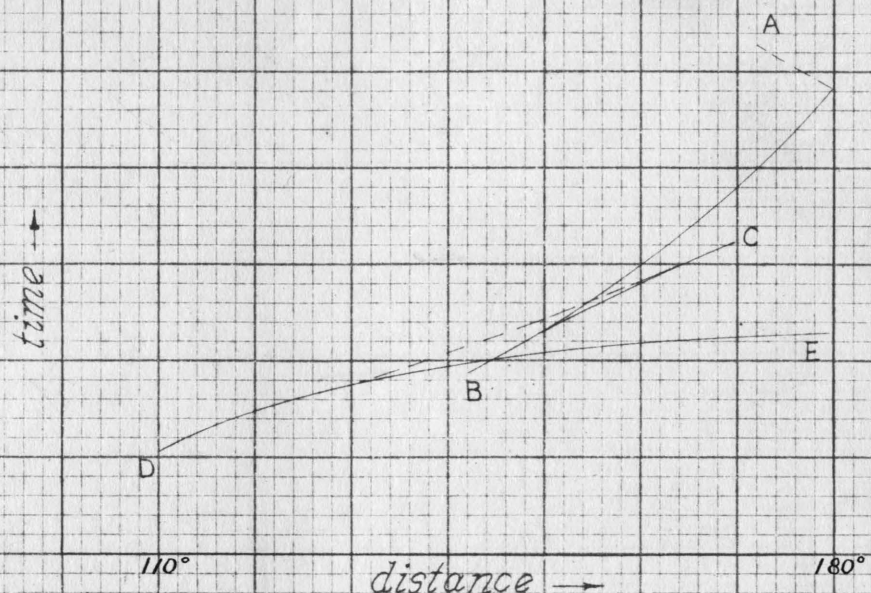

a. Form of P'core waves travel-time curve.

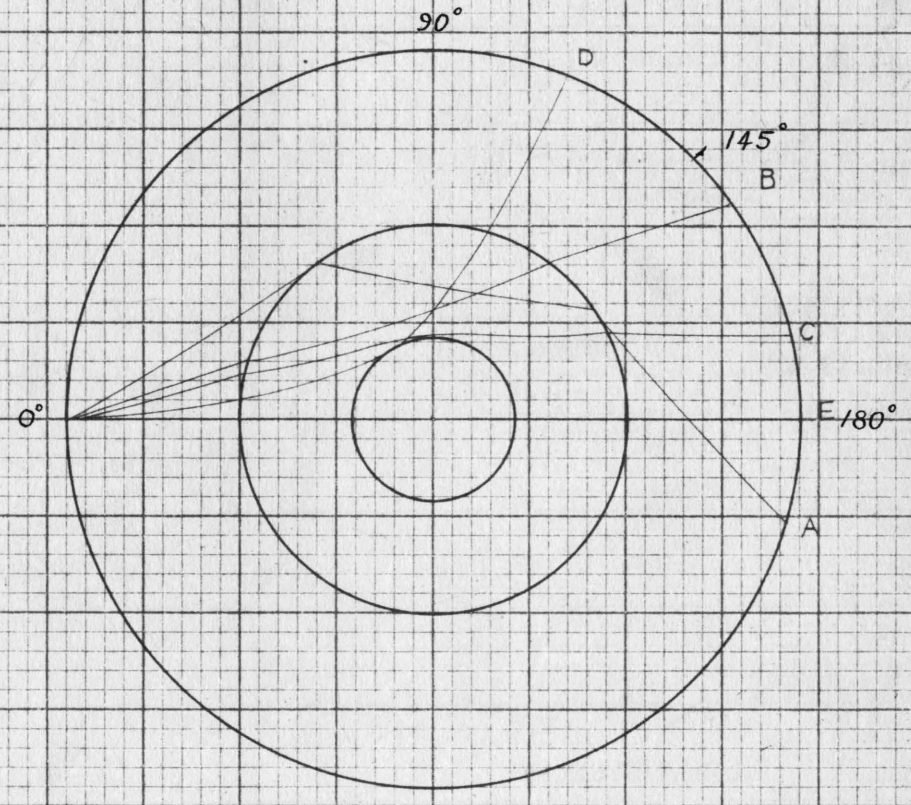

b. Path relationships of core waves.

Fig. 1

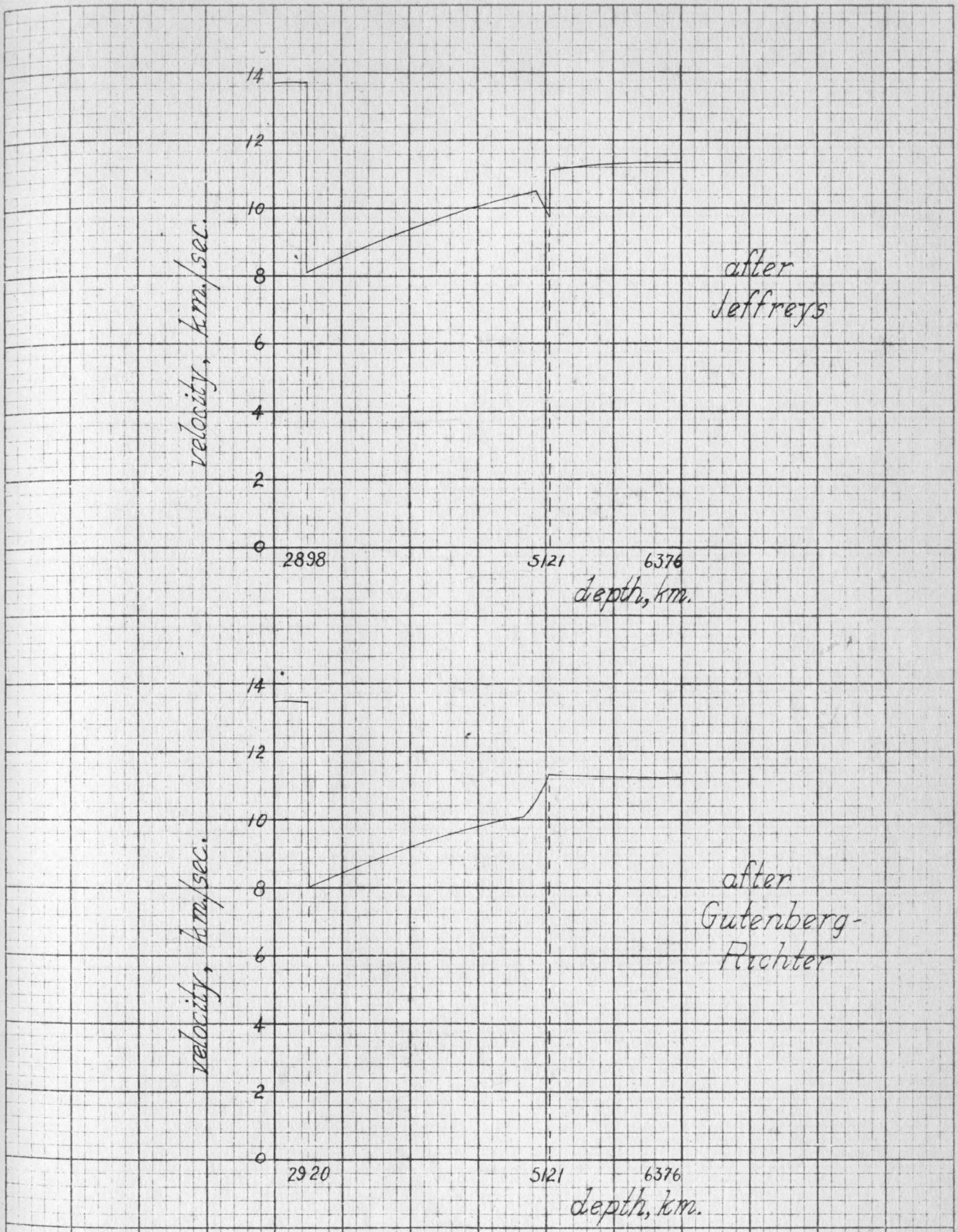

Fig 2. Velocity distributions within the earth's core

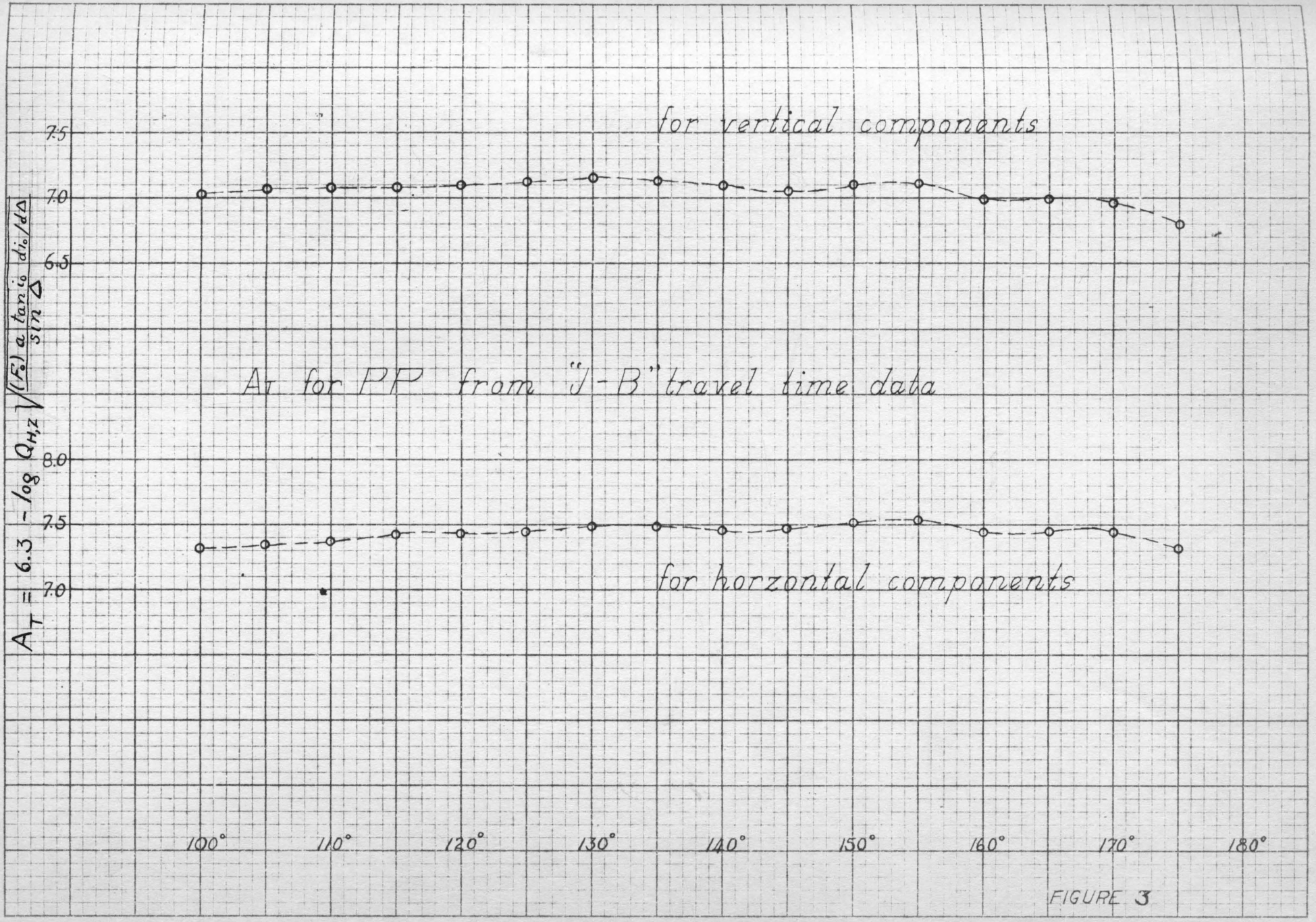
for vertical components
$A_T = 6.3 - \log Q_{H,z} \sqrt{\frac{(F_0)\ a \tan i_0\ di_0/d\Delta}{\sin \Delta}}$
A_T for PP from "J-B" travel time data
for horzontal components
7.5
7.0
6.5
8.0
7.5
7.0
100°
110°
120°
130°
140°
150°
160°
170°
180°

FIGURE 3

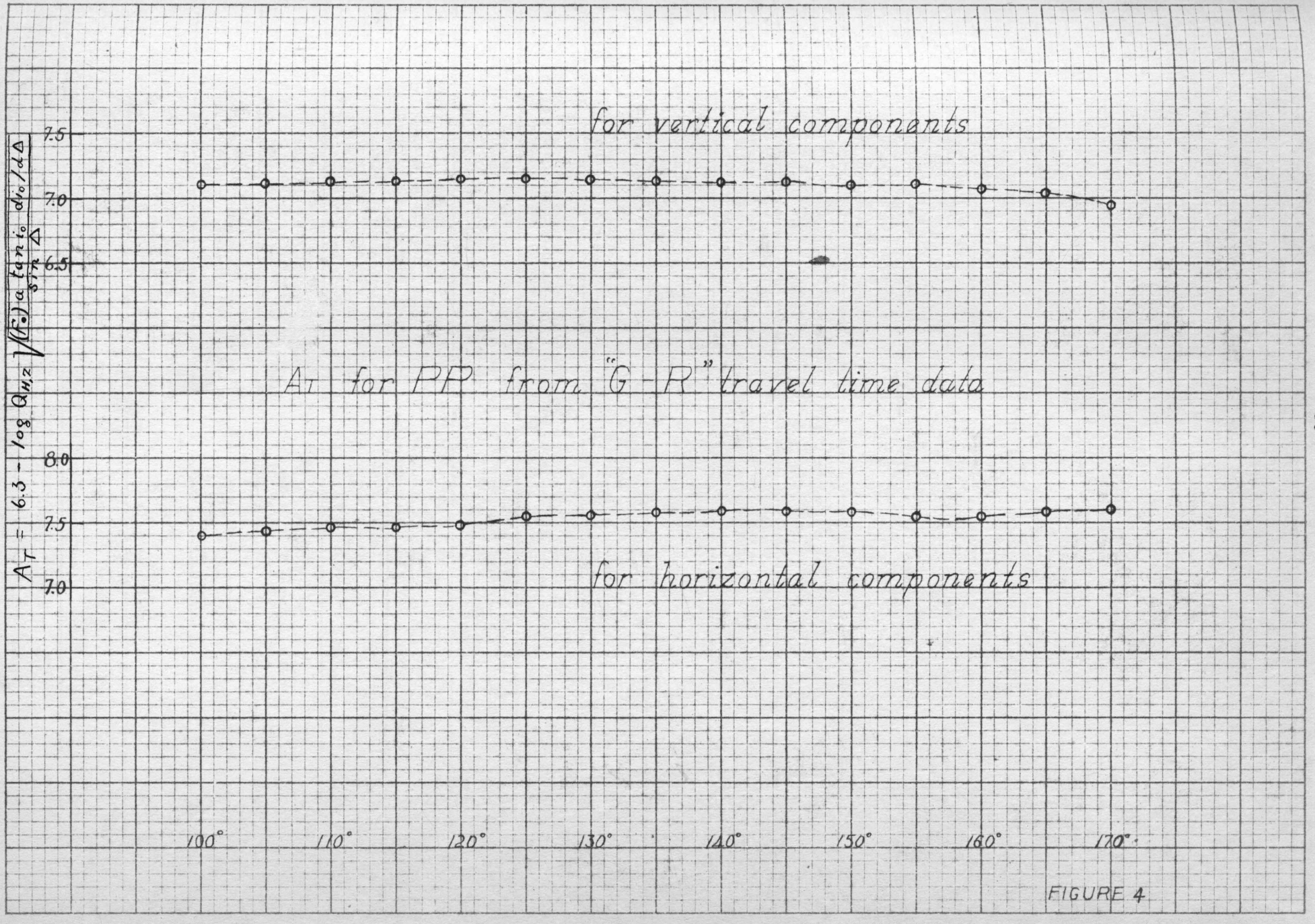
for vertical components
A_T for PP from "G-R" travel time data
for horizontal components
$A_T = 6.3 - \log Q_{HZ} \sqrt{(F_0)} \frac{a \tan i_0 \; di_0/d\Delta}{\sin \Delta}$
7.5
7.0
6.5
8.0
7.5
7.0
100°
110°
120°
130°
140°
150°
160°
170°

FIGURE 4

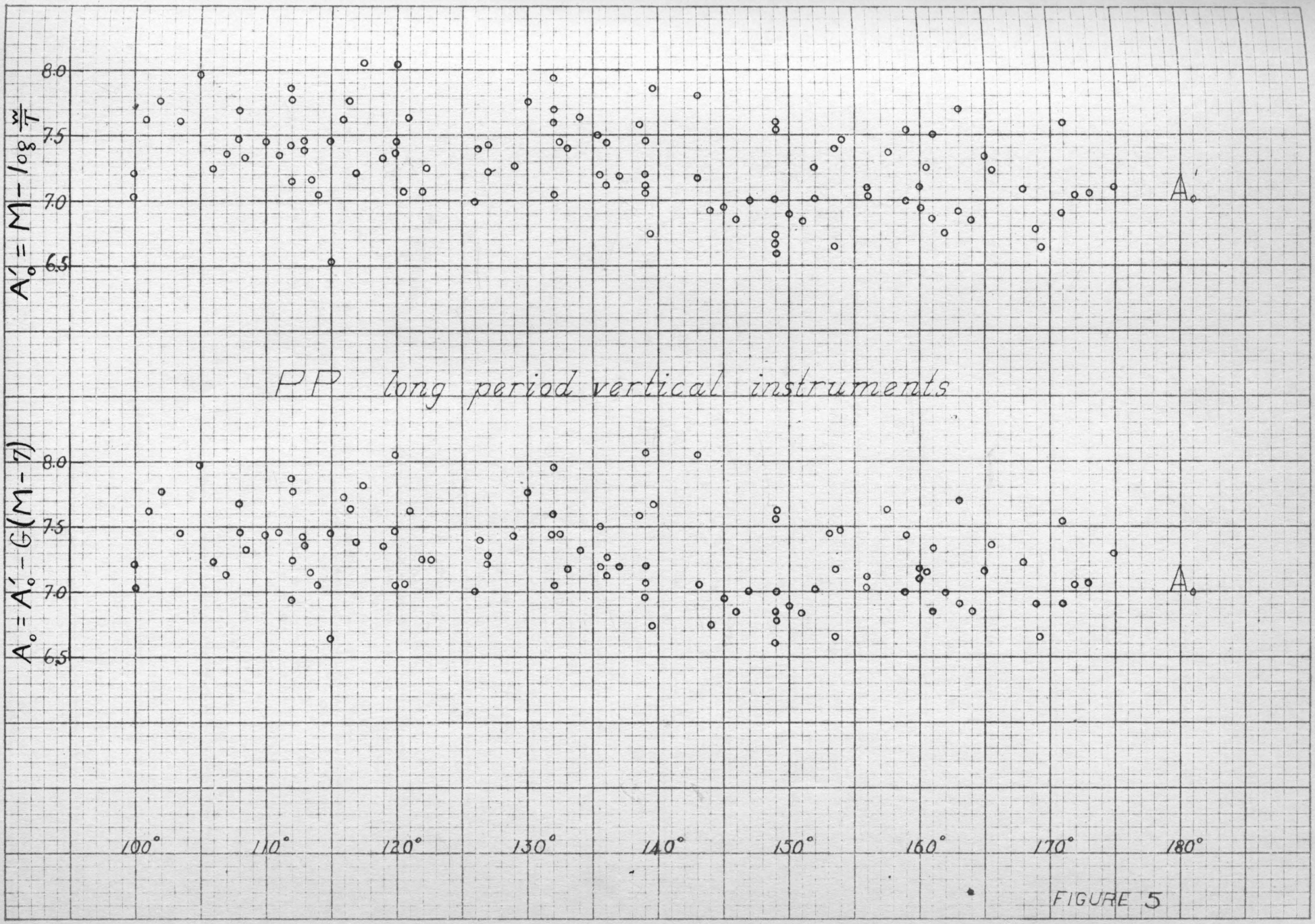
$A'_\circ = M - 10_8 \frac{w}{T}$
8.0
7.5
7.0
6.5
A'
PP long period vertical instruments
$A_\circ = A'_\circ - G(M-7)$
8.0
7.5
7.0
6.5
A
100°
110°
120°
130°
140°
150°
160°
170°
180°

FIGURE 5

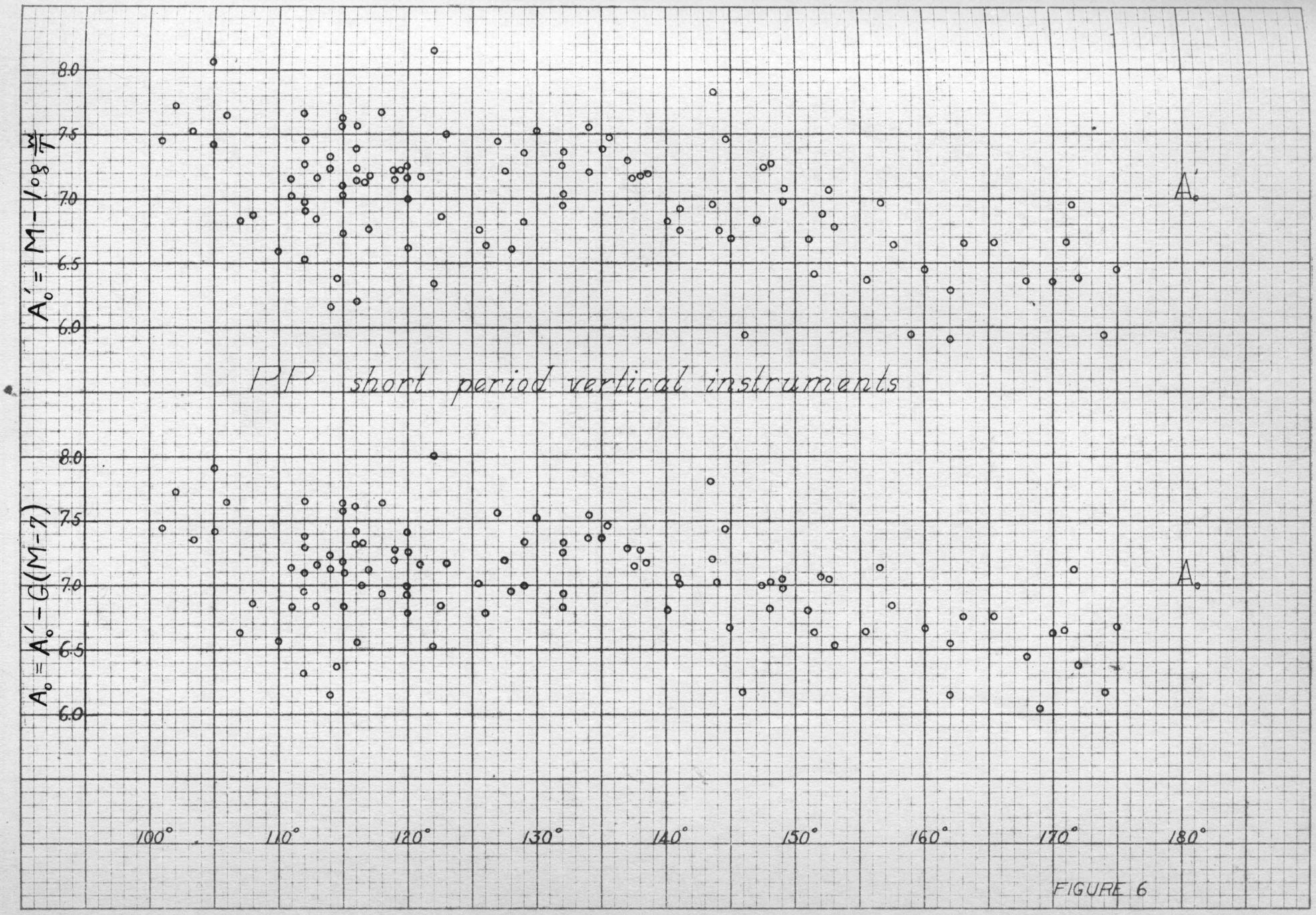
PP short period vertical instruments
$A_o' = M - \log \frac{w}{T}$
$A_o = A_o' - G(M-7)$
8.0
7.5
7.0
6.5
6.0
100°
110°
120°
130°
140°
150°
160°
170°
180°
A'
A

FIGURE 6

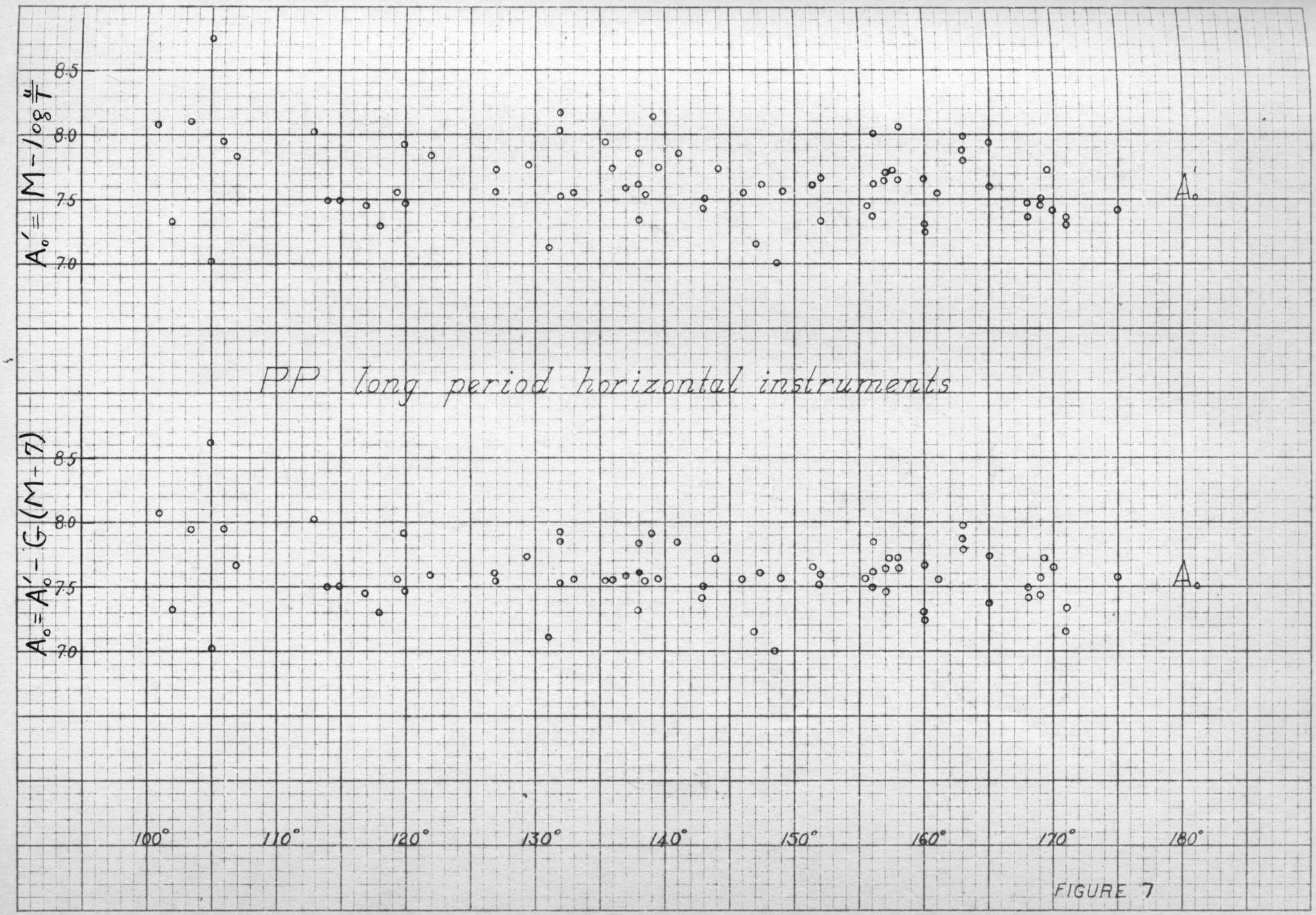
$A_0' = M - 10\frac{u}{T}$
8.5
8.0
7.5
7.0
PP long period horizontal instruments
$A_0 = A_0' - G(M+7)$
8.5
8.0
7.5
7.0
100°
110°
120°
130°
140°
150°
160°
170°
180°

FIGURE 7

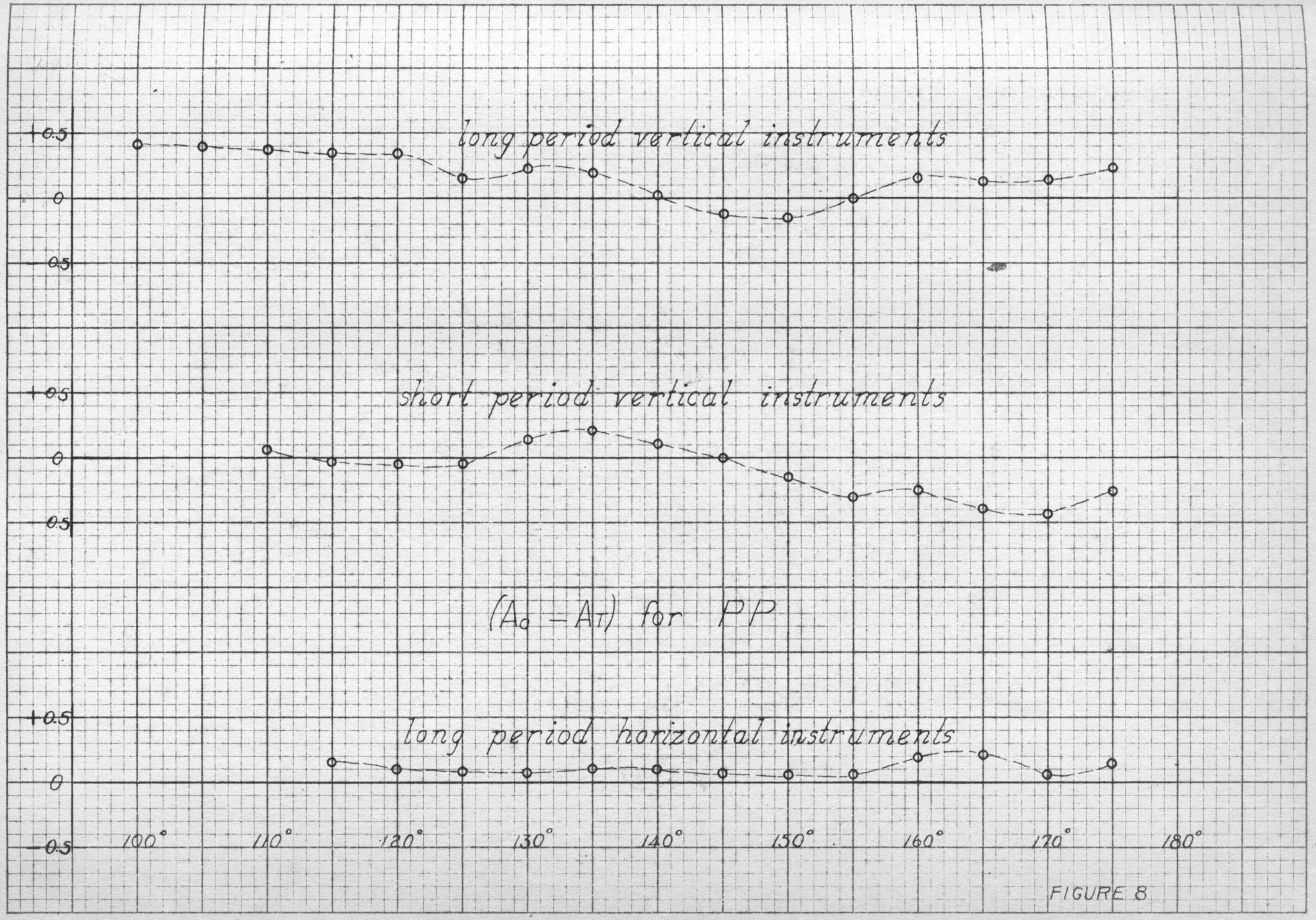
long period vertical instruments
+0.5
0
-0.5
short period vertical instruments
+0.5
0
-0.5
$(A_o - A_T)$ for PP
long period horizontal instruments
+0.5
0
-0.5
100°
110°
120°
130°
140°
150°
160°
170°
180°

FIGURE 8

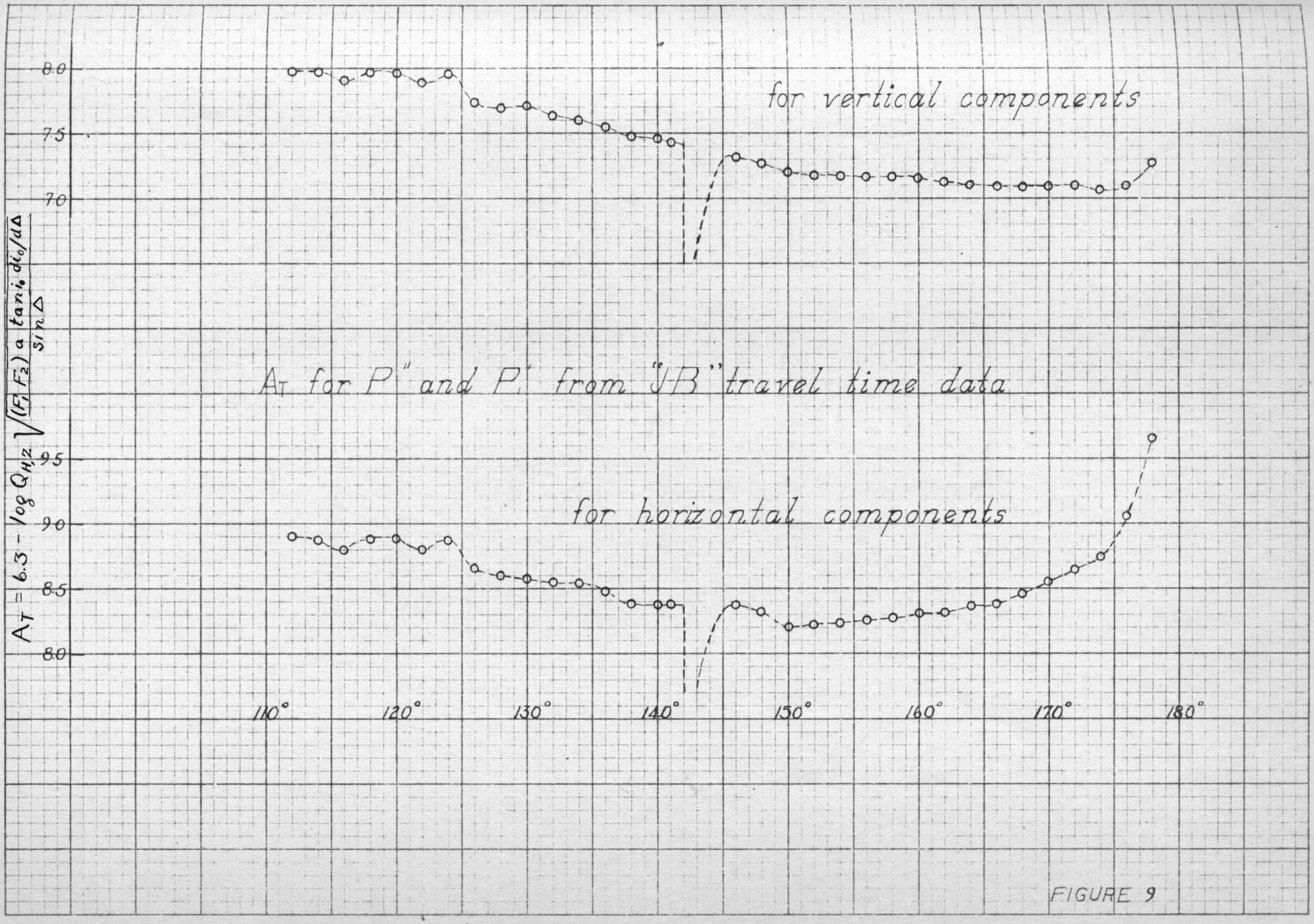
for vertical components
A_T for P'' and P' from "J-B" travel time data
for horizontal components
$A_T = 6.3 - \log Q_{H,Z} \sqrt{(F_1 F_2)} \, a \, \frac{\tan i \, d\iota_0/d\Delta}{\sin \Delta}$
8.0
7.5
7.0
9.5
9.0
8.5
8.0
110°
120°
130°
140°
150°
160°
170°
180°

FIGURE 9

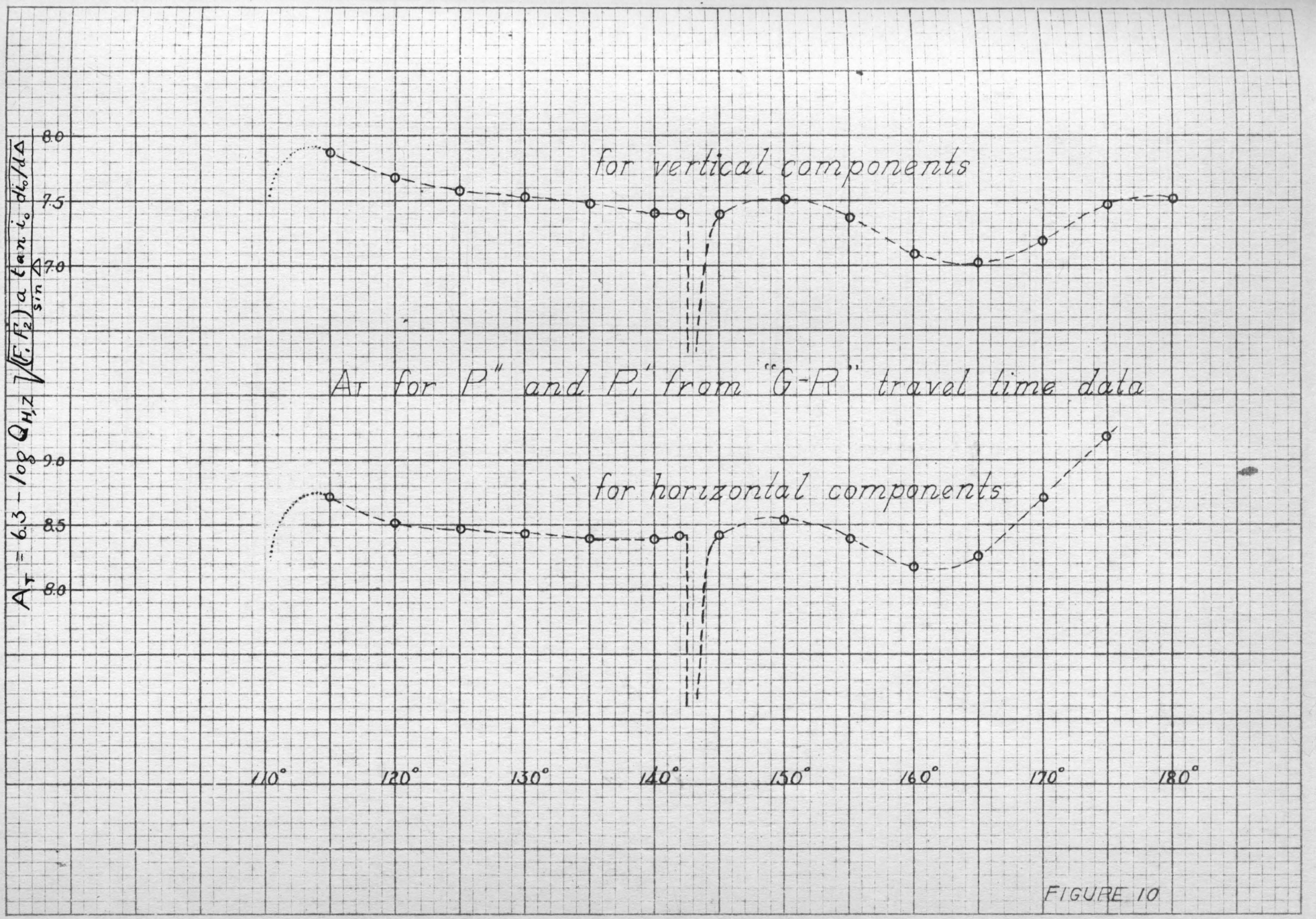
$A_T = 6.3 - \log Q_{H,Z} \sqrt{(F_1 F_2)} \frac{a \tan i_o \, di_o/d\Delta}{\sin \Delta}$
8.0
7.5
7.0
9.0
8.5
8.0
for vertical components
A_T for P'' and P_1' from "G-R" travel time data
for horizontal components
110°
120°
130°
140°
150°
160°
170°
180°

FIGURE 10

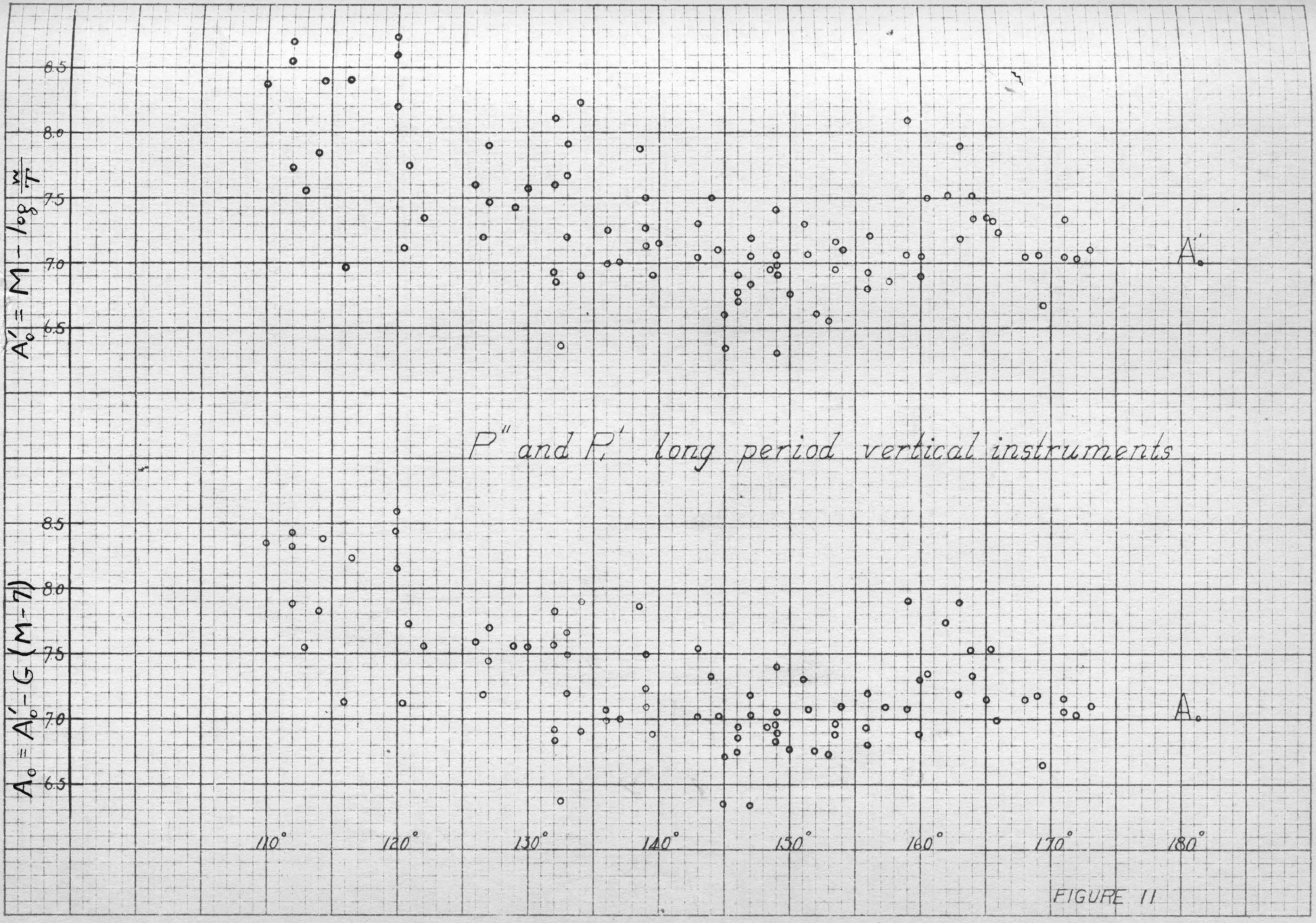
$A'_o = M - \log \frac{w}{T}$
8.5
8.0
7.5
7.0
6.5
A'o
P'' and P' long period vertical instruments
$A_o = A'_o - G(M-7)$
8.5
8.0
7.5
7.0
6.5
Ao
110°
120°
130°
140°
150°
160°
170°
180°

FIGURE 11

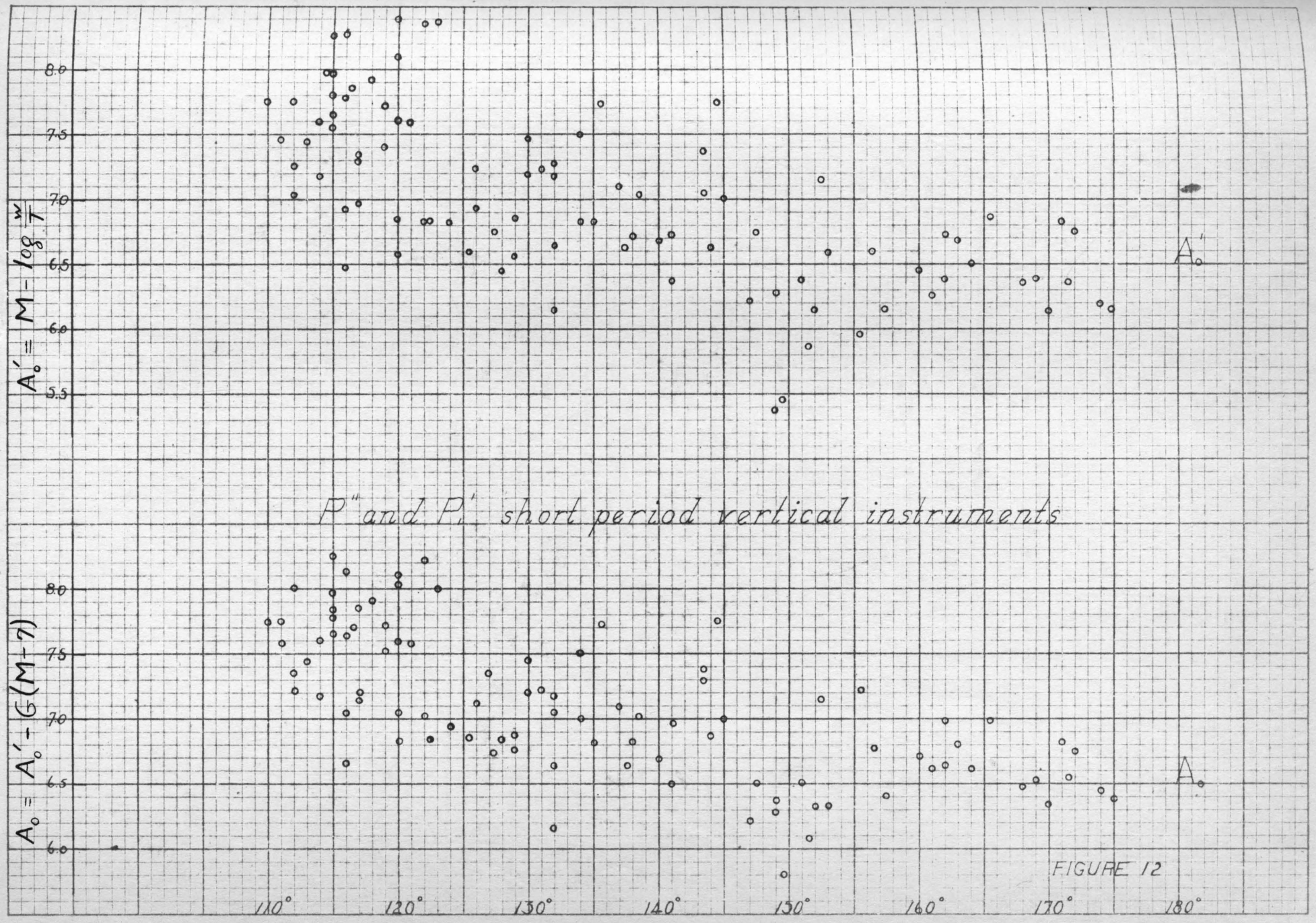
$A'_o = M - \log \frac{w}{T}$
8.0
7.5
7.0
6.5
6.0
5.5
A'
P" and P' short period vertical instruments
$A_o = A'_o - G(M-7)$
8.0
7.5
7.0
6.5
6.0
A
110°
120°
130°
140°
150°
160°
170°
180°

FIGURE 12

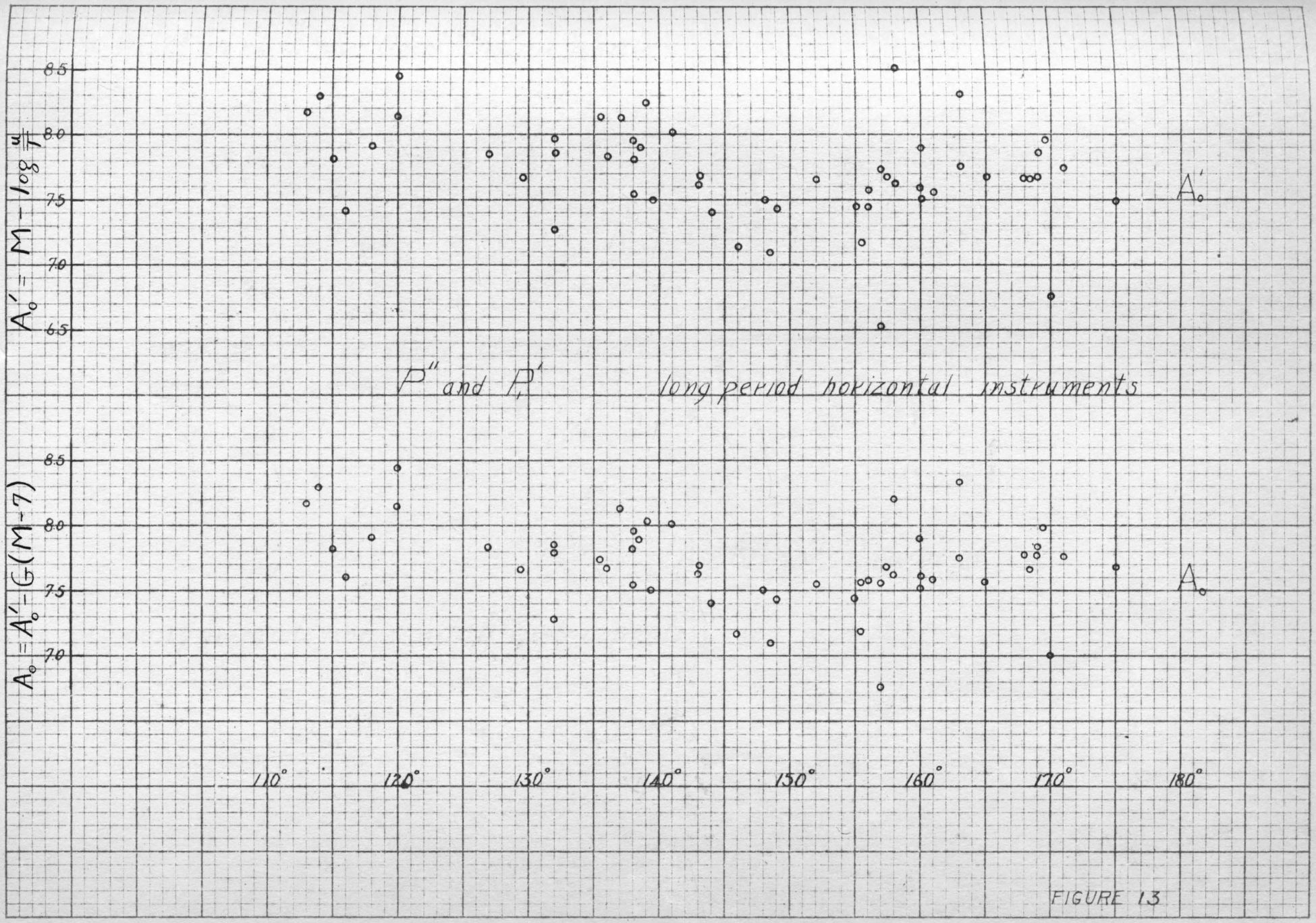
$A'_o = M - \log \frac{u}{T}$
8.5
8.0
7.5
7.0
6.5
A'_o
P" and P' long period horizontal instruments
$A_o = A'_o - G(M-7)$
8.5
8.0
7.5
7.0
A_o
110°
120°
130°
140°
150°
160°
170°
180°

FIGURE 13

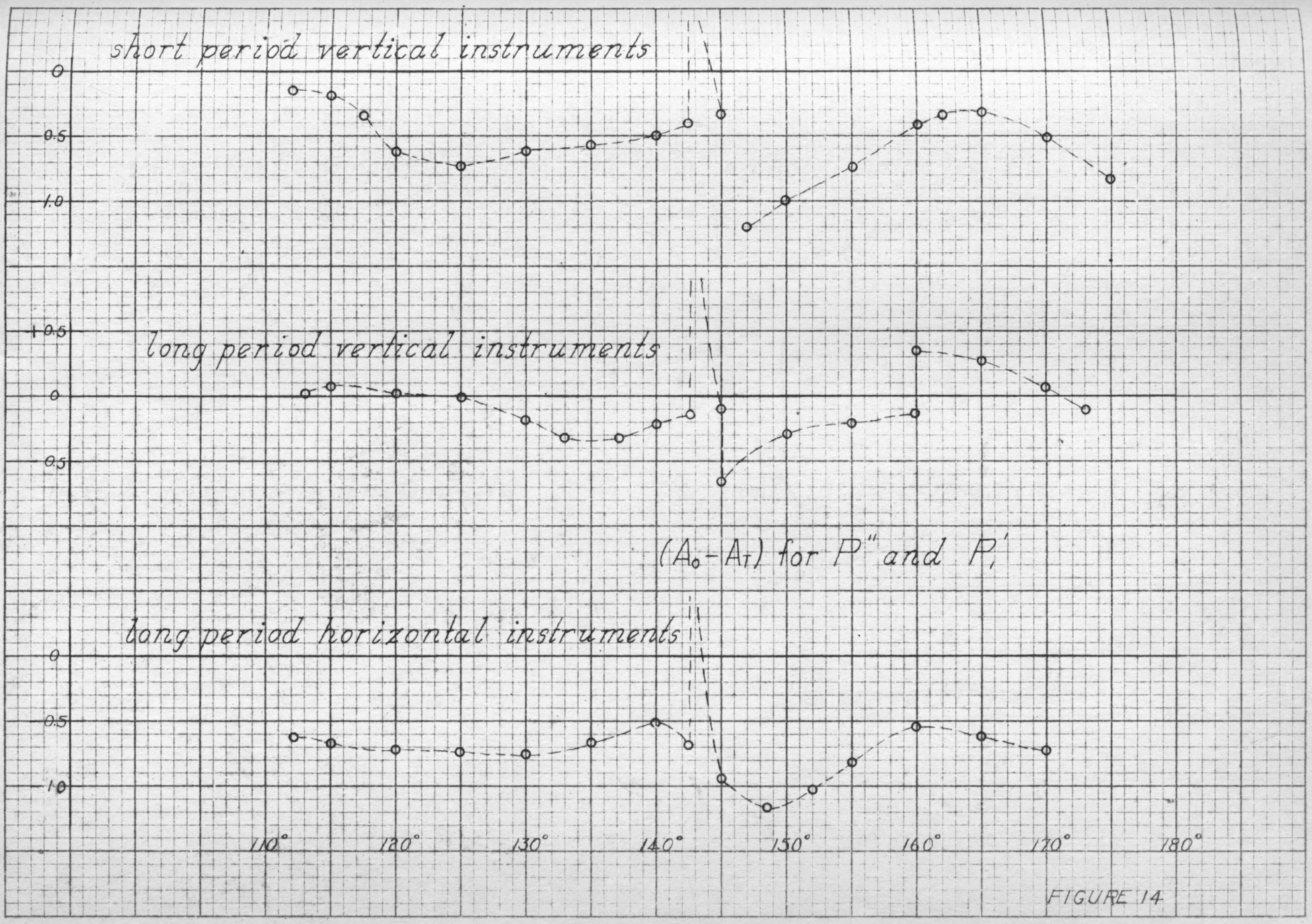
short period vertical instruments
0
0.5
1.0
+0.5
long period vertical instruments
0
-0.5
$(A_o - A_T)$ for P" and P,'
long period horizontal instruments
0
0.5
1.0
110°
120°
130°
140°
150°
160°
170°
180°

FIGURE 14

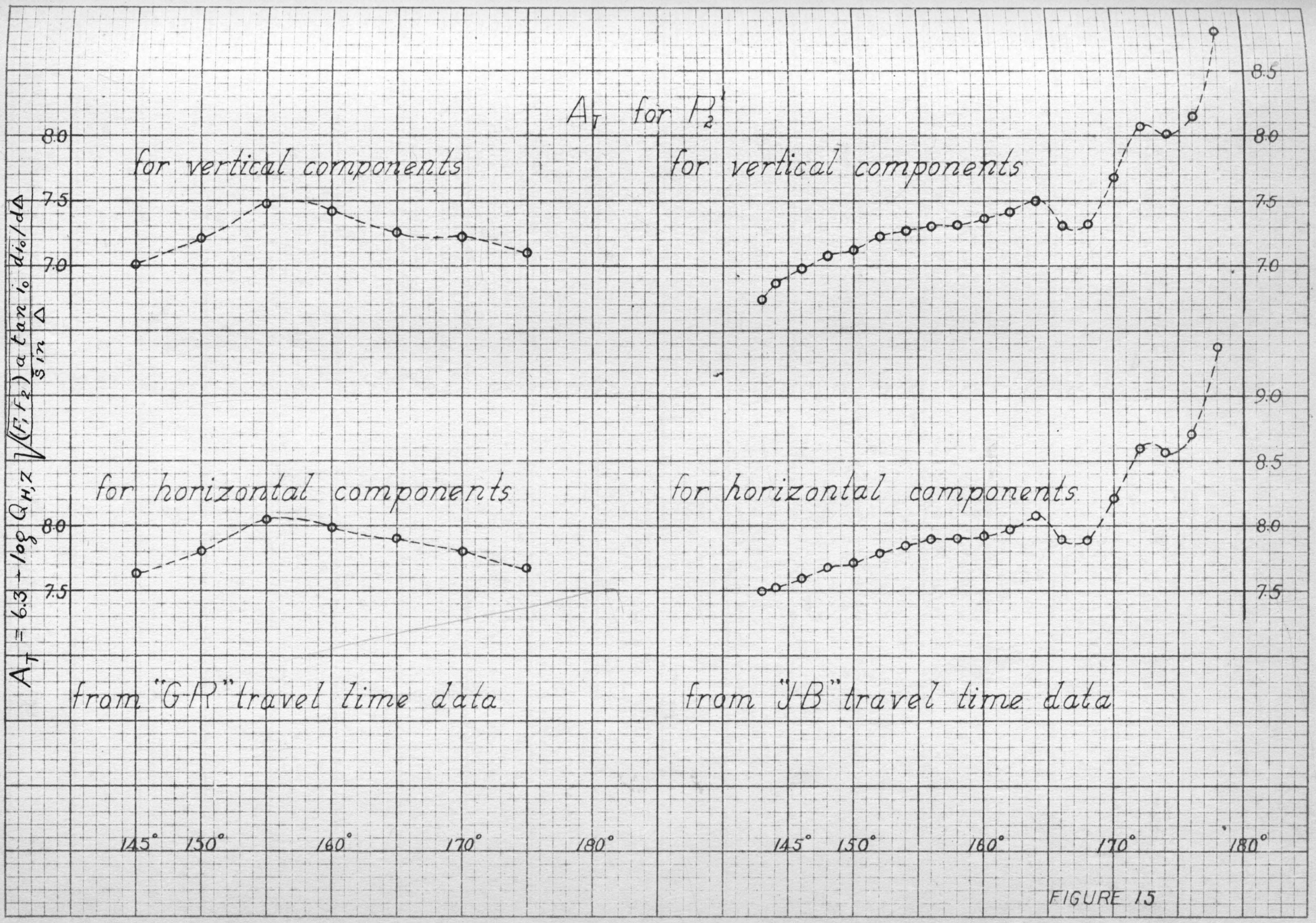
A_T for P_2'
for vertical components
for horizontal components
from "G-R" travel time data
$A_T = 6.3 + \log Q_{H,Z} \sqrt{(F_1 F_2)} \, a \tan i_0 \, di_0/d\Delta \sin \Delta$
8.0
7.5
7.0
8.0
7.5
145° 150° 160° 170° 180°
for vertical components
for horizontal components
from "J-B" travel time data
8.5
8.0
7.5
9.0
8.5
8.0
7.5
145° 150° 160° 170° 180°

FIGURE 15

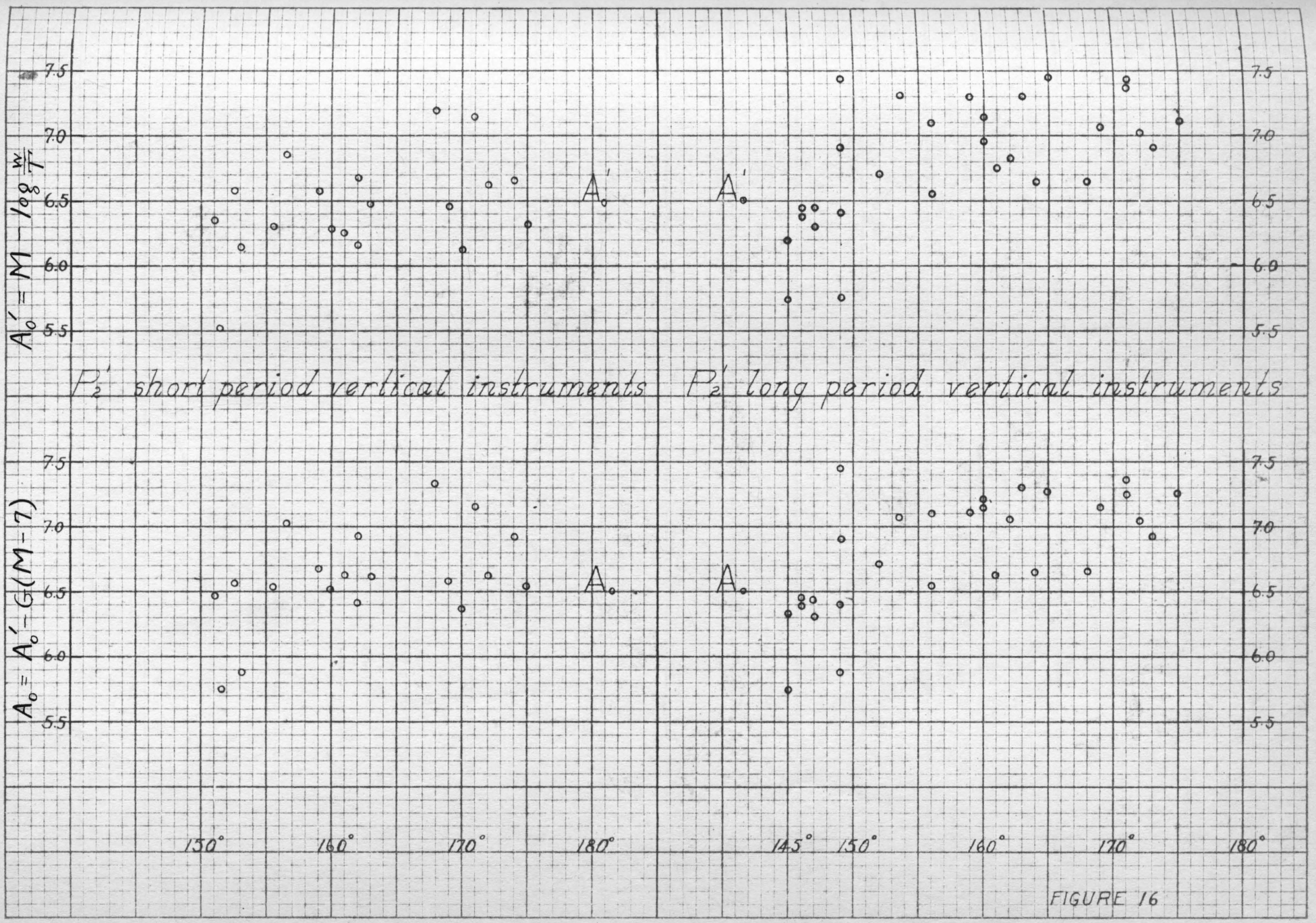
$A_0' = M - \log \frac{w}{T}$
$A_0 = A_0' - G(M-7)$
7.5
7.0
6.5
6.0
5.5
A_0'
A_0
P_2' short period vertical instruments
P_2' long period vertical instruments
150°
160°
170°
180°
145°
150°
160°
170°
180°

FIGURE 16

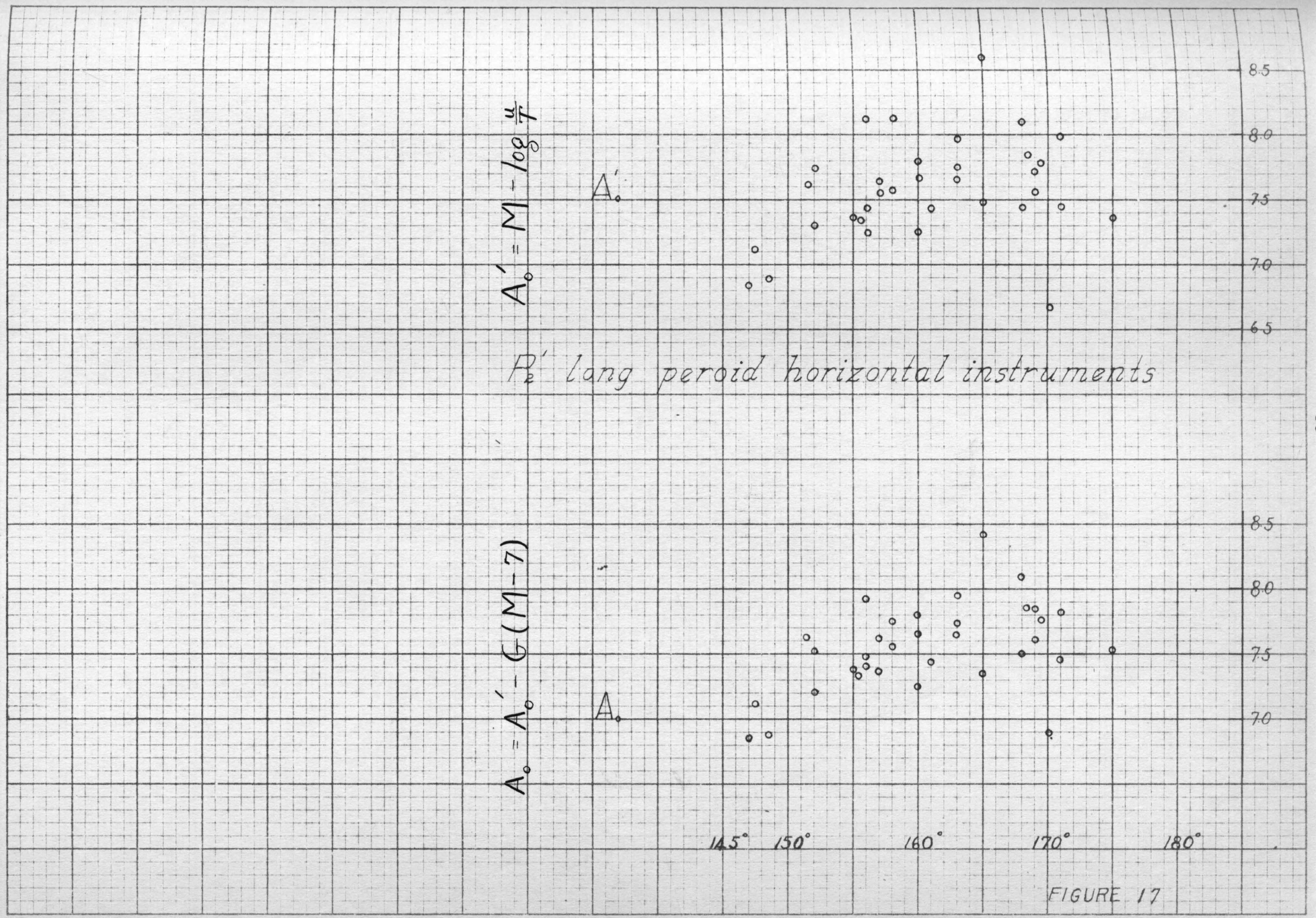
$A'_o = M - \log \frac{u}{T}$
A'_o
8.5
8.0
7.5
7.0
6.5
P_2' long peroid horizontal instruments
$A_o = A'_o - G(M-7)$
A_o
8.5
8.0
7.5
7.0
145°
150°
160°
170°
180°

FIGURE 17

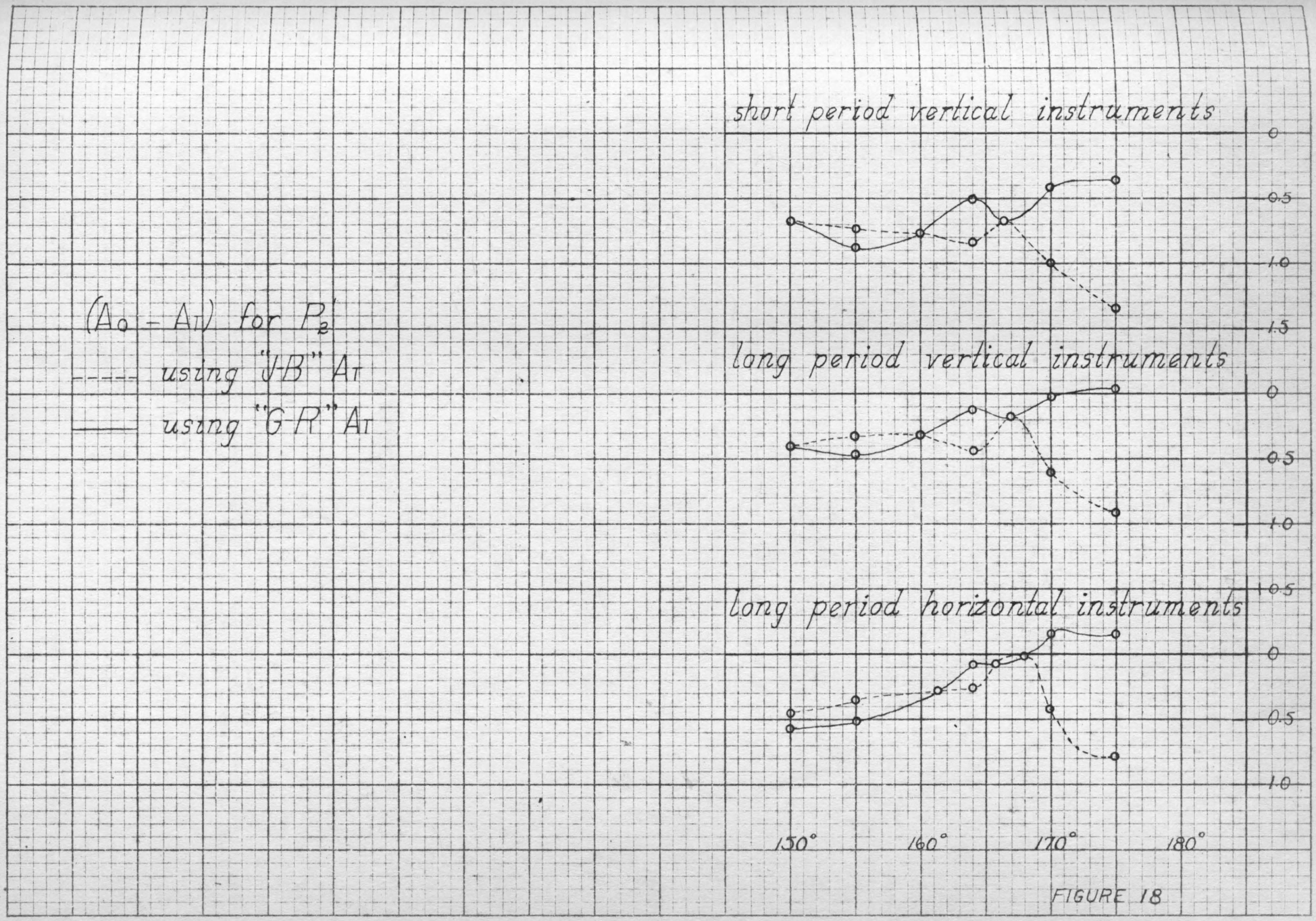
short period vertical instruments
long period vertical instruments
long period horizontal instruments
0
0.5
1.0
1.5
0
0.5
1.0
0.5
0
0.5
1.0
150°
160°
170°
180°
$(A_O - A_{II})$ for P_2
----- using "J-B" A_I
—— using "G-R" A_I

FIGURE 18

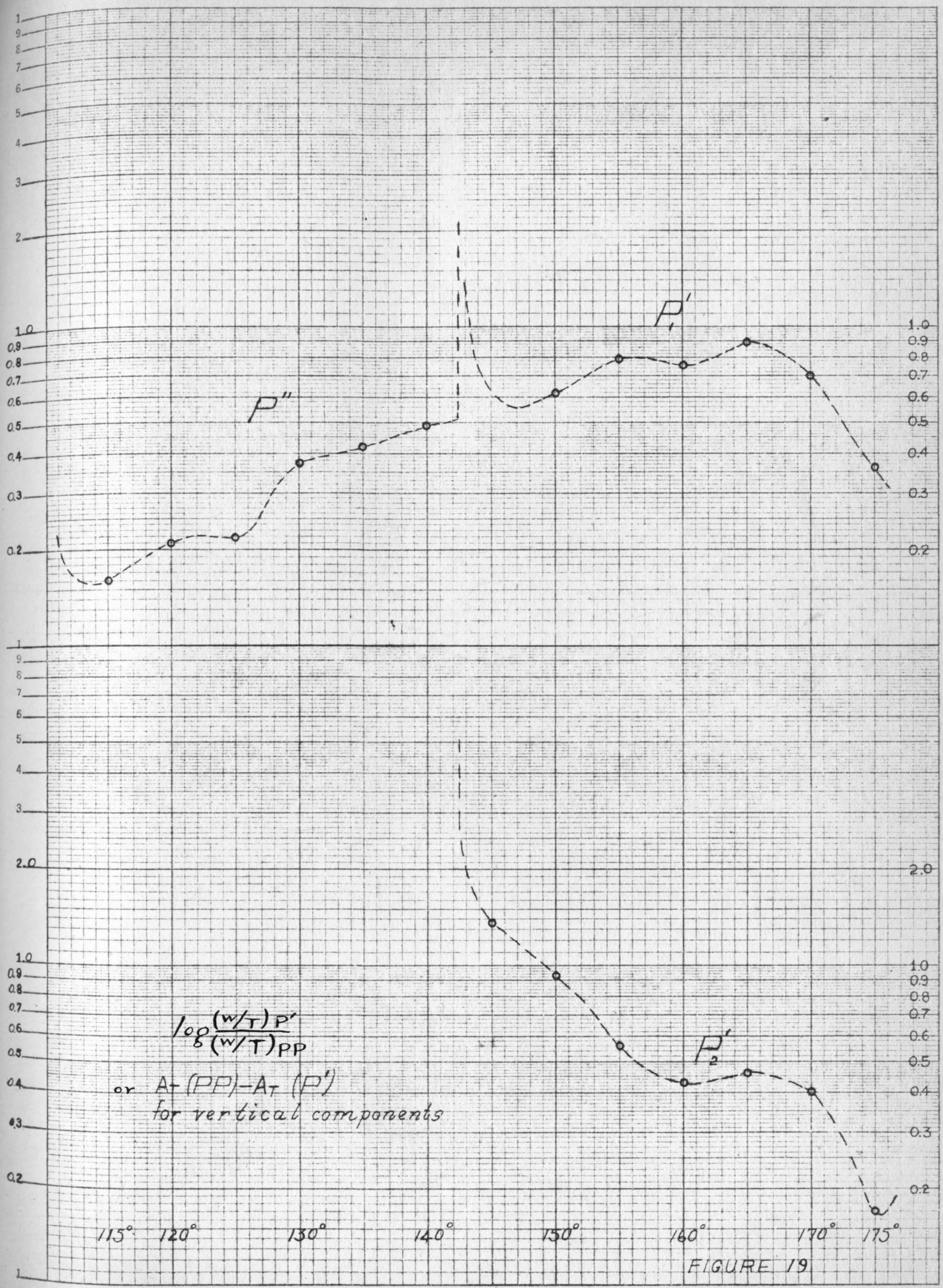
P''
P'
P'2
$\log \frac{(w/T)P'}{(w/T)PP}$
or $A_T(PP) - A_T(P')$
for vertical components
115°
120°
130°
140°
150°
160°
170°
175°

FIGURE 19

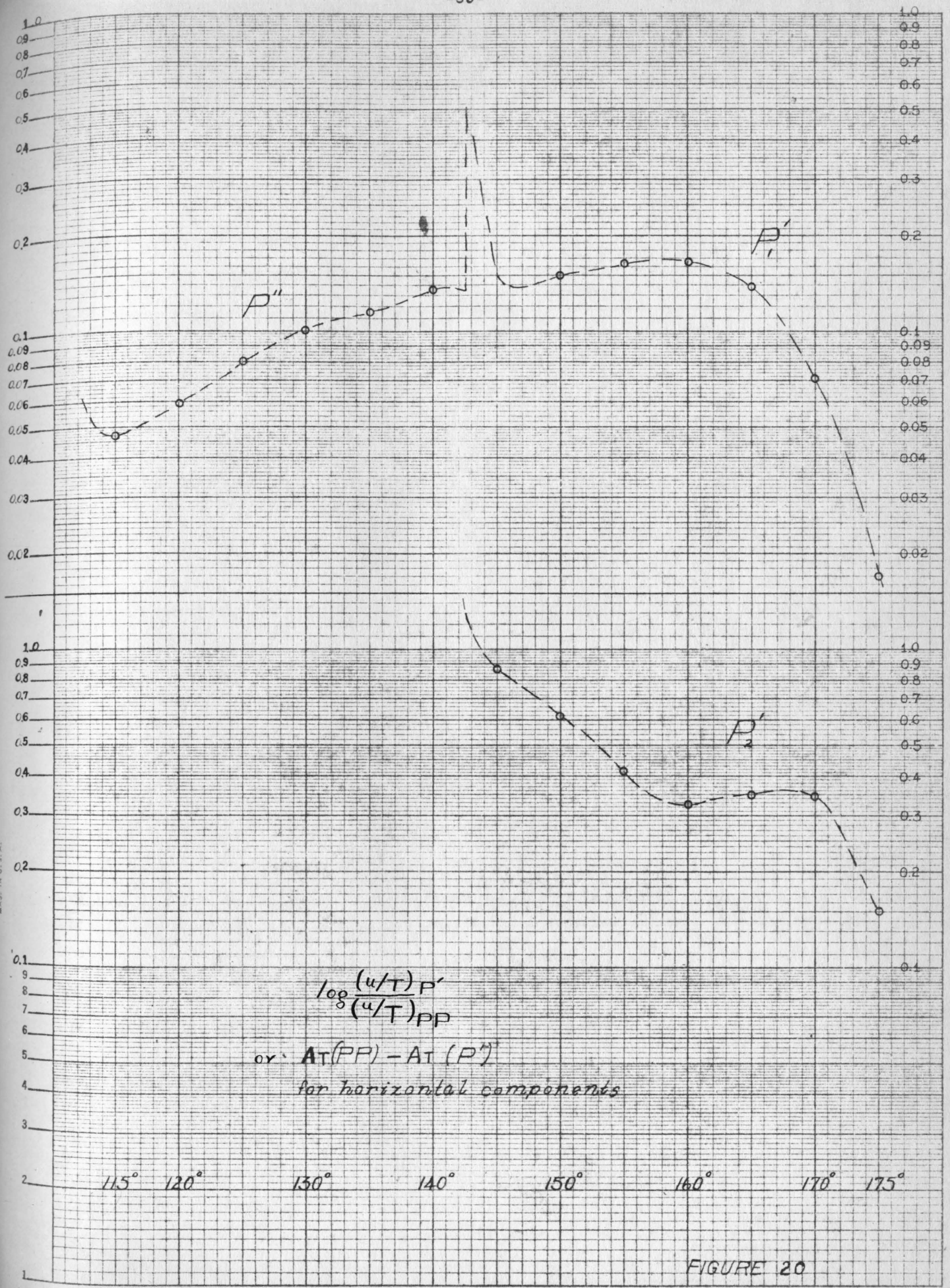

$$\log \frac{(u/T)_{P'}}{(u/T)_{PP}}$$

or $A_T(PP) - A_T(P')$

for horizontal components

FIGURE 20

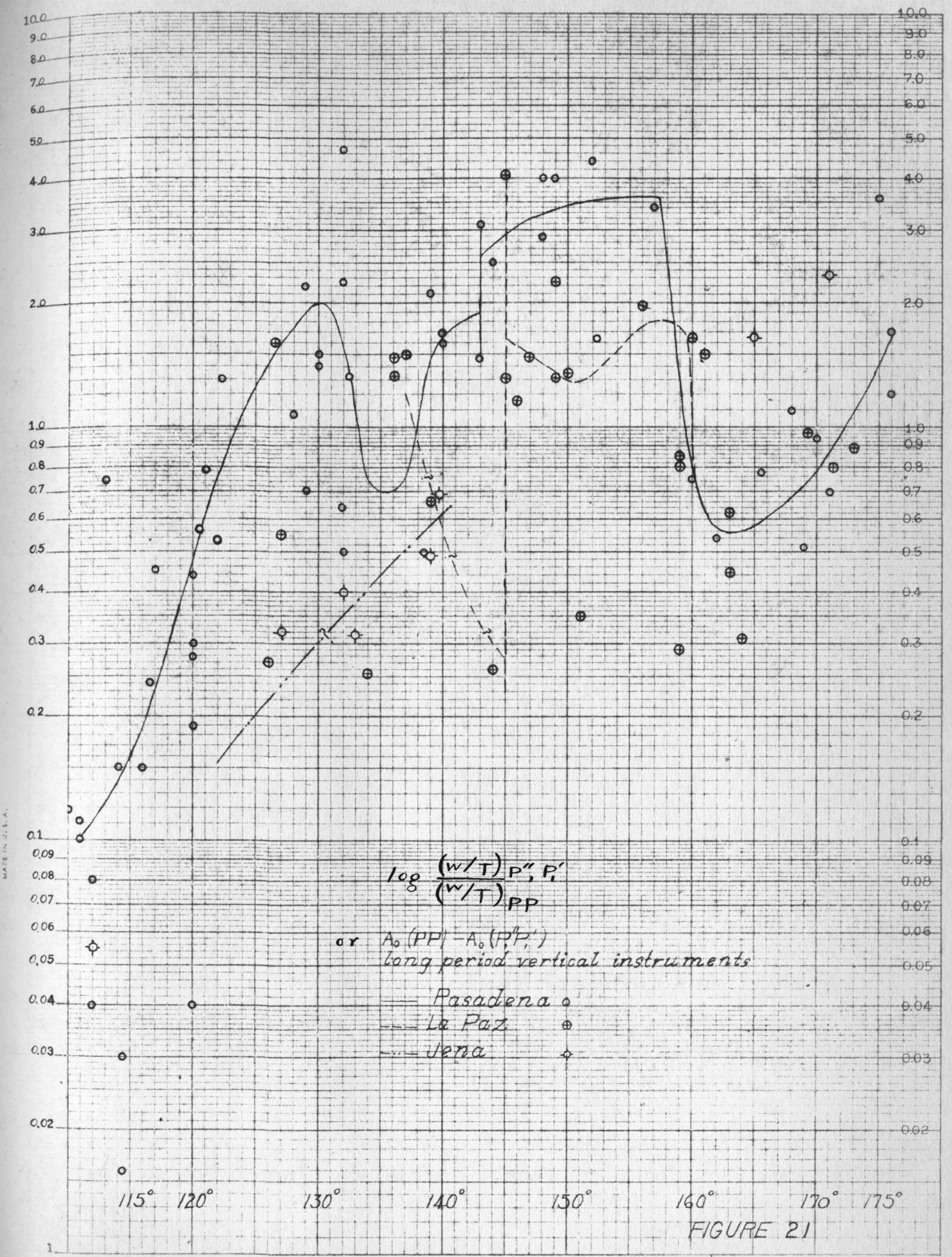

FIGURE 21

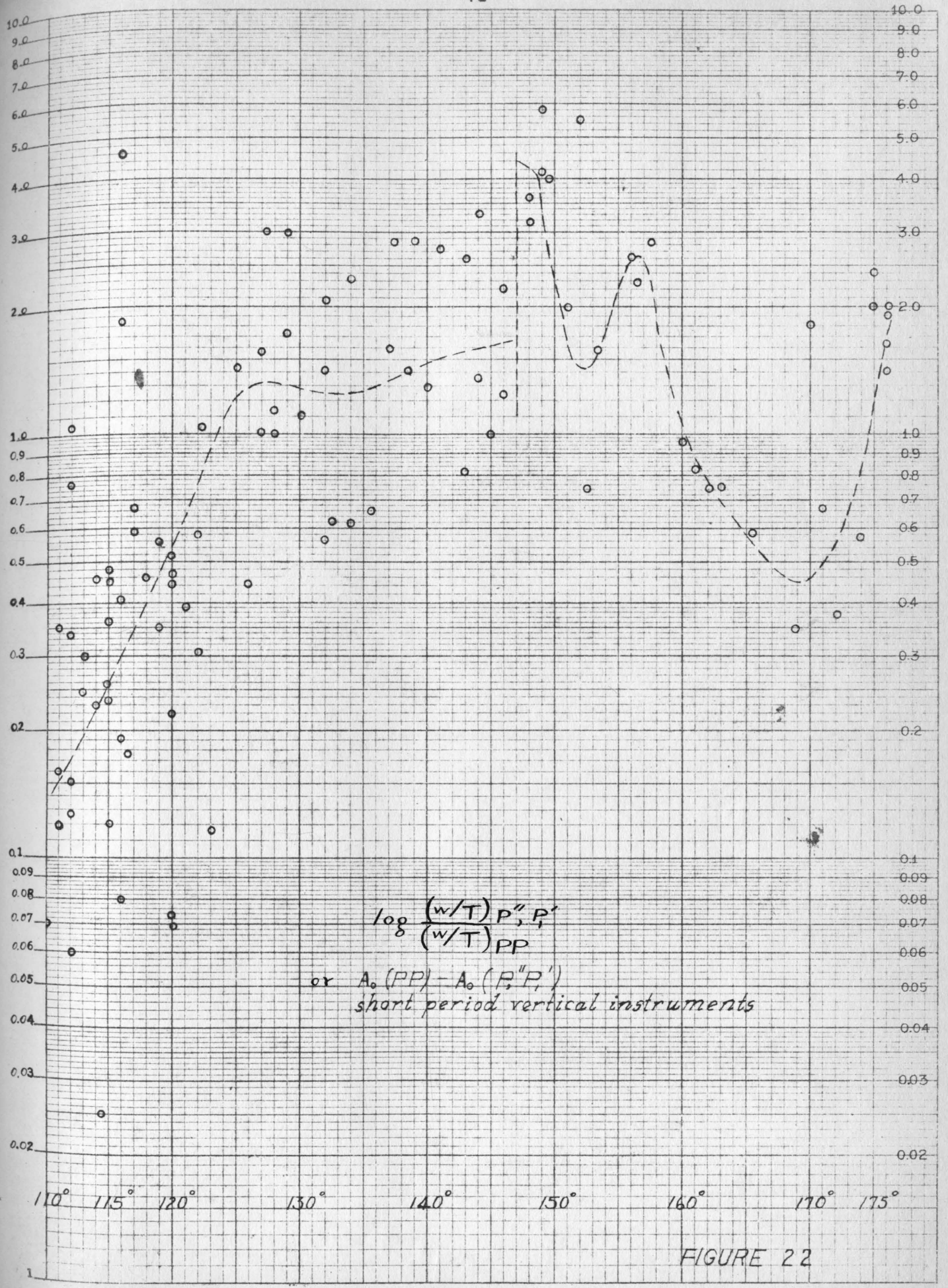
10.0
9.0
8.0
7.0
6.0
5.0
4.0
3.0
2.0
1.0
0.9
0.8
0.7
0.6
0.5
0.4
0.3
0.2
0.1
0.09
0.08
0.07
0.06
0.05
0.04
0.03
0.02
110°
115°
120°
130°
140°
150°
160°
170°
175°
$\log \frac{(w/T)_{P'', P_1'}}{(w/T)_{PP}}$
or $A_0(PP) - A_0(P_1'' P_1')$
short period vertical instruments

FIGURE 22

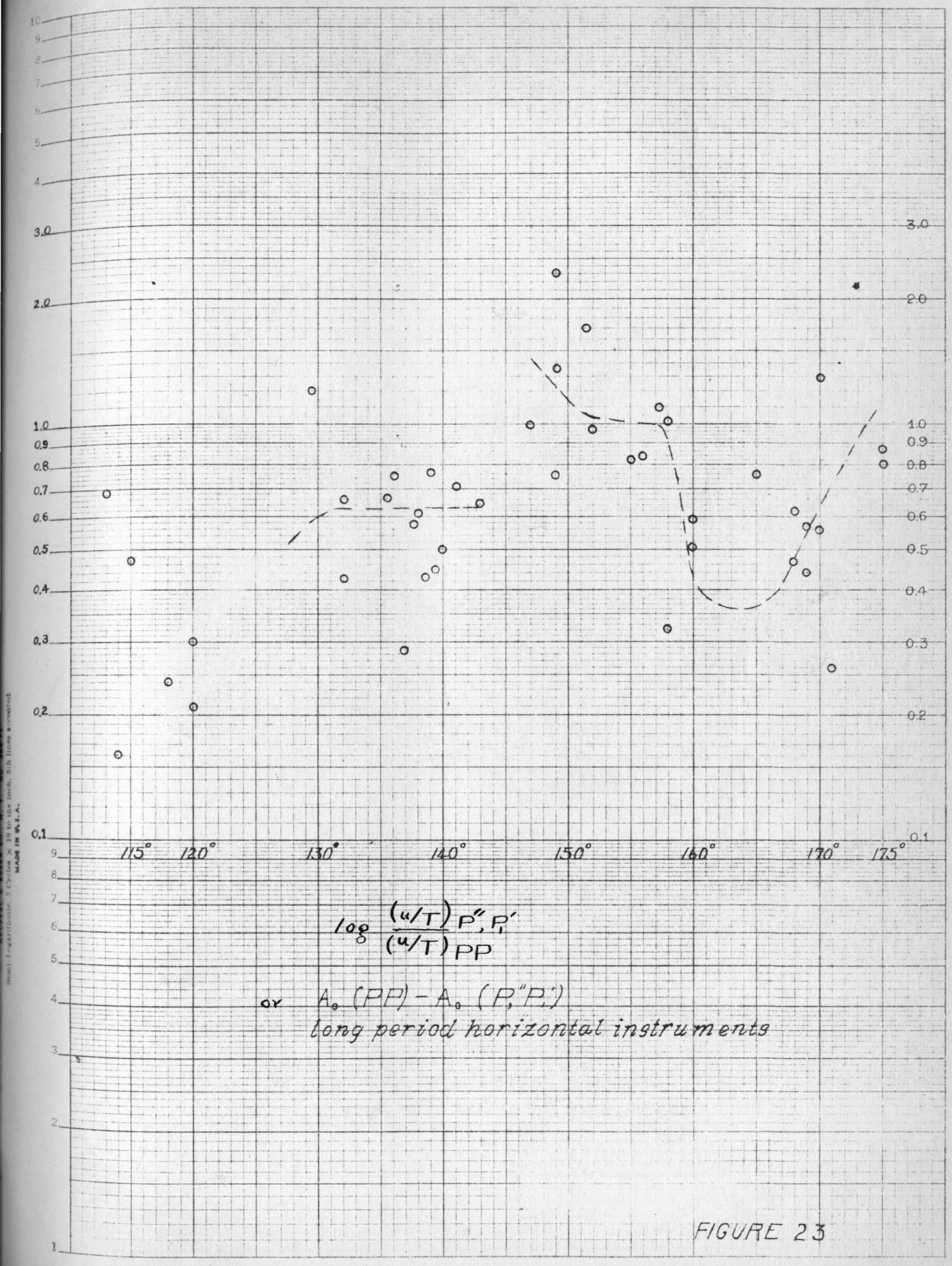
10
9
8
7
6
5
4
3.0
2.0
1.0
0.9
0.8
0.7
0.6
0.5
0.4
0.3
0.2
0.1
115°
120°
130°
140°
150°
160°
170°
175°
3.0
2.0
1.0
0.9
0.8
0.7
0.6
0.5
0.4
0.3
0.2
0.1
9
8
7
6
5
4
3
2
1
log (u/T) P'', P1' / (u/T) PP
or A0 (PP) − A0 (P1''P1')
long period horizontal instruments

FIGURE 23

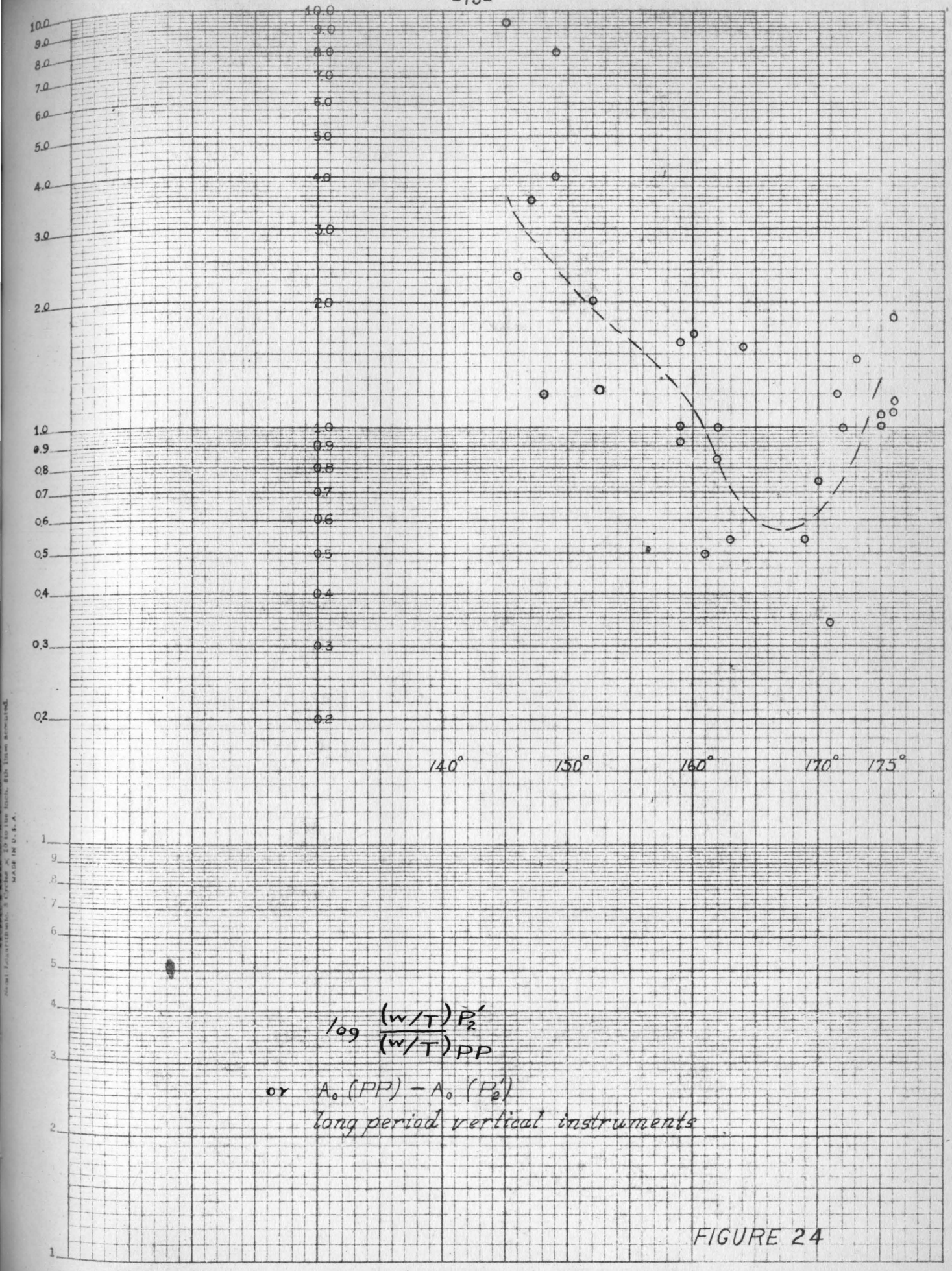

$$\log \frac{(w/T)\,P_2'}{(w/T)_{PP}}$$

or $A_0(PP) - A_0(P_2')$

long period vertical instruments

FIGURE 24

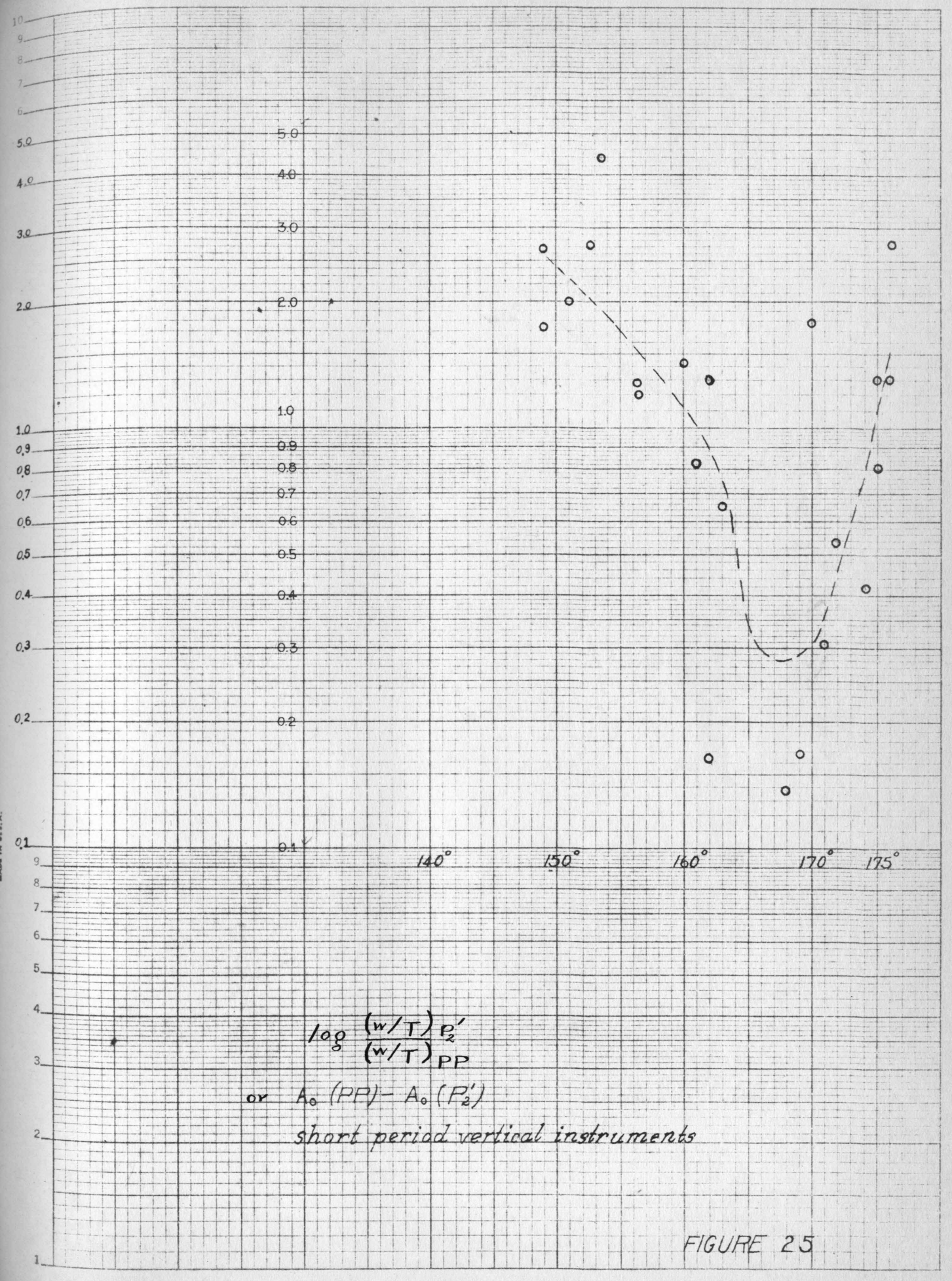

$$\log \frac{(w/T)P_2'}{(w/T)_{PP}}$$

or $A_0(PP) - A_0(P_2')$

short period vertical instruments

FIGURE 25

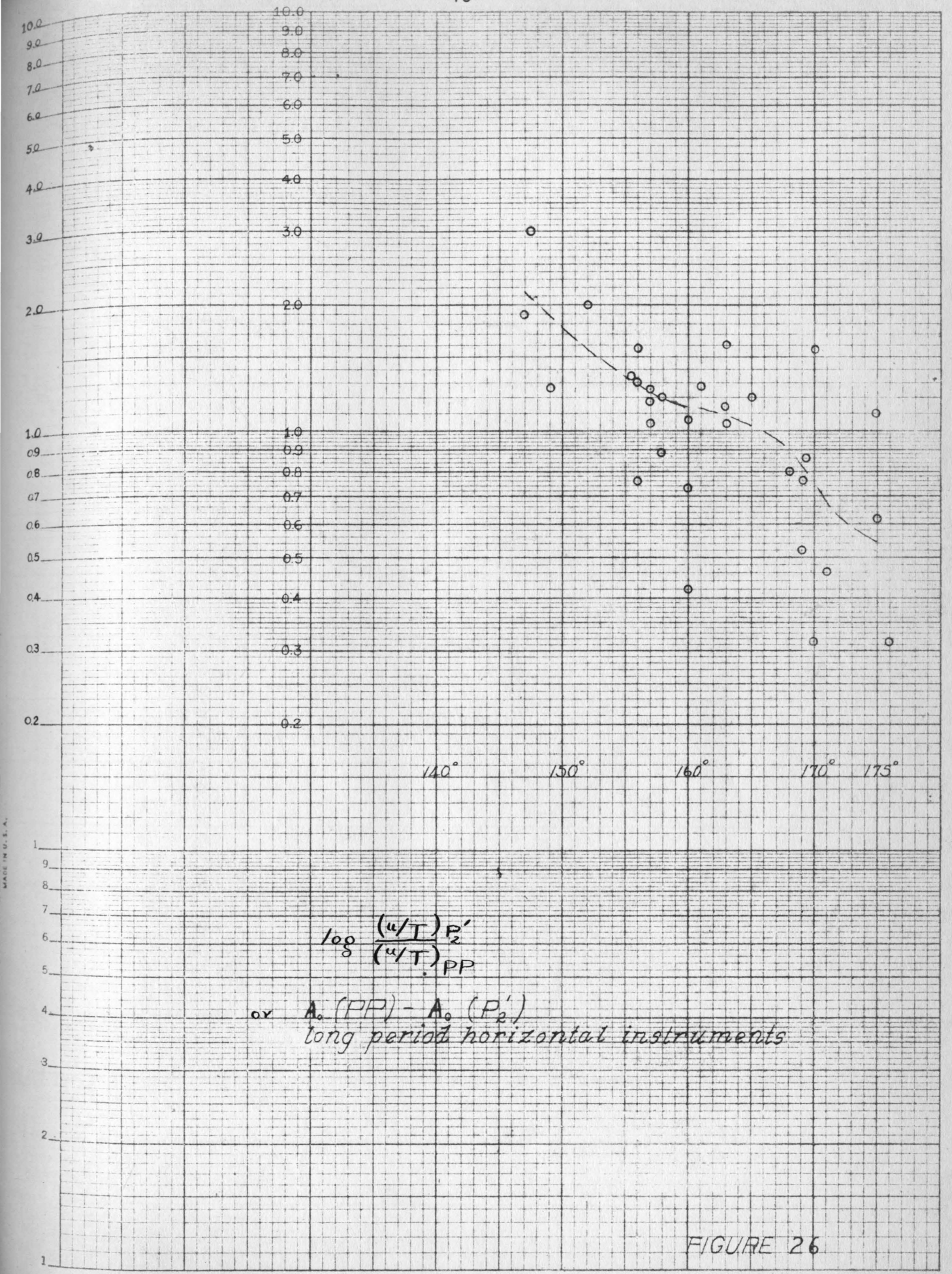
10.0
9.0
8.0
7.0
6.0
5.0
4.0
3.0
2.0
1.0
0.9
0.8
0.7
0.6
0.5
0.4
0.3
0.2
140°
150°
160°
170°
175°
$\log \frac{(u/T)_{P_2'}}{(u/T)_{PP}}$
or $A_0(PP) - A_0(P_2')$
long period horizontal instruments

FIGURE 26

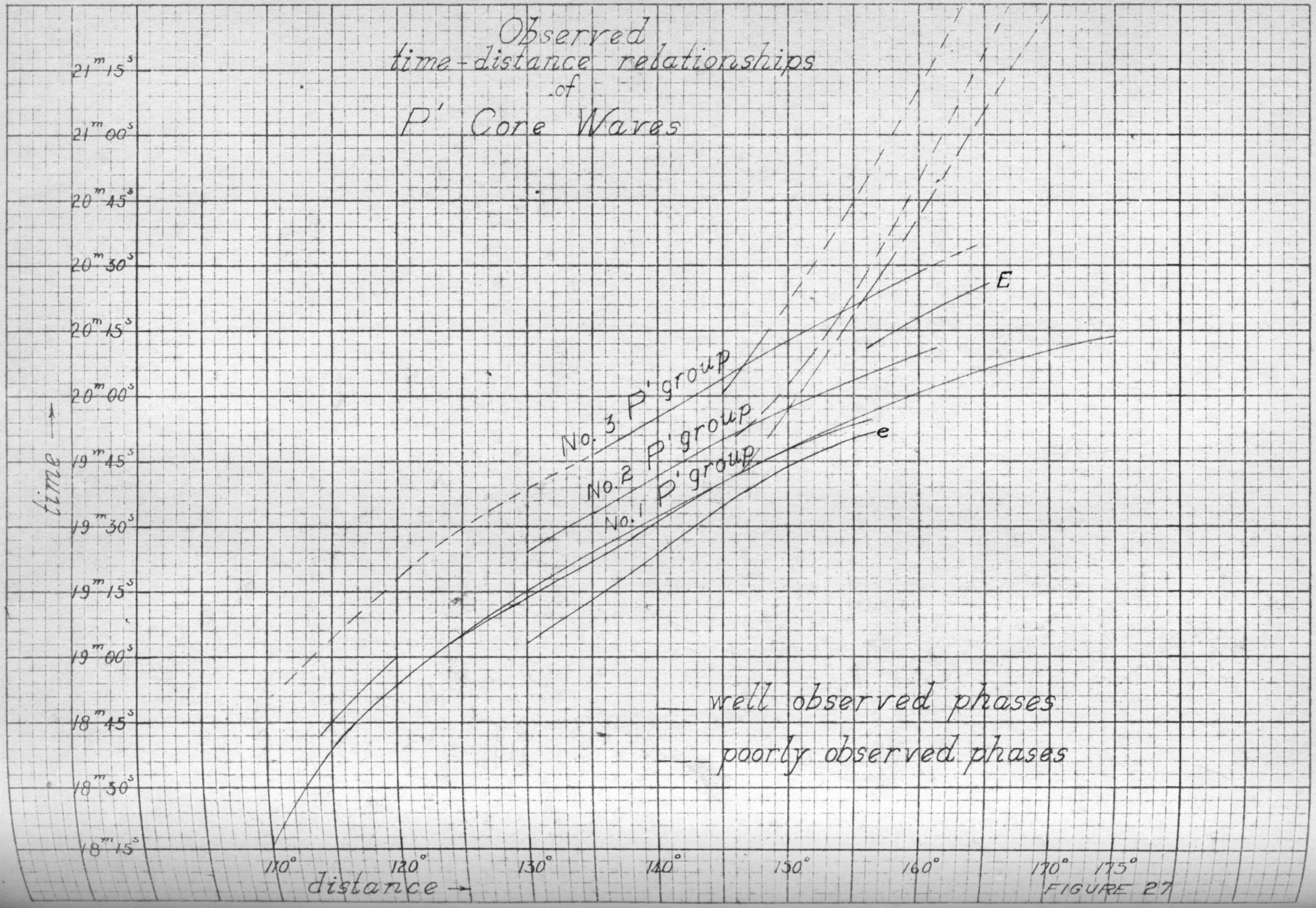

FIGURE 27

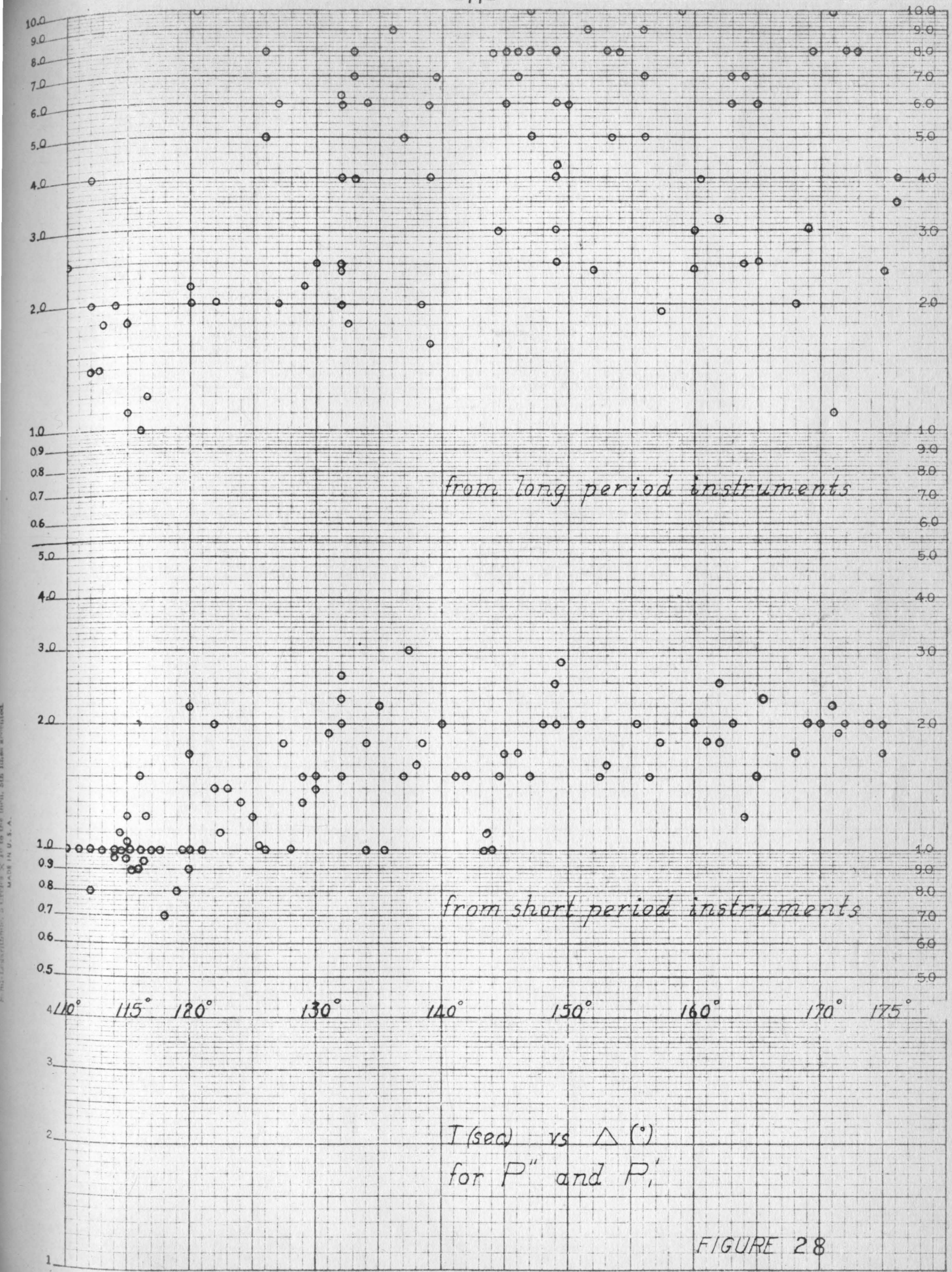

T (sec) vs △ (°)
for P" and P,'

FIGURE 28

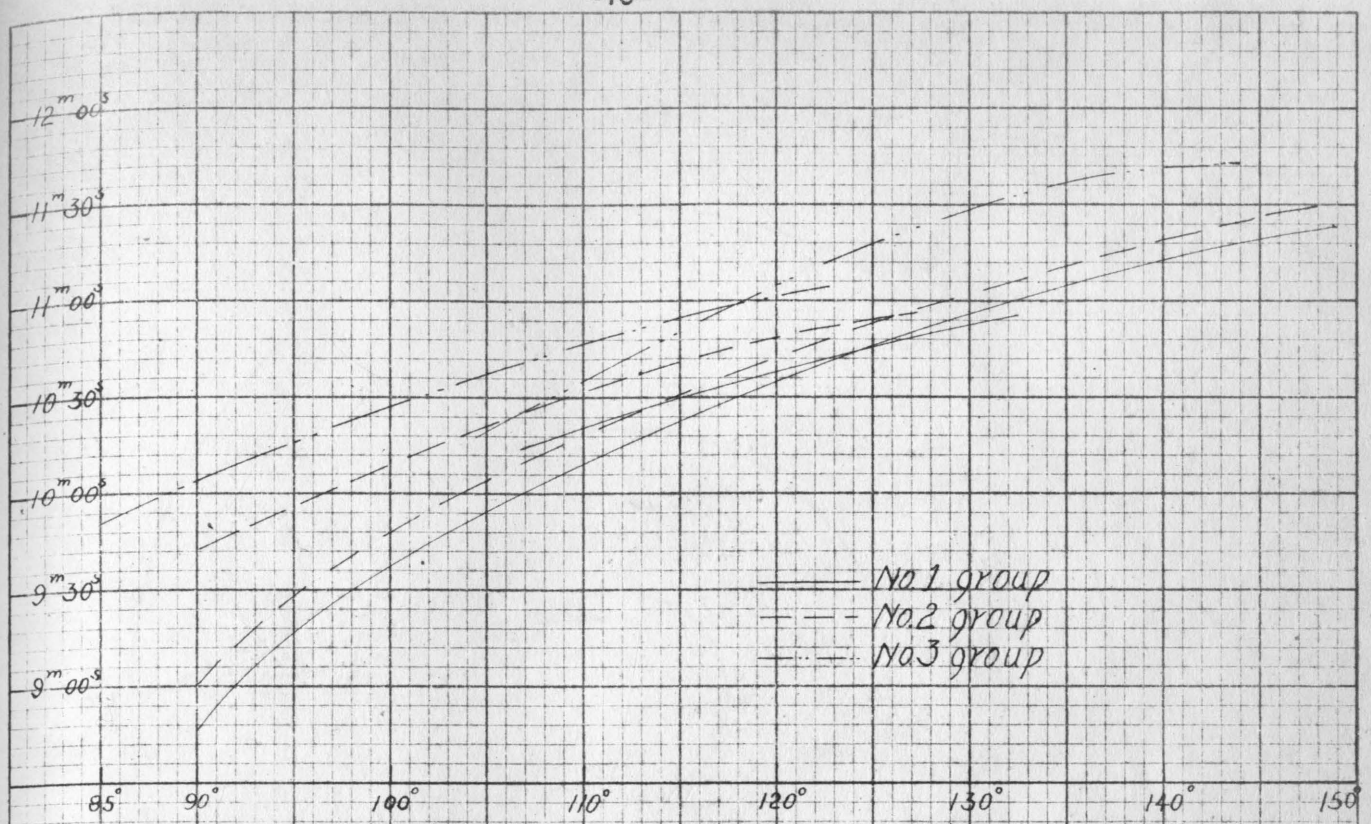

Fig. 29. Travel times of P waves within the core as calculated from unsmoothed observed data (between 120° and 165°)

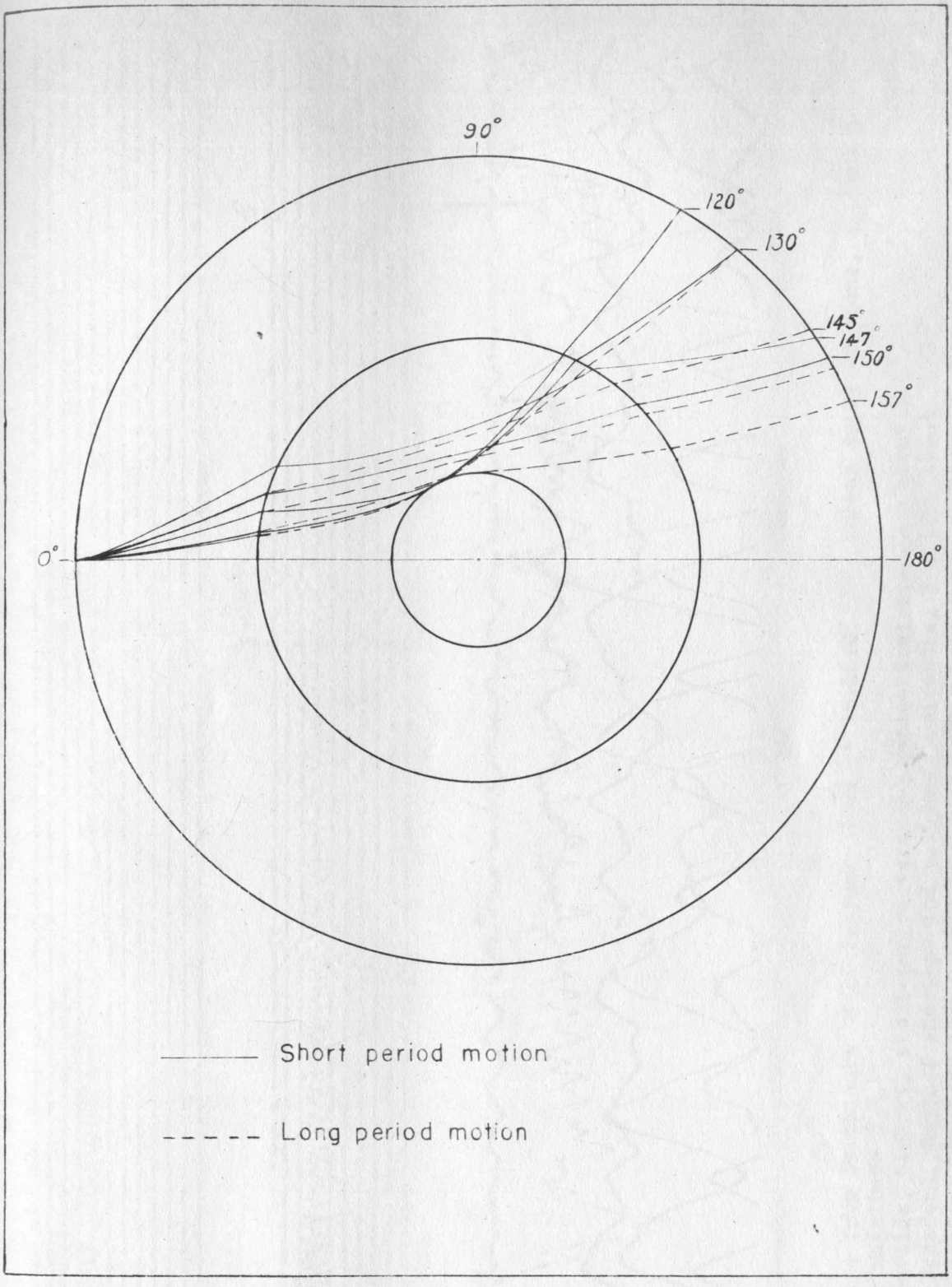

Fig.30. Path relationships of P' phases as suggested by travel time data.

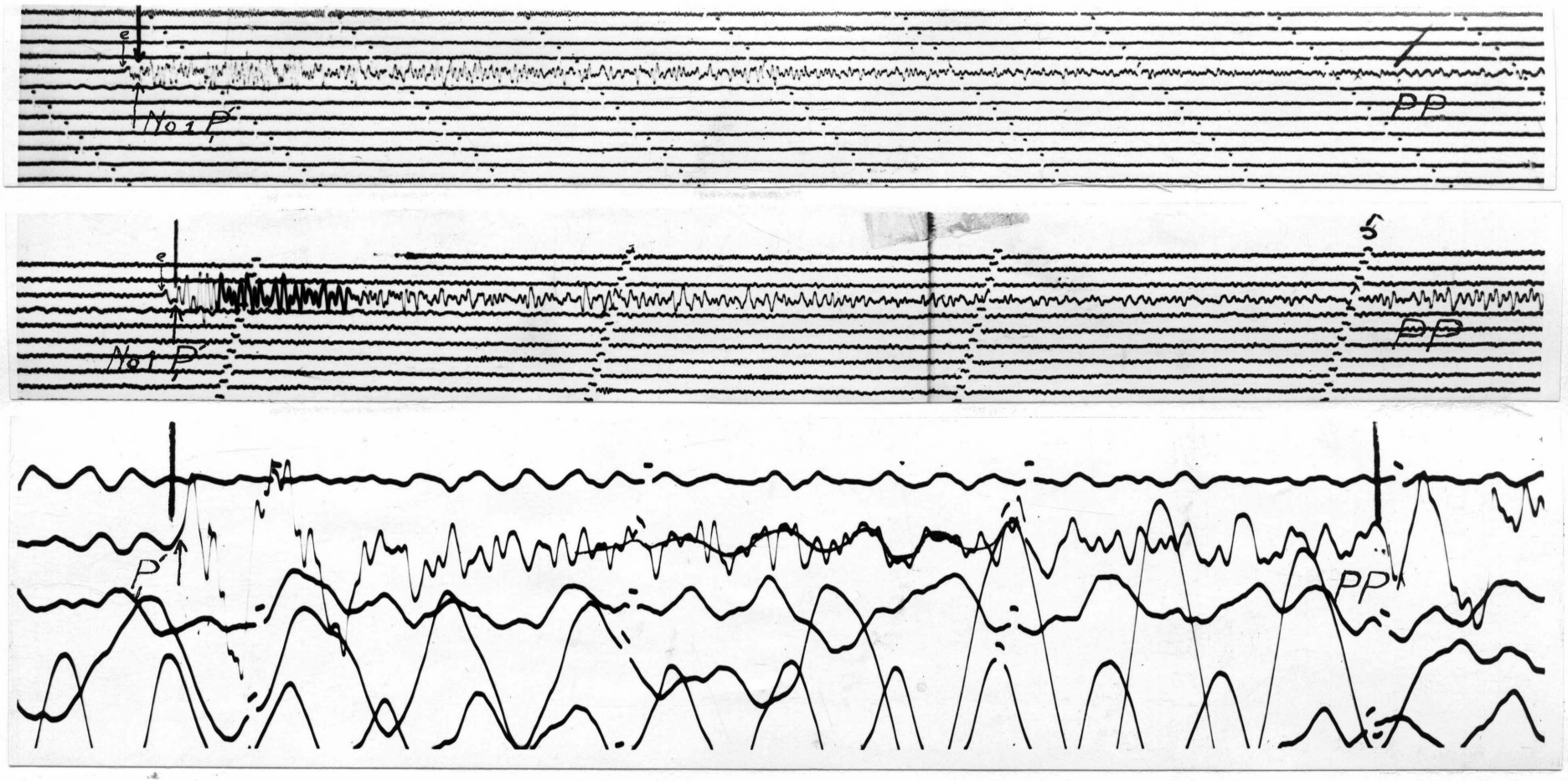

Plate I: Seismograms from earthquake of 29 February 1944 at 16:28:07 GCT, normal depth of focus, epicentre ½ N 76 E; magnitude 7.2.
Top: Riverside, Benioff, short-period vertical, epicentral distance about 144°.
Center: Pasadena, Benioff short-period vertical, epicentral distance about 143½°.
Bottom: Pasadena, Benioff long-period vertical, epicentral distance about 143½°.

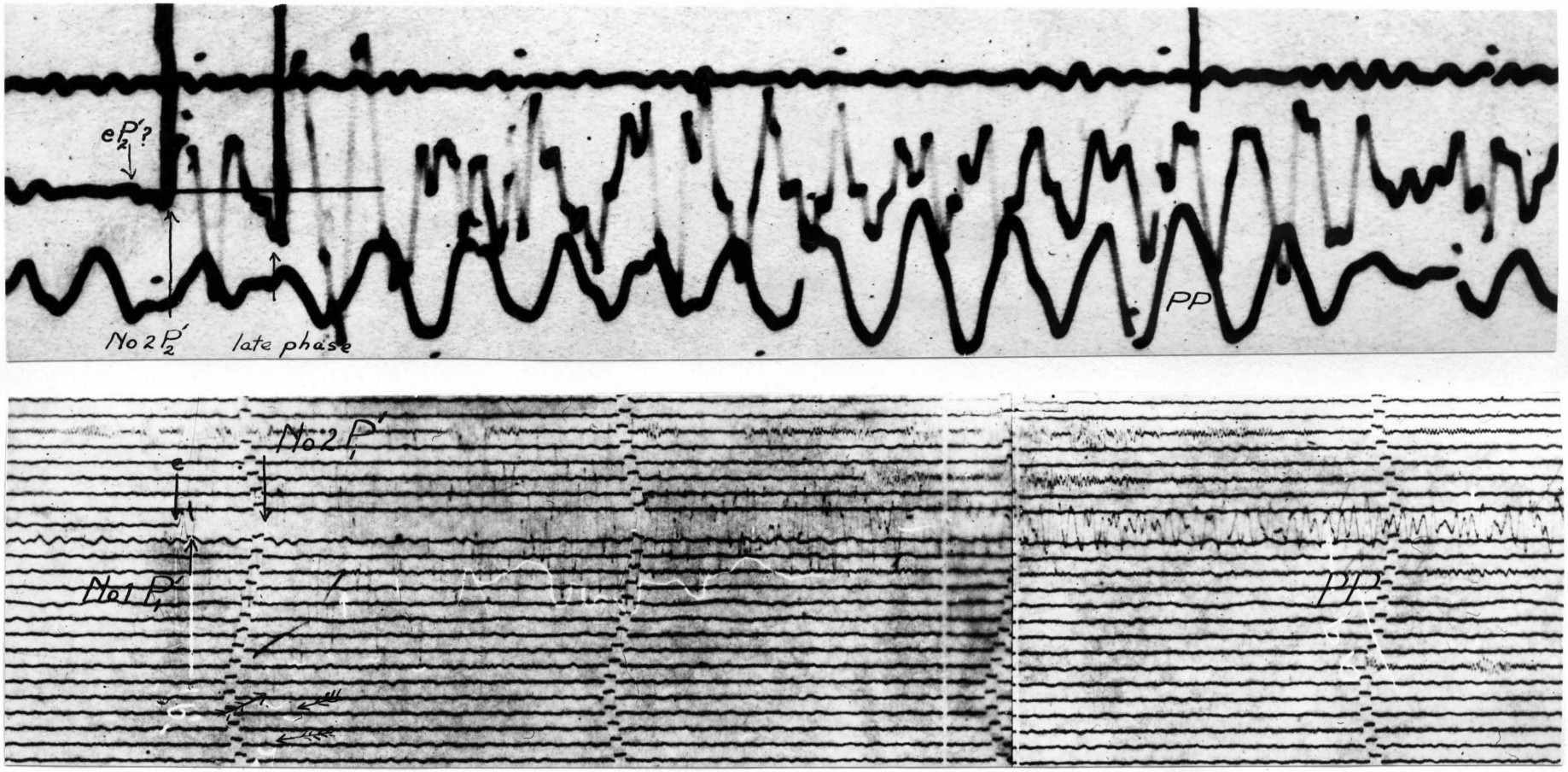

Plate II: Seismograms showing different phases in focal zone.
Top: Huancayo, long-period horizontal (EW component) seismogram from earthquake of 12 April 1936 at 20:51:00, normal depth of focus, epicentre 8 N 137½ E, magnitude 6 3/4, epicentral distance about 147°.
Bottom: Tucson photostat reproduction; same earthquake as described on Plate I; Benioff short-period vertical at about 147° epicentral distance registers abnormally high amplitudes (arrows).

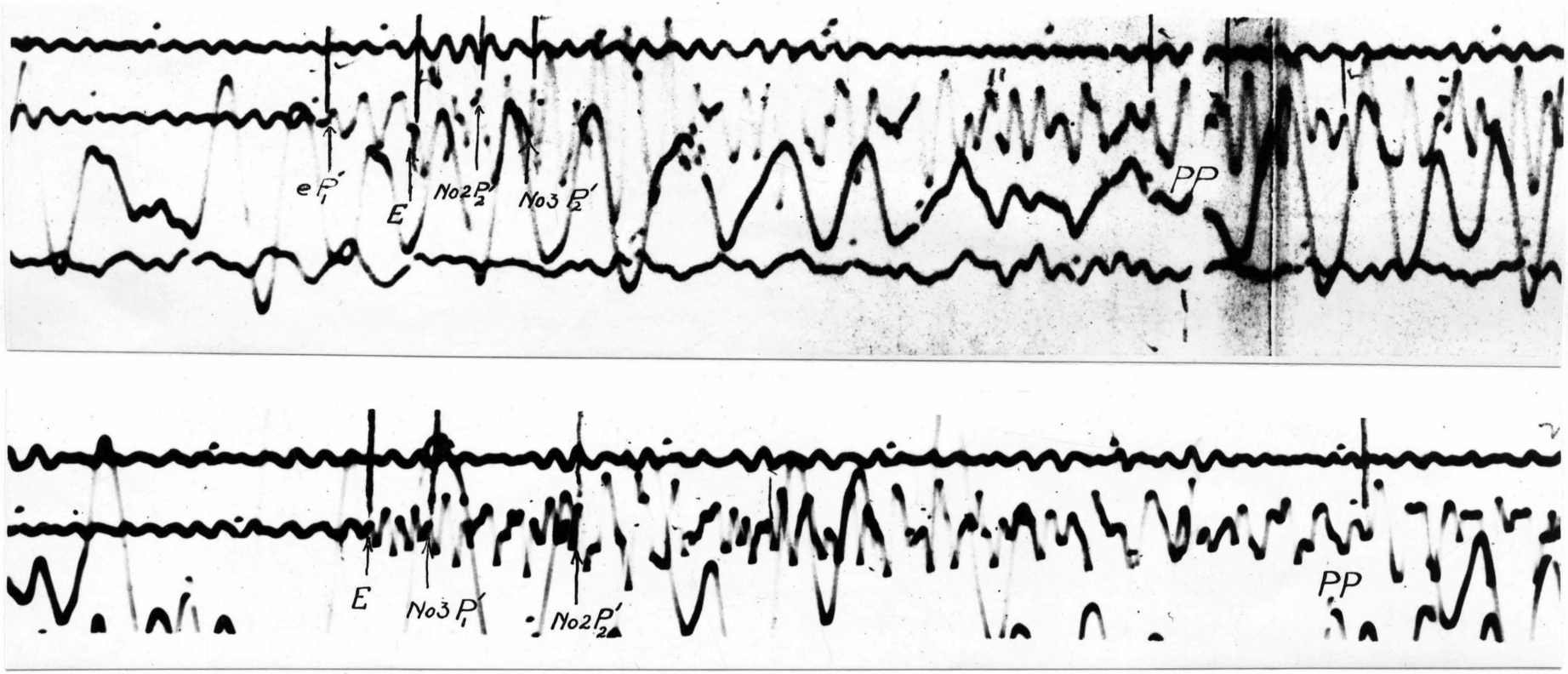

Plate III: Huancayo seismograms showing different phases on EW long-period horizontal components.
Top: 10 October 1938 at 20:48:05, normal depth of focus, epicentre $2\frac{1}{4}$ N 126 3/4 E, magnitude 7.3; epicentral distance about 156°.
Bottom: 20 August 1937 at 11:59:16, normal depth of focus, epicentre $14\frac{1}{2}$ N $121\frac{1}{2}$ E, magnitude 7.5; epicentral distance about 163°.

REFERENCES

Benioff, H. (1932) "A New Vertical Seismograph," Seis. Soc. Amer., Bull., Vol. 22, pp 155-169.

Bullen, K. E. (1947) An Introduction to the Theory of Seismology, Camb. Univ. Press.

Dana, S. W. (1944) "The Partition of Energy Among Seismic Waves Reflected and Refracted at the Earth's Core," Seis. Soc. Amer., Bull., Vol. 34, No. 4, pp 189-197.

Gutenberg, B. (1914) "Uber Erdbebenwellen," VIIA. Nachr. Ges. Wiss. Gottingen, math-phys. Kl., p 1.

(1925) "Bearbeitung der Aufzeichnungen einiger Weltbeben." Abh. der Senckenberg. Naturforsch. Ges., Vol. 40, p 57.

(1944) "Energy Ratio of Reflected and Refracted Seismic Waves," Seis. Soc. Amer., Bull., Vol. 34, No. 2, pp 85-102.

(1945a) "Amplitudes of P, PP, and S and Magnitudes of Shallow Earthquakes," Seis. Soc. Amer., Bull., Vol. 35, No. 2, pp 57-69.

(1945b) "Magnitude Determination for Deep-Focus Earthquakes," Seis. Soc. Amer., Bull., Vol. 35, No. 3, pp 117-130.

Gutenberg, B. and Richter, C. F. (1934) "On Seismic Waves" (first paper), Gerl. Beitr. Geophys., Vol. 43, pp 56-133.

(1938) "P' and the Earth's Core," Monthly Notices Roy.Ast.Soc., Geophys. Suppl., Vol. 4, No. 5, pp 363-372.

(1939) "On Seismic Waves" (fourth paper), Gerl. Beitr. Geophys., Vol. 54, pp 94-136.

(1942) "Earthquake Magnitude, Intensity, Energy, and Acceleration," Seis. Soc. Amer., Bull., Vol. 32, No. 3, pp 163-191.

(1949) Seismicity of the Earth, Princeton Univ. Press.

Jeffreys, H. (1926) "The Rigidity of the Earth's Central Core," Monthly Notices, Roy. Ast. Soc., Geophys. Suppl., Vol. 1, p 371.

(1939a) "The Times of Core Waves," Monthly Notices, Roy. Ast. Soc., Vol. 4, No. 7, pp 548-561.

(1939b) "The Times of Core Waves" (second paper), Monthly Notices, Roy. Ast. Soc., Vol. 4, No. 8, pp 594-615.

Jeffreys, H. and B. S. (1946) Methods of Mathematical Physics, Camb. Univ. Press.

Jeffreys, H. and Bullen, K. E. (1940) "Seismological Tables," British Assoc. Adv. Sci., London.

Knott, C. G. (1899) "Reflexion and Refraction of Elastic Waves, with Seismological Applications," Phil. Mag., 5th ser., pp 64-97.

(1919) "The Propagation of Earthquake Waves through the Earth, and Connected Problems," Proc. Roy. Soc. Edinburgh, Vol. 39, pp 157-208.

Lehmann, I. (1937) "P'," Publications du Bureau central seismologique international, Serie A: Travaux scientifiques, fasc. 14, pp 87-115.

Macelwane, J. B. (1925) "New evidence for a sharply rounded and very rigid core in the earth," Phys. Review, Vol. 25, p 721.

(1930) "The South Pacific Earthquake of June 26, 1924," Gerl. Beitr. Geophys., Vol. 28, pp 165-228.

(1936) Introduction to Theoretical Seismology, Part I, Geodynamics, John Wiley and Sons, Inc., New York.

Martner, S. T. (1948) "Observation on Seismic Waves Reflected at the Core Boundary of the Earth," Unpublished thesis, Calif. Inst. of Technology, Pasadena, Calif.

Mooney, H. M. (1950) "A Study of the Seismic Waves P and pP," Unpublished thesis, Calif. Inst. of Technology, Pasadena, Calif.

Munk, W. H. (1947) "Increase in the Period of Waves Traveling over large Distances: with Applications to Tsunamis, Swell, and Seismic Surface Waves," Trans. Amer. Geophys. Un., Vol. 28, No. 2, pp 198-217.

Oldham, R. D. (1906) "The Constitution of the Interior of the Earth, as revealed by Earthquakes," Quarterly Jour. Geol. Soc. London, Vol. 62, pp 456-475.

Richter, C. F. (1935) "An Instrumental Earthquake Magnitude Scale," Seis. Soc. Amer., Bull., Vol. 25, No. 1, pp 1-32.

Stoneley, R. (1949) "The Seismological Implications of Aeolotropy in Continental Structure," Monthly Notices, Roy. Ast. Soc., Geophys. Suppl., Vol. 5, No. 8, pp 343-353.

Zoeppritz, K. (1919) "Uber Erdbebenwellen," Nachr. Ges. Wiss. Gottingen, math-phys., VIIb, p 57.

Zoeppritz, K., Geiger, L., and Gutenberg, B. (1912) "Uber Erdbebenwellen," V, Nachr. Gesell, d. Wiss. Gottingen, math-phys. Kl., pp 121-206.

APPENDIX OF MATERIAL USED

Following is a list of the earthquakes which have been used for this study. These are listed in chronological order and are presented by serial numbers as given by Gutenberg and Richter in Tables 17 and 18 of Seismicity Of The Earth, 1949. An asterisk following the serial number denotes that the earthquake is listed in Table 18; no asterisk denotes that the earthquake is listed in Table 17. Earthquakes occurring from 1946 on are not listed in Seismicity Of The Earth; dates, origin times, locations, depths, and magnitudes for earthquakes during these years are taken from files at the Seismological Laboratory, Pasadena.

In listing stations the following abbreviations are used: P for Pasadena, H for Huancayo, J for Jena, T for Tucson, A for La Paz and V for Victoria. Station components and epicentral distances are given in the following manner:

76. 280-24: PSBZE, LBNE - 129½; HNE - 158; TZ - 135.

From earthquake number 280, region 24, table 17, readings were obtained at Pasadena, 129½°, from short-period Benioff vertical and east-west (SBZE) instruments, from long-period Benioff north-south and east-west (LBNE) instruments; at Huancayo, 158°, from north-south and east-west (NE) instruments--all of which are long-period instruments. All Tucson readings are from short-period Benioff instruments, all Jena and La Paz readings are from long-period instruments.

1927-1932

1. 560-33: PSBN - 175½.
2. 880-33: PSBN - 140.
3. 220-14: JNEZ - 151½.
4. 890-8: JZ - 112.
5. 630-11: JNEZ - 171.
6. 840-11: JNEZ - 165.
7. 845-11: JNEZ - 165.
8. 730-47: PLBZ - 116½.
9. 390-24: PSBZ - 132½.
10. 100-15: JZ - 133.
11. 465-23: PSLBZ - 111.
12. 225-23: HNE - 161.
13. 370-27: HNE - 152.

1933

14. 400-33: PSLBZ - 176; HNE - 115.
15. 210-19: HNE - 136.
16. 131-22: HNE - 157.
17. 750-24: PSLBZ - 128.
18. 150-19: HNE - 137.
19. 380-24: HNE - 163.
20. 500-33: PSLBZ - 176.

1933 cont'd

21. 70-26: HNE - 160.

22. 580-10: PSBZN, LBZ - 120.

23. 460-27: HNE - 149.

1934

24. 695-26: HNE-158; PSLBZ - 116.

25. 640-22: HNE - 165.

26. 260-18: HNE - 141.

27. 20-16: HNE - 117.

28. 140-15: HNE - 119½; JZ - 139.

29. 200-22: HNE - 157½.

30. 400-29*: HNE - 138; PSLBZ - 117.

1935

31. 675-26: HNE - 156.

32. 200-33: PSLBZ - 144.

33. 400-22: HNE - 160.

34. 870-47: PSLBZ - 116.

35. 180-24: PSLBZ - 120.

36. 640-10: PSLBZ - 120½.

37. 700-24: PSLBZ - 130; HNE - 169.

38. 550-10: PSBZ - 122½.

39. 360-19: HNE - 132.

1935 cont'd

40. 170-16: JZ - 117½; HNE - 139.

41. 460-17: HNE - 144.

42. 200-15: JNEZ - 139½.

43. 560-24: PSBZE, LBZ - 132.

1936

44. 195-24: PSBZE, LBZ - 122½.

45. 510-24: PSBZE, LBZ - 131½.

46. 540-10: PSBZE, LBZ - 122.

47. 750-16: HNE - 147.

48. 255-24: PSBZ - 124.

49. 965-33: PSBZE - 152.

50. 50-23: HNE - 157.

51. 150-17: HNE - 147.

52. 525-24*: PSBZE, LBZ - 129.

53. 320-15: JZ - 135½.

54. 850-24: PSBZE - 127.

55. 750-24*: PSBZE - 126.

56. 760-24*: PSBZE, LBZ - 126.

57. 730-26: PSLBZ - 114½; HNE - 154.

58. 520-19: HNE - 120.

59. 200-21: HNE - 160.

1936 cont'd

60. 215-33: PSBZNE, LBZ - 149.

61. 720-24: PSBZNE, LBZ - 130½; HNE - 169.

62. 250-10*: PSBZE - 117½.

63. 650-24: PSBZE, LBZ - 129; HNE - 169.

64. 360-23: PSBZE, LBZ - 110; HNE - 155½.

65. 140-19: HNE - 138.

66. 640-19: HNE - 118.

1937

67. 250-27: HNE - 156.

68. 60-15: JNEZ - 139½.

69. 950-16*: HNE - 148.

70. 630-24*: PSBZE - 123; TZ - 129.

71. 365-33: PSBZE, LBZN - 170; TZ - 174.

72. 590-22: HNE - 163.

73. 200-10*: PSBZE, LBZN - 118; TZ - 113.

74. 360-10: PSLBZ - 119.

75. 440-15: HNE - 127.

76. 280-24: PSBZE, LBNE - 129½; HNE - 158; TZ - 135.

77. 122-48*: PSBZ - 109.

78. 450-37: PSBZ - 134.

1938

79. 720-24*: PSBZ - 133.

80. 720-10: PSBZ - 114.

81. 40-24: PSBZ - 111.

82. 970-33: PSLBZNE - 149; TZ - 152½.

83. 80-16: JNE - 133; AZ - 137.

84. 585-23: PSBZNE, LBZN - 116½; TZ - 122; AZ - 161.

85. 68-19: AZ - 147.

86. 870-23: PSLBZ - 113; TZ - 117.

87. 120-20: AZ - 160.

88. 710-37: PSLBZ - 143; TZ - 140½.

89. 640-25: HNE - 163; AZ - 163.

90. 690-24*: PSBZ - 132; TZ - 139.

91. 240-23: HNE - 156.

92. 420-24*: PSLBNE - 118½; TZ - 122½.

93. 185-33: PSBZ - 143; TZ - 145.

94. 720-37: PSBZ - 155; TZ - 151.

1939

95. 340-15: JNEZ - 127.

96. 200-16*: AZ - 138½.

97. 220-15: JZ - 132; AZ - 126.

98. 865-33: PSLBZNE - 138½; TZ - 144½; AZ - 152.

1939 cont'd

99. 240-15: HNE - 122; JNEZ - 132.

100. 970-19: AZ - 146.

101. 275-18: AZ - 149.

102. 220-16: AZ - 145.

103. 310-33: PSBZ - 161.

104. 160-19: AZ - 144⅓.

1940

105. 180-14*: AZ - 113.

106. 140-18*: HNE - 138; AZ - 147.

107. 610-14*: AZ - 125.

108. 925-33: PSLBZ - 165½.

109. 180-16: AZ - 145.

110. 675-45: PSLBZ - 121.

111. 320-24: PSLBZNE - 132; AZ - 156.

112. 690-22*: AZ - 172.

113. 250-16: AZ - 146; HNE - 143.

114. 60-1: AZ - 120½.

115. 310-24: PSLBZ, SBNE - 131½; AZ - 154.

116. 730-37: PSLBZ, SBNE - 152.

117. 260-16: AZ - 147.

118. 120-24: PSBZ - 117; AZ - 153.

1940 cont'd

119. 570-23*: AZ - 160.

120. 210-46*: AZ - 148.

121. 195-23: TZ - 121.

122. 990-19: AZ - 144.

123. 700-20: AZ - 153⅓.

124. 500-15: AZ - 138.

125. 75-45: PSLBZ - 116.

126. 60-22*: PSBZ - 108⅓.

127. 780-24: PSBZ - 128.

128. 10-24: PSLBZ - 111.

129. 310-16: AZ - 149.

130. 600-37: PSLBZ - 146.

131. 240-18*: AZ - 148.

1941

132. 250-23*: PSLBZ , SBNE - 112.

133. 135-24: PSLBZ - 118.

134. 270-23: PSLBZNE - 113.

135. 640-23*: PSLBZ, SBNE - 113.

136. 60-37: PSBZN - 126.

137. 550-15: AZ - 134.

138. 600-26*: PSBZ - 113.

139. 500-26*: PSLBZ - 113.

1941 cont'd

140. 200-24*: PSLBZ - 112.

141. 405-23: AZ - 162.

142. 345-24*: AZ - 156; PSLBZ - 118.

143. 765-24*: PSLBZ - 132½.

144. 540-24*: PSBZ - 121.

145. 200-38: PSLBZNE - 132.

146. 350-38: PSBZ - 116.

147. 720-25: PSLBZ - 112.

148. 985-14: AZ - 122½.

149. 540-23: PSBZ - 112.

150. 555-23: PSLBZ - 112.

151. 655-23: PSLBZNE - 116.

152. 890-24: PSLBZNE - 126; TZ - 130.

153. 400-38: PSBZ - 116.

154. 325-33: PSLBZ - 162.

155. 885-24: PSBZ - 125½.

156. 440-16: AZ - 154.

157. 750-23*: PSLBZNE - 116.

158. 640-33: PSBZ - 156½.

159. 440-22: AZ - 171½.

160. 450-23: AZ - 164; PSLBZNE - 114.

161. 300-10*: PSLBNE, LBZ - 118½.

1941 cont'd

162. 540-20: AZ - 159.

163. 610-33: PSLBZNE - 168.

164. 420-24*: AZ - (166); TZ - 125; PSLBZNE - 125.

165. 860-23: PSLBZ - 117.

166. 50-21: AZ - 172.

167. 520-25: PSLBZ - 114.

1942

168. 700-16: AZ - 149.

169. 135-19: AZ - 146.

170. 510-22: PSLBZ, LBE - 107; TZ - 112.

171. 730-24: PSLBZ - 130.

172. 720-23*: PSLBZ, SBNE - 113; TZ - 120; AZ - 160.

173. 30-32: PSLBZ - 129.

174. 80-18*: AZ - 123.

175. 480-17: AZ - 151.

176. 765-23: PSLBZ - 110; TZ - 118; AZ - 156.

177. 975-33: PSLBZNE - 148; TZ - 152½.

178. 580-37: PSLBZNE - 140; TZ - 142.

179. 250-22: PSLBZ - 108.

180. 455-19: AZ - 122.

181. 405-24*: PSBZNE, LBZ - 118; TZ - 124; AZ - 153.

1942 cont'd

182. 720-33: PSLBZNE - 152½; TZ - 148.

183. 95-19: AZ - 147.

184. 640-19*: AZ - 141.

185. 640-18: AZ - 149.

186. 130-30: AZ - 108.

1943

187. 50-29: PSBZE, LBZ - 122; TZ - 120.

188. 190-48*: PSBZE, LBZ - 109.

189. 680-10: PSLBZNE - 120; TZ - 115.

190. 580-15: AZ - 126½.

191. 685-10: PSLBZ - 120.

192. 725-37: PSLBZ, LBNE - 157.

193. 360-24: PSLBZ - 132; AZ - 156.

194. 340-18*: AZ - 150.

195. 470-22: AZ - 173.

196. 190-22: AZ - 166.

197. 450-24: PSLBZNE - 132; AZ - 168.

198. 451-24: PSLBZNE - 132; AZ - 168.

199. 355-19: AZ - 145½.

200. 375-33: PSLBZN, SBE - 175; TZ - 171½.

201. 240-23*: AZ - 163½.

1943 cont'd

202. 360-24*: PSLBZNE - 119; TZ - 126.

203. 540-24*: PSLBZNE - 130; TZ - 137½; AZ - 154.

204. 120-11: PSBZNE, LBZ - 112; TZ - 114.

205. 640-20: AZ - 154.

206. 240-14: AZ - 111.

207. 600-48*: TZ - 112½.

208. 605-33: PSLBZN - 169; TZ - 163½.

209. 450-26: PSLBZNE - 113; TZ - 117; AZ - 160½.

210. 560-10: TZ - 115.

211. 561-10: TZ - 115.

212. 380-14: AZ - 113.

213. 750-24*: PSLBZNE - 132.

214. 550-16*: AZ - 144.

215. 470-15: AZ - 134½.

1944

216. 430-24: PSLBZ, LBNE - 133; TZ - 138½; AZ - 164½.

217. 850-33: PSLBZN, LBE - 143; TZ - 147.

218. 360-24*: PSLBZN, LBE - 118; TZ - 124; AZ - 153.

219. 420-16: AZ - 154½.

220. 390-16: AZ - 155.

221. 530-15: AZ - 135½.

1944 cont'd

222. 300-12*: AZ - 104½.

223. 390-23: PSLBZN, SBE - 110; TZ - 115; AZ - 161.

224. 305-24: PSLBZ - 130; TZ - 136½.

225. 575-19: AZ - 130.

226. 391-23: AZ - 161.

227. 745-26: TZ - 114.

228. 60-23: TZ - 113; AZ - 143.

229. 820-14: AZ - 113.

230. 80-18: AZ - 148.

231. 360-33: PSLBZNE - 171; TZ - 166.

232. 297-33: PSLBZ - 160; TZ - 162.

233. 110-1: AZ - 113½.

1945

234. 900-19: AZ - 150.

235. 100-19: AZ - 146.

236. 70-22*: AZ - 165.

237. 945-33: PSLBZ - 164.

238. 240-24*: PSLBZNE - 116; TZ - 123.

239. 905-26: PSBZ - 114.

240. 725-24: TZ - 134.

241. 420-19*: AZ - 141.

1945 cont'd

242. 530-23: AZ - 161.

243. 80-29: PSLBZNE - 120; TZ - 123; AZ - 134.

244. 650-15: AZ - 136.

245. 665-15: AZ - 136.

1946

246. 5 Jan. 0=19:57:20 16 S 167 E h = 50 M = 7.3
AZ - 117½.

247. 12 Jan. 20:25:37 59N 147 W n 7.2
AZ - 100.

248. 17 Jan. 09:39:35 7½ S 147½ E 100 7.2
AZ - 141.

249. 26 Mch. 17:09:03 3 S 102 E n 6 3/4
PSBZNE, LBZN - 132½; TZ - 137.

250. 1 Apr. 12:28:54 53 N 164 W n 7.4
AZ - 108½.

251. 11 Apr. 01:52:20 1 S 14½ W n 7.2
PSLBZNE - 101.

252. 3 May 22:23:40 5 S 153 E n 7.4
AZ - 133.

253. 8 May 05:20:22 0 99½ E n 7.1
PSLBZNE - 132; TZ - 137½; AZ - 159.

254. 12 Sept. 15:17:15 23 N 96 E n 7.5
AZ - 163½.

255. 23 Sept. 23:30:00 6 S 145 E (100) 7.2
AZ - 141.

256. 29 Sept. 03:01:55 5 S 154 E n 7 3/4
AZ - 133½.

257. 26 Oct. 00:21:03 60 S 35 W n 6 3/4
PSLBZ - 115.

1946 cont'd

258. 1 Nov. 11:14:24 51 N 174 W 40 7.0
AZ - 112.

259. 2 Nov. 1[illegible]:28:25 41½ N 72½ E n 7.6
PSBZ, LBZNE - 103½; AZ - 139.

260. 4 Nov. 21:47:47 39 3/4 N 54½ E n 7.5
PSBZ, LBZNE - 106; AZ - 127.

1947

261. 17 Mch. 08:19:32 33 N 99½ E n 7.6
PSBZE, LBNE - 105.

262. 2 Apr. 05:39:11 1½ S 138 E n 7.4
PSBZE, LBZNE - 102.

263. 27 May 03:34:54 8½ S 124 E 100 6
PSBZ - 126.

264. 27 May 05:58:54 1½ S 135½ E n 7¼
PSBZE, LBZNE - 105.

265. 12 June 09:02:30 1½ N 126½ E 40 7.2
PSBZE, LBZ - 111.

266. 23 July 17:13:22 55½ S 29 W n 6.5
PSLBZ - 115.

267. 29 July 13:43:22 28½ N 94 E n 7.5
PSLBZ - 112.

268. 23 Sept. 12:28:09 33½ N 59 E n 6 3/4
PSLBZ - 112.

269. 24 Dec. 05:22:00 (55 S 115 E) n 6½
PSBZE, LBZ - 141; TZ - 140.

1949

270. 23 Jan. 06:31:(15) 8 S 95 E (50) (6 3/4)
PSLBZ, LBNE - (140); TZ - (144).

271. 7 Oct. 12:02:(04) 33½ S 58 E n 6 3/4
PSLBZNE - (177); VSBZ - (165).

THE MADISON (MISSISSIPPIAN) LIMESTONE

OF THE

BIGHORN BASIN, WYOMING

Thesis by

Mayette Elner Denson, Jr.

In Partial Fulfillment of the Requirements

for the Degree of

Doctor of Philosophy

California Institute of Technology

Pasadena, California

1950

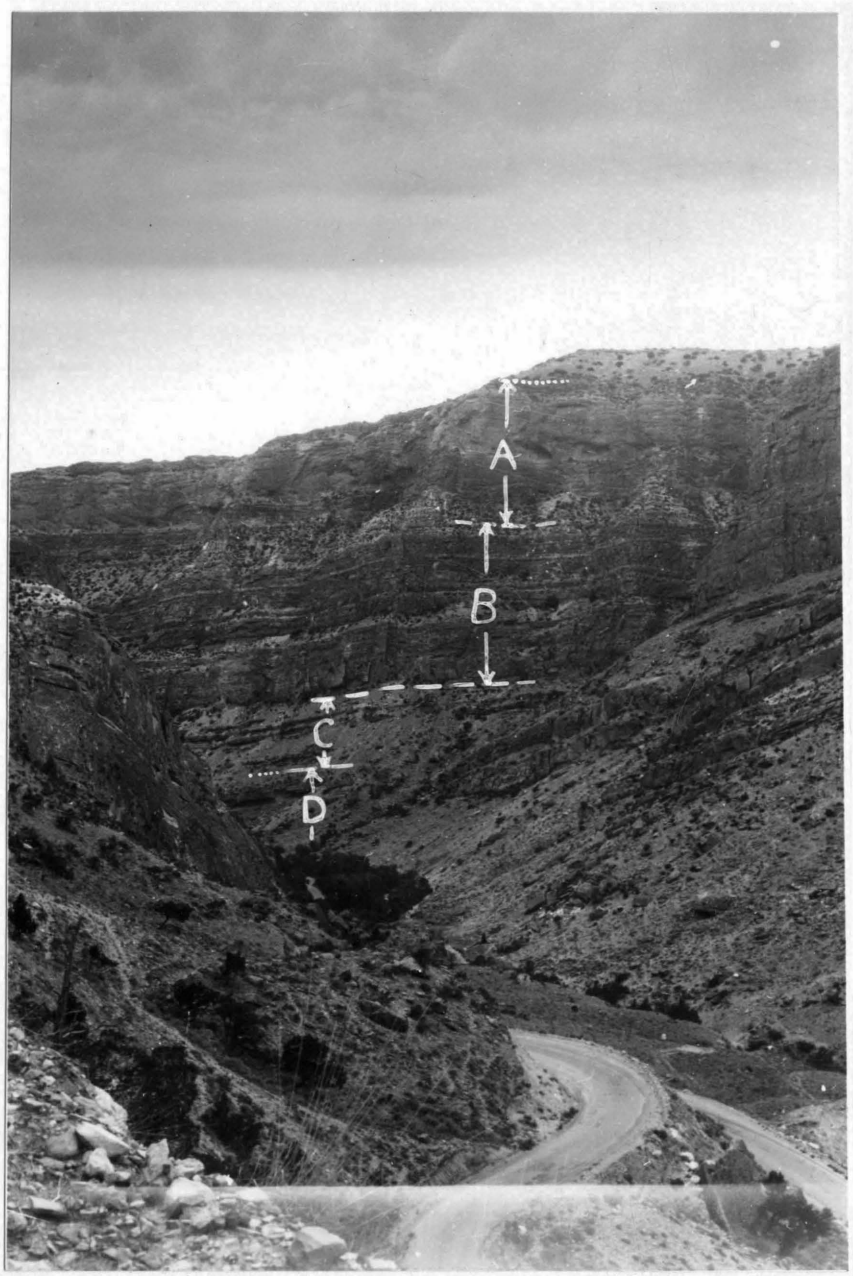

Madison Group, Shell Canyon, Wyoming. View taken from above second switchback looking west; approximate height of cliff 900 feet.
A, Mission Canyon Formation; B, Lodgepole Formation;
C, Upper Devonian? and Kinderhookian; D, Bighorn dolomite.

CONTENTS

PART I

General Relationships

PART II

Descriptive Data

FIGURES

CHARTS

PLATES

PART I

General Relationships

ABSTRACT

The Mission Canyon and Lodgepole formations of the Madison group are recognized throughout the Bighorn Basin, Wyoming. The features by which these formations and their members have been differentiated and correlated are described. Limited paleontologic determinations and lithologic similarities indicate that Kinderhookian and Upper Devonian strata may be present along the eastern margin of the Bighorn Basin. Variations which exist in porosity developments are herein related to solution activities, to the degree of dolomitization, and to the character of the original sediment. Lithology and insoluble residue descriptions are included in Part II.

INTRODUCTION

PURPOSE AND SCOPE OF INVESTIGATION

Since the early 1920's the Paleozoic calcareous sediments of Alberta, Montana, and Wyoming have yielded important quantities of petroleum. Yet within these formations much sedimentary detail is relatively unknown--particularly how it may bear on the importance of traps other than structural. Hence, the present study has been concerned with determination of the characteristics of the Madison (Mississippian) Limestone of the Bighorn Basin, Wyoming. The principal effort has been directed toward a correlation of lithologic horizons throughout the Basin. In this connection detailed sampling was carried out at advantageous locations and megascopic and microscopic properties of each unit were described.

LOCATION OF AREA

The area dealt with in this study is an elongate "basin" in northern Wyoming and southern Montana. The basin is bounded by the Bighorn and Pryor Mountains to the east and northeast, the Owl Creek and Bridger Ranges to the south, and the Absaroka Range to the west. Other geographic features are given in Fig. 1.

FIELD PROCEDURES AND EQUIPMENT

To determine to what extent correlations might be possible samples were obtained at six localities. These localities lie around the periphery of the Bighorn Basin (see Fig. 2.)

In sampling an attempt was made to obtain for each stratigraphic

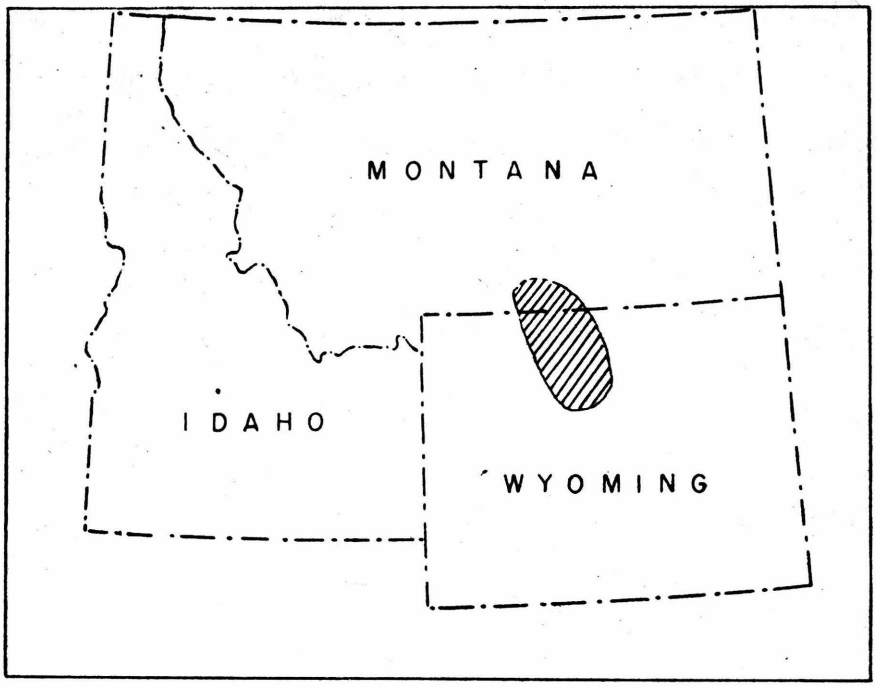

Figure 1. Index map showing location of area.

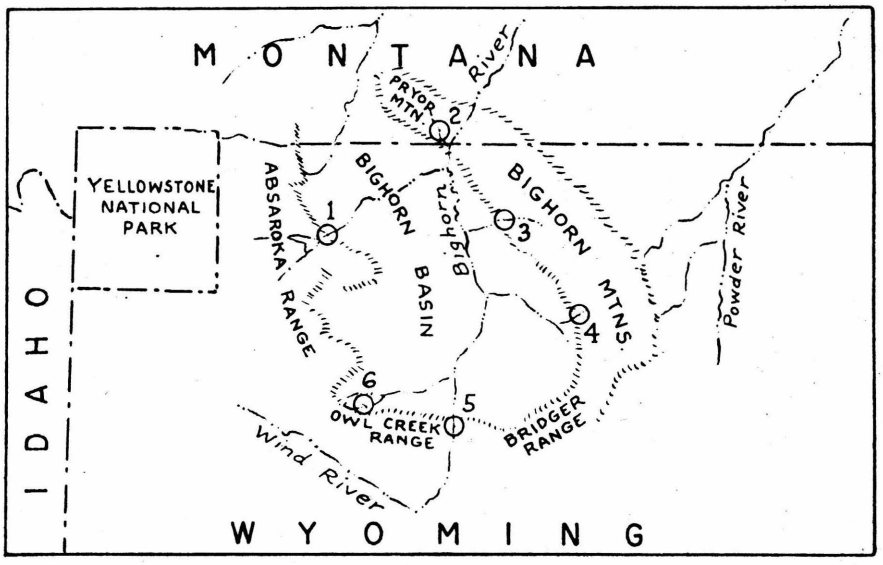

Figure 2. Index map showing sampling localities: 1. Shoshone River Canyon, 2. Crooked Creek Canyon, 3. Shell Canyon, 4. Tensleep Canyon, 5. Wind River Canyon, 6. South Fork of Owl Creek Canyon.

interval a sample of rocks that approached a channel sample in representation. Intervals were chosen on lithology or on bedding characteristics; the average interval chosen was five and one-half feet. Samples of chert were taken at all horizons where it was noted megascopically. A 12x hand lens was used in making field descriptions. Calcium carbonate rocks were differentiated from magnesium carbonate rocks with dilute HCl.

Steel tapes, hand levels, and Brunton compasses were used in measuring stratigraphic intervals. Overall thicknesses were checked with a mountain-type, "high-boy" alidade and with a fifty-foot linen tape. Four-pound mauls and cold chisels were used to break fragments from the outcrop.

The Exploration Research Department of Stanolind Oil and Gas Company prepared insoluble residues from the field samples. These were described with a 36x binocular microscope. Accessories, quartz, and cherts from the residues were immersed in index oils and studied under the petrographic microscope. Clay fractions of the residues were not separated from the coarser fractions.

Lithologic descriptions were made with a binocular microscope. Particular outcrop samples were studied by means of thin sections, stained by K_2CrO_4 following a method advocated by Holmes (1921). Many samples were studied by means of HCl etching on a smooth surface.

TERMS AND STANDARDS

The terminology and classification of H. A. Ireland, et al, (1947)

is followed in the description of insoluble residues. The general adjective, "modified", is used to designate a quartz or chert whose natural form has been altered, e.g. dolomoldic, dolomorphic, oolitic, etc. The general adjective, "unmodified", refers to the unaltered or unmarred state, e.g. subhedral, euhedral, etc.

In the stratigraphic descriptions, an arbitrary set of bedding standards was adopted. These standards were largely dictated by the mode of occurrence of the Madison. The following classification was found convenient:

Massive--largely devoid of stratification breaks.

Massive-bedded--beds of greater than 7 feet thickness.

Thick-bedded--beds from 3 feet to 7 feet thickness.

Medium-bedded--beds from 1 foot to 3 feet thickness.

Thin-bedded--beds less than 1 foot in thickness.

In lithologic descriptions terms from Shrock (1948) and Pettijohn (1949) are used. Size classifications of clastic and nonclastic particles follow the Wentworth scale; however, "micro" is prefixed for clay size particles. The following definitions may clarify their usage here:

Granular or grained--this term, applied chiefly to dolomites, designates rocks consisting of clastic or allocthonous particles; the criteria used to determine this property were cross-bedding, degree of fossil preservation, percentage and character of clastic insoluble residue, and particle shapes in thin section. The distinction

has been made since appreciable differences exist between Madison "grained" or "granular" dolomites and "crystalline" dolomites.

Crystalline--refers to an "in situ" growth.

Lithographic to sublithographic--denotes extreme minuteness of individual particles, granularity not being evident under the hand lens.

Fragmental--refers to a lithified rock consisting of 25% or more of megascopically visible, clastic, calcareous particles; particle variation may be from 1/16 to 4 mm. This term is analagous to the "calcarenite" and "calcirudite" of Pettijohn (1949, p 300).

Calcareous Sand--a friable, clastic carbonate consisting of 1/16 to 2 mm. particles.

Color designations are made in accordance with the standards established by the Rock Color Chart Committee and distributed by the National Research Council in 1948.

Porosities were estimated during binocular examination. Designations are made in accordance with Stanolind standards, i.e. "none", "poor", "fair", "medium", and "good"; in the chart on Stratigraphic Sections and Correlations the following are used as equivalents: inappreciable for "none to poor", intermediate for "poor to fair", and appreciable for "fair" or better. Variable porosity means porosity which varies laterally and vertically.

PREVIOUS INVESTIGATIONS

Naming of the Madison limestone and its first description are credited to A. C. Peale (1893). Peale designated the age of the Madison at the type locality in the Madison range near Three Forks, Montana, as Lower Carboniferous. For the nearly correlative sequence

in the Bighorn Mountains, Darton (1904) proposed the name "Littlehorn" in view of indefinite stratigraphic limits; the term "Madison" has been extended notwithstanding the indefinite stratigraphic limits.

Following definition of the upper Mississippian Brazer formation by Richardson (1913), Mississippian sediments of southeast Idaho have been divided into Madison and Brazer, the Madison being of lower Mississippian age and the Brazer of upper Mississippian age. The Carboniferous of southern Montana and northwest Wyoming was studied by Scott (1935). He showed that Peale's "Quadrant" formation correlates with the dual period Amsden as defined by Darton, op cit (1904), in north central Wyoming. Between the Amsden and the Madison of the Three Forks vicinity Scott delimited the Big Snowy group. Branson (1937) proposed the name "Sacajawea" for a portion of the Mississippian Amsden; Love (1939) has preferred to continue use of "Amsden" since Sacajawea sediments are not regarded by him as a mappable unit; however, Pierce (1947) has indicated Sacajawea strata at Shell Canyon. Basal limits of the Big Snowy, Brazer, and Amsden (as used) are not correlative nor are they clearly defined, except as overlying the "Madison". As no detailed study of faunas and stratigraphy relates the age groups of the Mississippian of Wyoming, Montana, and Idaho the delimitation of the Madison is not definite.

The Madison has been considered both as a "formation" and as a "group". This paper follows the "group" designation initiated and discussed by Sloss and Hamblin (1942).

ACKNOWLEDGEMENTS

The help which the author has received is gratefully acknowledged. The Stanolind Oil and Gas Company made field work for this study possible. Personnel from the Stanolind Casper office have given helpful suggestions and advice. Completion of this work has been aided materially by the Stanolind Oil and Gas Fellowship which was awarded to the writer during the school years 1948-49 and 1949-50.

Philip C. Scruton, Frank H. Jacobeen, and John S. Haddock assisted in the field operations. These men aided immeasurably in the more arduous phases of the sampling program; without their help sampling could not have been carried to the extent desired.

Laboratory procedures and interpretations have been supervised by Dr. Ian Campbell, Professor of Petrology at the California Institute of Technology. His advice and suggestions have contributed greatly to the completion of this study.

Dr. G. A. Cooper, Curator of the Smithsonian Institute, Dr. Wilbert H. Hass, U. S. Geological Survey, and Dr. David Dunkle, U.S. National Museum have identified fossil material which was submitted. Their identifications have made for a clearer understanding of basal Mississippian and upper Devonian stratigraphy in the Bighorn Basin.

The writer is indebted to the California Institute for the making of thin sections.

STRATIGRAPHIC RELATIONSHIPS

PALEOZOIC STRATIGRAPHY

Excepting the Silurian, all Paleozoic periods are recognized within

the Bighorn Basin. The stratigraphy is summarized below.

CAMBRIAN

Cambrian terminology varies with locality, although lithology at different localities is similar.

Wind River Canyon	Shoshone Canyon
Boysen Formation	Gallatin limestone
Depass Formation	Gros Ventre Formation
Gros Ventre member	Flathead quartzite
Flathead member	

Shoshone Canyon terminology follows earlier designations of Peale (1893) with modifications by Blackwelder (1918). The Wind River divisions and terminology were established by Miller (1936) and modified by Deiss (1938).

Upper portions of the Cambrian consist of thin-bedded limestone conglomerates, limestones, and shales; glauconitic horizons have been noted by Tourtelot and Thompson (1948) in both the Gallatin and the Gros Ventre formations. Lower strata consist of coarse- to fine-grained sandstones with quartzitic facies. The basal contact is with pre-Cambrian metamorphics. Thickness about 1200 feet.

ORDOVICIAN

Bighorn dolomite, Darton (1904): massive to thick-bedded dolomites, relatively free of terrigenous material; locally characterized by pitted surface due to differential weathering, Blackwelder (1913). Beds of reworked sandstone locally denote the basal contact; thickness increases northward from about 150 to about 400 feet.

SILURIAN

None recognized.

DEVONIAN

Jefferson formation, Peale (1893): brown to black, bedded limestones and dolomites; subdivided by Sloss and Laird (1946) into lower limestone and upper dolomite members in central Montana. Jefferson sediments have been recognized at Shoshone Canyon by Stipp (1947a). The basal contact

of the Jefferson is placed with difficulty when adjacent to Bighorn dolomite. Thickness at Shoshone Canyon±20 feet.

Darby formation, Blackwelder (1913): varicolored shales, dolomites and sandstones. Beds of Darby age may be in part equivalent to or younger than Jefferson sediments. Darby beds have been recognized locally in the Owl Creek Mountains by A. E. J. Engel (personal communications) and by Love (1939). Thickness in the Owl Creek Range varies from 0 to about 150 feet.

Three Forks formation, Peale (1893): a varied sequence of shales, dolomites, and limestones; locally with sandy facies in upper portions (Sappington Sandstone, Berry 1943; Sloss and Laird 1946). Three Forks (?) beds have been recognized along the western margin of the Bighorn Basin; thickness ± 200 feet.

The presence of Three Forks beds along the eastern margin of the Bighorn Basin has not been verified. As noted, page 22, the presence of Devonian (?) beds along the eastern margin is suggested from faunal and stratigraphic evidence.

MISSISSIPPIAN

Madison "formation", Peale (1893)--raised to "group" rank, Sloss and Hamblin (1942).

Madison sediments have been variously subdivided. Peale (op cit) recognized an upper jaspery unit, a central massive unit, and a basal laminated unit. Darton (1904) recognized a lower, moderately massive-bedded member and an upper more massive member. Sloss and Hamblin (op cit) following an earlier division of Collier and Cathcart have proposed that in Montana the Madison group be recognized as consisting of two formations--the upper Mission Canyon formation and the lower Lodgepole formation. The divisions established by these authors are summarized below:

Mission Canyon formation: Osagean; buff weathering, coarse to medium crystalline, massive limestones with varying amounts of white chert; intermittent breccias.

Lodgepole formation:

Woodhurst member: Osagean; laminated and bedded limestones with varying amounts of fossil debris and varying high amounts of clastic material.

Paine member: Kinderhookian; bedded, shaly limestones with varying amounts of brown chert, fossil debris, and clastic material.

To the writer's knowledge, the formations of the Madison group have not been previously recognized within the Bighorn Basin. To delimit these as closely as possible a section in the Pryor Mountains, about 15 miles southwest from the section described by Sloss and Hamblin (op cit p 323) was sampled and described. The areal geology between these sections was investigated to insure that no large scale stratigraphic irregularities existed undetected. Details on which this correlation was based are shown on Chart I, in pocket.

Around the Bighorn Basin bedded dolomites and fossiliferous oolitic dolomitic limestones characterize the upper Lodgepole sediments; banded, gradational limestones to dolomites are more characteristic of the lower Lodgepole sediments. Only thin remnants of the Kinderhookian Paine member are noted in the Bighorn outcrops. Massive, cherty limestones and dolomitic limestones characterize the Mission Canyon formation.

The basal Madison contact when adjacent to the Bighorn dolomite is often difficult to define; when adjacent to Devonian sediments the gray to green shales and sandstones of the Devonian delimit the contact. Thickness in the Bighorn Basin varies from 450 feet to around 700 feet. From central Wyoming northward the Madison thickens at a rate of between 3 to 5 feet per mile.

Brazer limestone, Richardson (1913): a series of massive- to thin-bedded, sandy limestones and sandstones; basal beds of this age may, in part, be equivalent to the upper Mission Canyon formation of the Bighorn Basin. The basal Brazer contact is not always clearly defined. The

possible presence of Brazer (or Big Snowy) age sediments in the Bighorn Basin outcrops is recognized in the present study.

LOWER PENNSYLVANIAN AND UPPER MISSISSIPPIAN

Amsden formation, Darton (1904): medium-bedded, cherty limestones and dolomites with interbedded shales and sandstones; locally red shales, residual cherts, limestone conglomerates, or thick-bedded sandstone (Darwin member, Blackwelder, 1918) occur near the basal contact. Thickness 100 to 400 feet.

Sacajawea formation, Branson (1937): this name was suggested for the Amsden beds of pre-Chester, Mississippian age. Amsden has since then been applied, however, to include all beds of Mississippian age above the Madison.

PENNSYLVANIAN

Tensleep sandstone, Darton (1904): white to tan sandstones which are commonly cross-bedded; locally with calcareous facies. The basal contact is poorly defined. Thickness 50 to 400 feet.

PERMIAN

Phosphoria formation, Richards and Mansfield (1912), Thomas (1934): partly correlative with Embar, Darton (1906) and Park City, Condit (1916); a phosphatic series of red and yellow sandstones, intermittent gypsum, and interbedded shales; the basal contact is delimited by more thickly bedded sandstones below; locally a thin, red shale occurs at or near the base, Stipp (1947). Thickness 50 to 250 feet.

MADISON GROUP OF THE BIGHORN BASIN

INTRODUCTORY STATEMENT

Correlations of the Mission Canyon and Lodgepole formations of the Bighorn Basin are here established. Five members have been recognized. General stratigraphic relationships and descriptive data of the members are discussed below and delineated on Chart II (in pocket). Detailed descriptions are given in Part II; stratigraphic correlations are shown in Chart III.

Beds of questionable age occur below the Madison as here described; these beds are also discussed.

GENERALIZED DESCRIPTIONS AND RELATIONSHIPS

The Amsden-Madison Contact

This contact has been established in the current study by (1) evidence of unconformities, (2) lithology. At the Owl Creek Mountain, Tensleep Canyon, Shell Canyon, and Shoshone Canyon locations, an appreciable thickness of gradational beds occurs between the massive, cliff-forming Madison limestones and the superjacent, locally resistant beds of Amsden sandstone. Unconformities exist within these gradational beds; an unconformity which exists at the upper limit of these beds and at the base of a sandstone series has been chosen as the Amsden-Madison contact. The "Madison" as thus defined includes this sequence of thin- to medium-bedded, gradational strata. By virtue of stratigraphic position and unconformities the age of these beds may vary from Osagean, to Meramecian, to Chesterian. Greater thicknesses and apparent conformable basal contacts to the west suggest that this sequence may be remnants of Big Snowy or Brazer equivalents. Identifications by Helen Duncan, Pierce (1947 p 37), of fossils from the Shell Canyon locality have also suggested a late Mississippian age for these beds. These Madison (?) strata will be herein referred to as Mission Canyon member MC 1.

Evidences of unconformity noted at the Madison-Amsden contact are (1) limestone conglomerates, (2) irregular, transgressing contacts,

(3) channeling, (4) residual cherts, (5) sand-filled mud cracks (those mentioned by Darton (1906) as occurring at Shell Canyon were found on the south side of the canyon about one-half mile above the Paton Ranch bridge).

The Mission Canyon formation

This formation is subdivided into three members, designated from youngest to oldest as MC 1, MC 2, and MC 3 (see frontispiece).

Member MC 1: Osagean (?) to Chesterian (?); thickness 10 to 80 feet.

Outcrops of this member are often obscured by talus debris or a heavy mantle of soil; where observed they weather from dark brown to slate gray. Iron derivatives from the superjacent Amsden sands locally yield red stains which "cascade" over the sediments below. Outcrop surfaces are hackly and rough in the dolomites; irregular in the limestones. This member is composed of a series of medium- and thin-bedded fragmental limestones and crystalline dolomites. Thin stringers, 1/8 inch to 1/4 inch thick, of quartzitic sandstone and yellowish-orange to brown, flaky, calcareous shale are intercalated with the limestones and dolomites. A facies of yellow-tinged, chalk-like, platy, calcareous dolomite embodying small, limonite-centered, clay concretions is locally present.

Porosities within this member are commonly poor. Brown to dark gray, irregularly shaped, nodular aggregates of subporcelaneous cherts and quartz are infrequent to common.

Insoluble residues consist of quartzitic sandstone aggregates, infrequent silicified fossil fragments, occasional coarse sand grains, dolomorphic quartz, dolomorphic and dolomoldic cherts, and clay (see Plate I); percentages are variable (1 to 10%) but greater than the member below.

The basal contact is locally slightly unconformable. It delimits the massive limestone below, insoluble residues of which consist predominantly of small amounts (±1%) of silicified fossil fragments and unmodified cherts.

Member MC 2: Meramecian (?) to Osagean (?); thickness 80 to 110 feet.

Outcrops of this member are dominantly massive and possess a distinct blue-gray color on the weathered surface. The outcrop surface is locally characterized by a pattern of silica rivulets resembling "rillensteine" which stand out as the result of differential weathering. Silicified brachiopods and corals which weather dark brown dot the surface; frequently the embedded portions of the fossils are not silicified. This silicification is believed to be a surface phenomena; however silicified fossil fragments were found in rock of the relatively deep interior. Locally, small horizontal ledges or shelves, discontinuous laterally, denote horizons where thin films of argillaceous matter collected during deposition. Irregularly shaped nodules of white and gray, chalcedonic cherts which weather brown to light gray are very common.

The lithology of this member varies, from south to north, from a brown, sublithographic, sparsely fragmental, fossiliferous limestone to a white and brown, fossiliferous, fragmental and oolitic, locally coquinoidal, partly sublithographic limestone. Intraformational limestone conglomerates are noted locally in the uppermost portions. This member grades downward into a cavernous breccia and conglomerate, characteristics and thickness of which vary. Lenses of quartzitic sandstone and green shale occur sporadically within the breccia which lies on an irregular eroded surface.

Porosities within this member are very poor.

Insoluble residues from upper portions of the member consist of low percentages (±1%) of siliceous fossil fragments and unmodified chert while high percentages (10-20%) of clays, quartz, and sand are derived from the basal breccia (see Plate II, III). Green shale fragments in the residue from the breccia are unique in the Mission Canyon sediments.

Member MC 3: Osagean; thickness 140 to 160 feet.

This member, which generally appears as a massive outcrop when viewed from a distance, is a series of thick to medium beds separated by only indistinct partings. To the west the massive character gives way to distinct thick and medium beds; to the south the outcrops appear massive in the lower portions while upper portions are thinly bedded. Solution breccias occur sporadically.

Surface colors vary from light gray on the fresh surfaces to medium brown on well-weathered outcrops. The surface of the dominant lithology is very smooth, a distinctive feature. Granular, laminated cherts weather dark brown and occur in persistent beds and lenses.

Symmetrically shaped "baseballs" of zoned, chalcedonic chert characterize well-bedded portions of this member; the outer surface of these weathers to a light gray tripoli.

In this member embayments of secondary quartz coincide with dolomitized portions; these may be traced across bedding planes by the darker color they display on weathering.

The dominant lithology is a white to medium gray, dolomitic limestone with dolomite facies. The outstanding features are the uniformity of texture and the near absence of fossils.

Porosity within this member varies from "none" in silicified portions to "fair (?)" in the dolomitic limestones.

Insoluble residues consist largely of varying percentages of secondary, micro-crystalline quartz and dark gray, granular to subporcelaneous chert (see Plate IV). Where quartz is not a major constituent, the residue consists of light gray clays and dolomoldic chert.

The basal contact is slightly undulatory and marked by breccias. High percentages of subhedral quartz grains and silts in the insoluble residue from the member below delimit the basal contact.

The Lodgepole formation:

This formation is subdivided into two members, designated from younger to older as Member L 1 and Member L 2.

Member L 1: Osagean; thickness 140 to 200 feet.

This member crops out as a series of thick- and medium-bedded limestones and dolomites. The outcrop is characterized by a weathered color distinctly darker than the overlying Mission Canyon sediments; the occurrence of beds which weather from light gray to white characterize the upper portions (see frontispiece). Outcrop surfaces are irregular; in the upper portions differential weathering produces pitted surfaces locally. Cross-bedding occurs frequently and characteristically.

Lithology of the upper portions varies from fragmental and oolitic limestones to algal-like limestones to granular (clastic) and crystalline dolomites. Unaltered fossil shells are common in the granular dolomites.

Lower beds of the member include a hematitic, sandy, fossiliferous facies lying just above a basal, erosional unconformity.

Chert is conspicuously absent throughout most of the member but is present at the base. This occurrence is in the form of one-half inch thick, laminated beds of granular gray chert, and vari-sized, smooth, symmetrical nodules of oolitic chert and fossil fragments in a jaspery matrix; the nodules have a thin tripolitic coating.

Porosities throughout this member vary from "none" to "fair";"medium" porosities occur infrequently.

Insoluble residues consist of moderate percentages (± 2%) of residual quartz and chert in upper portions and of frosted sand grains, silts, grains resembling oolites, hematite flour, and clay in the lower portions (see Plate V).

The basal contact is delimited by the sandy hematitic facies just above a chert-marked unconformity; below are banded, crystalline dolomites and fragmental limestones. The residue consists of high percentages of frosted sand grains, silts and clay fractions above the contact, while euhedral, twinned quartz crystals, residual anhedral quartz grains, silicified fossils, and dolomorphic hematite in decreasing percentages characterize the uppermost part of the member below.

Member L 2: Osagean; thickness 70 to 170 feet.

Upper sediments of this member frequently display laminations or banding. These are produced by alternate, gradational bands (± 3 feet thick) of crystalline dolomites and fragmental limestones. The limestone bands weather to form smooth, blue-gray concavities; the dolomites weather to form rough, gray-black, pitted prominences. Where dolomite characterizes the entire member, laminations or bands are fainter and possess varying degrees of roughness. Basal portions are bedded and on the weathered surfaces these greatly resemble the Bighorn dolomite; chert is conspicuous by its absence.

Lithology in this member varies from dolomites consisting of anhedral through euhedral crystals to fragmental oolitic limestones; these latter becomes more magnesian to the south.

Throughout this member porosities are appreciable.

Insoluble residues are characterized, locally, by very low percentages of petroliferous residue; uppermost strata contain varying percentages of clay, dolomoldic hematites, clay pellets and quartz (see Plate VI).

Nearness to the basal contact is denoted by shales and sandstones; unconformable relations are not always apparent. The residue is delimited by increasing percentages of clay in the basal Madison and by the occurrence of large amounts (20%) of frosted sand grains and green shale fragments at the contact (see Plate VII).]

Unnamed Devonian (?) or Kinderhookian

Beds of Devonian age have not been distinguished along the eastern margin of the Bighorn Basin. However, Stipp (1947, p 122) makes mention of beds lying between the Madison and the Bighorn which resemble the Three Forks (?) at Shoshone Canyon. His observations referred to outcrops at Tensleep Canyon, Shell Canyon, and east of Kane. The present discussion refers to similar beds noted by the writer at or near these same localities.

The contact of the recognized, cliff-forming basal Madison with the underlying sediments is a well marked unconformity. This horizon and the strata immediately below are characterized by some or all of the following features at the localities noted above:

1. An eroded irregular surface of two feet vertical relief.
2. Phosphatic concretions up to 3-inch size.
3. Abundant fish bones.
4. Well-compacted stringers of hematite or laterite on the eroded surface.
5. Glauconite grains.
6. Conglomeratic beds.
7. Channeling and solution.
8. Silicification of underlying sediments where porous.
9. Locally with intercalated black shale stringers immediately below the contact.

The lithology immediately below the erosional horizon consists of quartzitic sandstones, black shales, and varicolored dolomites. At Tensleep black shales are absent but sandstone occurs in lenses from 0 to 2 feet thick; here the sandstone lies in erosional channelways and fills solution caverns approximately 15 feet below its upper surface. At Shell Canyon black shale stringers are intercalated with thin lenses of sandstone and argillaceous varicolored dolomites to a depth of about ten feet. At Crooked Creek Canyon limited outcrops are found to consist of incompetent, thin-bedded, fetid dolomites; these are cherty, crystalline, and contain vugs partly filled with black carbonaceous material.

From the sandstones at the base of the cliff-forming Madison, Dr.

Wilbert H. Hass, U. S. Geological Survey, has identified the following conodonts and commented:

"Collection 187...Among them are many specimens of Siphonodella duplicata, S. quadruplicata, Polygnathus inornata, and Spathognathodus aciedentatus together with a fewer number of Siphonodella sexplicata and Polygnathus communis. Dinodus cf. D. fragosus, Gnathodus sp., and Pseudopolygnathus sp. are each represented by a single specimen. This fauna is definitely from the lower Mississippian. There are, however, four specimens of Icriodus in the material that was examined; their presence indicates not only that the fauna is a mixed one but also that rocks of Devonian age may be present in the vicinity of Shell Canyon. Dr. David Dunkle of the U. S. National Museum examined the fish fragments of collection 187. He recognized them as belonging to a member of the Bradyodonte sharks. These fish are typical of the Carboniferous though he states that a few have been reported from the Upper Devonian.

Collection 93...The collection contains a single recognizable lower Mississippian conodont, Polygnathus inornata. However, a larger collection would need to be examined before any positive statement could be made regarding the age of the rocks from which the collection came."

On the fossils from the dolomite into which the conodont-bearing sandstone of Tensleep has channeled, Dr. G. A. Cooper, Smithsonian Institute, has commented:

"...specimens..93..poor....The Spirifers look like Three Forks Devonian Spirifers but on the other hand they could be Mississippian.....Nothing in the collection is even suggestive of Jefferson which has an entirely different suite of Spirifers.."

The base of this sequence of doubtful age has been placed below a sequence of indurated, laminated, calcareous claystones at Tensleep. Here a three-foot series of eroded, conglomeratic carbonates is believed to denote the top of the Ordovician.

At Shell Canyon (see frontispiece) the base of the Devonian (?), Kinderhookian (?) sequence has been established on the basis of lithology

and fauna. Lithologically, the base underlies a series of shales, sandstones, and dolomites with high percentages of clastic residue. Dr. G. A. Cooper has identified the following specimens from the sediments below the Devonian (?) - Kinderhookian (?) sequence and commented as follows:

"Locality Numbers 207 to 210 belong in the high Ordovician. The specimens are listed as follows:

207-208
Calymene sp. ?
Sowerbyella
E. Streptelasma
Rhynchotrema perlamellosa
Dalmanella aff. tersa

209 Austinella ? sp.
Rhyncotrema perlamellosa?
Opikina?

210 Dalmanellid
Sowerbyella
....."

In light of the foregoing, it is here suggested that remnants of Kinderhookian (?) beds are present both at Tensleep Canyon and at Shell Canyon. By reason of faunal similarities, mixed fauna, and stratigraphy similar to that at Shoshone Canyon the beds immediately below the Kinderhookian (?) beds are designated as Upper Devonian (?). As postulated above the maximum thickness of Kinderhookian (?) beds is about 10 feet.

LIMESTONES AND DOLOMITES

With exception of the Madison section at Tensleep, the two upper members of the Mission Canyon formation in the Bighorn Basin consist

mostly of limestones. In the remainder of the Madison section, limestone percentages vary with locality and member. The table belowshows this estimated variation.

Approximate Percentage of limestone and dolomitic limestone

	Owl Crk	Wnd Rvr	Tnslp	Shll	Crkd Crk	Shshne
MC 1 & 2	65%	80%	30%	90%	70%	85%
MC 3	20%	-5%	-5%	20%	-5%	25%
L 1	70%	-5%	-5%	40%	35%	50%
L 2	(0% exp)	-5%	0	25%	35%	5%
% of section	56%	19%	13%	43%	32%	43%

Average percentage of section in basin----35%.

The dominant limestones are fragmental, including both calcarenites and calcirudites (see Plate X). Madison limestones are very similar to the second type of Pettijohn (1949, p 306). The existence of silicified fossil fragments in a rock wherein whole fossils are unsilicified provides evidence of the character of these sediments which may in part be washed debris from biohermal growths. At the southern extremities of the basin the limestone lithology varies to calcilulites or sublithographic limestones with clastic affinities. This variation toward the south is accompanied by a color change from shades of gray to shades of brown; also, fossil content decreases to the south. These changes in color, texture, and fossil content may well be related to distance from the Mississippian shore line.

Sloss (1947, p 110) cites the Mission Canyon formation of central Montana as an example of a normal marine platform deposit. Upper Mission Canyon sediments of the northern Bighorn Basin may with modifications be similarly classed. From variations exhibited, upper Mission Canyon sediments to the south may be more properly classified as marginal deposits; it seems reasonable that in such an environment chemical sublithographic sediments may be present.

The dolomites of the Madison occur predominantly in the Lodgepole formation and are most extensively developed in the L 2 member. That these sediments may have been deposited as normal marine limestones is suggested by: (1) variations in dolomite texture which can be interpreted as reflecting original limestone structures; (2) fossil content; (3) association with what appear to be normal marine, fossiliferous, fragmental limestones in the upper portions. Whether an inferred diagenetic dolomitization proceeded penecontemporaneously is, of course, problematical.

The dolomites of the uppermost L 2 member appear to have been formed penecontemporaneously or deposited chemically. Persistent dolomite bands grade abruptly into limestone bands above and below; while this mode of occurrence does not make for a unique interpretation, it suggests, nonetheless, that dolomitization or dolomite deposition proceeded prior to deposition of the overlying gradational limestone bands. Thin sections of the dolomite, of the gradational dolomitic limestone zone, and of the limestone show every gradation

from fragmental limestone through partly dolomitized, fragmental limestone to dolomite. Near the contact zone relic outlines of limestone fragments are preserved in the dolomites. Epigenetic or diagenetic dolomitization which could select clear-cut continuous stratigraphic intervals should be evidenced in some manner by insoluble residue contents or partings between bands; such are not apparent. Cloud and Barnes (1946, p 94) and Hewett (1931) have discussed similar occurrences of dolomite. It is interesting to note that these banded, gradational, dolomites and limestones in the Madison occur below an unconformity; and further, the percentage of clastic insoluble residue increases as the unconformity is approached from below. It would seem reasonable in light of this that these banded dolomites are related to changes in sea level. The statement of Twenhofel (1932, p 348) that magnesium carbonate enrichment may be related to a base level of deposition could reasonably be invoked to explain these banded, gradational, dolomite deposits.

The carbonates of the L 1 member vary from dolomites through calcitic dolomites to dolomitic limestones. A characteristic feature of this member is the clastic nature of its sediments. The dolomitic limestone and calcitic dolomite facies contain oolites, carbonate fragments, frosted quartz grains and quartz anhedrons; these sediments embody dolomitized fossil casts. Dolomitic facies are locally well cross-bedded and consist of anhedral, corroded, closely packed dolomite grains and quartz silts with a small amount of interstitial calcite

"flour" (see Plate XII). These sediments enclose fossil shells which appear to be of original material as evidenced by their pearly lustre. This suggests that from an original dolomitic limestone, the dolomite particles were separated, by virtue of their resistant nature, size, or other physical property, and redeposited under current action. Close packing of these clastic dolomites would prevent subsequent leaching; coarser detrital limestones would, a priori, admit of subsequent solution work and leaching to a greater degree than would obtain in the clastic dolomites. Pettijohn (1949, p 315) has remarked that limestones which are incompletely dolomitized diagenetically show euhedral dolomite rhombs, while complete recrystallization produces medium to coarsely crystalline anhedral dolomites. Examples of diagenetically dolomitized limestones from the uppermost L 1 member are shown in Plate VIII. Textural variations between facies of the L 1 member are interpreted as resulting from varying degrees of diagenetic dolomitization with subsequent solution and leaching by marine waters. Features listed by Van Tuyl (1916a, p 258) which suggest this type of dolomitization are: (1) failure of dolomitization to follow secondary structures, (2) existence of perfect dolomite rhombs in imperfectly altered limestones, (3) uniform distribution of mottling, (4) dolomites overlain by limestones or thick shale beds.

The presence of abundant fossils in the L 1 beds may account for the dolomitization observed; the unconformity above may be a necessary factor. Sloss (1947, p 111) has mentioned that the cross-bedded,

barred-basin dolomites of Montana are unfossiliferous, and evidence precipitation from abnormally concentrated solutions. The presence of abundant fossils in the cross-bedded dolomites of the L 1 member tends to preclude this otherwise applicable interpretation.

The lower Mission Canyon rocks may be variously interpreted. These sediments show variations from dolomitic limestone to dolomites (see Plate IX). The extreme paucity of fossils and uniformity of texture and color suggest chemical affinities. Daly's theory (1909) of direct dolomite precipitation is held to be objectionable by many; the precipitation of dolomite is considered by Twenhofel (1932, p 339) to lie entirely within the realms of theory. Nonetheless, the character of these fine-grained sediments of Mission Canyon age are believed related more to sedimentary environmental factors than to diagenetic processes. Below the MC 3 sediments is an unconformity marked perhaps by desiccation (?) breccias, solution-worked deposits, or penecontemporaneous conglomerates. Within the MC 3 rocks are extensive collapse breccias; below them are no collapse breccias. Solution activities in the MC 3 Mission Canyon sediments appear to have been confined, in the main, to small areas. The inference that these sediments are related to partially landlocked basins, perhaps with local evaporite affinities, while speculative, seems reasonable.

INSOLUBLE RESIDUES

The history of insoluble residues and their application to correlation studies in Missouri was first published by McQueen (1931).

Independent developments elsewhere indicated the widespread application of insoluble residues to stratigraphic studies. A standard nomenclature was necessitated by the provincial terms established; standardization was completed by Ireland et al (1947). Recently, Grohskopf and McCracken (1949) have published an informative statement on Missouri Paleozoic residues; those unfamiliar with residue preparation and analysis will find this paper a very useful guide. Insoluble residues have been evaluated, generally, in regard to their correlation properties; this has been their prime application. Few results have been published which interpret residue material in light of sedimentary environments or in light of post depositional processes to which the sediment has been subject.

Different workers have obtained outcrop samples for insoluble residues both by channeling and by spot sampling. The variations resulting from an application of these different methods have been discussed by Goldich and Parmelee (1947); in their study no great differences were noted. In the present study an effort was made to obtain a continuous channel sample. It is believed that sedimentation processes can be extrapolated more exactly from the results of channeling procedures. In correlation work constituents of insoluble residues are most generally used. A lesser use has been made of residue percentage. Cheney (1940, p 71, fig. 3) has incorporated percentage information in correlating Mississippian and Ordovician formations in Texas. Sloss and Hamblin (1942, p 331) have presented amounts of insoluble residues as

volume percentages in their Montana Madison study. In the current study percentages of residue by weight have been found of value. However, the use of volume percentages is time saving and should provide satisfactory results.

The residues of the Madison in the Bighorn Basin include varying percentages of silicified fossil debris, modified and unmodified cherts, modified and unmodified quartz, sands, limonite, hematite, clays, collophanite, and minor accessories. Insoluble residue logs and correlations of the Bighorn Madison are shown on Chart IV in pocket. The following criteria are established in relation to these residues and their correlation properties:

(1) Fine to coarse quartz sand with finely pitted grains denotes the base of Osagean Madison.

(2) Waxy, green shale fragments in conjunction with high percentages of clastic material mark the base of the Mission Canyon MC 2 member. Low percentages of residue consisting of abundant fossil fragments characterize the upper part of the MC 2 member.

(3) Aggregates and silts of very finely dolomoldic, microcrystalline quartz, finely dolomoldic cherts, and clays characterize the MC 3 member.

(4) Chert forms resembling aggregates of small oolites or grains in association with clays, quartz sand, silts, and hematite "flour" characterize the Lodgepole L 1 member.

(5) The virtual absence of residue, with few exceptions, characterizes the Lodgepole L 2 member.

(6) Relatively high percentages of clays in association with anhedral to euhedral quartz frosted by micro-crystalline quartz growths, cherts, and silicified fossil fragments denote unconformity zones.

(7) Changes with depth (i.e. increases or decreases) in the percentage curve of the clastic insoluble material may be used for correlation. As may be seen on Chart IV a close correspondence exists between variation in amounts of clastic material *or in* kinds of siliceous residue.

With the exception of the first two correlation criteria noted above no single residue can be used to define positively a stratigraphic interval; several residues from an interval must generally be used for this purpose.

It is believed that from channel sample residues changes in the direction of slope of the clastic residue content curve may be of value. By interpreting this information in combination with occurrences of modified siliceous residue, environmental and postdepositional processes should become more clear.

BRECCIAS

Breccias are well developed in the Madison of the Bighorn Basin. Certain of these bear relation to correlatable unconformities. In this regard special mention is made of the Madison breccias.

Three types of breccias may be differentiated in the Bighorn Madison; characteristics differentiate them. The first type is believed to be a landslide or slump breccia. Distinctive features include (1) plastic deformation of cobbles, (2) gnarly, contorted laminations, (3) erratic basal contact over short distances, (4) relatively small stratigraphic thickness, (5) no foreign fragments, (6) impersistency and lateral variations and (7) undisturbed bedding immediately above and below.

Somewhat similar occurrences have been described by Kuenen (1948), v Straaten (1949), and numerous others. Deformations of this type may be attributed to submarine landsliding precipitated by pressure variations from wave action, by seismic disturbances, or by gravity flow. These breccias bear no apparent relation to stratigraphic position, unconformity, or porosity. Examples are noted at Tensleep (390 feet) and at Shoshone Canyon (200 feet).

The second type of breccia occurs at the Mission Canyon-Lodgepole contact and locally at the base of the L 1 Lodgepole member. This type which bears definite relation to stratigraphic position, is believed to be a modified "desiccation" or "sharpstone conglomerate" breccia. Some or all of the following characteristics are noted: (1) persistency over long distances, (2) angular, pebble size fragments of hackly character locally associated with subrounded, semi-smooth pebbles, (3) occurrence of two or more beds of breccia within a given stratigraphic interval, (4) chert fragments, (5) associated intraformational conglomerates and

sedimentary hematite at nearby horizons above, (6) lithologic transitions above the breccia conglomerate interval with local collapses caused by solution, (7) large amounts of residual quartz frosted by micro-crystalline secondary growths, (8) relatively large amounts of clastic residue. (It was noted that in the intraformational conglomerates oolites with hematite and sand nuclei served as a matrix for well-rounded pebbles composed of similar oolites.)

Breccias with similar characteristics have been described by Norton (1917, p 176), Shrock (1948, p 67, 69), Pettijohn (1949, p 210). From the above associated features these breccias are believed to have originated partly as the result of dessication and partly as penecontemporaneous "sharpstone conglomerates".

The third type of breccia occurs only at the base of the Mission Canyon MC 2 member and is the most extensively developed in the Madison. It bears definite relation to stratigraphy and porosities; lateral variations in its characteristics appear significant. Typical outcrops are found at all localities, while variations are noted at the northern and southern extremities of the Basin.

The distinctive features of this breccia are: (1) persistency accompanied by lateral variations in lithologic features, (2) locally graded with smaller fragments at base of breccia, (3) conglomeratic affinities at base, (4) fragments with exotic lithology, (5) subangular and angular fragments as well as plastically deformed fragments, (6) varying degrees of cementation by a marly matrix, (7) gradational upward

into massive limestone, (8) locally, boulders of breccia occur in the breccia, (9) irregular basal contact marked by sporadic occurrences of green shale, (10) locally with contorted, indistinct bedding planes, (11) fragments, whose lithology and insoluble residues are similar to those of underlying beds, occur high up in the breccia sequence, (12) the breccia delimits very fossiliferous, fragmental rocks above from unfossiliferous, nonfragmental rocks below.

At what is believed to be the same horizon in the Pryor Mountains, Sloss and Hamblin (1942, p 323) refer to this interval as "solution breccia". In the Bighorn Basin diverse lithology was noted; fluorite-bearing dolomites in the breccia at Shoshone were found elsewhere in the Madison only at a horizon about 150 feet below the breccia; at Wind River 1 foot thick sandstone lenses were found in the breccia; at Tensleep discordant bedding planes were noted; at Owl Creek lenses of dolomite were found in the breccia; at all localities green shale fragments were found in the marly matrix. Berry (1943, p 16) mentions a limestone conglomerate at the base of the massive "jaspery limestones" of the Madison "formation" west of Three Forks, Montana. This conglomerate appears to be stratigraphically correlative with the breccia described herein. Tourtelot and Thompson (1948) have noted this same breccia in the Boysen Area, Wyoming. Near Alcova, Wyoming, Lee (1927, p 52) makes mention of an "uneven contact as if by erosion" 73 feet below the Amsden-Madison contact and at the base of a massive limestone;

this surface appears to be stratigraphically correlatable with this same breccia sequence. If the horizons noted by Lee and Berry are correlative, indications are that the causes of the breccia-producing processes were manifested over a wide area. Breccias with some characteristics similar to those noted above are described by King (1948, p 63, 86), McKee (1938, p 126), Woodford and Harriss (1928, p 279), Miser (1934), and Van Tuyl (1916b, p 122).

The characteristics which the breccias exhibit may be interpreted as suggesting an origin related to deformation while sediments were yet plastic in addition to erosional and depositional processes following a tectonic disturbance. The breccias are thicker and more angular at the northern localities than at the southern localities. Red Amsden silts which permeate the breccia at Crooked Creek evidence postdepositional activities. It seems reasonable that tectonic uplift may have resulted in submarine landsliding of plastic MC 3 sediments; this uplift may have formed land masses to the south from which sands and green shales were derived. Continued uplift may have resulted in shallow basins where sorting and deposition continued. Locally, the lithology and many of the features exhibited by the breccias suggest the presence of reef structures. It is conceivable that tectonic uplift may have created environments favorable for bioherm development; the overlying fossiliferous, fragmental limestones lend additional support to this view. An unconformity of considerable extent resulting

from tectonic uplift is believed evidenced. While these breccias may have an alternative explanation, it is difficult to conceive how they may be explained solely as collapsesfrom solution of evaporites or limestones, or from wave action. However, it is indeed possible that uplift may have resulted in the formation of landlocked basins wherein evaporites and limestones were deposited. Continued uplift followed by erosion and by solution of the evaporites and limestones appears reasonable from this point of view.

POROSITIES

Development of porosity in calcareous rocks has long been a controversial subject. Insufficient analyses prevent a detailed discussion of porosity at present. However, the features observed in the Madison which pertain to this problem are summarized below.

(1) Progressing from southeast to northwest across the Bighorn Basin (going seaward) the ratio of dolomites to limestones decreases. Steidmann (1911) has discussed the relative solubility of limestone and dolomite. The variation noted here may be a function of relative solubilities. From the reasoning of Van Tuyl (Cloud and Barnes, 1948) this variation may be related to water depth and temperature.

(2) Unconformities, dolomitization, and porosities within the Madison sediments of the Bighorn Basin are qualifiedly related:

(a) Appreciable porosities were observed in dolomites and dolomitic limestones below unconformities; on the other hand, some

dolomites below unconformities were observed to have very inappreciable porosity. The discrepancy appeared to be solely a function of varying resistance to leaching. Appreciable porosities were noted in clean dolomites embodying large vugs, many of which retained relic fossil outlines, and in partially dolomitized limestones from which some calcite appeared to have been selectively removed. Inappreciable porosities were occasioned by unleached fossils and intergrain calcite "flour". One notable difference obtains between these rocks. Those which have little porosity consist of clastic, cross-bedded dolomites. This suggests that clastic dolomite facies were compacted to such a degree that percolation or flushing phenomena were prohibited. Porosity developments in these sediments appear to be directly related, not to the amount of dolomite nor to the degree of dolomitization, but to the "cleanness" of the dolomitized rock.

(b) The degree of dolomitization in the Mission Canyon MC 3 member was intimately related to growths of secondary, micro-crystalline quartz which could easily be traced across bedding planes by observing weathered color and hardness; the quartz was associated only with crystalline dolomite. In addition to modified quartz aggregates in the residue, a fine pattern of fracture-filling quartz was observed. Evidently, here fractures below an unconformity formed channelways for solutions which deposited silica thus reducing the porosity. Calcitic rock which remained undolomitized even though porous contained no

appreciable quartz. Here, the close association of quartz and dolomite implies a related growth. Silicification was more intensive in the younger strata and outcrop relations suggested that the solutions came from above.

(3) A singular occurrence of dolomitization may be seen at Shoshone Canyon. Dolomitized portions occur as resistant, isolated, bedded concretions or pseudo-boulders in a bed of highly-fractured, fragmental and micro-granular limestone. These forms resemble small bioherms, which their bedded nature shows to be untrue (see Plate XIII). Dolomitization in this case seems to have proceeded upwards from the fluorite-bearing beds immediately below. Forms similar to those noted above have been described by Van Tuyl (1916a, p 255). Isolated patches of dolomitization in areas of ore deposition have been described by Hewett (1928). This mode of occurrence suggests an origin related to artesian percolation somewhat similar to that suggested by Landes (1946). That dolomitization here was epigenetic seems most probable. If these features are correctly interpreted, the circulation of artesian waters may have had significance in the dolomitization of the Madison sediments of the Bighorn Basin.

CORRELATION DATA

STRATIGRAPHIC CHERT

Within the Madison formations, both the presence and absence of chert proved helpful in correlating. The following generalizations are

drawn between character, mode of occurrence, and stratigraphic position.

Cherts vary from abundant to scant within the Mission Canyon formation. Three distinct types, with modifications, were noted. These types, although not wholly analogous to the types described by McKee (1938) show definite similarities.

Type 1 cherts occur in irregularly shaped nodules which weather dark gray to brown. They consist of granular to subporcelanous chert enclosing varying percentages of quartz crystals or grains. Microscopic analysis shows a gradation from well developed, coarse quartz crystals through micro-crystalline quartz to finely granular silica. The same kind of chert is noted as occurring infrequently in thin beds; this mode of occurrence shows paucity of quartz crystals or grains but embodies abundance of silicic micro fossils and silicic fossil fragments.

Type 2 cherts occur as irregularly shaped nodules and as concretions; these are yellow, red, white, gray, and brown zoned cherts. No fossils or recognizable nuclei were found in these forms. They appear to vary from "jasper" to chalcedony. The surface is commonly covered with a tripolitic coating.

Type 3 cherts occur in lenses conformable with bedding planes and locally as layers in thin cross-beds; these consist of laminated, dark to light gray, granular silica which weathers dark brown to yellowish-brown. The bedding surfaces of these cherts are modified by depressions

which resemble casts; however, weathering may have produced this effect.

Cherts of type 1 are dominant in the MC 1 member; they occur sporadically in the MC 2 member. Cherts of type 2 are dominant ih the MC 2 member only. Cherts of type 3 are dominant in the MC 3 member but their presence is also noted in member MC 1. Modified forms of chert residuals are found in the Wind River MC 1 member (see Plate I, A).

Within the Lodgepole formation cherts are generally absent or scant. They are present erratically in the top beds of the formation and at the L 1--L 2 contact. The erratic cherts in the Lodgepole are nearly always nodular or in small pod-like lenses. These lie conformable with the bedding.

A singular occurrence of white, granular chert which varied to chalcedonic chert was noted in the Lodgepole formation at Shoshone Canyon and at Crooked Creek.

The chert at the L 1 to L 2 contact, described on page 18, was unique. Oolites in this chert have quartz centers which are surrounded by fine bands of red and yellow, "jaspery" chert, all of which are enclosed in a red to gray matrix of chalcedonic to porcelanous chert.

INSOLUBLE RESIDUE CHERTS AND MODIFIED QUARTZ

Some noteworthy examples of modified siliceous residue were obtained from the Madison sediments. Clay fractions were not separated from the coarser portions of the insoluble residue; separation of the clay size fractions would have permitted readier distinction of the constituents.

Dolomoldic and dolomorphic "cherts" and unmodified cherts were observed to be of stratigraphic prominence at or near unconformities, e. g. MC 3--MC 2, L 1--L 2 as shown on Chart IV. These "cherts" were generally of a finely granular variety. They commonly vary to finely granular quartz. The modified forms of these tended to be of larger average size than those of scattered occurrence in the section; however, many exceptions to this exist.

Silicified fossil remains and quartz (both modified and unmodified) were observed below unconformities, e.g. L 1--L 2 as shown on Chart IV. The two were not always noted in conjunction. Silicification has been related to unconformities by Howell (1931) in his study of beekite rings. Whether silicified fossils and quartz at given horizons, may represent silicification during hiatuses of deposition or during a subsequent percolation is not known. However, higher relative amounts of anhedral frosted quartz may suggest residual deposits; euhedral and subhedral quartz crystals may be interpreted to indicate growth unimpeded by enclosing sediments which can be visualized as occurring on the sea bottom during hiatuses in deposition or in unsolidified sediments.

A preponderance of dolomoldic and dolomorphic cherts was obtained from Mission Canyon sediments (see Chart IV). These cherts occur in the breccia at the base of the MC 2 member, sporadically in the MC 1 member, and in minor amounts in the MC 3 member; large fragments of chert with infrequent casts (?) or pits on the surface were found predominantly in the MC 2 member.

Oolitic granular cherts occur in the MC 2 and L 1 members at Shell and Tensleep. From stratigraphic position those in the L 1 member are correlated with oolitic limestones at other localities. Within the L 1 member these "oolites" exhibit no concentric structure and occur singly as grains or in aggregates, which are commonly surrounded by a delicate shroud of quartz.

Filigree, dolomoldic quartz is preponderant only in the MC 3 member (see Plate IV). Frequently associated with this quartz are small chert granules. The granules grade from dark gray chert at their interior through light colored chert and quartz to micro-crystalline quartz at the exteriors. This is believed to result from solution activity which was concomitant with or followed the MC 2 unconformity.

SAND AND QUARTZ

Sand and quartz from insoluble residues of Madison sediments furnish the most reliable single correlation criterion. In this study quartz is divided into (1) unmodified and (2) modified. The unmodified refers to drusy quartz clusters and euhedral through anhedral quartz; modified refers to dolomorphic and dolomoldic quartz. Using this classification the following generalizations can be stated:

(1) Unmodified quartz and allocthonous quartz grains are characteristic of the Lodgepole L 1 member. A sandy facies is present at the base of the member; this sand is composed of rounded chert grains and well rounded quartz grains which have finely pitted surfaces. Size distribution varies from silt-size to very fine with occasional fine-sized grains.

(2) Medium-sized, angular sand grains occur within the MC 2 breccia in conjunction with high percentages of clay, low percentages of diagnostic green shale, and cherts. From their associations these sands are easily differentiated from those in the L 1 member and those at the base of the L 2 member.

(3) Unmodified quartz of irregular shape and varied size, as well as euhedral and subhedral quartz, marks the top of the Lodgepole formation and the top of the L 2 member; these grains are commonly frosted with growths of micro-crystalline quartz.

(4) Finely frosted sand grains of coarse to medium size characterize the base of the Madison at all exposed localities. These are associated with infrequent grains of glauconite and accessories.

GRAIN SIZE

Grain sizes are of definite value in establishing correlations within the Madison group. Broadly speaking, the Mission Canyon formation consists of micro-sized carbonate particles. The Lodgepole formation consists of coarse to very fine particles. The following data are found valuable for distinguishing the formation members.

The MC 1 and MC 2 members consist predominantly of irregularly shaped, varisized particles which consist of micro-granular carbonate. Numerous micro and mega fossils are associated with these fragments. The matrix varies from sublithographic limestone to coarsely crystalline calcite; infrequently dolomite occurs as matrix material. The dominant texture is micro-granular to sublithographic (see Plate X).

The MC 3 member consists of micro- to very fine dolomite particles in a micro-granular calcite matrix. Uniformity of texture is very noticeable. Locally the calcite has been leached away leaving a micro- to very finely crystalline dolomite (see Plate IX).

The L 1 member may be differentiated from the overlying MC 3 member by comparing particle sizes. In the clastic cross-bedded dolomites the difference is not quite so apparent(see Plates XII,VIII). The crystal and grain size of the uppermost L 1 varies from coarse to very fine, distinct from the fineness of the MC 3 sediments above. Crystal development varies between individual L 1 beds; very finely crystalline dolomite and calcite form the matrix of oolitic limestones in lower L 1.

The L 2 member is not easily differentiated by its grain size. An extreme variability is noted. The more porous portions are characterized by medium to very fine sizes of euhedral and subhedral dolomite crystals. The more compact portions seem to be of smaller sized, anhedral crystals or grains (see Plate XI).

ACCESSORY AND CLAY MINERALS

No correlations could be substantiated on the basis of kinds or amounts of accessories present. The presence of fluorite at Shoshone Canyon (both in the MC2 breccia and beds below) proved to be unique in the Madison. King (1948, p 160) mentions a similar occurrence in the Permian of Texas. Milner (1940) has discussed sedimentary occurrences of this mineral. No explanation is offered for its presence in the Madison.

Clay minerals have been little analyzed in this study. Throughout the L 1 and MC 2 members appreciable percentages of clays were noted. Increases and decreases of these percentages offer corroborative correlation evidence, as exemplified by the basal sediments of the Madison, the L 1--L 2 contact, and the MC 2 breccias. Relatively high percentages of clay in certain zones may possibly relate to subaerial soil developments. Correlation work by Grim (1937, 1947) has indicated that clays may be an important factor in correlations and in petroleum recovery. It is not impossible that the kind of clay in carbonate rocks may be a factor in dolomitization.

GEOLOGIC HISTORY AND SUMMATION OF SUGGESTED ROCK GENESIS

Exposed areas which contributed the clays and sands to upper Devonian sediments had been reduced by late Kinderhookian time to near base level. Mild diastrophism during lower Mississippian time may have caused redistribution of existing sediments, thus giving rise to the unconformity described on page 21. In view of features characterizing the unconformity, local subaerial exposure seems probable. Osagean Madison sedimentation is assumed to have commenced with a lowering of land levels which caused a southeastward transgressing sea and gave rise to varying amounts of clay in the basal Osagean, Lodgepole carbonates. Continued sinking and flooding gave rise to deposition of fragmental and normal marine limestones. Muds and oozes of these sediments were probably dolomitized before solidification; fossils and fragments appear to have been leached after solidification when the

rock had strength to maintain the voids produced during leaching processes. During late L 2 time sediments were built close to a base level of deposition; that dolomitization followed changes of the base level is suggested by the banded deposits discussed on page 25. Shallow water environments at the end of L 2 time are postulated in light of increasing amounts of insoluble residue believed in part to be redistributed products from eroded L 2 carbonates. Erosion in excess of deposition marked the transition from L 1 to L 2 time, as indicated by lithology. Subaerial exposure within the area of the Bighorn Basin during late L 2 time does not seem probable.

Following the hiatus at the end of L 2 time, clastic fragments of limestone and sands were deposited in a shallow L 1 sea. L 2 sediments of southern areas were conceivably transported further from shore. Sedimentation proceeded with sinking of the L 2 basin. Intraformational oolitic conglomerates with sandy, hematitic, and oolitic matrixes were formed in shallower waters, presumably from wind and wave action. Current action prevailed during this time of comparatively rapid deposition with clastic sediments predominating. Culmination of this period of deposition was caused by depletion of source sediments or cessation of basin sinking; organic forms became abundant and widespread. That the uppermost sediments were partially dolomitized diagenetically through marine processes is suggested by textural variations; psuedobreccias were formed during the dolomitization process.

Conglomerates and depositional breccias were laid down during the L 1 to MC 3 hiatus; subaerial exposure may locally have been effected. Conceivably, the formation of partly landlocked basins marked the end of L 1 time.

Deposition in MC 3 time may have proceeded in more highly saline and magnesian waters since organic remains are not in evidence. Uniformity of texture and fossil scarcity suggest that sedimentary processes during this time interval were dominated by chemical factors. The end of MC 3 time appears to have been marked by differential changes of sea level. At this time tectonic activity, suggested by breccia fragments of diverse lithology, may have brought about environments suitable for algal and coral growth. A widespread period of erosion and solution is reasoned to have ensued. During this period solution may have caused local collapse breccias in the MC 3 member. Distribution of secondary silica, dolomitization, and calcite solution in MC 3 sediments are believed to have characterized this erosional interval.

In MC 2 time a moderately shallow water, marine environment is assumed in light of the lithology described on page 24. Life became prevalent; reef and biohermal growth may have prospered. Gradual regional uplift may have caused lagoonal and shoal environments, as suggested by sublithographic textures in the MC 2 sediments. Fragmental limestones may have originated from earlier deposited sediments or as erosional debris from MC 2 sediments.

The transition from MC 2 to MC 1 time seems characterized by influx of clay and sand. Additional influx of terrigenous material effected by regional uplift supposedly marked the beginning of lower Amsden time.

ECONOMIC POSSIBILITIES

Aside from structural traps oil possibilities within Bighorn Madison sediments are governed by existence of porosity variations, fracture permeabilities, unconformities, and reefs. It seems not improbable that conditions favorable for economic accumulations may exist within the Basin, and that favorable conditions may be indicated in adjoining areas.

No appreciable porosity exists within the Mission Canyon MC 1 and upper MC 2 members which form an impervious cap over older sediments. Porosity below the MC 2 member is apparently related to the MC 2--MC 3 unconformity. Within the MC 3 member porosities at Shell, Crooked Creek, and Wind River are lacking in large part at Tensleep, Shoshone, and Owl Creek; this lateral variation seems to be a function of dolomitization, solution, and silicification. Solution breccias in the MC 3 member at Crooked Creek and Tensleep indicate removal of appreciable quantities of material. This solution activity may have created caverns and voids which are locally supported by competent silicified carbonates, similar in form to occurrences of secondary porosity in the Kevin-Sunburst Field in Montana.

Porosities within the Lodgepole L 1 member vary; appreciable porosities exist at Tensleep and Shell. While dolomitization within this member has been extensive at Wind River, primary porosities here are inappreciable and secondary porosities are not abundant.

Appreciable porosities occur in the L 2 sediments. These developments are largely a function of leaching and dolomitization; secondary developments are more dominant than primary. Sediments of Shell Canyon yielded an oily to tarry insoluble residue throughout this member.

The importance of unconformities in carbonate rocks has long been known. Those unconformities within the Madison which delimit porous zones are the MC 2--MC 3 unconformity and the L 1-- L 2 unconformity. Extended correlation of these in conjunction with isopach data may indicate areas worthy of investigation.

From examination of the Shoshone section, which has been subjected to stresses, it would seem that the abundant fracture patterns contribute much to the porosity developed there. Appreciable degrees of fracturing were noted particularly in lower Mission Canyon rocks.

Worthy of mention is the possibility of reef structures within Madison sediments of the Bighorn Basin and adjoining areas. Osagean Mississippian reefs in New Mexico have been recognized by Laudon and Bowsher (1941). The striking similarity of many features exhibited in the MC 2 breccia to features of known Mississippian reefs suggests

their presence in the Bighorn Madison. It seems reasonable that environments suitable for reef formation in the Wyoming Madison may have existed by reason of (1) transgressing seas during lower L 2 time, (2) regressing seas during upper L 1 time, (3) basin deposition during lower MC 3 time and (4) shallow water environments during MC 2 time. With little else to indicate location of favorable environments, the areal extent of evaporite deposits in Montana may have significance. Sloss (1947) has noted that the margins of tectonically negative areas should be favorable for biohermal growth. Partial change of facies is noted within the MC 3 member; fine-grained, uniformly textured, chalky carbonates in the south vary to clastic limestones in the northwest. This might be interpreted as suggesting that during upper MC 3 time the northern Bighorn Basin was a near limit of basin deposition.

RECOMMENDATIONS FOR FURTHER STUDY

Analyses of Madison samples to determine the CaO--MgO ratio might aid in delimiting zones. Further advantages may be realized in dealing with facies changes and porosity variations.

The occurrence of oily residue at Shell Canyon in the Lodgepole L 2 member and at Owl Creek at the top of the L 1 member may warrant further investigation. Dried carbonaceous (?) material in a vuggy, crystalline dolomite at the base (?) of the Madison at Crooked Creek may likewise be significant.

Clay fractions noted in insoluble residues during examination appeared in significant amounts. The character of these clays may relate directly both to dolomitization and to porosity through solution. Analyses of clay fractions from different calcareous sediments for correlation with lithologic features is believed worthy of consideration.

SUMMARY AND CONCLUSIONS

The Mission Canyon and Lodgepole formations (Madison group) of central Montana are recognized throughout the Bighorn Basin, Wyoming. These formations may be differentiated by lithology and by insoluble residues. In the main Mission Canyon strata are more massive and are characterized in residues by modified and unmodified cherts, fossil debris, and quartz. Lodgepole sediments are bedded and are characterized by insoluble content of clays and sands or silts. The Mission Canyon sediments are divisible into three members: an uppermost member consisting of bedded, calcareous sediments with intercalated sands and shales; a central member consisting of fossiliferous, massive limestone and basal breccia; a lower member consisting of massive and bedded, unfossiliferous, even-textured, calcareous rocks which exhibit lateral change of facies. The Lodgepole sediments are divisible into two members: an upper member consisting largely of bedded, fossiliferous, clastic, calcareous sediments; a lower banded and bedded member consisting largely of dolomite.

Remnants of Kinderhookian (?) and upper Devonian (?) sediments occur along the eastern margin of the Basin.

Madison sediments consist, in large part, of dolomite the percentage of which decreases seaward (northward and westward). Some of these dolomites are potentially petroliferous. The dominant porosity is secondary and is related principally to leaching; the degree to which leaching has been completed is dependent upon the character of the original sediment. Below unconformities leaching appears to have been more appreciable.

Lithologic features suggest that Madison sediments were deposited in marginal platform and basin environments. Thickness variations and clastic content indicate that distribution of the lower and middle Mississippian sediments was controlled by regional uplift to the southeast. Local deformations during upper Osagean time are evidenced by lithologic features and by unconformities.

PART II

DESCRIPTIVE DATA

ABBREVIATIONS

The abbreviations and contractions given below have been used in the descriptive data that follows.

arg	argillaceous	or	orange
bl(-)	black(ish)	pk(-)	pink(ish)
br(-)	brown(ish)	qtz	quartz
calc	calcareous	rnd(ed)	round(ed)
cg	conglomerate	sl	slight(ly)
crse(ly)	coarse(ly)	sndy	sandy
dol(s)	dolomite(s)	ss	sandstone
drk	dark	trc(s)	trace(s)
fn(ly)	fine(ly)	v	very
gr(-)	gray(ish)	w	with
gran	granular	wh	white
ls(s)	limestone(s)	xl(s)	crystal(s)
lt	light	xln	crystalline
med	medium	yel(-)	yellow(ish)

LITHOLOGY DESCRIPTIONS

OWL CREEK CANYON

Sampling was started in the NE/4, Sec 31, T 43, N, R 100 W, at a location due south of a deserted homesteader's shack in the adjacent valley to the north. This locality lies about five miles upstream from the Anchor Ranch.

Amsden formation

20'	Cliff-forming, massive sandstone.
37'	Thin-bedded, blocky sandstones and dolomites with partings of shale and claystone.

Mission Canyon formation

Units 639 to 635 constitute a thin-bedded sequence of dolomites which weather brown to gray (number 639 marks the top of the sequence, number 636 the base). Breccia intervals occur within this sequence. The top of the Madison has here been picked by lithologic change from carbonates to sandstone. This was done also at the other localities. However, this sequence is not separated from the Amsden by any indications of erosion or unconformity. Argillaceous dolomites characterize the uppermost beds, while unconformity zones may be evidenced by breccia intervals below.

639.	0-2.0	dol: arg, v lt gr, micro-gran; porosity none.
638.	2.0-3.5	dol: arg, v lt gr to lt pk-gr, micro-gran; brown flecks; porosity none.
637.	3.5-13.3	dol: lt pk-gr to lt gr, micro-xln; infrequent med vugs, occasional crse calcite xls; 3' cherty, breccia zone at base of unit; porosity none.
636.	13.3-20.3	ls: fossiliferous, br-gr, micro-gran and crsly fragmental w micro-gran matrix; porosity none.

Unit 635 is a massive bed of limestone which weathers blue-gray and brown. The top of this unit is a breccia with scattered quartz grains. This breccia appears to correlate with outcrops of red-stained soil which are noted in the locality. The top of this unit is believed to mark an unconformity because of the relations mentioned.

635.	20.3-32.3	ls: fossiliferous, fragmental, crsely to med-gran w micro-gran matrix; breccia at top of unit w sndy, gran dol matrix; porosity none.

Units 634 to 630 inclusive constitute a series of incompetent beds which are generally obscured by mantle. Bedding varies from thin to very thin. No cherts are noted. (Number 630 marks the base of the sequence.)

634.	32.3-40.3	dol: lt br-gr, w pk stains, silt-size gran; interbedded w v lt gr, arg, micro-gran dol; 1/8" seams of fnly-gran ss; porosity none.
633.	40.3-49.3	ls: fossiliferous, partly fragmental, br-gr, crse to fn fragments and micro fossils in a micro-gran matrix; porosity none.
632.	49.3-58.3	ls: fossiliferous, same as above but largely micro-gran; v lt gr, micro-gran dol interbedded; porosity none.
631.	58.3-67.3	dol: v lt gr as above; porosity none.
630.	67.3-76.3	dol: sl silty, arg, v lt gr, micro-gran; infrequent, crse calcite nests; porosity none.

Units 560 to 572 constitute a massive limestone which weathers brownish-gray and blue. Chert nodules and silicified fossils weather to a dark brown on the outcrop surface. The outcrop surface is irregular with scallops and ridges formed by differential weathering. Massive character in interrupted by a banding caused by fracture patterns and weathered color. The base of this sequence grades into a breccia and conglomerate.

560.	76.3-80.8	ls: cherty, fossiliferous, fragmental, oolitic, lt br-gr to gr-br, crse to med ls fragments and oolites in a micro-gran matrix; porosity none.
561.	80.8-88.3	ls: same as above; porosity none.
562.	88.3-96.3	ls: same as above but fnly to med-gran; porosity none.
563.	96.3-101.3	ls: same as above, partly w clear xln calcite matrix; porosity none.
564.	101.3-107.0	ls: same as above; a few v crse fragments; porosity none.
565.	107.0-112.5	ls: same as above; porosity none.

566.	112.5-120.5	ls: same as above; pebble to granule fragments in a fragmental matrix; porosity none.
567.	120.5-127.0	ls: same as above w micro to fnly-xln calcite matrix; porosity none.
568.	127.0-138.0	ls: same as above; largely fnly gran w micro xln calcite matrix; porosity none.
569.	138.0-150.0	breccia: cherty, fragmental and micro-xln, gr-br to lt br-gr, angular ls cobbles to v crse fragments in a micro-gran, arg dol matrix; infrequent cobbles of drk gr, micro-gran dol; porosity none.
570--571	150.0-166.5	breccia: cherty, angular to subrnded pebbles to small cobbles of micro-gran, med lt gr dols and infrequent micro-gran lss in a v fnly gran, arg dol matrix; lenses of v fnly gran, med drk gr, dol pass through unit; frequent hematite pseudomorphs; porosity none.

Units 572 to 599 constitute a poorly defined sequence of thick and medium beds. The contacts are very obscure and are largely gradational. These "pseudo-beds" weather to form a gray and brown, banded sequence in the upper portions. In the lower portions bedding is more definite and the outcrop is not so prominently banded. Laminations occur sporadically, while the characteristic smooth surface noted at other localities is present only on some of the bands. Cherts occur sporadically in lenses. Fossils are largely lacking.

572.	166.5-176.8	ls: gr- br, micro-gran; tiny calcite veinlets and occasional large calcite xls; porosity none.
573.	176.8-180.3	dol: v lt gr, micro-gran; tiny calcite veinlets; indistinctly outlined med lt gr, micro-gran, angular pebbles of dol; porosity none.
574.	180.3-188.9	dol: cherty, calc, v lt gr to lt br-gr, micro- to silt-size-gran; porosity none.
575.	188.9-196.1	dol: cherty, calc, partly banded, br-gr, silt-size-xln; porosity none.
576.	196.1-205.3	dol ls: cherty, lt yel-gr, micro-to silt-size-xln dol w calcite flour matrix; porosity none.

577.	205.3-209.3	dol: cherty, partly breccia, lt br gr, micro-xln; hematite flecks; 4" of angular pebble size fragments at base in a micro-gran, calc, arg matrix; porosity none.
578.	209.3-215.5	dol: cherty, lt br-gr, silt-size to v. fnly xln; porosity none.
579.	215.5-219.6	dol: lt br-gr, v fnly to silt-size xln; infrequent, fn, calcite-lined vugs; porosity poor to none.
580.	219.6-226.5	dol: cherty, same as above; grades into a breccia w chalky-looking, micro-gran, calc dol matrix; porosity none to poor.
581.	226.5-232.0	dol: cherty, silicic, v lt gr to lt gr, v fnly xln; porosity none.
582.	232.0-237.0	dol: fossiliferous, partly silicic, lt gr to med lt gr, silt-size-xln; infrequent med vugs lined w anhedral calcite; hematite anhedrons; porosity none.
583.	237.0-241.0	dol: cherty, partly silicic, same as above; porosity none.
584.	241.0-248.5	dol: cherty, sl calc, partly silicic, same as above; porosity poor.
585.	248.5-255.8	dol: cherty, sl calc, same as above, porosity poor to none.
586.	255.8-262.3	dol: very cherty, calc, lt gr; 2' med-to crsely xln w intergran calcite flour, hematite flecks; porosity poor. 4.5' micro-xln; porosity none.
587.	262.3-268.3	dol: very cherty, partly calc, partly fossiliferous, v lt gr, micro- to silt-size-xln; infrequent leached fossil vugs; porosity none.
588.	268.3-273.8	dol: cherty, calc, v lt gr, silt-size-xln; porosity none.
589.	273.8-275.8	dol ls to calc dol: arg, wh to v lt gr, micro-gran; hematite and pyrite trcs; porosity none.

590. 275.8-282.8 dol ls: cherty, v lt gr to br-gr, fnly to med-xln dol w interfragment calcite flour; porosity none.

591. 282.8-287.9 dol: silicic, v lt gr, silt-size-xln; porosity none.

592. 287.9-290.6 dol: silicic; same as above; porosity none.

593. 290.6-293.6 dol: sparsely fossiliferous, med lt gr, micro- to v fnly xln; infrequent fn vugs; porosity poor to none.

594. 293.6-299.3 dol: sparsely fossiliferous, same as above; porosity poor to none.

595. 299.3-303.7 dol: sparsely fossiliferous, calc, same as above; porosity poor to none.

596. 303.7-313.9 dol: lt br-gr, micro-xln; 3" layers of breccia at base; porosity none.

597. 313.9-318.4 dol: breccia, cherty, silicic, angular cobble to pebble fragments of v lt pk-gr, micro-xln; infrequent calcite xls and veinlets in a micro-gran, calc dol matrix; porosity none.

598. 318.4-324.7 dol ls: med gr to med lt gr, fn to med dol grains in a micro- to silt-size-gran ls matrix w occasional crse xls of calcite; porosity none.

Lodgepole formation

Units 599 to 622 constitute a cliff-forming series of thick and medium bedded strata which weather to a dark chocolate brown. Chert is absent. Fossils are relatively abundant. Cross-bedding occurs sporadically in the upper portions and is prevalent in lower portions of the sequence.

599. 324.7-331.7 dol ls: very cherty, partly silicic, med gr to med lt gr, med grains of ls and oolite-like forms in a micro-gran dol matrix; partly pebble to cobble breccia w med-gran, dol matrix; porosity none.

600. 331.7-332.9 ls: fossiliferous, oolitic, med to crse oolites and infrequent fragments in a micro-gran and micro-xln matrix; porosity none.

601.	332.9-340.3	dol ls: cherty, sparsely oolitic, v lt gr to lt yel-gr, silt-size to v fnly xln; abundant fn vugs; partly a micro-xln, calc dol; porosity poor to fair.
602.	340.3-348.4	ls: oolitic and fragmental, lt br-gr to gr-br, v fn to med-sized grains and oolites in a micro-xln, calcite matrix; porosity none.
603.	348.4-353.4	ls: same as above; porosity none.
604.	353.4-359.4	ls: same as above but more crsely gran; porosity none.
605.	359.4-360.4	dol: calc, lt yel-gr to lt br-gr, med- to fnly xln; porosity poor to fair.
606.	360.4-365.6	ls: oolitic and fragmental, lt br-gr to gr-br, v fnly to crsely gran w micro-xln calcite matrix; porosity none.
607.	365.6-373.0	ls: same as above, partly w v fnly gran dol in matrix; porosity none.
608.	373.0-379.5	dol: sparsely fossiliferous, calc, lt br-gr, silt-size-xln; infrequent fn vugs; porosity none to poor.
609.	379.5-388.8	dol: same as above; porosity none to poor.
610.	388.8-396.5	ls: oolitic, lt br-gr, med to crse oolites in a micro- to fnly xln, calcite matrix; porosity none.
611.	396.5-402.5	ls: same as above which grades to a dol ls of v fnly to silt-size-gran dol enclosing indistinct oolites and irregular ls fragments; porosity none.
612.	402.5-406.2	ls and dol ls: fossiliferous; same as above; porosity none.
613.	406.2-408.2	dol: banded, med lt gr to med gr, v fnly gran; hematite subhedrons; porosity none.
614.	408.2-417.9	dol ls: fossiliferous, partly fragmental, lt br-gr w red streaks, crsely to med-gran fragments of ls in fnly-gran dol matrix; infrequent rnded dol pebbles; porosity none.

615. 417.9-424.1 ls to dol ls: stylolites, lt br-gr to med lt gr, crsely to med gran ls w varying content of v fnly gran dol and calcite flour matrix; porosity none.

616. 424.1-431.1 ls to dol ls: fossiliferous, stylolites, fragmental, partly oolitic, banded, crsely to med-gran w oolites in a v fnly gran dol and micro-gran calcite matrix; porosity none.

617. 431.1-439.6 ls to dol ls: same as above; porosity none.

618. 439.6-445.6 dol ls to dol: same as above, grading to a fnly to silt-size-gran, calc dol; hematite flecks and stains; infrequent fn vugs; porosity poor to none.

619. 445.6-451.6 dol: calc, fossiliferous, sparsely crinoidal; med gr to med lt gr, fnly- to silt-size gran; infrequent fn, br-stained vugs; porosity poor.

620. 451.6-460.1 dol: sl calc, gr-br to lt med gr, micro- to silt-size-gran; porosity none.

621. 460.1-465.1 dol: arg, wh to v lt yel-gr, micro-gran; porosity none.

Units 622 to 629 constitute a distinct massive-appearing sequence. The uppermost beds (622-624) are very thin-bedded and slabby; they slump to form a ledge on top of the thick bedded units below. Locally the outcrop has a pitted surface caused by differential weathering. Chert is absent. Fossils and fragments are noted.

622. 465.1-466.6 ls: cherty, fragmental, oolitic, sl sndy, med- to fnly gran; infrequent grains of chert (?) or qtz; porosity none.

623. 466.6-468.6 dol ls: wh to v lt gr, micro-xln dol in micro-gran, calcite matrix; porosity none.

624. 468.6-473.8 dol: calc, pale pk-gr to wh, silt-size-xln; porosity none.

625. 473.8-476.6 dol: sl calc, pale pk-gr to v lt gr, silt-size-xln, partly saccharoidal; porosity fair to poor.

626. 476.6-485.3 dol: sl calc, fossiliferous, v lt gr, silt-size-xln, partly saccharoidal; infrequent fn vugs and occasional crse leached fossil vugs which are drusy w anhedral calcite; porosity fair to poor.

627.	485.3-493.6	dol: sl calc, fossiliferous, sparsely crinoidal, med gr to lt yel-gr to pale pk-gr, micro- to silt-size-xln; partly w abundant, fn vugs; infrequent crse calcite xls; porosity poor.
628.	493.6-497.6	dol: calc, lt br-gr, micro- to silt-size-xln; partly w black flecks surrounded by haloes of stain; porosity poor.
629.	497.6-509.7	dol: calc, fossiliferous, lt br-gr to lt yel-gr to pale pk-gr, micro-xln w med-xln fnly vuggy patches; porosity poor.

Base of section is not exposed.

WIND RIVER CANYON

Sampling was started in the NE/4 of Sec 32, T 7 N, R 6 E, at a location about 850 feet south of a point 1100 feet east of the quarter corner of sections 29 and 32. This location is about nine miles south of Thermopolis.

Amsden formation

No good outcrop of the lower Amsden sediments is found at this locality. Thin beds of sandstone and shale have been picked to mark the Amsden-Madison contact. The lower Amsden forms a mantle-covered saddle between the resistant Madison below and the uppermost, dolomitic Amsden. The uppermost beds of the Madison are thin- and medium-bedded. From residual cherts and varying thicknesses of this upper bedded portion, an erosional unconformity of appreciable extent is believed to mark the top of the Madison at this locality.

Unconformity—evidenced by residual cherts and varying thicknesses of uppermost Madison beds.

Mission Canyon formation

Units 466 to 470 constitute a thin- and medium-bedded series of limestones and dolomites which weather gray and brown. Chert nodules and lenses are present. Contacts between uppermost units are sharp.

466.	0-11.0	ls: cherty, lt br-gr, micro-gran and enclosing fn to med, indistinctly outlined chert grains; porosity none.
467.	11.0-18.5	dol: cherty, calc, wh, v fnly xln; porosity poor to none.
468.	18.5-23.3	ls: cherty, fossiliferous, fragmental, br-gr, med- to crsely gran w clear calcite matrix; porosity none.
469.	23.3-27.1	dol: calc, lt gr to med lt gr, v fnly to silt-size-gran, partly saccharoidal; porosity poor.

Units 470 to 484 constitute a massive sequence of limestones which weather to a blue-gray color. Chert nodules weather out brown; exposed fossils are silicified and weather brown also. Scattered, discontinuous, depositional breaks interrupt the massive character of the sequence. The outcrop surface is characterized locally by small valleys and ridges resulting from differential weathering. At its base this sequence grades into a breccia.

470.	27.1-35.2	ls: cherty, fossiliferous, lt br-gr, micro-xln; partly fragmental w fn to crse fragments in a clear xln calcite matrix; porosity none.
471.	35.2-41.2	ls: cherty, same as above; porosity none.
472.	41.2-49.2	ls: cherty, fossiliferous, fragmental, lt br-gr, fnly to v fnly gran w micro-xln matrix; porosity none.
473.	49.2-53.?	ls: cherty, same as above; porosity none.
474.	53.2-55.9	ls: cherty, same as above; porosity none; varies to a lt br-gr, micro-gran, calc dol; porosity none.
475.	55.9-62.4	ls: cherty, fossiliferous, fragmental, same as above; porosity none.
476.	62.4-68.4	dol ls and calc dol: cherty, fossiliferous, v lt gr, fnly to med-gran ls fragments w micro-xln, dol matrix; varies to a silt-size-xln, fossiliferous, dol; porosity none to poor.
477.	68.4-73.9	dol ls and calc dol: cherty, same as above; porosity none.
478.	73.9-83.4	dol ls and calc dol: cherty, same as above; porosity poor to none.
479.	83.4-89.8	dol ls and dol: partly same as above, partly a micro-gran, med lt gr dol w infrequent crse nests of calcite; porosity none.
480.	89.8-92.8	ls: conglomeratic, lt yel-gr to br-gr, micro-gran w infrequent nests of calcite; partly composed of granules to pebbles of lss in a matrix of fn to med, angular ss and fragmental lss; porosity poor.

481--483.

92.8-111.8 breccia: cherty, angular to subrnded cobbles to granules of lt gr, arg dols and v infrequent granular lss in an arg, sndy, calc matrix; euhedral pyrite, calcite veinlets in cobbles and in matrix; fragments of green sh in matrix; porosity none.

Units 484 to 492 constitute a sequence of thin-bedded strata which weather gray. These are generally covered by talus and mantle, making outcrops poor. Contacts are sharp to indefinite. Cherts are present in symmetrically shaped, gray-weathering spheroids. Fossils are absent.

484. 111.8-124.0 dol: partly breccia, lt gr, arg, micro-gran w scattered crse xls of pk calcite; basal portion a breccia of sndy, arg dols in a med-xln, partly arg, dol matrix enclosing fragments of sh; porosity poor.

485. 124.0-126.5 dol: med gr to med drk gr, micro-gran; infrequent crse, calcite-lined vugs; porosity poor.

486. 126.5-131.2 dol: med gr to med lt gr, micro-gran; veinlets of calcite; porosity none.

487. 131.2-136.7 dol: cherty, sl calc, lt gr to v lt gr, micro-gran; porosity none.

488. 136.7-139.7 dol: cherty, same as above w occasional angular granules of drk gr to v lt gr, micro-gran dol embedded; porosity none.

489. 139.7-144.0 dol: cherty, same as above; porosity none.

490. 144.0-149.0 dol: cherty, med gr, micro-gran w infrequent crse vugs; partly brecciated w lt gr, micro-gran dol filling fractures and cracks; conglomeratic at base; porosity none.

491. 149.0-155.3 dol: cherty, lt gr to med lt gr, micro-gran; infrequent fn vugs; hematite trcs; porosity none.

Units 492 to 511 constitute a cherty sequence of beds which weather tan and gray. Chert is present in nodules and lenses. The outcrop surface is smoothly granular and locally finely laminated. Beds vary in thickness from thin to medium, but locally they outcrop as a massive sequence. Fossils are absent.

492.	155.3-162.5	dol: cherty, partly banded, med gr, micro- to v fnly xln; infrequent crse vugs and nests of hematite; upper portion brecciated w calcite filling fractures; porosity poor to none.
493.	162.5-164.5	dol: cherty, conglomeratic, med lt gr; angular pebbles to granules of micro-xln dol in a wh, calc, micro-xln dol and crsely-xln calcite matrix; porosity poor.
494.	164.5-169.5	dol: cherty, med lt gr, micro-xln; porosity poor to none.
495.	169.5-173.8	dol: partly calc, partly banded, same as above w infrequent fn vugs; porosity none to poor.
496.	173.8-178.7	dol: calc, cherty, same as above; porosity none.
497.	178.7-181.7	dol; ls; med lt gr, intermixed micro-xln dol and calcite; porosity none.
498.	181.7-185.7	dol, ls: cherty, same as above; porosity none to poor.
499.	185.7-188.1	dol, ls: cherty, same as above.
500.	188.1-193.1	dol: cherty, v lt gr, micro-xln; porosity poor to none.
501.	193.1-201.1	dol: calc, partly banded, cherty, lt gr to v lt gr, micro-xln; porosity poor to none.
502.	201.1-206.9	dol: calc, cherty, lt gr, micro-xln; infrequent vugs w calc linings and calcite xls; porosity poor.
503.	206.9-213.3	dol: calc, partly banded, cherty, lt br-gr to med lt gr, micro-xln; porosity poor.
504.	213.3-218.5	dol: calc, very cherty, same as above; partly conglomeratic w angular pebbles and granules of chert, qtz, and dol in a xln calcite and arg, calc matrix; porosity none to poor.
505.	218.5-221.3	dol: cherty, med gr, micro-xln; occasional crse vugs partly lined w br-stained, anhedral calcite; porosity none.

506. 221.3-226.0 dol: cherty, same as above; porosity none.

507. 226.0-231.8 dol: calc, med gr, micro- to fnly gran; moderate fn vugs; porosity poor to fair.

508. 231.8-235.8 dol: sl calc, med gr to med lt gr, v fnly to silt-size-xln; moderate med vugs w br-stained calc linings; porosity poor to fair.

509. 235.8-244.8 dol: cherty, same as above w infrequent fn vugs; porosity poor to fair.

510. 244.8-250.3 dol: cherty, calc, same as above; porosity poor to none.

Units 511 to 525 constitute a series of indistinctly separated beds which weather to form bands with different shades of color. Cherts do not occur as lenses or beds; scattered gray nodules are present. The Mission Canyon-Lodgepole contact is difficult to define; lower portions of this sequence are brecciated; sediments above the brecciated interval resemble Mission Canyon sediments in lithology and outcrop form -- those below resemble Lodgepole sediments. The Mission Canyon-Lodgepole contact is believed to lie within the brecciated interval.

511. 250.3-253.0 dol: cherty, sparsely fossiliferous, calc, micro- to silt-size-xln; partly w abundant fn round vugs; porosity fair.

512. 253.0-256.7 dol: cherty, calc, conglomeratic, med lt gr to lt gr, micro-xln, sub-rounded dol fragments in a lt gr, micro-xln dol and xln calcite matrix; porosity none to poor.

513. 256.7-260.7 dol: cherty, med drk gr, micro-xln; moderate v crse vugs lined w anhedral calcite; porosity none.

514. 260.7-262.9 dol, calc to dol ls: med lt gr, micro-gran; infrequent crse vugs; porosity none.

515. 262.9-266.5 dol, breccia: cherty, med lt gr and v lt gr, angular, granule to pebble size fragments of micro-xln dol in a crsely-xln calcite and lt yel-gr dol matrix; soft, porous chert; porosity none to poor.

516--521. 266.5-288.9 dol, breccia: cherty, brecciated, same as above, porosity none.

522. 288.9-293.9 dol: cherty, brecciated, lt gr to med lt gr, micro-xln; interfragment calcite; infrequent crse vugs; porosity none.

523. 293.9-299.1 dol: calc, partly brecciated, med gr, micro-gran; porosity none.

524. 299.1-303.2 dol: cherty, sl calc, partly brecciated, lt br-gr, micro- to silt-size-xln; infrequent vugs surrounded by fnly-xln, dolomitized haloes; porosity poor to none.

Units 525 to 557 constitute a series of medium and thick beds (predominantly) which weather to black and shades of gray. Cherts are absent. Locally, thin-bedded portions slump to cause ledges and cliffs. Poorly discernible color bandings are present in the lower portions.

525. 303.2-305.7 dol: calc, lt br-gr, silt-size to v fnly xln and micro-xln; 1" of sndy dol w euhedral and subhedral qtz grains; porosity poor.

526. 305.7-308.2 dol: med gr, silt-size to v fnly xln; infrequent med vugs; porosity none.

527. 308.2-311.3 dol: calc, v lt gr, fnly to silt-size gran w intergranular calcite flour; partly a micro-gran, med gr dol; porosity poor to none.

528. 311.3-317.8 dol: conglomeratic at top w interfragment calcite, lt br-gr w wh mottlings, micro-gran dol; numerous fn to crse fragments of zoned chert; qtz grains; infrequent, drk red dolomitic inclusions w indistinct outlines; hematite stains in fractures; porosity none.

529. 317.8-319.3 dol: drk gr, fnly xln; porosity none.

530. 319.3-325.3 dol: partly banded, v lt gr, partly pk-gr, micro-xln; infrequent crse vugs drusy w calcite; porosity none to poor.

531. 325.3-331.6 dol: partly fragmental, wh to pk-gr to lt br-gr, silt-size to micro-xln; partly w indistinctly outlined, med to crse fragments of v fnly xln dol w a calcite matrix; porosity poor.

532.	331.6-334.8	dol: partly calc, pk-gr to lt yel-gr, micro- to silt-size-xln; infrequent crse vugs w dolomitized haloes; porosity poor.
533.	334.8-339.3	dol: med lt gr to lt br-gr, micro- to v fnly xln, partly med to fnly xln; porosity poor to none.
534.	339.3-342.3	dol: fossiliferous, pk-gr to lt br-gr, v fnly to micro-xln; partly w abundant fn vugs; porosity fair.
535.	342.3-345.8	dol: partly calc, lt yel-gr to lt br-gr, micro- to fnly xln; porosity poor to none.
536.	345.8-350.0	dol: fossiliferous, sl calc, pk-gr to lt br-gr, v fnly to fnly xln; infrequent fn vugs; porosity poor.
537.	350.0-354.1	dol: same as above; porosity poor.
538.	354.1-358.8	dol: same as above; porosity poor.
539.	358.8-360.5	dol: banded, lt yel-gr to med lt gr, v fnly xln; infrequent fn vugs; porosity none.
540.	360.5-362.7	dol: arg, lt gr to v lt gr, micro-gran; porosity none.
541.	362.7-369.4	dol: fossiliferous, med lt gr, v fnly to fnly xln; infrequent blue-gray, indistinctly outlined, calc inclusions; porosity poor to none.
542.	369.4-374.4	dol: same as above; porosity none to poor.
543.	374.4-379.7	dol: calc, partly conglomeratic w well-rnded granules and pebbles of med drk gr, micro-gran dol in a lt gr, micro- to silt-size-xln dol matrix; hematite stains; porosity none.
544.	379.7-385.5	dol: conglomeratic, rnded and angular granules and pebbles, same as above; calcite in fractures; sh, 1" fissile, green w qtz clusters; porosity none.

545.	385.5-389.2	dol: fossiliferous, calc, lt gr to med lt gr, micro- to v fnly xln; partly moderately crsely vuggy (leached fossil casts); porosity poor but quite variable.
546.	389.2-391.2	dol: fossiliferous, calc, same as above; infrequent vugs; porosity as above.
547.	391.2-395.7	dol: fossiliferous, calc, v fnly xln w micro-xln patches; moderate v fn to fn vugs; porosity as above.
548.	395.7-401.1	dol: cherty, fossiliferous, calc, same as above w or-yel stained fractures; frequent crinoid casts; porosity as above.
549.	401.1-407.6	dol: fossiliferous, calc, v fn to micro-xln; partly w occasional crse to fn vugs; frequent crinoid casts; porosity as above.
550.	407.6-414.1	dol: fossiliferous, calc, same as above; porosity as above.
551.	414.1-419.1	dol: fossiliferous, calc, same as above w or-yel calcite linings in vugs; porosity as above.
552.	419.1-423.3	dol: fossiliferous, calc, same as above; porosity as above.
553.	423.3-430.8	dol: fossiliferous, calc, same as above; porosity as above.
554.	430.8-436.8	dol: fossiliferous, calc, same as above; porosity poor.
555.	436.8-441.5	dol: partly fossiliferous, lt br-gr to lt gr, fnly to v fnly xln, partly w moderate fn and med vugs; porosity poor to none.
556.	441.5-446.2	dol: same as above; porosity poor to none.

Units 557 and 558 form a transition zone between "good" Madison and "good" Bighorn. The upper contact of unit 557 is somewhat gradational while the lower contact of 558 is an irregular, mildly undulating surface. This interval, which marks the Madison-Bighorn unconformity, may be Devonian.

557.	446.2-451.9	dol: calc, v lt gr, med- to crsely xln; camps of green, waxy sh; hematite anhedrons and subhedrons; porosity poor to fair.
558.	451.9-453.4	dol: calc, sandy; ss: same as above, grading into a crsely to med-gran, partly friable ss of spherical, subrnded to rnded qtz grains; porosity poor to fair.

Bighorn Dolomite

559.	453.4--	dol: v sl calc, lt gr w moderate red stains, fnly xln w patches v fnly to micro-xln; occasional crse vugs; infrequent crinoid section casts; porosity poor to fair.

TENSLEEP CANYON

Section measured in Sec 5, T 47 N, R 87 W. Sampling started just north of the Doyle residence located about two miles downstream from the State Fish Hatchery. Surveyed thicknesses varied from 475 feet to 525 feet.

Amsden formation

30'-50' Cross-bedded sandstone of subrounded to angular, medium-granular, quartz; locally stained red from overlying sediments.

0'-10' Thin-bedded, red, silty shale; characteristic of basal Amsden in nearby areas but absent at this locality.

Unconformity--An undulating surface of varying amplitude; limestone conglomerates and sand-cemented breccias common; channeling action to 10 feet depth.

Mission Canyon formation

Units 1-10 constitute a ledge-forming series of thin to medium-bedded strata which weather from buff to tan and are locally red-stained. Contacts between units sharp and partly marked by shale breaks.

1.	0-5.5	dol: calc, sl sandy, yel-gr, v fnly gran w occasional crse calcite xls; minor fn vugs; porosity poor.
2.	5.5-9.3	dol: cherty, sparsely crinoidal, lt yel-gr, v fnly to fnly gran; sparse, crse, br-stained vugs drusy w calcite and qtz; porosity poor to fair.
3.	9.3-12.5	dol: partly sndy, sparsely crinoidal, lt gr, v fnly to micro-gran; moderate med and crse vugs stained brown by hematite; partly brecciated; porosity none to poor.
4.	12.5-19.8	dol: partly arg, lt gr, v fnly to micro-gran; infrequent crse clacite xls and veinlets; partly breccia w pale green, calc matrix; porosity none to poor.
5.	19.8-22.9	dol: partly sndy and arg, yel-gr to tan, micro-gran; infrequent v crse vugs drusy w qtz; $\frac{1}{4}$" seam of v fn, angular qtz ss; 3" of lensing, yel-green sh; porosity none to poor.

6.	22.9-30.9	dol: partly arg, pk-gr to tan, micro- to fnly gran; infrequent med vugs; haloed hematite anhedrons; porosity poor to none.
7.	30.9-35.4	dol: partly arg and sndy, yel-gr to tan, micro-gran; infrequent v crse vugs w calcite; porosity poor.
8.	35.4-49.9	dol: calc, arg, cherty, yel-gr, micro-gran; fnly xln haloes surround crse, br-stained, drusy qtz vugs; partly pebble breccia w v crse calcite nests in calc matrix; porosity poor.
9.	49.9-52.1	dol: calc, yel-gr, micro- to fnly gran; fnly xln haloes surround moderate fn to crse vugs partly drusy w qtz and calcite; porosity poor to fair.
10.	52.1-54.9	dol: med gr, partly br-flecked, micro-gran; porosity none.

Units 11-31 constitute a laterally varying sequence which weathers blue-gray to tan. Uppermost portions are thickly to thinly bedded. Basal sections grade from massive rocks to rocks which are vaguely stratified with discordant attitudes. This sequence grades into a conglomerate-breccia.

11.	54.9-58.9	dol: cherty, calc, med gr to lt yel-gr, micro-gran; varies to yel-gr, fnly to med-xln dol w moderate med drusy qtz vugs; porosity fair to poor.
12.	58.9-62.4	dol: same as above.
13.	62.4-70.9	dol: same as above.
14.	70.9-73.2	dol: calc, cherty, drk to lt gr, partly br-stained, micro-gran w moderate crse and med vugs; partly breccia w v crse calcite xls in calc matrix; porosity poor.
15.	73.2-75.2	dol: cherty, med lt gr to yel-or, micro-gran; locally fractured w interfracture qtz xls; porosity poor to none.
16.	75.2-78.7	dol: calc, lt pk-gr to lt yel-gr w br hematite flecks, micro-gran w crse calcite xls; occasional vugs drusy w calcite; porosity poor to none.

Sample 17 marks the top of a distinct massive sequence which forms an irregularly rounded outcrop. In uppermost portions of the sequence depositional horizons weather out locally to produce a bedded effect.

17.	78.7-86.9	ls: partly sndy and siliceous, cherty, stylolites, lt br-gr to med lt gr, micro-gran to sublithographic w occasional crse calcite xls; partly v fnly to v crsely fragmental and oolitic w micro-xln matrix; porosity none.
18.	86.9-96.2	dol: v calc, cherty, lt med gr to lt yel-gr, partly br-gr, v fnly to fnly xln, scattered fn vugs; porosity poor. ls: 1'; fossiliferous, lt br-gr, fnly xln; porosity none.
19.	96.2-101.0	dol: 1.8'; calc, lt yel-gr, v fnly xln w occasional fn, partly calcited vugs; porosity poor. ls: fossiliferous, partly crinoidal, cherty, med lt gr, fnly to med-xln; porosity poor to none.
20.	101.0-106.5	dol: 2'; calc, cherty, lt yel-gr, partly br-flecked, fnly xln w crse calcite xls; occasional fn vugs; porosity fair. ls: cherty, fossiliferous, lt gr to lt yel-gr; v fn to crse, irregularly-rnded fragments in a micro-xln matrix; porosity poor to none.
21.	106.5-110.8	ls: fossiliferous (partly silicified), cherty, med lt gr, fnly xln; partly w med to crse, irregularly-rnded fragment s in a micro-xln, calcite matrix; porosity none.
22.	110.8-118.0	ls: same as above.
23.	118.0-123.4	ls: same as above.
24.	123.4-133.6	ls: same as above

25-31—these samples are listed collectively since they were taken laterally.

133.6-144.1 ls: same as above; basal portions a cg consisting of cobbles of fragmental ls in a fragmental matrix; locally cavernous.

Units 32-36 constitute a persistent breccia sequence of varying thickness which weathers out to form caves with overhanging cliffs. Uppermost units are characterized by occasional cobble to small boulder erratics embedded in massive rock. Downward this grades from a cobble to a granule breccia with laterally vanishing, rude lines of stratification. The base of this sequence is an irregular, undulating surface.

32. 144.1-154.3 dol ls: fossiliferous, med lt gr to v lt gr, fnly and med-xln; poorly outlined granules of pale greenish-gr material embedded; scattered med vugs drusy w calcite; laterally contains cobbles of br-gr fragmental ls, br-gr fnly gran ls, gr fnly xln dol, and chert; porosity poor.

33. 154.3-161.3 ls: cherty, med drk gr, micro- to fnly xln; varies laterally to a poorly sorted breccia w fragments of yel-or silt-size to v fnly gran dol, med gr fnly to micro-xln ls, lt br-gr micro-xln ls, fragmental dol ls, and chert in a lt yel-or to lt yel-gr, calc, arg dol matrix; porosity poor to none.

34. 161.3-169.8 breccia: subrnded to angular, cobble to granule fragments of dol, ls, dol ls, cherts, and breccia in a micro-gran, arg, partly hematitic dol matrix; fragments partly outlined w hematitic stains; porosity none.

35. 169.8-179.0 breccia: same as above.

36. 179.0-184.5 breccia: rnded to angular pebbles and granules of lt br-gr, micro-xln to sublithographic lss and med gr, micro-xln dols in a gr, calc, arg dol matrix w hematite streamers; porosity none.

37. 184.5-190.3 dol: arg, med lt gr to pk-flecked gr to yel-gr, micro-gran w tiny calcite veinlets and dendritic hematite seams; porosity none.

Units 38-54 constitute a distinct cliff-forming series; thickly bedded near top and pseudo-bedded downward by laminations on weathered surface; fresh surfaces massive; solution breccia at base of sequence. On weathered surface color varies from light brown in silicified portions to medium gray in unsilicified portions. Chert lenses and beds are less conspicuous than in the above sequences.

38.	190.3-193.3	dol: partly arg, med gr to med lt gr, v fnly to micro-xln w occasional crse calcite xls; infrequent fn vugs; porosity none to poor.
39.	193.3-199.5	breccia: pebbly, angular fragments of fnly to v fnly xln, med gr dol; matrix of lt gr-yel, micro-gran dol and crsely xln calcite; porosity poor.
40.	199.5-206.0	dol: partly silicic, cherty, med gr to lt yel-gr, v fnly to micro-gran; calcite veinlets; porosity none.
41.	206.0-218.5	dol: silicic, sl cherty, pk-gr to lt gr, v fnly xln w scattered med vugs drusy w qtz; porosity poor.
42-45--	218.5-251.9	dol: same as above.
46.	251.9-254.8	dol: v calc, lt yel-gr, v fnly to fnly xln; porosity poor (?).
47.	254.8-261.6	dol: silicic, yel-gr, v fnly to fnly xln; porosity poor to none.
48.	261.6-267.2	dol: partly silicic; partly calc, yel-gr to lt gr, v fnly xln; porosity none to poor.
49.	267.2-272.8	dol: same as above w drusy qtz in scattered crse vugs; porosity poor.
50.	272.8-279.8	dol: same as above.
51.	279.8-284.8	dol: same as above; cherts; basal contact irregular; porosity poor.
52.	284.8-295.5	dol: solution-worked breccia; cobble to pebble fragments of partly silicic, cherty, calc, yel-gr to lt gr, v fnly to fnly xln dol in matrix of same material; porosity none.
53-54--	295.5-308.7	dol: solution-worked breccia, same as above; basal contact of 54 irregular.

Lodgepole formation

Units 55-65 constitute a cliff-forming sequence of thick to thin beds, which weather light gray to dark brownish gray distinct from the above sequence. Lowermost portions of this sequence weather to form a talused slope. Bedding planes are characterized by calcareous, shaly partings. Chert is conspicuous by its absence on the outcrop. Cross bedding is sporadically present.

55.	308.7-318.6	dol: partly oolitic and calc, lt gr w bl flecks, fnly xln; scattered med vugs drusy w qtz; partly yel-gr, micro-xln; porosity fair.
56.	318.6-322.4	dol: same as above, porosity fair to med.
57.	322.4-326.3	dol: same as above, porosity fair.
58.	326.3-333.6	dol: same as above, silicic and w drusy qtz in occasional crse vugs; porosity fair.
59.	333.6-347.9	dol: same as above w fewer oolites; scattered crse calcite xls; porosity fair.
60.	347.9-349.0	dol: calc, partly silicic, lt br-gr to med gr, micro-gran to fnly xln; porosity poor to none.
61.	349.0-355.8	dol: calc, partly silicic, yel-gr to sl pk-gr, fnly to med-gran; moderate med vugs w drusy calcite and qtz; 0-3" bed of calcite at base; porosity poor.
62.	355.8-361.7	dol: calc, partly silicic, lt gr, v fnly gran; minor fn vugs w drusy qtz; partly yel-gr, fnly xln, abundant fn vugs; porosity fair.
63.	361.7-365.1	dol: calc, lt gr to lt yel-gr, v fnly to fnly gran w occasional crse calcite xls; porosity poor.
64.	365.1-373.3	dol: calc, lt med gr, v fnly to fnly xln; occasional fn vugs drusy w qtz; partly a lt yel-gr, fnly to med-gran ls; porosity poor to none.
65.	373.3-378.4	dol: sl calc, med drk gr to med lt gr, v fnly gran; occasional fn vugs drusy w qtz; small nests of crsely xln calcite; porosity poor.

66. 378.4-381.2 dol: sl fossiliferous, sl calc, gr-bl to med gr, v fnly xln w a few crse calcite xls; minor br-stained fn vugs; porosity none.

67. 381.2-382.9 dol: partly calc, med lt gr to lt pk-gr, fnly gran; occasional vugs; porosity poor.

68. 382.9-385.5 dol: med lt gr to pk-gr, fnly gran w nests of crse calcite; moderate pin point vugs; porosity poor.

69. 385.5-394.2 dol: sl fossiliferous (?), lt gr and partly pk-gr, fnly to v fnly gran; occasional crse, yel-stained vugs; nests and xls of crsely xln calcite; deformed lines of stratification; porosity poor.

70. 394.2-396.0 dol: partly calc, med gr to sl pk-gr and yel-gr, v fnly and fnly gran; porosity poor.

71. 396.0-398.1 dol: partly sl calc, gr-bl to pk-gr, micro-gran w moderate to abundant crse vugs drusy w calcite; porosity poor.

72. 398.1-406.7 dol: fossiliferous, med gr to or-pk, and lt br-gr, v fnly to micro-gran; occasional fn yel-stained vugs; porosity poor.

73. 406.7-411.7 dol: fossiliferous, lt br-bl to lt pk-gr, partly stained drk yel-or, v fnly gran; scattered fn, yel-stained vugs; indistinctly outlined, gr-green, calc, arg, granule-sized inclusions; partly med lt gr, v fnly to med-gran ls; porosity poor to none.

74. 411.7-414.7 dol: fossiliferous, sparsely crinoidal, laminated by hematitic bands, lt med gr, partly br-stained, v fnly to micro-gran; infrequent med vugs; porosity poor.

75. 414.7-417.1 dol: partly arg, partly fossiliferous, sl yel-gr to pk-gr, fnly gran; crse rnded xls of calcite; moderate crse vugs; med gr pebbles of arg dol; porosity poor to none.

76. 417.1-423.1 dol: lt med gr to yel-gr w color bandings, micro- to silt-size gran; deformed lines of stratification; porosity none.

77. 423.1-426.0 dol: partly arg, med gr to yel-gr, micro-gran; scattered clusters and xls of qtz, nests of crsely xln calcite; partly a pebble size cg of rnded to subrnded fragments of micro-gran, lt med gr dol in arg, calc matrix; contacts irregular; porosity poor to none.

78. 426.0-433.7 dol: partly arg, med gr to br-gr w color handings, micro-gran; crse calcite xls; partly cobble to pebble cg of green, pk and gr dol in yel-gr matrix w scattered chert and qtz grains; porosity poor.

Units 79-91 constitute a series of thick and medium beds which outcrop as a banded massive sequence. Units are medium-bedded near top and base of sequence, more thickly bedded in center. This sequence is characterized by a sporadically pock-marked, irregular surface which weathers from a grayish-black through deep grayish-brown to moderate brown, distinct from the above sequence.

79. 433.7-446.1 dol: partly calc, sparsely fossiliferous, partly banded, med lt gr w br and pk stains, v fnly and fnly xln; infrequent crse vugs; trcs of qtz grains; porosity poor.

80. 446.1-450.8 dol: calc, partly fossiliferous, med lt gr, v fnly to fnly xln; drusy calcite in br-stained vugs; porosity poor to fair.

81. 450.8-456.8 dol: med gr, micro-xln, thin horizons of leached fossil vugs drusy w calcite; porosity poor.

82. 456.8-462.8 dol: sparsely crinoidal, med lt gr, v fnly to micro-xln; scattered fn to crse vugs drusy w calcite; partly breccia w rudely stratified, soft calc, arg, matrix; porosity poor.

83. 462.8-466.4 dol: same as above; basal contact irregular; porosity poor to fair.

84.	466.4-472.1	dol: sl calc, partly silicic, fossiliferous, lt gr to sl yel-gr w pk stains, fnly xln; partly moderately crsely vuggy from leached fossils; porosity poor to fair.
85.	472.1-478.6	dol: same as above.
86.	478.6-482.6	dol: same as above
87.	482.6-491.5	dol: same as above.
88.	491.5-497.0	dol: same as above.
89.	497.0-505.0	dol: same as above
90.	505.0-515.5	dol: arg; same as above; porosity poor.
91.	515.5-518.7	dol: arg, fossiliferous, med lt gr, micro-gran to v fnly xln; minor or-stained fn to med vugs; trcs hematite anhedrons; porosity poor to none.
92.	518.7-522.0	dol: arg, fossiliferous, silty, yel-or to yel-gr to lt med gr w thin hematitic laminations, micro-gran; drusy and anhedral calcite in or-stained vugs; porosity poor.

KINDERHOOKIAN(?) and DEVONIAN(?)

Unconformity in Unit 93.

93.	522.0-524.0	ss to pebbly cg: 0-2'; conodonts, fish remains, sh and dol pebbles and accessories in ss of med to crse, well-rnded and angular, partly highly frosted, spherical, silica-cemented qtz; the ss which overlies and channels into a 2' bed of dol is capped by a 1/8" layer of micro-gran, compact hematite. dol: 2'-0'; fossiliferous, lt gr w or-yel flecks and stains, v fnly xln; yel-or-stained vugs; porosity poor to none.
94.	524.0-544.0	dol:, ss:, sh:, sndy dol: large scale solution action and lensing in this unit.

Unit 94 cont'd		dol: v cherty, sparsely fossiliferous, partly siliceous, bright sulphur yel, saccharoidal; partly sndy, drk red, micro-gran; partly v cherty, fossiliferous, lt gr to red, v fnly gran. Sediments of unit 94 embody large solution cavities (up to 10') filled with ss and sh.
95.	544.0-564.0	dol: arg, v fnly laminated, thinly bedded, pale red to lt gr, micro-gran; thin, solution-worked conglomeratic horizons of wh, micro-gran, calc dol to ls at base.

Bighorn formation

SHELL CANYON

Sampling started on the north side of the canyon in Sec 17, T 53 N, R 90 W at a location about ¼ mile above the highway bridge across Shell Creek just upstream from the Paton Ranch. Madison thickness is measured from the Amsden-Madison unconformity. Surveyed thicknesses varied from 625 feet to 650 feet.

Amsden formation

20' approximately — Thick bedded, finely to medium-granular sandstone which weathers brownish-gray.

0'-10' — Red, waxy-looking, impure siltstone to silty shale which crops out very infrequently.

Unconformity--The unconformable Amsden-Madison contact on the south side of the canyon is best viewed from across the canyon. From here variations in weathered color are easily discernible. The contact is an irregular, undulating surface of varying amplitude and is characterized by sand cemented breccias, thin sandstone lenses, sandstone filled channels, and cavity fillings to a depth of 60 feet below the contact.

Mission Canyon formation

Units 96-100 constitute a poorly defined, deeply weathered sequence of ochre colored beds which are generally covered on the north side of canyon. Contacts are obscured by breccia action, channeling, and sandstone cavity fillings. Outcrops are generally poor.

96. 0-12 — ls: 9'; silicic, v sparsely crinoidal, sndy, lt br-gr, micro-xln w infrequent crse calcite xls, occasional fn vugs; partly med gr, v fnly to med-gran ls grains in a micro-xln matrix; hematite and solution stains along fractures and in vugs, partly a cherty breccia w sndy matrix; porosity poor to none.
ls: 3'; algal.

97. 12.0-22.0 — ls: cherty, lt olive br, partly pk-stained, micro-xln to sublithographic w v crse nests of crsely xln calcite; porosity none.

98. 22.0-26.0 — ls: cherty, pale pk to lt olive br, micro-xln, w small settlements of qtz; hematite stains; porosity none.

99. 26.0-30.0 ls: partly silty and arg, lt yel-gr to red, v fnly to micro-gran; porosity poor to none.

100. 30.0-40.0 ls: arg, silty, pk to lt red, partly laminated, micro-gran w scattered fn qtz subhedrons and clusters; partly w pebbles of med gr, fragmental ls; porosity none.

Units 101-106 constitute a cliff-forming sequence--medium- to thick-bedded at top and massive at the base--of rocks which weather blue-gray to orange-gray and are locally red-stained. Contacts are sharp but undulatory, and partly marked by shale breaks. The basal massive portion varies in thickness and grades into a breccia.

101. 40.0-49.6 ls: cherty, styolites, lt br-gr to lt gr, sublithographic to micro-xln; hematite saturations along fractures; porosity none.

102. 49.6-54.7 ls: cherty, yel-gr, micro-xln w occasional crse calcite xls; hematite tros; porosity none.

103. 54.7-61.2 ls: fossiliferous, partly pk-stained, same as above; porosity none.

104. 61.2-69.6 ls: same as above.

105. 69.6-75.1 ls: fossiliferous, partly conglomeratic, sparsely cherty, red- and br-stained, gr, micro-xln and micro- to fnly fragmental w micro-xln matrix; occasional crse to fn calcite xls; well-rnded pebbles of micro-xln to sublithographic, lt br-gr ls embedded; porosity none to poor.

Near the top of this sequence boulder to cobble erratics of fragmental ls are enclosed in a micro-xln ls matrix; this grades into a granule to cobble breccia of dols and lss w a micro-gran to med-gran, partly red-stained matrix. Laterally vanishing lines of rude stratification are present in lower portions.

106. 75.1-91.9 ls: fossiliferous, cherty, lt yel-gr to pk-flecked gr to wh, fnly to crsely xln; porosity none.

107-108.
91.1-108.1 ls: same as above; partly fragmental.

109-110.		
	108.1-125.9	ls: cherty, fossiliferous, lt gr, crsely gran, rnded fragments enclosing indistinctly outlined, rnded cobbles of same; porosity poor.
111.	125.9-136.9	ls: same as above at top grading downward to a well-defined, persistent breccia which weathers out caves and forms abrupt cliffs; porosity poor.
	136.9-157.0	This sequence is plainly visible but inaccessible; the base of this breccia is an irregular, undulating surface of varying amplitude; porosity at base varies from good to none.
112.	157.0-167.0	dol: partly chalky-looking, sl calc, arg, v lt gr to lt yel-or; partly pk-stained, micro-gran; hematite seams; locally find up to 6' thick lenses of greenish-gr to pale yel-green, calc, silty, non-fissile shale overlying this unit; porosity none.

Units 113-129 constitute a cliff-forming sequence of thick and medium beds which are ledge-forming in the lower units and which appear massive when viewed from a distance. Weathered color varies from orange-gray to grayish-black; laminations are present on the weathered surface, absent on fresh surfaces; chert is present in lenses and beds. Bedded breccia is present at base of sequence.

113.	167.0-173.5	dol: sl cherty, med lt gr, micro-gran infrequent crse vugs; partly a pebble breccia of v lt gr to wh dol in a green to yel-or, arg, calc matrix; porosity poor to none.
114.	173.5-187.5	dol: cherty, partly silicic, partly calc, v lt gr to wh, micro- to v fnly xln; mihor fn vugs; porosity poor to none.
115.	187.5-196.0	dol: same as above; not silicic.
116.	196.0-202.8	dol: same as above w moderate med vugs drusy w anhedral calcite and chert; porosity poor.
117-119		
	202.8-224.7	dol: same as above; silicic.

120.	224.7-230.5	dol: v calc, chalky, gr-wh to lt yel-gr, v fnly xln; trcs of hematite; porosity poor to fair.
121.	230.5-240.5	dol: sparsely fossiliferous (?), silicic, med lt gr, micro- to fnly xln; scattered qtz xls; porosity poor.
122.	240.5-256.1	dol: sl arg, v calc, gr-wh, micro-gran; porosity poor.
123-124.	256.1-275.2	dol: same as above; silicic.
125.	275.2-282.4	dol: cherty, partly silicic, lt gr, micro- to fnly xln; porosity poor.
126.	282.4-293.5	dol: cherty, partly silicic, sparsely fossiliferous, med lt gr to lt yel-gr, partly pk-gr, v fnly xln; porosity poor to fair.
127.	293.5-305.5	dol: cherty, sl calc, hematite trcs, med lt gr to lt yel-gr, micro-gran w infrequent crse and med vugs; porosity fair (?).
128.	305.5-310.0	dol: same as above.
129.	310.0-317.0	dol: breccia; pebble to v crse fragments of silicic dol w micro-gran, arg, calc matrix; lenses of lt yel-gr, v fnly xln dol in the breccia; porosity poor to fair.

Lodgepole formation

Units 130 to 154 constitute a cliff-forming series of thick and medium beds which weather to a darker shade than the above bedded sequence but have beds which weather light gray at top of sequence. Chert is conspicuous by its absence on the weathered surface. Cross-bedding is sporadically present.

Units 154-164 constitute a darker weathering series which outcrop as a band throughout canyon. The base of this sequence is marked by channeling, breccias, and the appearance of chert; basal units weather to form a small talused slope.

130.	317.0-321.9	dol: calc, partly arg, v lt gr to wh, micro-gran, w occasional crse vugs partly filled w hematite; 3" breccia zone in center of unit; porosity poor.
131.	321.9-328.9	dol: cherty, v lt gr, v fnly to micro-gran; hematite trcs; porosity poor.
132.	328.9-335.5	dol: cherty, calc, med gr, partly gr-or, irregularly shaped patches of micro-xln, silicic dol in v fnly xln dol; moderate med br-stained vugs lined w fn chert ovoids; porosity poor to fair.
133-134.	335.5-344.8	dol: same as above.
135.	344.8-349.8	dol: fossiliferous, med gr, v fnly to micro-xln, moderate med vugs w anhedral hematite flecks and stains; porosity fair.
136.	349.8-354.8	dol: same as above; more vuggy; porosity fair.
137.	354.8-363.1	dol: same as above; partly w lt br color; porosity poor to fair.
138.	363.1-371.0	dol ls: fossiliferous, wh and med gr speckled; fnly to med-xln, dol rhombs mixed w and embedded in v fnly to crsely gran ls; porosity none to poor.
139.	371.0-377.3	dol: fossiliferous, calc, lt br-gr, v fnly gran w intergrain calcite flour, partly w moderate crse vugs; porosity poor.
140.	377.3-385.1	dol: same as above; porosity poor.
141.	385.1-388.1	dol ls: wh and med gr speckled; v fn to crsely gran; subrnded to angular remnants of micro-gran, lt br-gr ls in a matrix of v fnly xln dol; porosity none to poor.
142.	388.1-394.2	dol and dol ls: gradational lithology of 140 and 141; porosity poor.

143.	394.2-402.6	dol: med lt gr and pale gr-or, v fnly gran w minor med vugs, hematite trcs; porosity poor to fair.
144.	402.6-409.9	dol: med gr w yel-or flecks and stains, v fnly xln; partly enclosing crse rnded ls slx; porosity poor.
145.	409.9-414.9	dol: calc, med lt gr, micro-gran w minor fn vugs; porosity none.
146.	414.9-418.1	dol: calc, lt br-gr to lt gr, micro- to fnly gran; moderate med vugs w or-gr, calc linings; porosity poor to fair.
147.	418.1-424.5	dol: same as above; porosity poor to fair.
148.	424.5-432.7	dol ls: stylolites, mottled lt yel-gr and lt gr, crsely and med-gran ls fragments ? in a v fnly gran dol matrix; porosity poor.
149.	432.7-442.7	dol: fossiliferous, stylolites, lt br-gr to med gr, v fnly gran, w minor med vugs; porosity poor to fair.
150.	442.7-448.0	dol ls: med gr and wh speckled, crsely and med-gran, rnded ls fragments ? in a v fnly xln dol matrix; porosity poor to none.
151.	448.0-449.2	dol: med drk gr w yel-or flecks, micro-xln w v crse nests of crsely xln calcite; porosity none.
152.	449.2-454.0	dol ls: fossiliferous; med gr and wh speckled, crsely and med-gran rnded ls fragments ? in a v fnly xln dol matrix; porosity none.
153.	454.0-459.0	dol ls: same as above; partly micro-gran, drk reddish-gr dol; porosity none.
154.	459.0-463.7	dol ls: fossiliferous, silty, med gr to pale purple; med- and crsely gran, rnded ls fragments in a micro-gran dol matrix; partly w hematite flour cement; porosity none.
155.	463.7-467.4	dol ls: same as above, gr to reddish-purple, hematite cement; porosity none.

156. 467.4-472.9 dol ls: same as above; partly a cg of well-rnded granules and small cobbles of fragmental and oolitic, purple ls in a similar matrix; porosity none.

157. 472.9-479.2 dol ls: same as above; oolitic; minor amounts of dol matrix; porosity hone.

158-159 479.2-487.5 dol ls: same as above, but w minor amounts of dol matrix; porosity none.

160. 487.5-490.3 dol: v calc; v dusky reddish purple to gr-red and purple to med lt gr, laminated, micro-gran; hematite flour; fnly vuggy; partly w ls fragments embedded; porosity poor.

161. 490.3-498.1 dol: arg, pale purple to gr-purple, micro-gran; porosity poor.

162. 498.1-502.9 dol: arg, med lt gr to pale reddish-purple laminations, partly pk-gr to v lt gr, micro-gran dol; channeling actions; 6" lensing zones of calc pebbles; basal contact irregular; porosity none.

163. 502.9-510.3 dol: cherty, arg, gr-wh to wh, micro-gran; 6" to 1' of breccia in center and 2' to 1' of breccia at base w abundant nests of crsely xln calcite; porosity none.

Deposition of unit 162 clearly followed after brecciation had occurred, for bedding laminations are completely conformable to the irregular surface of the uppermost breccia.

164. 510.3-516.8 dol: arg, partly brecciated, same as above.

Units 165-179 form a distinct cliff-forming sequence which is well-banded. Banding is caused by variations in lithology which weather differently--dolomite to a dark brownish gray; limestone (dolomite limestone) to a bluish-gray to medium gray. The dolomite and limestone bands though clear and distinct are gradational into each other.

165. 516.8-522.0 ls: lt br-gr to lt gr, micro-gran; partly med-gran w micro-xln matrix; hematite anhedrons, infrequent qtz xls; porosity poor to none.

166.	522.0-528.3	ls: stylolites; sl cherty, lt gr to v lt gr, v fn and partly crse fragments and oolites in a micro-xln matrix; porosity none.
167.	528.3-534.5	dol: sl calc, v sl cherty, med gr to moderate br, v fnly xln, saccharoidal; scattered med vugs; porosity medium to good. ls: 8", lt gr, fragmental.
168.	534.4-538.9	ls: stylolites, med gr to moderate br, v fn fragments and oolites in a micro-xln matrix; porosity none.
169.	538.9-548.9	dol: 1', br-gr, fnly xln, saccharoidal; porosity good. ls: 9',lt gr, v fn to med fragments and oolites in a micro-xln matrix; porosity none.
170.	548.9-556.8	ls: 4',same as above, wh grades to saccharoidal dol as above w br-stained vugs; unit porosity poor to fair.
171.	556.8-562.2	ls: fossiliferous, oolitic, lt br-gr to lt med gr, med-gran; grades to a dol ls at base w ls oolites in a v fnly xln dol matrix; porosity poor to fair.
172.	562.2-567.6	dol: 2', partly crinoidal, br-gr to med lt gr, v fnly to fnly xln, saccharoidal; porosity good. dol ls: 3.4', stylolites; lt med gr to lt br-gr, fn to crse ls fragments and oolites in a v fnly xln dol matrix; porosity none.
174.	571.6-576.0	dol: calc; same as above; infrequent fn vugs w anhedral calcite; porosity poor to fair.
175.	576.0-584.8	dol: 3.5', br-gr to med lt gr, v fnly xln, partly saccharoidal; porosity fair. dol ls: 4.5', fossiliferous, lt br-gr, to lt gr, fn to v crse ls fragments and oolites in a v fnly xln, calc dol matrix; porosity none.

176. 584.8-591.3 dol ls: 4.6', fragmental as above.

dol: 1.7', calc, br-gr to med lt gr, v fnly xln w inter-xl calcite flour; porosity poor to none.

177. 591.3-597.1 dol: calc, partly saccharoidal, lt br-gr, partly stained pale red, v fnly xln; minor fn vugs; porosity poor.

178. 597.1-605.3 dol: same as above; porosity poor to fair.

Units 179-187 constitute a medium-bedded sequence which locally weathers out to cause slumping and talus. Weathered surface is cavitied and pitted.

179. 605.3-614.1 dol: calc, fossiliferous, lt gr, v fnly xln and partly micro-xln w abundant fn and med vugs and leached fossil fragments which are br-stained and drusy w anhedral and subhedral calcite; porosity fair.

180. 614.1-618.4 dol: same as above w numerous crinoid casts; porosity poor.

181. 618.4-622.7 dol: same as above w br-stained vugs; porosity none to poor.

182. 622.7-629.4 dol: same as above; porosity none to poor.

183. 629.4-635.7 dol: same as above; porosity none to poor.

184. 634.7-639.7 dol: calc, lt gr, micro-xln; moderate vugs w or-gr calc linings; numerous leached fossil fragments; porosity none to poor.

185. 639.7-647.0 dol: calc, stylolites, lt gr, partly w or-yel stains, micro-gran; partly laminated w 1/8" red-stained layers of med gr calc sh; porosity none to poor.

186. 647.0-650.8 dol: calc, stylolites, lt gr, partly w or-yel stains, micro-gran; porosity none.

187. 650.8-651.5 dol: 7", sndy, arg; lt med gr, micro-gran.

ss: 2"-1', crse to fn, well-rnded and frosted, partly angular, high sphericity qtz w infrequent glauconite grains and accessories; porosity none.

sh: ½"-0, black, fissile, calc.

KINDERHOOKIAN(?) and DEVONIAN(?)

Locally this ss of varying thickness becomes quartzose, and contains large, pebble-size, phosphatic, sandy, concretions. Fish bones, immature brachiopods, and conodonts are found in the ss. Locally a 1/8" layer of micro-gran hematite covers the irregular ss bed. A marked unconformity exists within unit 187 just above the sandstone; this sandstone is believed to be older than Osagean.

Units 188-202 constitute a ledge-forming sequence which locally forms a talused slope below the Madison. Chiefly dolomites, these rocks are argillaceous and silty to sandy with some beds of pebble to granule conglomerate. Lensing and channeling characterize the uppermost units, which vary in color from pink to pale green to light brown to yellowish-gray to gray. Shale partings and shaly horizons are common.

188. 651.5-655.0 dol: sndy, sl calc, lt gr, micro-gran w v crse nests of crsely xln calcite; fn frosted qtz grains; hematite; porosity none.

189. 655.-0-659.3 dol: arg, lt gr, micro-gran, hematite; porosity none.

190. 659.3-659.8 sh: bl, irregularly fissile; grades laterally to a laminated, arg, drk gr dol.

191. 659.8-665.1 dol: lensed and channeled; arg, sndy, lt gr, pale green, yel-or, med pk, micro-gran; locally this unit is capped by a 1/8" layer of micro-gran hematite which lies on an irregular bedding plane; porosity none.

192-201.
665.1-737.5 a bedded sequence of dols; sndy, silty, arg.

202-203.
737.5-756.5 cliff-forming dol; silty, sndy, arg, partly conglomeratic. Irregular basal contact.

204. 756.5-776.5 incompetent, platy ($\frac{1}{2}$"), arg dol.

Ordovician-Bighorn Dolomite

205-208

776.5-809.0 dol: cliff-forming, partly fossiliferous, med lt gr, partly lt purplish-gr, micro- to v fnly xln; partly crsely vuggy; porosities none to poor.

CROOKED CREEK CANYON

This section was measured in the SE/4, Sec 21, R 27 E, T 8 S, in the Pryor Mountain Game Reserve, Montana. Sampling was started on the west side of the canyon about 1.7 miles below the "Wyoming" Camp Ground, Montana.

Amsden formation

Dolomites, sandstones, and shales overlie the lowermost Amsden sediments. Outcrops are generally obscured by a heavy mantle of soil.

0'-30' These beds produce a red, silty soil; outcrops are poor. The thickness of this interval is estimated from topographic expression. In view of the apparent variations in thickness and topographic forms these beds are believed to lie on an irregular erosion surface.

Unconformity--an apparently undulating surface.

Mission Canyon formation

Units 355-372-C constitute a cliff-forming sequence which weathers brownish-gray. Medium beds characterize the uppermost portions, while the lower portions are more massive. Fossils weather out on the surface. Varicolored chert nodules are common throughout the massive portions; these nodules weather to a light gray to brown. At the base this sequence grades into a silt impregnated breccia and conglomerate.

355.	0-8.0	ls: cherty, fossiliferous, fragmental, lt br-gr; granule to fnly gran w a clear calcite matrix; red stained fractures; porosity none.
356.	8.0-11.7	dol ls: cherty, fossiliferous, lt br-gr to lt yel-gr; v fnly gran dol and micro-gran calcite; infrequent crse vugs drusy w calcite; porosity none.
357.	11.7-16.5	ls: cherty, fossiliferous, stylolites, fragmental; lt br-gr, fnly gran w micro-xln matrix; porosity none.
358.	16.5-25.3	ls: cherty, fossiliferous, lt br-gr w pk stains, med-gran, rnded fragments and oolites--no matrix; porosity poor.

359.	25.3-28.8	ls: cherty, fossiliferous, fragmental, lt br-gr, crsely to fnly gran w clear calcite matrix; porosity none.
360.	28.8-35.8	ls: cherty, same as above, partly w micro-xln matrix; porosity none.
361	35.8-42.6	dol ls: fossiliferous, partly banded, arg, lt gr to gr-pk, partly dusky red, micro-gran; porosity none.
362.	42.6-50.4	dol ls to ls: same as above w pk stained stylolites grading into fragmental ls--v crse to fn gran w clear calcite matrix; porosity none.
363.	50.4-57.2	ls: fossiliferous, fragmental, lt br-gr, fn to micro-gran; porosity none.
364.	57.2-66.7	ls: fossiliferous, partly crinoidal, fragmental, oolitic, lt br-gr, partly w pk stains, v crsely to fnly gran w micro-xln to micro-gran matrix; porosity none.
365.	66.7-77.8	ls: same as above, w infrequent crse red-stained vugs drusy w calcite; porosity poor to none.
366.	77.8-84.1	ls: same as above, partly micro-gran; porosity none.
367.	84.1-90.1	ls: cherty, same as above; porosity none.
368.	90.1-100.3	breccia: cherty, fractured, micro-xln and fnly fragmental lss w arg, red-stained fractures drusy w calcite; porosity none.
369.	100.3-107.6	breccia: cherty, micro-xln and fragmental ls w red siltstone in fractures; porosity none.
370.	107.6-115.8	breccia: cherty; dark gr crsely xln to lt gr micro-xln lss and lt br to lt gr micro-gran dols; pale green sh and lt br to yel-gr calc, arg matrix; porosity (matrix only) poor to fair.

371. 115.8-125.1 breccia: cherty; micro-gran and fragmental lss, infrequent micro-gran dols; green sh and arg calc matrix; porosity none to poor.

372. 125.1-135.1 breccia: cherty; dominantly yel-gr, arg dols; infrequent lt br-gr, micro-xln lss; green sh and lt br, arg, calc matrix; porosity none to poor.

Units 372-C to 391 constitute a gray and gray-brown weathering, banded sequence. On the weathered surface this sequence is pseudo-bedded. Brownish-weathering cherts are present in beds and lenses. Infrequent laminations are noted; surfaces are rough, but regular. Bedded breccias are present in the uppermost portions. Collapses are noted in the basal portions. Fossils are generally absent.

372-C. 135.1-140.1 dol: arg, calc, v lt gr, micro-gran; varying thickness; porosity none.

373. 140.1-145.6 dol: laminated, med lt gr to lt gr, micro-gran; partly fnly xln w abundant fn to med vugs; porosity poor to none.

374. 145.6-148.7 breccia, dol: partly fossiliferous, med lt gr, micro-gran; crse, leached fossil vugs and casts; crsely xln calcite matrix; porosity poor.

375. 148.7-151.6 dol: lt gr to v lt gr, micro- to v fnly xln; moderate fn and med vugs; crse nests of calcite xls; porosity none.

376. 151.6-155.4 dol: cherty, same as above; partly a breccia; porosity none.

377. 155.4-162.2 dol: cherty, med lt gr, micro-gran; partly a breccia w wh, micro-xln, sl calc dol matrix; porosity poor to none.

378. 162.2-172.4 dol: cherty, partly brecciated, same as above; med lt gr and wh; porosity poor to none.

379. 172.4-178.4 dol: cherty, partly calc, v lt gr to lt gr, micro-xln; porosity poor to none.

380. 178.4-184.9 dol: cherty, v lt gr to lt gr, micro-xln to v fnly xln; partly w crse vugs stained lt br; calcite nests; porosity poor to none.

381. 184.9-193.2 dol: lt gr to v lt gr, fnly and micro-xln; infrequent v crse calcite xls; moderately fnly vuggy; porosity poor.

382. 193.2-198.0 dol: cherty, sl calc, same as above, partly fnly xln; abuhdant fn vugs; partly saccharoidal; porosity poor to fair.

383. 198.0-205.0 dol: cherty, sl calc, med lt gr to lt gr, micro-xln; infrequent fn vugs; porosity none.

384. 205.0-210.0 dol: sl calc, lt gr to v lt gr, micro-xln; infrequent crse calcite xls; porosity none to poor.

385. 210.0-217.0 dol: fossiliferous, lt yel-gr to med lt gr, micro-xln; infrequent fn vugs; porosity none to poor.

386. 217.0-229.7- dol: lt yel-gr to lt gr, micro-xln and fnly xln; infrequent fn vugs; occasional crse calcite xls; porosity poor.

387. 229.7-239.2 dol: cherty, sl calc, wh to v lt gr, micro-xln; calcited fractures; porosity none.

388. 239.2-244.0 breccia, dol: cherty, same as above, w hematite anhedrons and stains in fractures; porosity none.

389. 244.0-249.5 breccia, dol: cherty, wh to v lt gr fragments in a med gr, micro-gran matrix; large interfragment calcite nests; porosity none.

390. 249.5-253.5 breccia, dol: cherty, calc, wh to v lt gr, micro-xln; chalky-looking; porosity poor.

Units 391 to 400 constitute a poorly bedded, cliff-forming sequence which weathers to a grayish-brown. Fresh surfaces are light grayish in color. Thin beds and lenses of brown and gray cherts are present. Collapses are noted in the basal portions. Fossils are absent.

391. 253.5-257.6 dol: calc, med gr to br-gr, micro-gran; porosity none.

392. 257.6-264.7 dol: partly calc, lt br-gr to yel-gr, micro-gran and v fnly xln; partly moderately fnly vuggy; porosity poor.

393. 264.7-270.1 dol: sl calc, same as above; porosity poor to none.

394. 270.1-279.1 dol: v lt gr, micro-xln; infrequent med and fn vugs lined w anhedral calcite; porosity none.

395. 279.1-289.5 dol: crsely brecciated, cherty, med gr, micro-xln fragments in a wh to v lt gr micro-xln, calc matrix; interfragment calcite xls; porosity poor to fair (?).

396. 289.5-302.3 breccia, dol: cherty, sparsely fossiliferous; wh to med gr, micro-xln fragments in a wh to v lt gr, micro-xln calc matrix; porosity poor to none.

397. 302.3-308.7 breccia, dol: same as above, no chert, no fossils; porosity poor to none.

398. 308.7-318.7 breccia, dol: same as above; porosity poor.

399. 318.7-323.7 breccia, dol: same as above; porosity poor to none.

Lodgepole formation

Units 400 to 439 constitute a well cross-bedded series which weathers to a brownish-tan. Fossils are abundant. Chert is largely absent. This sequence is medium- to thin-bedded in upper and lower portions while medium to thick bed characterize the center.

400. 323.7-335.9 dol: cherty, fossiliferous, lt gr to med lt gr, micro- to v fnly gran; porosity poor.

401. 335.9-342.6 dol: cherty, fossiliferous, lt gr to med lt gr, micro- to v fnly gran; partly w darker-colored, more compact, irregularly shaped portions; porosity poor.

402. 342.6-346.6 dol: cherty, same as above; porosity poor.

403. 346.6-352.1 dol: no chert, same as above; porosity poor.

404. 352.1-356.2 dol: same as above, partly fnly xln and saccharoidal; porosity fair.

405. 356.2-358.4 dol: sparsely fossiliferous, med gr to lt br-gr, micro- to v fnly gran; porosity none.

406. 358.4-363.7 dol: med gr to lt gr, fnly gran w infrequent br-stained vugs; porosity fair.

407. 363.7-367.7 dol: fossiliferous, calc, yel-gr to v lt gr, v fnly gran; moderate fn vugs drusy w anhedral, br-stained calcite; occasional well-rnded, poorly outlined, micro-gran, med gr, dol granules; porosity fair.

408. 367.7-373.5 dol: fossiliferous, calc, med lt gr, micro- to v fnly gran: infrequent fn vugs drusy w anhedral br-stained calcite, hematite anhedrons and stains; porosity none.

409. 373.5-376.8 dol: fossiliferous, lt br-gr to med lt gr fnly to med-gran; occasional v crse calcite xls; porosity none.

410. 376.8-381.9 dol: fossiliferous, same as above; porosity none.

411. 381.9-386.3 dol ls, 1.4': fossiliferous, fragmental, fn to med-gran calcite w scattered grains of micro- to v fnly gran dol; porosity none.
dol 3': fossiliferous, med drk gr, fnly to v fnly xln; porosity poor.

412. 386.3-393.8 dol ls to calc dol: fossiliferous, yel-br (micro yel-flecked), micro-gran dol rhombs in a calcite flour matrix; lenses of drk gr, fnly gran dol w scattered crse calcite xls; porosity none to poor.

413. 393.8-400.5 dol ls to calc dol: same as above; porosity none to poor.

414. 400.5-410.5 dol ls to calc dol: same as above; minor fn vugs; porosity poor.

415. 410.5-415.0 calc dol: same as above; porosity poor to none.

416. 415.0- 420.2 calc dol: same as above w rnded pebbles of drk gr, micro-xln, dol; basal portions grade to a fragmental and fossiliferous ls of med-gran, rnded fragments; porosity poor.

417.	420.2-426.9	ls 4': fragmental, med- to crsely gran w infrequent fn vugs drusy w calcite; porosity poor to none. dol ls, 2.7': fragmental, same as above w fragments in a micro-gran dol matrix; porosity none.
418.	426.9-437.0	dol ls to calc dol: gradational from the above to a med gr w or-yel stains, fnly to v fnly xln, calc dol; porosity poor.
419.	437.0-445.1	dol: calc, same as above, partly a med lt gr, micro-gran, dol w abundant micro-hematite flecks and stains; partly dol ls, fragmental as above; porosity poor to none.
420.	445.1-448.6	dol calc to dol ls: fragmental, fossiliferous, med gr, fnly to med-gran, ls w v fnly gran dol matrix, hematite flecked; porosity none.
421.	448.6-451.0	dol ls: same as above, partly w well-rnded pebbles; porosity none.
422.	451.0-455.3	dol: calc, br-gr w pk stains, v fnly to micro-gran, w frequent subhedral and euhedral hematite pseudomorphs after pyrite; porosity none to poor.
423.	455.3-458.5	dol calc, 1': same as above, wh grades to fnly to med-gran, med gr dol ls w hematite stains in fnly to micro-gran dol matrix; porosity none.
424.	458.5-463.4	dol ls to calc dol: partly fragmental as above; partly v fnly gran dol w rnded granules of micro-gran, med lt gr dol; porosity none.
425.	463.4-466.8	dol: calc, fossiliferous, med drk gr w or-yel stains, v fnly to silt-size gran; fn vugs stained or-yel; hematite anhedrons; indistinctly outlined, rnded granules and pebbles of micro-gran, med lt gr dol; porosity none.
426.	466.8-469.9	dol: calc, same as above.

427.	469.9-474.7	dol: sl calc, banded and laminated, br-gr to med gr w lt br partings and pk stains, micro- to silt-size gran; occasional crse calcite xls; porosity none.
428.	474.7-480.2	dol: same as above; porosity none.
429.	480.2-486.3	dol: same as above; porosity none.
430.	486.3-489.8	dol: same as above and dol ls, fragmental, oolitic, fossiliferous, sparsely crinoidal; fn to med fragments in a v fnly gran dol matrix; porosity none.
431.	489.8-495.4	ls to dol ls: fragmental, fossiliferous, oolitic, crinoidal, lt br-gr to pale purple to gr-red, crse to fn fragments in a matrix of clear calcite, hematite and dol rhombs; porosity none.
432.	495.4-501.7	ls to dol ls: same as above; porosity none.
433.	501.7-507.0	calc dol and dol ls: laminated and banded, partly same as above, partly a silt of hematite, dol rhombs and calcite flour; porosity none to poor.
434.	507.0-510.0	dol ls: fragmental as above, w 1/8" stringers of micro-gran hematite; porosity none.
435.	510.0-514.0	ls: fragmental, fossiliferous, oolitic, crinoidal, bands of med gr to pale purple, fnly to med-gran; hematite and calcite matrix; porosity none.
436.	514.0-517.8	ls: same as above; partly calc dol, med lt gr, micro- to v fnly gran; porosity none.
437.	517.8-520.6	dol ls: fossiliferous, med gr w br and or-yel stains, fnly to v fnly gran dol and med- to v fnly gran ls; porosity none to poor.
438.	520.6-529.6	dol: med drk gr, micro-gran; micro-hematite flecks; porosity poor to none.

Units 439 to 453 constitute a distinctly bedded series which weathers to white and different shades of brown. Concavities and prominences result from varying degrees of resistance to weathering.

439.	529.6-533.1	dol ls: fragmental, fossiliferous, lt br-gr, fnly to med-gran ls w a v fn to micro-gran matrix; porosity none.
440.	533.1-540.0	ls: lt gr to lt br-gr, sublithographic-looking ls w small bands of fnly gran ls embedded; porosity none.
441.	540.0-540.8	ls: lt br-gr to br-gr, micro-gran w drk red streamers and partings; porosity none.
442.	540.8-546.4	dol: arg, irregularly laminated, yel-gr to lt br, micro-gran; porosity none.
443.	546.4-549.4	dol, calc and calcite: cherty, v lt gr micro-xln dol; partly subhedral to euhedral calcite w only irregular patches of dol remaining; "brecciated-looking"; porosity good to med.
444.	549.4-553.2	ls: lt br-gr to lt gr, micro-gran to fnly gran; occasional xls of dol; hematite anhedrons and stains; porosity none.
445.	553.2-557.7	dol, calc and calcite: lt gr, v fnly xln, (saccharoidal dol) which replaces xln calcite; porosity med to good.
446.	557.7-562.6	dol ls and dol: lt gr, fnly to v fnly gran ls and xln dol interbedded w drk gr, micro-xln dol; porosity none to poor.
447.	562.6-566.6	dol: lt gr, micro-xln wh varies to calcite and fnly xln dol at base; porosity fair.
448.	566.6-569.6	ls: lt br-gr to br-gr, micro-gran (sublitho-graphic-looking) which varies to a dol ls at base; porosity none.
449.	569.6-573.4	ls: lt br-gr to br-gr, micro- to fnly gran; dol, calc; lt yel-gr, micro-xln w infrequent fn vugs; partly saccharoidal and replaced by calcite; porosity fair to poor.
450.	573.4-575.6	dol: med lt gr, micro-xln, partly v fnly xln; varies to a micro-gran, br-gr ls at base; porosity poor.

451. 575.6-579.1 dol: cherty, partly calc, lt br-gr, v fnly xln, partly saccharoidal; porosity poor to fair.

452. 579.1-580.3 dol: lt yel-gr to yel-gr, v fnly xln, saccharoidal; porosity good.

Units 453 to 462 constitute a cliff-forming sequence of medium-bedded strata which weather brown to gray. Bedding planes occur only as depositional partings. The weathered surface is characterized by differential weathering pits.

453. 580.3-582.8 dol: sl calc, lt yel-gr, v fnly xln, w tiny lenses and bands of cross-laminated, wh, micro-gran, chert; porosity fair to med.

454. 582.8-587.5 dol: fossiliferous, lt gr to med lt gr, v fnly to silt-size xln; crinoid sections and fossil fragment casts; partly w moderate fn to med leached vugs; porosity fair.

455. 587.5-592.1 ls: fragmental, partly dolomitic, lt gr to br-gr, micro- to med-gran, rnded fragments (and oolites?) w scattered grains and nests of silt-size dol xls; porosity none to poor.

456. 592.1-596.5 dol: cherty, br-gr, v fnly to silt-size xln, partly saccharoidal; porosity poor.

457. 596.5-603.7 dol: fossiliferous, med lt gr, micro- to silt-size xln; infrequent crse calcite xls; moderate fn to med vugs; crinoid and fossil fragment casts; porosity poor to none.

458. 603.7-609.7 dol: same as above, partly micro-gran; porosity poor to none.

459. 609.7-618.5 dol: same as above, w infrequent bl-lined (asphaltic?) v crse vugs; porosity poor.

460. 618.5-623.0 dol: fossiliferous, lt gr, v fnly to silt-size xln; abundant fn vugs and crinoid casts; porosity fair.

461. 623.0-626.6 dol: same as above, partly micro-gran; porosity poor to fair.

462. 626.6-632.6 dol: cherty, same as above; porosity poor.

Below unit 462 the outcrop becomes thinly-bedded and slumps away to leave an overhanging cliff above. This interval below 462 to 465 may mark the base of the Mississippian. Strata below are not similar lithologically to the Bighorn dolomite sediments.

463. 632.6-635.1 dol: cherty, siliceous, partly same as above; partly drk gr to med drk fr, fnly to v fnly xln w infrequent nests of crsely xln calcite; irregularly shaped ¼" nodules and streaks of wh, partly porous chert?; porosity poor.

464. 635.1-639.5 dol: fossiliferous, cherty, med gr to or-yel, v fnly to silt-size xln; partly w abundant fn vugs and moderate v crse, bl-lined (asphaltic?) vugs; porosity poor to fair.

465. 639.5-647.9 dol: cherty, drk yel-or to lt yel-gr w drk gr mottlings, v fnly to micro-xln; porosity poor.

Base of section is not exposed.

SHOSHONE CANYON

Sampling started on the north side of the Shoshone River in Sec 4, T 52 N, R 102 W, at a location about 1/8 mile above the inverted syphon. Madison thickness is measured from the Amsden-Madison lithologic contact. Surveyed thicknesses varied from 700 feet to 750 feet.

Amsden formation

0'-30' (approximately) Poor outcrops of incompetent beds of varying thickness are obscured by a red-colored mantle; the basal contact of these beds appears to be very irregular. Because of varying thickness, sporadic occurrence, and an apparently undulatory basal contact of varying amplitude the base of these beds is believed to mark an unconformity.

Unconformity(?)--

7' --Conglomerate: limestone and dolomite cobbles to granules in a sandy, argillaceous matrix.

18' --Interbedded sandstones and limestones.

2' --Sandstone: brownish-gray weathering, fine to medium granular.

Mission Canyon formation

Units 211 to 222 constitute a series of thin- and medium-bedded strata which weather blue-gray to tan. These beds weather to form a series of ledges near the top of the sequence, but crop out as a massive unit in the lower portions. Chert lenses and nodules are frequent. Contacts between units are sharp near the top and become progressively more vague downward.

211.	0-3.5	ls: cherty, lt br-gr, micro-xln; porosity none.
212.	3.5-7.7	ls: cherty, lt br-gr, micro-xln; partly a lt yel-gr, micro-xln, calc dol; minor fn vugs drusy w qtz xls; porosity none.
213.	7.7-15.2	ls: cherty, stylolites, sparsely fossiliferous, lt br-gr to lt yel-gr, micro-xln; partly fragmental; at base a dol ls w infrequent fn vugs lined w bl, carbonaceous (?) material; porosity none.

214.	15.2-21.0	ls: cherty, stylolites, lt br-gr w yel flecks, micro-xln; partly a lt yel-gr w yel-or stains, micro-xln dol w infrequent cse vugs drusy w qtz and calcite; porosity none to poor.
215.	21.0-24.8	dol: cherty, stylolites, partly silicic, calc, lt yel-gr to med lt gr, micro-xln; yel-or stained fractures, minor fn vugs; porosity poor to none.
216.	24.8-28.3	dol: calc, cherty, lt yel-gr to lt gr, micro-xln; porosity none to poor.
217.	28.3-32.8	dol: calc, cherty, med gr to med lt gr, micro- to v fnly xln; infrequent leached fossil fragments; infrequent large nests of crsely xln calcite; porosity poor.
218.	32.8-37.8	dol: cherty, calc, lt yel-gr to med lt gr, micro-xln; partly w med xls of calcite; infrequent fn vugs; porosity poor.
219.	37.8-44.3	ls: fossiliferous, fragmental, oolitic, med lt gr to lt gr, fnly to med-gran; occasional well-rnded ls granules and pebbles and abundant oolites in a micro-xln matrix; partly w infrequent fn rhombs of dol; porosity none to poor.
220.	44.3-49.9	ls: cherty, fragmental, lt br-gr to lt gr, fn to med fragments in a micro-xln matrix; partly a v fnly xln, med lt gr calc dol w hematite pseudomorphs; porosity none.
221.	49.9-52.9	dol to dol ls: cherty, lt yel-gr to v lt gr, v fnly xln w abundant crse calcite xls and inter-xl calcite flour; porosity poor to none.

Units 222 to 235 constitute a massive, cliff-forming sequence which weathers blue-gray to grayish-brown. Depositional planes and intervals are evidence by fracture patterns and varying degrees of weathering. Sporadic chert nodules weather out brown to pale yellow. At the base, this sequence grades into a breccia and conglomerate, which locally caves under to form a talused ledge.

222.	52.9-55.9	ls: cherty, fossiliferous, v lt gr to lt br-gr, v fn to granule size fragments in a micro-xln matrix; infrequent v crse vugs drusy w calcite; porosity none.
223.	55.9-68.6	ls: cherty, fossiliferous, partly crinoidal; v fn to v crse fragments in a micro-xln matrix; varies to a lt br-gr, micro-xln ls; hematite pseudomorphs; porosity none to poor.
224.	68.6-70.9	ls: fossiliferous, lt gr to lt yel-gr, v fnly to micro-gran; porosity none.
225.	70.9-75.4	ls: cherty, fossiliferous, stylolites, lt gr to v lt br-gr, fn to v crse fragments w micro-gran and micro-xln matrix; scattered rnded granules; porosity none.
226.	75.4-79.9	ls: same as above; porosity none.
227.	79.9-87.0	ls: fossiliferous, lt gr to med lt gr, v fnly to med-gran fragments in a micro-xln matrix; locally a cg of subrnded pebbles to cobbles of fragmental ls in a micro-gran to crsely gran ls matrix; porosity none.
228.	87.0-91.0	ls: cherty, fossiliferous, lt gr to v lt br-gr, v fnly to med-gran fragments and oolites in a micro-xln matrix; porosity none.
229.	91.0-103.8	ls: cherty, fossiliferous, oolitic w a med- to v crsely xln matrix; porosity none. dol, 2½': calc, lt yel-gr, micro-xln; lensing; porosity poor to none.
230.	103.8-109.1	dol: cherty, partly v calc, v lt gr to lt yel-gr, v fnly to micro-xln; porosity poor.
231.	109.1-114.6	ls: v fossiliferous, lt br-gr, micro-gran at top; grades into a poorly compacted, v crsely fragmental ls w a micro-gran matrix; partly crinoidal; hematite trcs; v large brachiopod casts (3½"-4½"), large crinoid sections and numerous horn corals are present among the ls fragments; porosity poor to fair.

232. 114.6-125.6 ls: fragmental, same as above, cherty; porosity poor. (Laterally varies to a boulder breccia.)

233. 125.6-128.6 ls: fragmental, same as above; partly conglomeratic w well-rnded pebbles of fragmental ls set in a fragmental matrix; v fossiliferous w large ($\frac{1}{2}$" cross-section) crinoid stems and large (2"-4") fossil shell casts; locally v friable; porosity poor to fair and variable laterally.

234. 128.6-148.6 breccia and cg: (a maximum thickness was measured) rnded to angular boulders to granules of varied lithology; boulders of well-cemented breccia w different matrices present; cobbles to pebbles of translucent micro-xln ls and gr-bl, fnly xln dol are lined w micro-gran, and subhedral hematite; anhedral micro-pseudomorphs of hematite are scattered through matrices; fragments of chert lenses and nodules; fragments of fluorite-bearing dol; a pale green to yel-or, shaly, calc, arg matrix is lineated around fragments locally.

Units 235 to 255 constitute a series of medium- and thickly-bedded strata which weather brownish-gray. Thin-bedded strata occur over short stratigraphic intervals. Laminations and banding are frequent. Sporadic breccias occur. Chert lenses and beds are common. At the base of this sequence is a highly fractured, massive bed which contains conformably bedded, pseudo-boulders of dolomite. Fossils are generally absent.

235. 148.6-153.4 dol: arg, med lt gr to lt gr, micro-gran; infrequent med vugs; porosity none.

236. 153.4-166.7 dol: calc, cherty, lt yel-gr to lt gr, micro-gran; veinlets and nests of calcite; cg at base of subrnded pebbles to cobbles of yel-gr to med gr, micro-gran to micro-xln dol in an or-yel, calc matrix; porosity none to poor.

237. 166.7-172.2 dol: chalk-looking, partly silicic, arg, micro-gran; porosity none.

238. 172.2-174.7 dol: cherty, med lt gr, partly w hematite stains, micro-xln; porosity none.

239.	174.7-182.8	dol: calc, med gr to br-gr, micro-gran; basal 3" a dol ls of v fn rhombs in a calc matrix; porosity none.
240.	182.8-189.6	dol: cherty, calc, sparsely fossiliferous, med lt gr, micro-gran; partly micro-saccharoidal; porosity poor to fair.
241.	189.6-198.6	dol: cherty, same as above; porosity fair.
242.	198.6-203.4	dol ls and calc dol: grades from a med gr, micro-gran calc dol to a lt br-gr, dol ls of silt-size dol rhombs in a calc matrix; porosity none.

Local unconformity--marine erosion.

243.	203.4-210.9	ls: thinly banded, lt br-gr, micro-gran; also, well-rnded granules of micro-gran ls in a micro-gran matrix; porosity none.
244.	210.9-218.2	dol: cherty, conglomeratic; subrnded to angular, cobbles to granules of med lt gr to v lt gr, micro-gran, calc dol in a matrix of br-gr to yel-gr, micro-gran to v fnly gran dol; porosity poor.
245.	218.2-222.0	ls: lt br-gr, micro-gran; nests and veinlets of calcite; porosity none.
246.	222.0-228.6	dol: sl calc, v lt gr to med lt gr, micro-gran; porosity none.
247.	228.6-230.4	ls: cherty, lt br-gr, micro-gran; partly w red-stained streaks; porosity none.
248.	230.4-234.5	dol: cherty, calc, med lt gr, micro- to v fnly gran; irregularly shaped, granule-size inclusions of v lt gr, micro-gran to v fnly gran dol; porosity none.
249.	234.5-238.3	ls: partly fragmental, lt br-gr, micro-gran; partly w v crse to med fragments in a micro-gran, calc matrix; porosity none.

250.	238.3-241.6	dol: silicic (?), partly banded, lt yel-or ti med lt gr, micro-gran; porosity none.
251.	241.6-250.1	ls: cherty, lt br-gr, micro-gran; partly fragmental w crse to v fn fragments in a micro-gran calc matrix; porosity none.
252.	250.1-256.2	ls: cherty; same as above; partly a dol ls w silt-size dol rhombs enclosing fn to crse fragments of ls; porosity none.
253.	256.2-261.2	dol ls: cherty; same as above; minor v crse vugs drusy w calcite; porosity none.
254.	261.2-263.1	dol calc to dol ls: cherty, med lt gr, micro- to v fnly xln dol w interstitial micro-gran calcite; porosity poor.
255.	263.1-266.5	dol: cherty, sndy, arg, v lt gr, micro-gran; frequent grains of fn angular qtz and aggre-gates of qtz xls; 1" beds of v fnly xln fluorite-bearing dolomite; porosity poor.

Units 256 to 270 constitute a thin- and medium-bedded series of strata which weather grayish-brown. Cherts are sporadically present in lenses and nodules which weather to gray and brown colors. Small scale channeling is present throughout upper portions of the sequence. Fossils are absent. The Mission Canyon-Lodgepole contact is marked by a series of hematitic and conglomeratic beds which outcrop in the basal portions of this sequence.

256.	266.5-269.3	ls: v cherty, lt br-gr, micro-gran; flecked w micro-hematite; porosity none.
257.	269.3-274.5	dol ls: v lt gr, micro-gran dol w micro-gran calcite; porosity none.
258.	274.5-276.0	ls: lt br-gr, micro-gran; flecked w micro-hematite; porosity none.
259.	276.0-282.1	dol ls: v lt gr to lt br-gr, micro-gran dol w interstitial micro-gran calcite; porosity none.
260.	282.1-287.9	dol: cherty, banded; med lt gr, v fnly to micro-gran w thin 1/8" bands and streaks of wh, porous chert; porosity none.

261. 287.9-301.5 ls: sl cherty, lt br-gr, fnly to med-fragmental w scattered dol rhombs; porosity none.

262. 301.5-303.3 dol: cherty, lt gr to med lt gr, micro-gran; porosity none.

263. 303.3-305.7 dol: cherty, calc, laminated, lt gr to v lt br-gr, micro-gran; porosity none.

264. 305.7-308.5 ls: lt br-gr, micro-gran; porosity none.

Lodgepole formation

265. 308.5-310.9 dol: arg, banded; lt gr partly stained yel-or, micro-gran; pebbles and lenses of bl-gr, micro-gran, arg dol; hematite anhedrons; porosity none.

266. 310.9-312.2 dol: cherty, arg, lt gr to yel-or mottled, micro-gran; infrequent nests and veinlets of calcite; porosity poor.

267. 312.2-315.0 ls: cherty, lt br-gr, fnly fragmental to micro-gran; porosity none.

268. 315.0-318.8 dol: cherty, calc, v lt gr, micro-gran; porosity none.

269. 318.8-323.8 dol: cherty, silty, conglomeratic, lt gr to or-yel, silt-size gran dol w subrnded to angular pebbles of v lt gr, micro-gran, arg dol; micro-hematite anhedrons; nests of calcite; porosity none.

Units 270 to 320 constitute a cliff-forming series of medium- and thin-bedded strata which weather to a darker gray than the above sequences. Cherts are not present. Cross-bedding and laminations occur sporadically. Fossils are abundant to moderate. Pseudo-bedding is formed by stylolite occurrences.

270. 323.8-327.8 dol: cherty, silty, calc, v lt gr to lt yel-gr, micro-xln; infrequent silt-size to v fn chert and qtz grains; minor fn vugs; porosity none to poor.

271. 327.8-332.8 dol: cherty, partly arg, v lt gr to yel-or, micro-xln; partly micro-saccharoidal; porosity poor to fair.

272.	332.8-333.8	dol: cherty, silty, v drk red to gr-yel, fn to med-gran dol; irregularly shaped med size grains of qtz and chert; hematite anhedrons and stains; porosity poor to none.
273.	333.8-335.0	dol: cherty, yel-gr to gr-yel, partly stained drk red, micro-gran to micro-xln; partly micro-saccharoidal; porosity poor.
274.	335.0-336.5	ls: concretionary, lt br-gr, micro- to v fnly gran, partly w med size nests of micro-gran dol; cobble size, zoned, well-rnded concretions of med gran, micro-xln, calc dol; porosity none.
275.	336.5-341.2	dol: v lt gr, and stained yel-or, micro-gran; occasional xls of calcite; anhedral hematite in fractures; porosity none to poor.
276.	341.2-352.2	dol ls: sparsely fossiliferous, med lt gr w or-yel flecks, micro-xln to v fnly xln dol rhombs in micro-gran ls; porosity none to poor.
277.	352.2-355.5	dol ls: same as above; porosity none to poor.
278.	355.5-357.4	ls: sl dolomitic, fossiliferous, fragmental; lt br-gr, granule to med fragments in a micro-gran to v fnly gran dol ls matrix; porosity none.
279.	357.4-360.2	dol: calc, med lt gr, v fnly to micro-gran; calcite in fractures; porosity none to poor.
280.	360.2-364.4	ls: fragmental, sparsely fossiliferous, ot br-gr, granule to fn ls fragments in a xln calcite matrix; porosity none.
281.	364.4-365.5	dol ls: cherty, v lt gr, micro-to fnly xln dol rhombs in micro-gran ls; scattered v crse vugs drusy w calcite; porosity none.
282.	365.5-368.5	dol ls: fossiliferous, fragmental, lt br-gr, granule to fn ls fragments in a micro-gran, calc dol matrix; porosity none.
283.	368.5-374.6	dol ls: lt br-gr, micro-xln dol rhombs in micro-gran ls; porosity none.

284.	374.6-377.5	dol: calc, fossiliferous, v lt gr to yel-or, micro-gran to v fnly gran; partly a micro-gran dol ls; porosity none.
285.	377.5-386.5	ls: fossiliferous, oolitic, fragmental crse to fn ls fragments and oolites in a xln calcite matrix; porosity none.
286.	386.5-390.5	ls to dol ls: fossiliferous, oolitic, fragmental, same as above grading into a fragmental ls w micro-gran dol matrix; carbonaceous lined stylolites; $\frac{1}{4}$" crinoid sections; porosity none.
287.	390.5-395.0	dol ls: fragmental, same as above; porosity none.
288.	395.0-396.5	dol: calc, med gr w or-yel flecks, micro-gran; porosity none to poor.
289.	396.5-403.1	ls: fossiliferous, oolitic, fragmental; crse to fn fragments w xln calcite matrix; partly w dolomitic matrix; porosity none.
290.	403.1-404.9	dol ls: lt gr to lt yel-gr, micro-gran dol w inter-grain calcite; porosity poor.
291.	404.9-409.8	dol ls: fragmental and oolitic, lt br-gr, crsely to fnly gran w a micro-gran dol matrix; porosity none.
292.	409.8-414.8	ls: fossiliferous, oolitic, stylolites, lt br-gr, fnly to crsely gran w a micro-gran dol matrix; porosity none.
293.	414.8-417.4	ls: sl dolomitic, fragmental, oolitic, lt br-gr, fn to crse fragments in a matrix of micro-gran ls and dol; porosity none.
294.	417.4-421.5	ls: fragmental, oolitic, lt yel-br, fn to crse fragments in a matrix of clear, xln calcite, micro-gran calcite and micro-gran dol; porosity none.
295.	421.5-424.9	dol: calc, pale yel-br, micro- to v fnly gran; calmite veinlets; porosity poor to none.

296.	424.9-430.1	ls: sl dolomitic, fragmental, yel-br, v crse to fn fragments in a matrix of clear xln calcite and micro-gran dol; porosity none.
297.	430.1-433.7	dol: calc, pale yel-br w or-yel stains, v fnly to micro-xln; porosity poor to none.
298.	433.7-435.9	dol ls to calc dol: cherty, partly fragmental ls w micro-gran dol matrix; partly micro- to v fnly gran dol w inter-grain calcite; porosity none.
299.	435.9-440.9	dol: lt gr to lt yel-gr, micro- to fnly xln; occasional calcite-lined vugs; porosity poor to fair.
300.	440.9-446.4	ls: oolitic, fragmental, crse to fn rnded fragments in a micro-gran and fnly xln matrix; porosity none.
301.	446.4-448.9	ls: same as above w hematite stains and flecks in matrix; porosity none.
302.	448.9-455.4	dol ls: fragmental as above, partly crinoidal; partly pale lavender w hematite and fnly gran dol matrix; partly a med gr, v fnly gran dol at top; porosity none to poor.
303.	455.4-464.9	ls: cherty, fragmental, oolitic, partly crinoidal; well-rnded granules through fn fragments in a micro-gran ls and dol matrix; porosity none.
304.	464.9-472.8	ls: same as above; porosity none.
305.	472.8-478.5	ls: same as above w occasional crse, subhedrons of pseudomorphic hematite (after pyrite); frequent hematite stains; porosity none.
306.	478.5-486.2	dol ls: fragmental as above w micro-gran dol matrix; frequent v fn to micro-sized hematite anhedrons; porosity none.
307.	486.2-489.7	dol ls: same as above which grades into a banded, med gr w yel-or flecks, v fnly gran dol; porosity none.

308.	489.7-493.9	dol ls: fossiliferous, same as above w abundant pyrite and hematite flecks; porosity none.
309.	493.9-498.0	dol: calc, banded, lt br-gr, micro-gran w layers of abundant hematite and pyrite; partly v calc and partly arg at base; porosity none.
310.	498.0-501.5	dol ls and dol: scantily fossiliferous, yel-br and med gr, partly fragmental w micro-gran dol matrix; grades to a v sl calc, drk bl-gr and or-yel speckled dol; dcl oolites poorly preserved; hematite and pyrite flecks throughout; porosity none.
311.	501.5-508.0	dol: silty, calc, med gr w yel-or flecks to drk yel-br, micro-gran dol; porosity none.
312.	508.0-513.0	ls: silty, fragmental, partly w abundant pyrite and hematite in matrix; bl-gr speckled to red-gr speckled to pale purple; porosity none.
313.	513.0-516.3	dol ls: speckled lt to med gr, oolites and ls fragments in a micro-gran dol matrix; grades to a micro-gran, med gr, calc dol; porosity none.
314.	516.3-519.6	dol ls: cherty, med gr to pale purple, oolites and fragments in a micro-gran, dol matrix; partly w abundant hematite and pyrite; porosity none.
315.	519.6-523.3	dol ls: fragmental, fossiliferous, lt br-gr to yel-br, w med gr granules of micro-gran dol; occasional crse vugs drusy w calcite; porosity none.
316.	523.3-526.3	dol: cherty, sl calc, lt yel-gr, micro-gran; porosity none.
317.	526.3-531.5	ls: cherty, stylolites, lt br-gr, micro-gran; porosity none.
318.	531.5-540.7	dol: cherty, fnly laminated, lt yel-gr to med gr, micro-gran; partly micro-saccharoidal; porosity poor.

319. 540.7-547.5 dol: 3', lt yel-gr, micro-gran; porosity none.
ls breccia: 3.8', angular cobbles to pebbles of lt yel-br, oolitic ls in lt yel-gr, micro-gran dol matrix; porosity none.

Units 320 to 347 constitute a dark weathering, cliff-forming sequence; laminations occur sporadically in bedded sequences of limestones and dolomites. Cherts are absent except near the top of the sequence where they occur in large nodules. Lowermost portions of the sequence are thin- and medium-bedded, while upper portions are thick- to massive-bedded.

320. 547.5-552.0 ls: cherty, lt br-gr, micro-xln; calcite veinlets and fracture fillings; porosity none.

321. 552.0-555.9 dol: cherty, calc, pale yel-br to lt yel-or, micro-xln; partly saccharoidal; porosity poor.

322. 555.9-559.2 dol: cherty, med gr to lt yel-gr, v fnly to micro-gran; calcite veinlets; porosity poor.

323. 559.2-564.3 dol: cherty, same as above; porosity poor.

324. 564.3-569.1 dol: cherty, silicic, arg, med gr, micro-gran; varies to a v lt gr to med gr w yel-or stains, fnly xln ls w scattered dol grains; porosity poor to none.

325. 569.1-574.8 dol: cherty, laminated, arg, med lt gr to lt gr, micro-gran; porosity none to poor.

326. 574.8-579.6 dol, l': cherty, calc, lt br-gr, v fnly to micro-gran; porosity poor.

dol ls: 3.8'; fossiliferous, crinoidal, partly fragmental, med gr to moderate yel-br w bl stains; fn to crse ls fragments in a micro-gran dol matrix; porosity poor to none.

327. 579.6-587.6 dol: calc, lt yel-br, v fnly xln; varies to a med lt gr, micro-gran dol; calcite veinlets; porosity poor.

328. 587.6-595.4 dol: calc, yel-br, v fnly to micro-xln; nests of crsely xln calcite; partly oolitic, micro-gran ls; porosity none.

329. 595.4-601.8 dol ls: partly fragmental and crinoidal, med lt gr to lt yel-br, micro-gran to v fnly xln dol rhombs in a micro-gran ls matrix; partly fn to med ls fragments and oolites in a micro-gran dol matrix; porosity none.

330. 601.8-607.0 dol ls to calc dol: fossiliferous, v fnly xln to micro-xln dol rhombs and micro-gran ls; partly fnly xln, calc dol; porosity poor.

331. 607.0-612.1 dol to dol ls: a calc, lt yel-br, micro- to v fnly xln dol which varies to a fnly xln dol w med to crse xls of calcite; porosity poor.

332. 612.1-620.2 dol: calc, med lt gr to lt yel-br, v fnly xln; infrequent fn vugs; porosity poor.

333. 620.2-624.7 dol: calc, same as above w occasional large vugs drusy w calcite and br-stained calcite xls; porosity poor.

334. 624.7-639.7 dol: fossiliferous, sparsely crinoidal, med lt gr to lt yel-gr, v fnly to fnly xln w crse calcite xls and nests; infrequent leached fossil vugs; br stains in fractures; porosity poor.

335. 639.7-645.7 dol: fossiliferous, crinoidal, med lt gr to lt yel-gr, micro- to v fnly xln; moderate med vugs and leached fossils; porosity poor.

336. 645.7-649.4 dol: sl cherty, same as above.

337. 649.4-655.2 dol: no chert; same as above w moderate crsely xln calcite nests; porosity poor.

338. 655.2-664.2 dol: same as above; porosity poor.

339. 664.2-670.4 dol: cherty; same as above; hematite anhedrons and stains; porosity poor.

340. 670.4-674.3 dol: cherty; same as above, arg, flecks of foreign material; porosity poor to none.

341. 674.3-676.4 dol: cherty; same as above; porosity poor to none.

342. 676.4-678.3 dol: cherty; same as above; partly w bl carbonaceous material; porosity poor to none ?.

343. 658.3-681.4 dol: cherty; same as above; porosity poor ? to none ?.

344. 681.4-685.6 dol: same as above; no chert; porosity poor ? to none.

345. 685.6-690.6 dol: same as above; porosity poor ? to none.

346. 690.6-693.6 dol: arg, med gr, micro-gran w occasional crse xls of calcite; tiny drk red streamers and flecks; porosity none.

347. 693.6-695.2 dol: same as above w occasional large nests of red, micro-gran hematite; porosity none.

DEVONIAN(?) - THREE FORKS SHALE(?)

348. 695.2-702.2 sh: green to drk gr w large qtz clusters; hematitic fossil remains; scolecodonts and conodonts; dendroids; porosity none.

349. 702.2-716.2 dol: partly ripple marked, arg, calc, yel-or, micro-gran; porosity none.

350. 716.2-722.2 ss, sh, dol:

thin beds (1"-2") of fn to med, v hi sphericity, frosted qtz grains in a dol matrix w numerous conodont fragments; varies to a green sndy sh to sndy dol; porosity none.

351. 722.2-732.2 ss, sh, dol.

352. 732.2- sndy, arg dol.

Madison Sample

353. Note: This sample is taken from pseudo-boulders in interval represented by samples 251 to 254.

dol, calc to dol ls: lt yel-gr to v lt gr, v fnly xln dol rhombs in a micro-gran calc matrix; porosity fair.

INSOLUBLE RESIDUE DESCRIPTIONS

OWL CREEK CANYON

MISSION CANYON FORMATION

Member MC 1

639. 0-2.0 10.02%
Whitish-gray, slightly slity clay.

638. 2.0-3.5 10.95%
Whitish-gray clay.

637. 3.5-13.3 1.84%
Lt gray clay, minor silt; accessory traces.

636. 13.3-20.3 2.48%
Crinoid debris; gray, silty clay; minor grains of chert and quartz; limonite traces; accessory traces.

635. 20.3-32.3 2.28%
Coarse quartz clusters with overgrowths of chert; fine to med anhedral quartz sands; crinoid debris.

634-630.
32.3-76.3 2.74%
Quartz euhedrons and subhedrons; lt gray clay; crinoid debris; traces of granular, gray chert.

Member MC 2

560. 76.3-80.8 1.21%
Quartz in clusters and in coarse to silt-size grains or anhedrons; black clay; crinoid debris.

561-62.
80.8-96.3 0.40%
Chalcedonic chert fragments; subhedral quartz clusters; black clay; silt-size grains of quartz.

563-64.
96.3-107.0 0.54%
Crinoid and brachiopod debris; silt of quartz and chert; dark gray to black clay.

565-67.	107.0-127.0	1.85% Brachiopod and crinoid debris; silt of quartz and chert; dark gray clay.
568.	127.0-138.0	1.94% Crinoid and brachiopod debris; fragments of porcelaneous, gray chert; dark gray clay.
569-71.	138.0-166.5	5.92% White clay; crinoid and brachiopod debris; chalcedonic, pearly chert; accessory traces; greeen shale traces; occasional grains of rounded, irregularly shaped quartz.
572.	166.5-176.8	0.89% Dark gray clay; crinoid and brachiopod debris; flakes of granular chert; traces of green shale; accessory traces; fine quartz grains.

Member MC 3

573-75.	176.8-196.1	1.82% Finely dolomoldic, porous chert; chalcedonic chert; dark gray clay.
576-77.	196.1-209.3	4.72% Unmodified granular chert; finely dolomoldic, granular chert; black clay, collophanite traces; accessory traces.
578.	209.3-215.5	1.15% Finely dolomoldic quartz and chert; micro-xln quartz silt; dark gray clay.
579-80.	215.5-226.5	0.69% Traces of finely dolomoldic quartz and chert; euhedral quartz of silt-size; black clay.
581-83.	226.5-241.0	4.80% Finely dolomoldic chert and lacy dolomoldic quartz.
584-85.	241.0-255.8	0.47% Black clay; traces of white, finely dolomoldic chert.

586.	255.8-262.3	3.64% Finely dolomoldic and compact, granular, dirty gray chert; black clay.
587-88.	262.3-273.8	0.97% Black silty clay; limonite traces; traces of dolomoldic gray chert; accessory traces.
589.	273.8-275.8	2.42% lt gray clay; quartz fragments; collophanite.
590-91.	275.8-287.9	11.0% Med dolomoldic chert; white, finely granular, compact, porcelaneous chert.
592.	287.9-290.6	11.16% Finely dolomoldic chert.
593-95.	290.6-303.7	0.42% Black, silty clay; finely dolomoldic chert.
596-97.	303.7-318.4	2.39% V finely granular, pearly chert fragments; flakes of granular chert; limonite traces; coarse to silt-size quartz subhedrons.
598.	318.4-324.7	0.75% Dark gray, silty clay.

LODGEPOLE FORMATION

Member L 1

599.	324.7-331.7	0.96% Silt of quartz and chert with dolomorphic-like quartz clusters; collophanite.
600.	331.7-332.9	0.60% Black, silty clay.
601.	332.9-340.3	4.97% Coarse, dolomoldic, granular, gray chert which grades to quartz; grains or fragments of quartz and chert; crinoid debris.
602-04.	340.3-359.4	0.72% Silt of quartz and chert; black clay; Crinoid debris traces.

605.	359.4-360.4	0.29% Oily material
606-07.	360.4-373.0	0.45% Black clay; silt.
608-09.	373.0-388.8	0.49% Gray clay; silt.
610-12.	388.8-406.2	0.83% Gray clay; silt of quartz; limonite traces; collophanite.
613.	406.2-408.2	4.24% Fine quartz silt; lt gray clay.
614-15.	408.2-424.1	1.28% Same as above.
616.	424.1-431.1	1.13% Same as above; collophanite.
617-19.	431.1-451.6	1.91% Quartz subhedrons and quartz silt with gray clay; collophanite.
620.	451.6-460.1	2.83% Quartz silt; gray clay.
621.	460.1-465.1	2.28% Gray clay; silt; limonite traces.

Member L 2

622.	465.1-466.6	2.65% Chert and quartz silt; overgrowths of quarts on silt fragments; gray clay.
623.	466.6-468.6	3.14% Whitish-gray clay; traces of quartz clusters.
624-26.	468.6-485.3	2.55% Whitish-gray clay; traces of quartz subhedrons.
627-28.	485.3-497.6	0.54% Black clay; crinoidal debris; irregularly shaped chert fragments.
629.	497.6-509.7	0.34% Black clay; traces of finely dolomoldic chert; minor fine silt.

WIND RIVER CANYON

MISSION CANYON FORMATION

Member MC 1

466.	0-11.0	1.35% Smooth, rounded, irregularly shaped grains up to granule size of granular, dirty white chert; traces of limonite; black silty clay.
467.	11.0-18.5	5.99% Chert as above but not so well-rounded; traces of yellow shale; limonite traces; accessory traces.

Member MC 2

468-69.	18.5-27.1	1.43% Black, silty clay; granular, porous chert; crinoid debris; subhedral quartz xls.
470-73.	27.1-53.2	0.65% Dark gray clay with silt of chert and quartz; crinoid and brachiopod debris; traces green shale; accessory traces.
474-75.	53.2-62.4	1.94% Gray clay; brachiopod and crinoid debris; unmodified, slightly porous, white chert.
476-78.	62.4-83.4	1.26% Oolitic ? aggregates of white chert; dolomorphic quartz aggregates; abundant brachiopod debris; unmodified, granular chert fragments; gray clay.
479.	83.4-89.8	4.36% Silt to v fine size of angular quartz and chert; finely dolomorphic chert; brachiopod debris; massive chert-cemented quartz aggregates; chalcedonic chert fragments.
480.	89.8-92.8	10.14% V angular,fine to silt-size, quartz grains; finely granular, porous, white chert; green shale traces.

481-83.	92.8-111.8	10.68% Lt grayish-white clay; fine to med sand grains; green shale; minor quartz clusters.
484.	111.8-124.0	15.78% Lt gray to white clay; quartz and chert silt; green shale traces; accessory traces.

Member MC 3

485.	124.0-126.5	0.48% Black, silty clay; minor dolomorphic (?) chert; unmodified, finely granular chert.
486.	126.5-136.7	0.32% Black, silty clay.
487-89.	136.7-144.0	1.51% Med gray clay; fragments of pearly chalcedonic chert; minor silts; accessory traces.
490-91	144.0-155.3	0.75% Traces of v finely dolomoldic chert; subhedral pyrite; med gray, silty clay.
492-93.	155.3-164.5	7.77% Gray, silty clay; med dolomoldic chert; v finely porous, compact chert; cemented oolite ? clusters.
494-97	164.5-181.7	1.81% Soft, finely dolomoldic (?), porous, white chert; med gray, silty clay; traces of unmodified, granular chert.
498-99	181.7-188.1	2.93% Micro-xln, dolomoldic, lacy quartz; finely dolomoldic chert; white and gray clay.
500.	188.1-193.1	0.85% Med dark gray, silty clay; traces of finely granular, porous, white chert.
501-04.	193.1-218.5	2.0% Angular quartz and chert fragments; minor dark gray clay; finely porous dolomoldic chert; clustered quartz xls.

505-06. 218.5-226.0 3.49% (30%)
White, hard, porous and granular, dolomoldic (?) chert; dark gray to black, silty clay; traces of soft, black, carbonaceous material.

507-08. 226.0-235.8 0.61%
Black and white clay; finely dolomoldic, white chert.

509-10. 235.8-250.3 0.47%
Black clay; finely dolomoldic chert.

511. 250.3-253.0 2.11%
Lt gray clay; limonite traces.

512-13. 253.0-260.7 1.33%
Dark gray clay minor; massive, granular chert mottled white and gray; finely granular, dolomoldic chert; chert and quartz fragments to silt-size.

514. 260.7-262.9 2.19%
Lt gray clay.

515-18. 262.9-277.2 2.72%
Granular, dolomoldic, white chert (finely porous); hard, granular, unmodified chert.

LODGEPOLE FORMATION

Member L 1

519-22. 277.2-293.9 10.52%
Dolomoldic or dolomorphic (?) chert; quartz clusters; anhedral quartz xls; gray clay.

523-24 293.9-303.2 0.68%
Black clay; v fine to med quartz subhedrons; free chert oolites (?).

525-26 303.2-308.2 2.13%
Euhedral and subhedral, v fine quartz xls (and clusters); black, silty clay minor.

527. 308.2-311.3 3.61%
Whitish-gray, slightly silty clay.

528-29	311.3-319.3	2.65% Coarsely dolomorphic (?) and anhedral quartz which grades to chert; minor black clay.
530-31.	319.3-331.6	1.32% Lt to med gray clay; coarse quartz clusters.
532-33	331.6-339.3	1.0% Same as above; lt gray clay with minor fine to med grains of quartz.
534.	339.3-342.3	0.59% Lt gray silty clay; crinoid traces.
535.	342.3-345.8	0.25% Black, silty clay.
536-38.	345.8-358.8	0.83% Lt gray, silty clay.
539.	358.8-360.5	2.56%
540.	360.5-362.7	11.94% Whitish-gray, slightly silty clay.
541-42	362.7-374.4	1.55% Lt gray, silty clay.
543.	374.4-379.7	5.09% Whitish-gray, slightly silty clay.
Member L 2		
544.	379.7-385.5	4.09% Pale pink clay; green, waxy shale; limonite traces; euhedral and subhedral quartz xls (partly clustered).
545-46.	385.5-391.2	1.61% Green shale traces; gray, v finely silty clay.
547-48.	391.2-401.1	1.0% Med dark gray clay; silts of chert and quartz; limonite traces.
549-50	401.1-414.1	1.10% Quartz silt; one cluster of quartz; med dark gray clay.

551-52. 414.4-423.3 0.24%
Med dark gray to black, slightly silty, clay.

553-54. 423.3-436.8 0.13%
Black, fluffy clay.

555-56. 436.8-446.2 0.10%
Same as above.

DEVONIAN?

557. 446.2-451.9 1.17%
White clay.

558. 451.9-453.4 13.37%
Angular to subrounded, spherical, med size quartz sand; traces of green shale; white clay.

BIGHORN DOLOMITE

559. 453.4- 0.20%
Traces of green, waxy, shale in fluffy clay; occasional fine quartz xls.

TENSLEEP CANYON

MISSION CANYON FORMATION

Member MC 1

1. 0-5.5 — 0.5%
Lt bright brown, flaky, silty clay; traces of sand grains (v fine); collophanite (?) traces; carbonaceous flakes.

2. 5.5-9.3 — 1.99%
Chalky-colored, silty clay; traces of v finely dolomoldic, granular chert; brachiopod fragments; crinoid rings; a few quartz and chert grains; limonite traces; accessories.

3. 9.3-12.5 — 2.49%
Chalky-colored, smooth, earthy clay; scattered carbon flecks; accessory traces; fossil fragments; one anhedral limonite grain.

4. 12.5-19.8 — 3.28%
Chalky-colored, smooth, earthy clay; accessory traces.

5. 19.8-22.9 — 18.32%
Well consolidated grains (?) of granular, dolomoldic chert; fine sand aggregates; minor chalky colored clay.

6. 22.9-30.9 — 5.86%
Dirty gray, powdery, weathered chert or silica; minor, coarse to fine quartz grains; anhedral limonite grains.

7. 30.9-35.4 — 10.14%
Dirty gray, powdery, weathered chert; spherical-shaped aggregates of quartz xls; limonite traces.

8. 35.4-49.9 — 5.18%
Same as above; no limonite.

9. 49.9-52.1 — 1.35%
Dirty gray, flaky clay; limonite and chert grains; traces of crinoid and brachiopod debris.

10. 52.1-54.9 5.24%
Dirty gray, powdery clay; brachiopod traces; limonite traces.

11. 54.9-58.9 3.23%
Finely granular, grayish-white chert with inclusions of drusy, subhedral quartz.

12. 58.9-62.4 0.11%
Silty, dirty brown clay.

13. 62.4-70.9 0.23%
Brownish-cast, powdery clay; slight amount of subporcelaneous chert; v infrequent quartz grains.

14. 70.9-73.2 5.11%
Unmodified, porcelaneous, smooth, white chert; lt gray clay.

15. 73.2-75.2 15.62%
Unmodified, porcelaneous chert; moderate amount of finely granular, drusy, subhedral quartz; powdery, dark gray clay.

16. 75.2-78.7 1.495%
Dark gray, flaky clay.

Member MC 2

17. 78.7-86.9 9.84%
Dolomoldic, med-granular chert; drusy, finely granular chert; subhedral quartz aggregates; scattered limonite.

18. 86.9-96.2 1.42%
Dull gray, earthy clay; unmodified, chalcedonic chert fragments; pyrite traces.

19. 96.2-101.0 1.25%
Pyrite traces; dull, earthy, silty clay; unmodified, chalcedonic chert fragments.

20. 101.0-106.5 1.065%
White, porcelaneous chert; fragments of banded, chalcedonic chert; limonite traces (minute particles); earthy, silty clay.

21. 106.5-110.8 0.93%
Traces of brachiopod debris; finely granular chert flakes; black, silty clay; traces of limonite.

22. 110.8-118.0 1.23%
White, porcelaneous, chalky chert; clustered and free oolites; brachiopod, crinoid, and gastropod debris; pyrite traces; silty clay.

23. 118.0-123.4 1.21%
Scattered, finely granular, fossil fragments; clustered oolites (?) of chalky chert; silty, brownish-gray clay;

24. 123.4-133.6 1.7%
Free and clustered, chalky, skeletal, concentric, elongated oolites (?); fine grained fragments of brachiopod and crinoid debris; silty clay.

Samples 25 to 31 inclusive are here listed separately. These are shown collectively in Chart II since they were taken from a short stratigraphic interval; thickness range of this interval is 133.6-144.1

25. 1.73%
Same as above; fossil debris (brachiopods) abundant; clustered and free, concentric oolites (?); clay.

26. 3.09%
Oolitic (?), chalky aggregates; unmodified, gray, chalcedonic chert fragments; granular fragments of fossil debris; gray, silty clay.

27. 20.59%
Translucent, chalcedonic fragments of fossil debris; finely granular, white oolite (?) clusters. These oolites (?) may be algal debris.

28. 1.55%
Translucent fragments of brachiopods and crinoids; limonite traces; infrequent, granular, white oolites (?).

29. 1.15%
Pearly, translucent, chalcedonic chert with tripolitic coating; fragments of white, porcelaneous chert; black, silty clay; collophanite traces.

30.		3.58% Banded, chalcedonic chert (white to translucent);free and clustered oolites (?) of chalky chert; powdery, silty clay.
31.		2.48% Dirty white, porous, chalky chert; powdery, silty clay.
32.	144.1-154.3	15.38% Oomoldic and oolitic, chalky (tripolitic ?) chert; infrequent, fossil fragments; traces of green shale and drusy quartz.
33.	154.3-161.3-	21.61% Unmodified, white, porous, subporcelaneous chert fragments with small, pearly, chalcedonic inclusions; limonite traces; subhedral quartz aggregates which vary to porcelaneous chert.
34.	161.3-169.8	2.75% Silty clay; limonite; v coarse grains of soft, weathered chert.
35.	169.8-179.0	7.19% Slightly silty, gray clay; traces of quartz anhedrons.
36.	179.0-184.5	10.13% White clay; porous, granular, gray chert; fine to med, subrounded, sand grains.
37.	184.5-190.3	2.04% Limonite and magnetite (corroded) traces; silt; dplomite centered quartz grains; green shale flakes; accessories.

Member MC 3

38.	190.3-193.3	0.085% Black, silty residue of clay with micro-sized, euhedral quartz xls; traces of collophanite.
39.	193.3-199.5	3.32% Minor clay; granular, white chert with v fine, irregular dolomolds; finely xln quartz clusters.

40. 199.5-206.0 12.78%
Aggregates of porous, granular chert with poorly defined dolomolds; hollow, concentric oolites (?) and oomolds (?); infrequent, fine grains of quartz; infrequent, fine euhedrons and subhedrons of quartz.

41. 206.0-218.5 8.57%
Micro- to silt-size, quartz subhedrons abundant; cellular, skeletal, finely xln, quartz networks which appear to be fracture fillings; minor, gray, chalcedonic chert; overgrowths of micro-xln quartz on granular, gray chert.

42. 218.5-223.5 17.03%
Micro-xln, quartz silt; some lacy, v finely xln, dolomoldic quartz aggregates; some cellular, white, chalk-like chert; several aggregates of chalcedonic, chert grains enclosed in micro-xln, quartz matrix;

43. 223.5-231.7 17.23%
Dolomorphic and dolomoldic, v finely xln, quartz clusters and silt; moderate amount of granular (v fine), compact chert; minor chalcedonic chert (as above).

44. 231.7-244.7 11.79%
Micro-xln, porous aggregates and silt of dolomorphic and dolomoldic quartz; minor, micro-xln networks of fracture filling quartz; fragments of nonporous, chalky, granular chert.

45. 244.7-251.9 11.77%
Micro-xln, quartz silt; trace of magnetite.

46. 251.9-254.8 .935%
V finely to micro-xln aggregates and silt of modified quartz; earthy, silty clay; pyrite trace (one chunk).

47. 254.8-261.6 20.46%
Micro-xln, dolomoldic and dolomorphic quartz aggregates; minor clay.

48. 261.6-267.2 8.90%
Micro-xln, dolomoldic and dolomorphic quartz; many angular fragments of quartz; minor clay.

49.	267.2-272.8	6.43% Micro-xln, modified, quartz silt and aggregates; minor, interstitial clay.
50.	272.8-279.8	4.14% Dolomoldic and cellular quartz to silt-size; increasing clay content; some scattered, med, quartz subhedrons; rounded fragments of porous chert.
51.	279.8-284.8	3.95% Clay; angular fragments of compact, granular (slightly porous) chert.
52.	284.8-295.5	1.63% Same as above; minor chert; pyrite traces.
53.	295.5-302.0	6.47% Dolomoldic and cullular quartz aggregates and silt; fragments of porous chert; minor clay.
54.	302.0-308.7	0.97% Finely to silt-size, xln quartz; clay; a few dark colored fragments of compact, finely granular, porcelaneous chert.

LODGEPOLE FORMATION

Member L 1

55.	308.7-318.6	2.4% Euhedral to subhedral, quartz xls; clusters of subhedral quartz; granular, compact chert; dolomoldic chert fragments.
56.	318.6-322.4	0.42% Med to silt-size grains of chert and quartz; dark colored clay.
57.	322.4-326.3	.355% Spongy mass of clay.
58.	326.3-333.6	16.99% Oomoldic (and containing oolites), white chert with interwoven, micro-xln quartz; silts.

59. 333.6-347.9 .98%
Dolomoldic, finely xln, quartz aggregates and silt.

60. 347.9-349.0 1.27%
Gray flakes of clay; minor silts.

61. 349.0-355.8 2.60%
Fragments of anhedral, xln quartz; traces of dolomoldic, lacy quartz; flaky, cellular aggregates of quartz.

62. 355.8-361.7 5.82%
Clay impurities; silt of anhedral quartz fragments; infrequent, chalky, chert oolites (?) or grains; infrequent clusters of silt-size, xln quartz.

63. 361.7-365.1 0.18%
Dark gray, silty, flaky clay; traces of magnetite.

64. 365.1-373.3 1.93%
Chalky, white, chert oolites (concentric), free and clustered; anhedral to subhedral, quartz xls and clusters; scattered flakes of fracture filling quartz.

65. 373.3-378.4 0.47%
Black, flaky clay; traces of limonite; minor amount of quartz silt; traces of a dark brown, spongy, cellular aggregate.

66. 378.4-381.2 2.72%
Thick flakes of v finely silty clay; traces of limonite and magnetite; traces of cellular, brown aggregate as above.

67. 381.2-382.9 1.12%
Magnetite trace; slightly silty clay with micro-size flakes of chert.

68. 382.9-385.5 2.10%
Relatively pure, lt gray clay; limonite trace.

69. 385.5-394.2 0.40%
Silty, gray clay.

70. 394.2-396.0 0.51%
Quartz clusters in quartz silt.

71. 396.0-398.1 .49%
Med gray, silty clay; magnetite trace.

72. 398.1-406.7 1.32%
Trace of black, anhedral material which diffuses in index oil; micro-silt in gray clay.

73. 406.7-411.7 22.4%
Micro-silt in gray clay as above.

74. 411.7-414.7 6.97%
Grayish-white, silty clay as above with a moderate amount of finely disseminated limonite.

75. 414.7-417.1 2.27%
Whitish-gray, silty clay as above.

Member L 2

76. 417.1-423.1 5.96%
Whitish-gray, micro-silty clay; microscopic accessories.

77. 423.1-426.0 2.54%
Sand and silt of tabular, prismatic, quartz grains frosted by micro-xln quartz; clusters of anhedral quartz.

78. 426.0-433.7 2.925%
Med to coarse sized, subhedral and euhedral, quartz xls (penetration twins) and aggregates; clay pellets (?).

79. 433.7-446.1 1.79%
Fine, anhedral quartz grains and quartz aggregates in clay; trace of collophanite.

80. 446.1-450.8 1.58%
Gray clay with a chalky, white material.

81. 450.8-456.8 1.91%
Gray clay.

82. 456.8-462.8 0.24%
Brown, micro-granular, silty clay.

83. 462.8-466.4 .025%
Same as above with fine quartz clusters.

84. 466.4-472.1 1.98%
Micro-sized xls and dolomorphic-like clusters of quartz; one crinoid ring.

85. 472.1-478.6 .165%
Micro-xln, quartz silt in dark gray clay.

86. 478.6-482.6 .16%
Same as above.

87. 482.6-491.5 .19%
Same as above.

88. 491.5-497.0 .38%
Lt gray, silty clay.

89. 497.0-505.0 .23%
Same as above.

90. 505.0-515.5 .82%
Med gray clay.

91. 515.5-518.7 4.58%
V lt gray clay.

92. 518.7-522.0 11.105%
Infrequent, micro-sized, finely pitted, sand grains in white clay.

KINDERHOOKIAN(?) and DEVONIAN(?)

93. 522.0-524.0 44.52%
V fine to coarse, spherical quartz grains; limonite traces; green shale traces; accessory traces.

94. 524.0-544.0 38.02%
Well-rounded, high sphericity, coarse to fine, quartz grains; fragments of porcelaneous chert.

95. 544.0-564.0 .83%
Silty clay with impurities (minor chert).

SHELL CANYON

MISSION CANYON FORMATION

Member MC 1

96. 0-12.0 — 1.82%
Numerous crinoid rings; grains of gray, granular chert and of rose quartz; clusters of oomoldic-like chert; clay; accessory traces.

97. 12.0-22.0 — 1.35%
Small fragments of porcelaneous chert; clustered and free oolites of chalky chert; dolomorphic (?) chert; magnetite specks; infrequent frosted sand grains; rose quartz fragments; crinoid debris; clay.

98. 22.0-26.0 — 2.66%
Ochre and gray flakes in a tan to lt brown clay; fragments of quartz xls; dark gray porcelaneous chert fragments; hematite flecks.

99. 26.0-30.0 — 9.62%
Finely disseminated hematite; silts and v fine sand grains in clay; limonite flecks; minor gray porcelaneous chert fragments.

100. 30.0-40.0 — 16.06%
Red silty clay with fragments of unmodified brown and red, chalcedonic chert; coarse to fine sand grains.

101. 40.0-49.6 — 4.45%
Minor fossil debris; chalcedonic chert fragments.

102. 49.6-54.7 — 0.94%
Gray, silty clay with v fine, frosted sand grains; accessories.

103. 54.7-61.2 — 26.87%
Rose, chalcedonic chert; micro-gran, gray chert; quartz fragments.

104. 61.2-69.6 — 1.01%
Fine to med quartz subhedrons in a silt of hematite, quartz and clay; minor micro-granular, grayish-brown chert fragments.

105. 69.6-75.1 .83%
Dark reddish-brown silt; infrequent granular chert fragments and quartz xls.

Member MC 2

106. 75.1-91.1 2.31%
Moderate to minor porous (oomoldic ?) chalky chert aggregates; granular, chalcedonic chert; fossil debris; tripoli (?); silty clay.

107. 91.1-99.1 .59%
Fossil debris (bryozoa); minor oomoldic (?), porous chert; chalcedonic chert fragments; brown silty clay.

108. 99.1-108.1 .23%
One crinoid ring; bryozoa, brachiopod debris; granular chert flakes; maroon, silty clay.

109. 108.1-114.1 .62%
Brachiopod debris; jaspery chert flakes; hematite flecks; traces of oomoldic (?) chalky chert.

110. 114.1-125.9 .59%
Coral, crinoid, and brachiopod debris; waxy red shale; granular chert aggregates; silt; some soft chalky chert.

111. 125.9-136.9 1.07%
Flakes of red shale; infrequent frosted quartz grains; large fragments of chalcedonic chert; limonite traces; some soft white material.

Inaccessible interval 136.9-157.0

112. 157.0-167.0 8.79%
One well-rounded, v fine, spherical magnetite ball; limonite, hematite, and minor chert grains in white clay; flakes of grayish-green shale.

Member MC 3

113. 167.0-173.5 .95%
Limonite; lt gray clay; minor finely granular, gray chert fragments.

114. 173.5-187.5 7.32%
Cellular, micro-xln fracture-filling quartz; micro-dolomoldic (lacy) quartz aggregates and silt; fragments of gray granular chert; traces of fine quartz subhedrons.

115. 187.5-196.0 0.04%
Dark brown, v fine silt.

116. 196.0-202.8 0.19%
Micro-xln quartz; black clay flakes.

117. 202.8-211.0 11.16%
Dolomoldic (lacy) quartz silt and aggregates.

118. 211.0-217.3 15.94%
Quartz as above with some white, chalky chert.

119. 217.3-224.7 11.61%
Quartz as above but slightly more coarse in texture; gray clay flakes.

120. 224.7-230.5 1.37%
Quartz as above; gray clay.

121. 230.5-240.5 2.24%
Dolomoldic and dolomorphic, lacy, micro-xln quartz; brown clay.

122. 240.5-256.1 1.56%
Clay flakes; lacy quartz silt; limonite trace.

123. 256.1-264.6 6.20%
Finely dolomoldic (lacy) quartz; finely xln quartz anhedrons to subhedrons; minor dark gray clay.

124. 264.6-275.2 2.62%
Lacy quartz as above.

125. 275.2-282.4 3.10%
Fluffy, lacy dolomoldic quartz.

126. 282.4-293.5 2.01%
Fragments of chalcedonic chert; dark gray, silty clay; lacy, micro-xln quartz silt.

127. 293.5-305.5 0.89%
Gray, silty clay; granular to chalcedonic chert fragments.

128. 305.5-310.0 0.48%
Med gray, finely silty clay; limonite traces.

129. 310.0-317.0 1.45%
Finely silty, lt gray clay; infrequent quartz grains.

LODGEPOLE FORMATION

Member L 1

130. 317.0-321.9 0.24%
Finely silty, med gray clay.

131. 321.9-328.9 0.69%
Fragments of granular to chalcedonic pink chert; clay; quartz silt with infrequent med quartz anhedrons.

132. 328.9-335.5 1.18%
Quartz silt; infrequent fine-sized ovoids; minor clay.

133. 335.5-340.5 0.74%
Quartz silt with infrequent, fine quartz anhedrons.

134. 340.5-344.8 0.46%
Clay; white material; trace limonite.

135. 344.8-349.8 2.79%
Grayish-white clay.

136. 349.8-354.8 1.42%
Powdery, fluffy gray clay; minor lacy quartz.

137. 354.8-363.1 0.38%
Dark gray clay; soft, white, weathered chert.

138. 363.1-371.0 0.29%
Slightly silty, gray clay.

139.	371.0-377.3	0.74%	Pale black clay.
140.	377.3-385.1	0.51%	Clay as above.
141.	385.1-388.1	0.95%	Clay as above.
142.	388.1-394.2	0.12%	Clay as above; traces of micro-sized oolitic ? chert aggregates.
143.	394.2-402.6	1.13%	Med gray clay; limonite flecks.
144.	402.6-409.9	1.80%	Clay as above; limonite trace.
145.	409.9-414.9	2.16%	Same as above; anhedral pyrite.
146.	414.9-418.1	2.79%	Same as above; limonite traces.
147.	418.1-424.5	0.85%	Darker gray clay; limonite traces.
148.	424.5-432.7	0.67%	Tiny limonite flecks in slightly silty clay.
149.	432.7-442.7	1.79%	Pyrite flecks in gray clay; v fine to med-size frosted quartz and chert grains.
150.	442.7-448.0	1.83%	Slightly silty gray clay.
151.	448.0-449.2	7.51%	Lt gray clay.
152.	449.2-454.0	0.95%	Slightly silty, lt gray clay; infrequent limonite flecks.
153.	454.0-459.0	0.84%	V slightly silty gray clay.

154. 459.0-463.7 1.21%
Slightly silty, gray clay with finely disseminated hematite.

155. 463.7-467.4 2.67%
Silty red clay.

156. 467.4-472.9 3.43%
Silty red clay.

157. 472.9-479.2 2.90%
Hematitic, clayey silt of equidimensional, high sphericity quartz.

158. 479.2-484.0 2.21%
Silt; hematite; infrequent v fine quartz grains; traces of fossil debris.

159. 484.0-487.5 2.69%
Silt; hematite; infrequent, v fine quartz grains.

160. 487.5-490.3 3.68%
Blue-gray clay; infrequent, v fine, quartz grains.

161. 490.3-498.1 9.62%
Gray clay.

Member L 2

162. 498.1-502.9 7.12%
Whitish-gray clay.

163. 502.9-510.3 2.21%
Dark gray, silty clay; outgrowth chert on v fine quartz; dark gray, chalcedonic chert.

164. 510.3-516.8 1.51%
Silty, black clay; euhedral quartz with penetration twins; anhedral clusters of quartz; hematite flecks.

165. 516.8-522.0 2.33%
Dolomorphic hematite to pyrite; limonite flecks; finely xln, anhedral to euhedral quartz which is corroded by micro-xln overgrowths; gray silt; accessories.

166.	522.0-528.3	0.95% Silty clay; hematite to limonite traces; one piece of chalcedonic chert; brachiopod (?) debris.
167.	528.3-534.5	0.63% Oily black clay.
168.	534.5-538.9	0.30% Same as above.
169.	538.9-548.9	0.42% Carbonaceous tarry material.
170.	548.9-556.8	0.44% Same as above.
171.	556.8-562.2	0.28% Same as above.
172.	562.2-567.6	0.79% Carbonaceous clay.
173.	567.6-571.6	0.82% Same as above.
174.	571.6-576.8	0.51% Same as above.
175.	576.8-584.8	0.58% Carbonaceous tarry residue.
176.	584.8-591.3	0.52% Carbonaceous tarry clay.
177.	591.3-597.1	0.56% Same as above.
178.	597.1-605.3	0.02% Same as above; one crinoid ring.
179.	605.3-614.1	0.79% Slightly tarry, brown clay; minor silts and accessories.
180.	614.1-618.4	1.27% Same as above; moderate magnetite.

18.	618.4-622.7	1.25% Same as above; moderate magnetite; one crinoid ring; one coarse quartz grain.
182.	622.7-629.4	1.07% Brown carbonaceous clay.
183.	629.4-635.7	5.61% Deliquescent tarry material.
184.	635.7-639.7	2.37% Brown clay and minor weathered chert (?).
185.	639.7-647.0	3.67% Gray clay; v infrequent, yellow flecks.
186.	647.0-650.8	10.82% Whitish-gray clay.

KINDERHOOKIAN(?) and DEVONIAN(?)

187.	650.8-651.5	19.76% Coarse, frosted, high sphericity, well-rounded, quartz grains in silty clay.
188.	651.5-655.0	4.92% Gray silt with infrequent frosted fine quartz grains.
189.	655.0-659.3	11.95% Gray clay.
190.	659.3-659.8	34.26% Powdery, gray clay.
191.	659.8-665.1	17.76% Slightly clayey silt with many quartz grains as above.
192.	665.1-670.4	33.01% Same as above but not so silty.
193.	670.4-678.4	32.56% Coarse to v fine quartz grains in silty clay.
194.	678.4-685.4	1.29% Brown silt with infrequent frosted med quartz grains.

k95.	685.4-691.4	15.48% V fine sand.
196.	691.4-702.9	1.54% Dark gray silty clay.
197.	702.9-707.5	25.03% Whitish-gray, clayey silt with some v fine quartz grains.
198.	707.5-716.9	11.6% Clayey silt with med and v fine quartz grains.
199.	716.9-722.7	36.85% Clay and v fine silt.
200.	722.7-731.1	6.89% Whitish-gray clay.
201.	731.1-737.5	6.75% Slightly silty, lt gray clay.
202.	737.5-746.5	6.20% Dark gray, clayey silt; fine to v fine quartz grains.
203.	746.5-756.5	8.85% Same as above.
204.	756.5-776.5	8.63% White, slightly silty clay.
		BIGHORN DOLOMITE
205.	776.5-784.0	1.25% Blue-gray, v slightly silty clay.
206.	784.0-787.8	0.52% Same as above.
207.	787.8-799.8	0.68% Same as above.
208.	799.8-809.0	7.35% Whitish-gray, slightly silty clay; fragments of milky granular chert and white chalcedonic chert.

209. 809.0-819.0 9.50%
Clay; clusters of milky chert and grains.

210. 819.0- 2.55%
Slightly silty clay; infrequent frosted fine quartz grains.

CROOKED CREEK CANYON

MISSION CANYON FORMATION

Member MC 1

355-56.	0-11.7	1.35% Dolomorphic and dolomoldic, granular chert; crinoid and brachiopod debris; magnetite traces; flakes of chert; gray clay; silt of quartz and chert.
357.	11.7-16.5	3.17% Fossil fragments; minor white, porcelaneous chert; lt gray clay.
358-62.	16.5-50.4	1.37% Crinoid, bryozoan, brachiopod debris; gray clay.

Member MC 2

363-65.	50.4-77.8	3.48% Spongy, oomoldic (?) chert; crinoid and brachiopod debris.
366-67	77.8-90.1	0.46% Black clay.
368-71	90.1-125.1	3.3% Spongy, porous chert; unmodified, granular, gray chert; green shale; silty, lt gray clay.
372 A-B	125.1-135.1	20.18% White clay; fragments of anhedral quartz; silt; green shale; limonite traces.
372 C	135.1-140.1	3.98% Dirty white, silty clay; quartz anhedrons.
373.	140.1-145.6	0.85% Med gray, silty clay.
374.	145.6-148.7	0.47% Dark gray clay; soft, porous clusters of white chert.

Member MC 3

375.76.	148.7-155.4	5.91% Dirty gray, silty clay; fragments of hard porous chert.
377-78.	155.4-172.4	2.53% Dolomorphic chert; unmodified, granular chert fragments; dirty gray, silty clay.
379.	172.4-178.4	1.35% Unmodified, granular chert fragments; silty clay.
380-83.	178.4-2-5.0	0.76% Slightly silty, gray clay.
384-86.	205.0-229.7	0.89% White, granular to porcelaneous chert.
387.	229.7-239.2	5.55% White, granular to porcelaneous chert; minor, porous, granular, gray chert; minor gray clay.
388-90.	239.2-249.5	6.14% Soft, dolomoldic (?) chert; hard, granular grayish-white, unmodified chert; anhedrons and fragments of quartz.
390 A	249.5-253.5	0.32% Blackish-gray, silty clay.
391.	253.5-257.6	0.15% Blackish-gray, silty clay; infrequent fragments of finely porous, white chert.
392-94.	257.6-279.1	0.08% Same as above.
395-96.	279.1-302.3	0.39% Med gray, silty clay; white, soft, tripolitic (?) chert.
395 A		0.72% Gray clay. (Lateral sample).

397-98.	302.3-318.7	2.03% Med gray, dolomoldic chert; unmodified, granular, lt gray chert; quartz clusters.
399.	318.7-323.7	(Not received).

LODGEPOLE FORMATION

Member L 1

400-401.	323.7-342.6	1.03% Subhedral to anhedral quartz; black clay and silt; rounded chert grains.
402-04.	342.6-356.2	0.30% Blackish-brown, silty clay.
405.	356.2-358.4	0.26% Same as above.
406.	358.4-363.7	0.28% Brownish-cast gray, slightly silty clay.
407.	363.7-367.7	1.44% Lt gray clay with infrequent silt-size fragments of quartz.
408-10.	367.7-381.9	1.68% Same as above.
411.	381.9-386.3	0.72% Slightly silty, med gray clay; flakes of chert and quartz.
412-13.	386.3-400.5	1.13% Gray clay; infrequent silt particles.
414-15	400.5-415.0	1.39% Slightly silty, gray clay.
416-19	415.0-445.1	1.15% Gray, silty clay; occasional anhedral quartz clusters.

420-24.	445.1-463.4	2.68% Gray, silty clay with subhedral pyrite.
425-26.	463.4-469.9	3.80% Gray, slightly silty clay.
427-30.	469.9-489.8	7.36% Gray, silty clay; infrequent grains or fragments of gray chert; v fine to med quartz grains.
431-32.	489.8-501.7	2.36% Coral ?, crinoid and brachiopod debris; flakes and fragments of gray chert; pyrite traces.
433-36.	501.7-517.8	4.85% Limonite flecks; gray clay; silt.
437.	517.8-520.6	3.23% Flattened oolites ? of chert; v fine quartz silt; subhedral pyrite; oomoldic (?), granular chert.
438-39.	520.6-533.1	6.49% Finely porous, limonite centered, clay concretions; fine quartz silt.

Member L 2

440-41.	533.1-540.8	6.83% Quartz anhedrons and clusters; gray clayey silt.
442-43.	540.8-549.4	4.01% Quartz euhedrons and anhedrons; granular, dirty gray chert; silt.
444-46.	549.4-562.6	0.71% Black, silty clay; scattered, fine xls of quartz; traces of carbonaceous material.
447-48.	562.6-569.6	0.64% V coarse to v fine quartz in xls, clusters, and grains; black silty clay.

449-50.	569.6-575.6	2.06% Traces of modified, cellular chert; fine sized quartz and chert grains; gray silty clay.
451.	575.6-579.1	14.14% V finely dolomoldic chert; porous, granular, white chert; chalcedonic, zoned chert.
452-53.	579.1-582.8	12.22% Finely dolomoldic, soft, white chert.
454.	582.8-587.5	3.34% Dirty gray clay; minor silt portions; traces of dolomoldic chert.
455-56.	587.5-596.5	1.26% Dolomoldic or oomoldic, white chert (granular) and chalcedonic chert; black, silty clay; traces of brown oomoldic ? clay.
457-58.	596.5-609.7	2.42% Oomoldic clay traces; crinoid debris; granular, semi-porous, white chert; dark gray, silty clay.
459-60.	609.7-623.0	0.58% Black clay; minor, v fine silt.
461-62.	623.0-632.6	0.40% Same as above.

DEVONIAN(?) or ORDOVICIAN(?)

463-64.	632.6-639.5	1.50% Black, silty clay; fragments of unmodified, granular, gray chert.
465.	639.5-647.9	1.06% Gray, slightly silty clay.

SHOSHONE CANYON

MISSION CANYON FORMATION

Member MC 1

211-13.	0-15.2	0.23% Pyrite; limonite; infrequent v fine quartz grains; finely dolomoldic chert; black clayey silt.
214.	15.2-21.0	1.33% Collophanite traces; chalcedonic chert fragments; subhedral quartz xls; flakes of chert and quartz; finely silty, gray clay.
215-17.	21.0-32.8	1.35% Slightly silty, dark gray clay; infrequent, fine sand grains; white porcelaneous chert fragments; chalky, porous, tripolitic chert.
218.	32.8-37.8	1.34% Slightly silty clay; flakes of white porcelaneous chert; white chalky, tripolitic chert.
219.	37.8-44.3	.615% Crinoid and brachiopod debris; black, silty clay.
220-21.	44.3-52.9	1.32% White and gray, chalcedonic chert in fragments and flakes; dark gray silty clay; white, soft, tripolitic chert.

Member MC 2

222-23.	52.9-68.6	.725% Crinoid, coral ?, brachiopod debris; chalcedonic chert fragments; black to dark gray, silty clay; traces of quartz clusters; white, spongy chert.
224.	68.6-70.9	0.96% Crinoid and brachiopod debris; anhedral quartz grains; micro-silty clay.

225-26.	70.9-79.9	1.04% Same as above with a cellular-like fossil; quartz anhedrons; granular, gray chert fragment; dark gray silt.
227-29.	79.9-103.8	0.52% Traces of pyrite and limonite; brachiopod debris in blackish-gray, clayey silt.
230-32.	103.8-125.6	1.65% Crinoid, coral ?, and brachiopod debris; chalcedonic and granular chert; quartz anhedrons; black, clayey silt.
233.	125.6-128.6	1.76% Same as above.
234.	128.6-148.6	18.63% Pyrite and limonite traces; blue-green shale; drusy quartz clusters; chalcedonic chert fragments; a soft, white, fibrous, length slow, low-birefringent material; silts; clay.

Member MC 3

235-36.	148.6-166.7	3.56% Aggregates of poorly dolomoldic (lacy), micro-xln quartz; granular chert fragments; black, clayey silt.
237-39.	166.7-182.8	0.72% Soft, shite, porous chert aggregates; black, silty clay.
240-41.	182.8-198.6	0.19% Black, silty clay.
242-43	198.6-210.9	0.17% Black, silty clay with one fine sand grain.
244.	210.9-218.2	1.11% Gray, silty clay.
245-47.	218.2-230.4	0.29% Fragments of porous, granular chert; silty clay.
248.	230.4-234.5	7.29% Black, silty clay; granular chert fragments; porous, v finely dolomoldic chert and quartz.

249.	234.5-238.3	0.115% Black, silty clay.
250.	238.3-241.6	(Not received).
251-53.	241.6-261.2	0.135% Black, silty clay.
254.	261.2-263.1	(Not received).
255.	263.1-266.5	7.0% Anhedral fluorite; fragments of chalcedonic and granular chert; gray, silty clay.
256-59.	266.5-282.1	3.02% Gray, silty clay; fragments of granular chert.
260-61.	282.1-301.5	4.8% Soft, porous, tripolitic chert; some irregularly shaped voids in more compact granular, gray chert; dirty gray clay.
262-64.	301.5-308.5	1.57% Compact, granular, gray chert; gray clay.

LODGEPOLE FORMATION

Member L 1

265.	308.5-310.9	7.59% Whitish-gray, silty clay; fine to med, anhedral to subhedral quartz; accessory traces.
266-68.	310.9-318.8	3.26% Granular and porcelaneous chert fragments; dirty gray clay; silt of quartz subhedrons and euhedrons.
269.	318.8-323.8	1.97% Small, white chert; oolites (?)--clustered and free; silty clay.
270-71.	323.8-332.8	2.85% Free and clustered quartz subhedrons; porcelaneous chert fragments; gray, silty clay.

272.	332.8-333.8	8.77% Fine and med, poorly dolomoldic chert; free and clustered quartz subhedrons of fine and med size; minor clay.
273-74.	333.8-336.5	0.37% Black, silty clay; minor, granular chert.
275-77	336.5-355.5	0.64% Silty, dark gray clay.
278-80.	355.5-364.4	0.41% Crinoid and fossil debris; amber to rose to clear-colored, micro- to fine sized quartz anhedrons; dark gray, silty clay.
281.	364.4-365.5	0.55% Massive, granular chert fragments; fine to silt-size quartz grains in a dark gray silty clay.
282.	365.5-368.5	1.95% Silty, gray clay; accessory traces; magnetite trace.
283-84.	368.5-377.5	2.9% Gray, silty clay with fragments of granular chert.
285-87.	377.5-395.0	1.16% Infrequent, fine quartz grains; pyrite to magnetite and impurities in gray silty clay.
288-89.	395.0-403.1	2.12% Gray, slightly silty, clay.
290.	403.1-404.9	(Not received).
291.	404.9-409.8	1.52% Gray, slightly silty clay.
292-93.	409.8-417.4	(Not received).
294-95.	417.4-424.9	0.73% Darker gray, silty clay.

296. 424.9-430.1 1.23%
Spongy, cellular, brown clay trace; v silty clay.

297. 430.1-433.7 2.59%
Fine quartz silt in clay; micro-flecks of limonite and magnetite; same large anhedral grains of quartz.

298. 433.7-435.9 1.05%
Numerous limonite flakes; fine quartz silt in clay; angular fragments of granular chert.

299. 435.9-440.9 1.83%
Limonite flecks; micro-quartz silt and clay.

300. 440.9-446.4 1.44%
Same as above.

301. 446.4-448.9 1.33%
Limonite flecks; gray clay.

302. 448.9-455.4 2.46%
Traces of limonite in silty, gray clay.

303. 455.4-464.9 1.09%
Numerous limonite flecks; med gray clay; quartz silt.

303. 464.9-472.8 1.65%
Limonite flecks; silty gray clay; occasional rounded chert grains.

305. 472.8-478.5 1.41%
Pyrite altering to limonite; silty gray clay; coarse limonite grains; micro-sized magnetite grains.

306. 478.5-486.2 3.47%
Magnetite, pyrite, and limonite flecks in gray clay; pink quartz xls (v fine); quartz and chert silt.

307. 486.2-489.7 3.30%
Same as above.

308. 489.7-493.9 1.75%
Lots of fine pyrite and limonite; gray clay and silt; infrequent, coarse, subrounded chert grains.

309. 493.9-498.0 2.83%
Gray clay and micro- quartz silt; tiny limonite flecks.

310. 498.0-501.5 4.21%
Lots of finely disseminated pyrite altering to limonite in silt and clay.

311. 501.5-508.0 7.82%
Gray clay and v fine silt.

312. 508.0-513.0 3.33%
Blue-gray clay and silt; numerous pyrite flecks; an occasional subrounded chert fragment.

313. 513.0-516.3 2.51%
Silt; reddish-tan clay; numerous flecks of limonite altering from pyrite; hematite; minor v fine to fine quartz grains.

314. 516.3-519.6 2.87%
Pyrite and limonite; chert oolites; silt; minor clay; infrequent irregularly shaped cherts; anhedral fragments of quartz.

315. 519.6-523.3 (Not received).

Member L 2

316. 523.3-526.3 2.46%
White, granular chert fragments in slightly clayey silt.

317. 526.3-531.5 3.67%
Pyrite and limonite traces in silt; oolites; zoned chert; infrequent fine quartz subhedrons.

318. 531.5-540.7 0.33%
Black, silty clay; oolite sections; clustered and free oolites of white chert.

319. 540.7-547.5 2.58%
Clusters of quartz anhedrons; subrounded chert fragments; silt with minor clay.

320. 547.5-552.0 0.76%
Chert and quartz grains or fragments; black, silty clay.

321. 552.0-555.9 0.67%
Traces of brown, oomoldic-like clay; numerous chert and quartz clusters; dolomoldic chert to quartz clusters; black, micro-silt.

322. 555.9-559.2 3.97%
Med dolomoldic and oomoldic, micro-granular chert.

323. 559.2-564.3 0.38%
Black, silty clay; dolomoldic chert.

324. 564.3-569.1 19.53%
Dolomoldic and dolomorphic, granular, gray chert; anhedrons to subhedrons of quartz.

325. 569.1-574.8 21.43%
V fine to micro-sized grains of dirty white, quartz and chert; angular fragments of granular chert.

326. 574.8-579.6 0.39%
Dolomorphic (?), granular chert; black, oily material; granular chert flakes and fragments of small size; black clay.

327. 579.6-587.6 0.25%
Oomoldic-like aggregates of brown clay; black, silty clay.

328. 587.6-595.4 0.24%
Black clay.

329. 595.4-601.8 0.23%
Dolomoldic chert trace in black to brown clay.

330. 601.8-607.0 0.24%
Same as above; no chert.

331. 607.0-612.1 0.19%
Same as above.

332. 612.1-620.2 0.25%
Brown to black clay; v slightly silty.

333. 620.2-624.7 0.17%
Brown to black clay.

334. 624.7-639.7 0.33%
Same as above.

335. 639.7-645.7 0.61%
Gray clay.

336. 645.7-649.4 0.88%
Rose chert (1) fragment; oomoldic-like, brown clay aggregate; blackish-gray clay.

337. 649.4-655.2 0.41%
Dark gray clay.

338. 655.2-664.2 0.12%
Minor ochre and black impurities in med gray, slightly silty clay.

339. 664.2-670.4 0.94%
Minor granular chert flakes in gray, slightly silty clay.

340. 670.4-674.3 2.8%
Slightly silty, lt gray clay.

341. 674.3-676.4 4.45%
Same as above.

342. 676.4-678.3 7.85%
Same as above.

343. 678.3-681.4 2.62%
Same as above.

344. 681.4-685.6 5.01%
Silty clay, dirty lt gray in color.

345.	685.6-690.6	5.7% Same as above.
346-47.	690.6-695.2	16.18% Same as above.

DEVONIAN?

348.	695.2-702.2	69.55% Silty clay and gray-green shale.
350-52.	702.2-732.2	Lt gray, silty clay; well-rounded, high sphericity, frosted quartz grains of coarse to fine size.

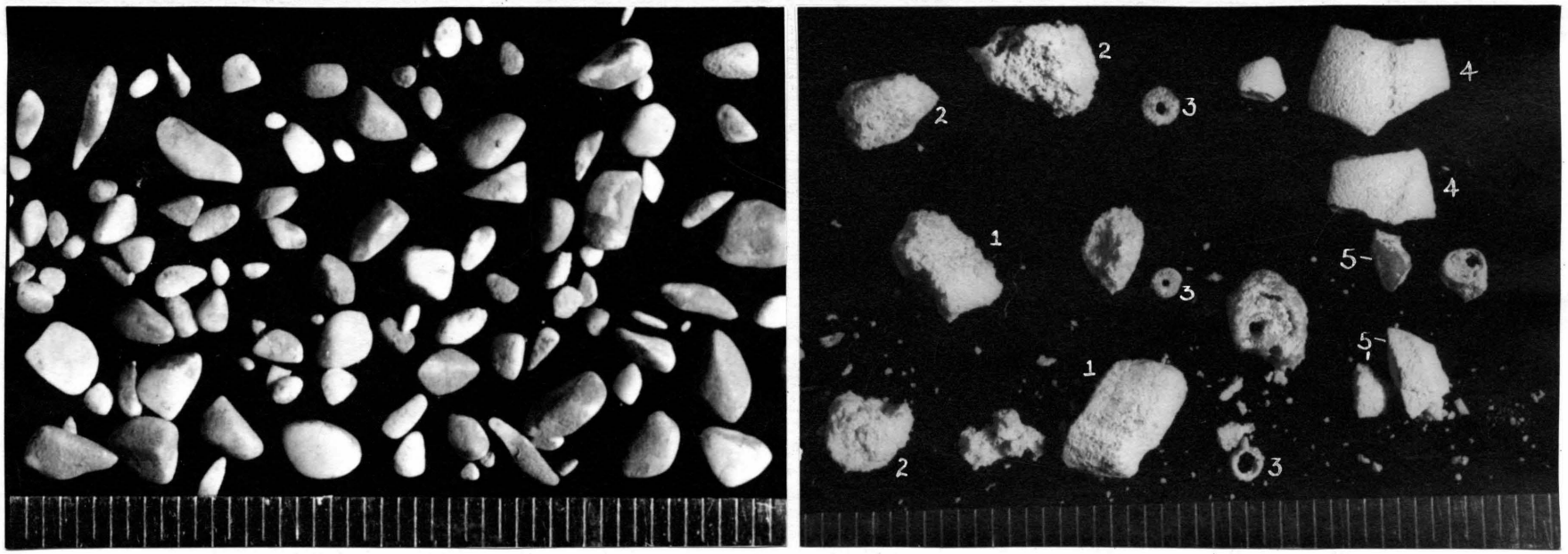

A B

Plate I: Member MC 1 Residues (smallest scale division 1/32").

A, Wind River Canyon: residual chert grains.

B, Tensleep Canyon: 1, aggregates of fine sand; 2, dolomoldic chert; 3, crinoid debris; 4, clay; 5, porcelaneous cherts.

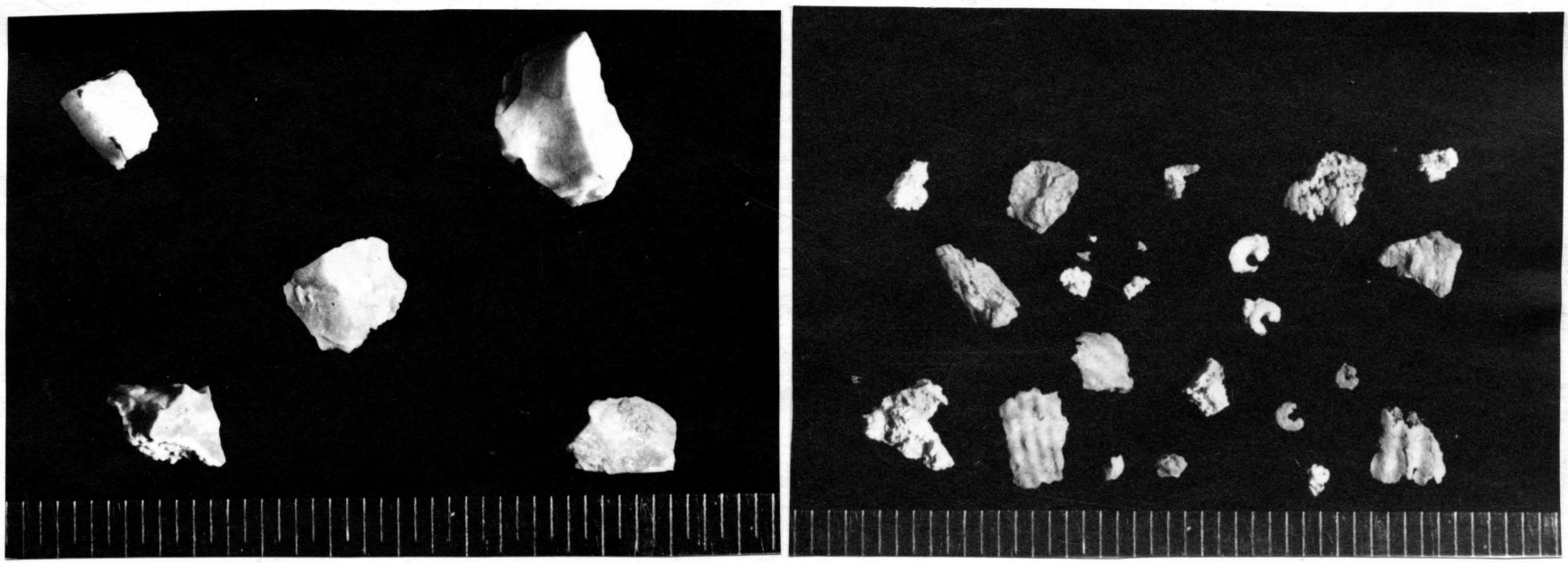

A B

Plate II: Upper MC 2 Residues (smallest scale division 1/32").

A, Shell Canyon: porcelaneous and chalcedonic cherts (note tripolitic border on lower left fragment).

B, Shoshone Canyon: fossil debris.

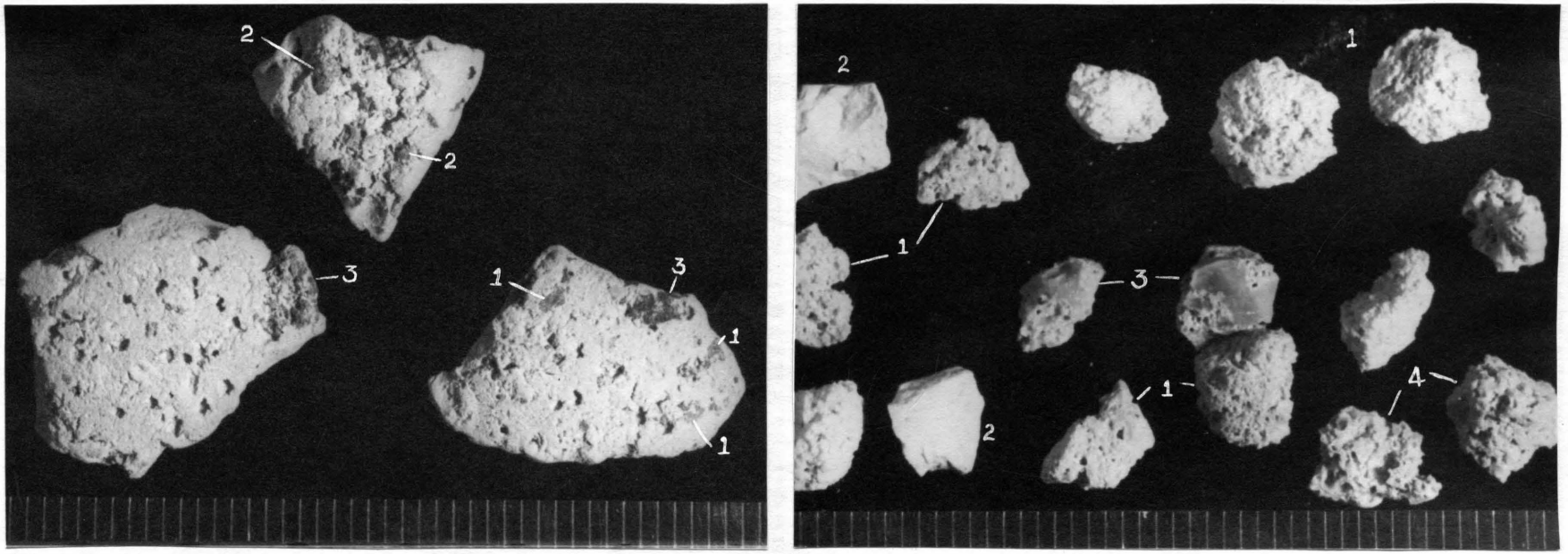

A B

Plate III: Lower MC 2 Residues (smallest scale division 1/32").

A, Tensleep Canyon: clay aggregates with embedded 1, green shale fragments; 2, quartz grains; 3, limonite.

B, Tensleep Canyon: 1, dolomoldic chert; 2, porcelaneous chert; 3, dolomoldic chert grading to unmodified, porcelaneous chert; 4, oolitic ? aggregates.

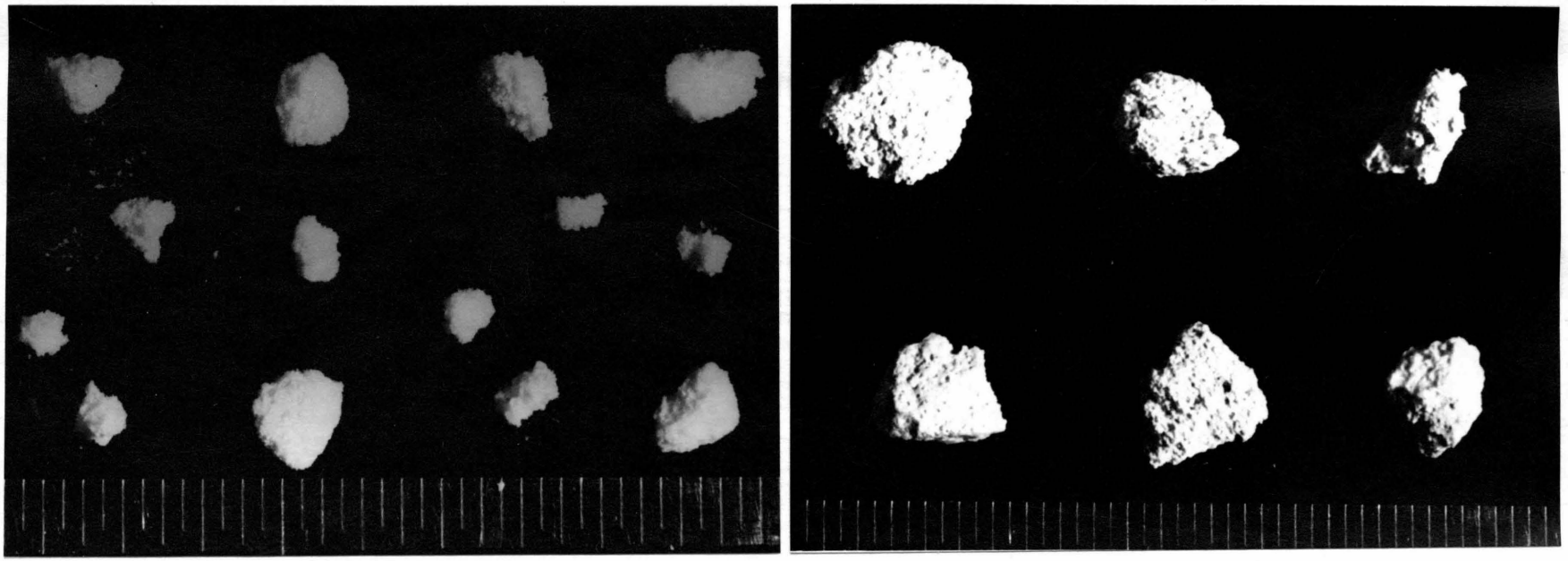

A B

Plate IV: Member MC 3 Residues (smallest scale division 1/32").

A, Shell Canyon: very finely dolomoldic and dolomorphic, lacy, micro-crystalline quartz.

B, Owl Creek Canyon: finely dolomoldic chert.

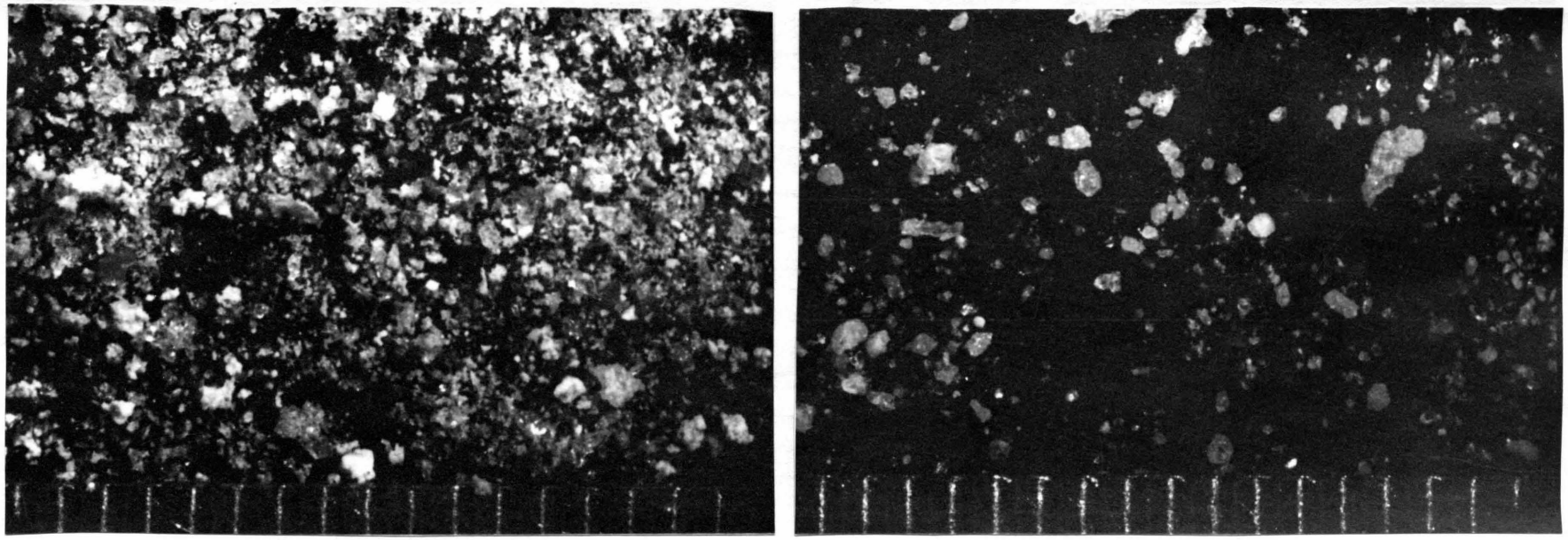

A B

Plate V: Member L 1 Residues (scale divisions 1/64").

A, Shoshone Canyon: silt of quartz and chert.

B, Shell Canyon: finely frosted sand grains and silt.

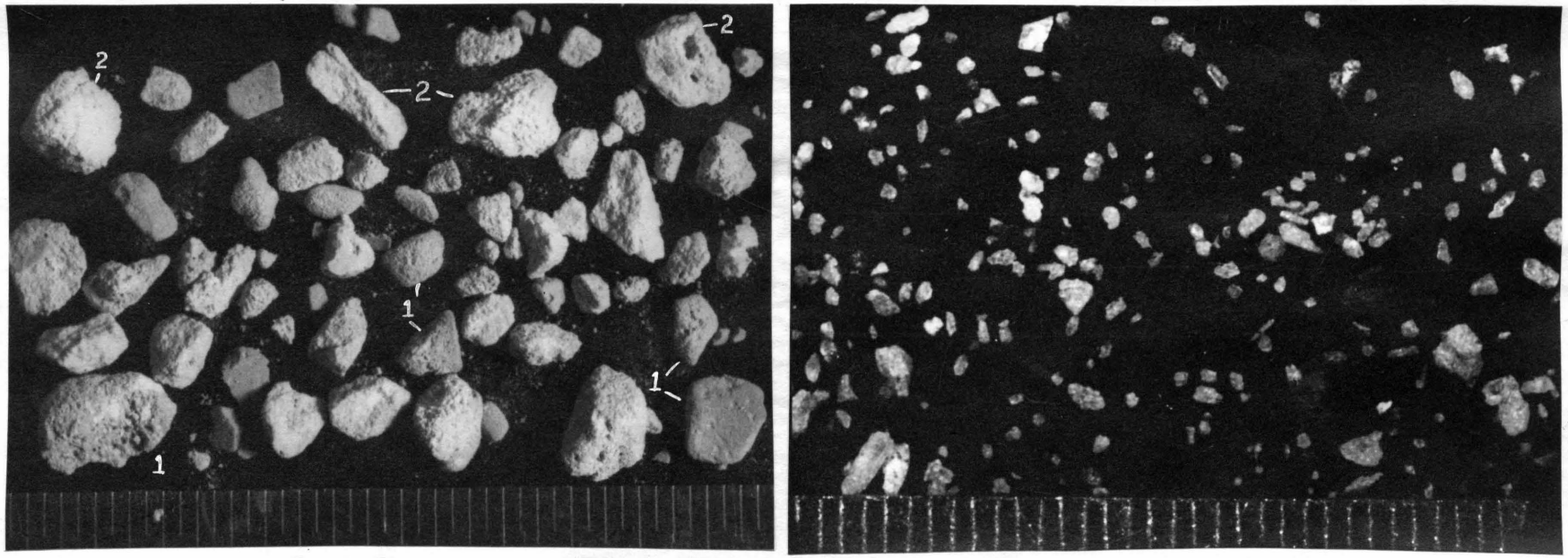

A B

Plate VI: Upper L 2 Residues.

A, (smallest scale division 1/32") Crooked Creek and Owl Creek Canyons: 1, clay pellets partly with crinoid casts; 2, spongy clay aggregates.

B, (scale division 1/64" to alternate lines) silt of euhedral and subhedral quartz crystals and grains frosted by micro-crystalline quartz.

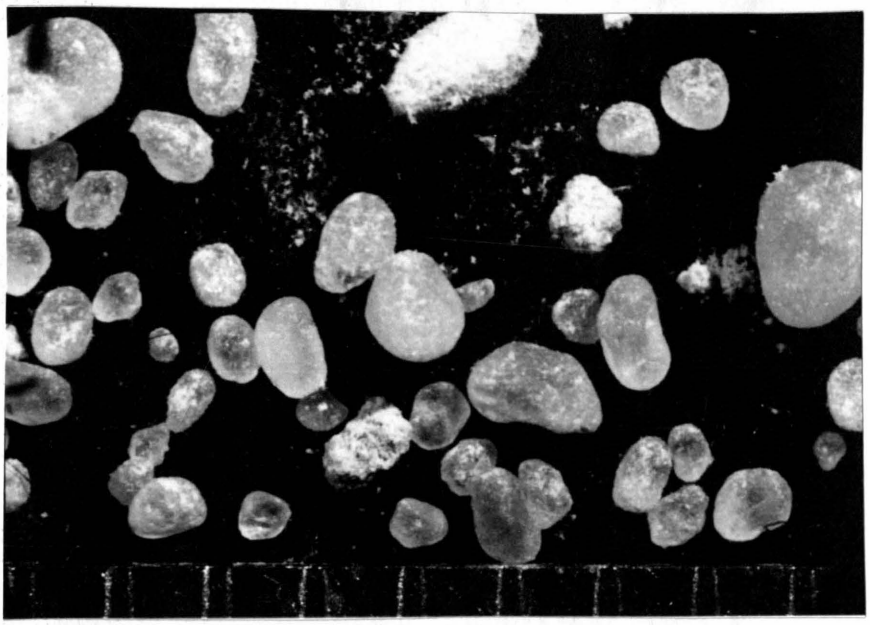

Plate VII: Uppermost Kinderhookian?-Upper Devonian? Residue (scale division 1/64").

Finely frosted, rounded quartz grains.

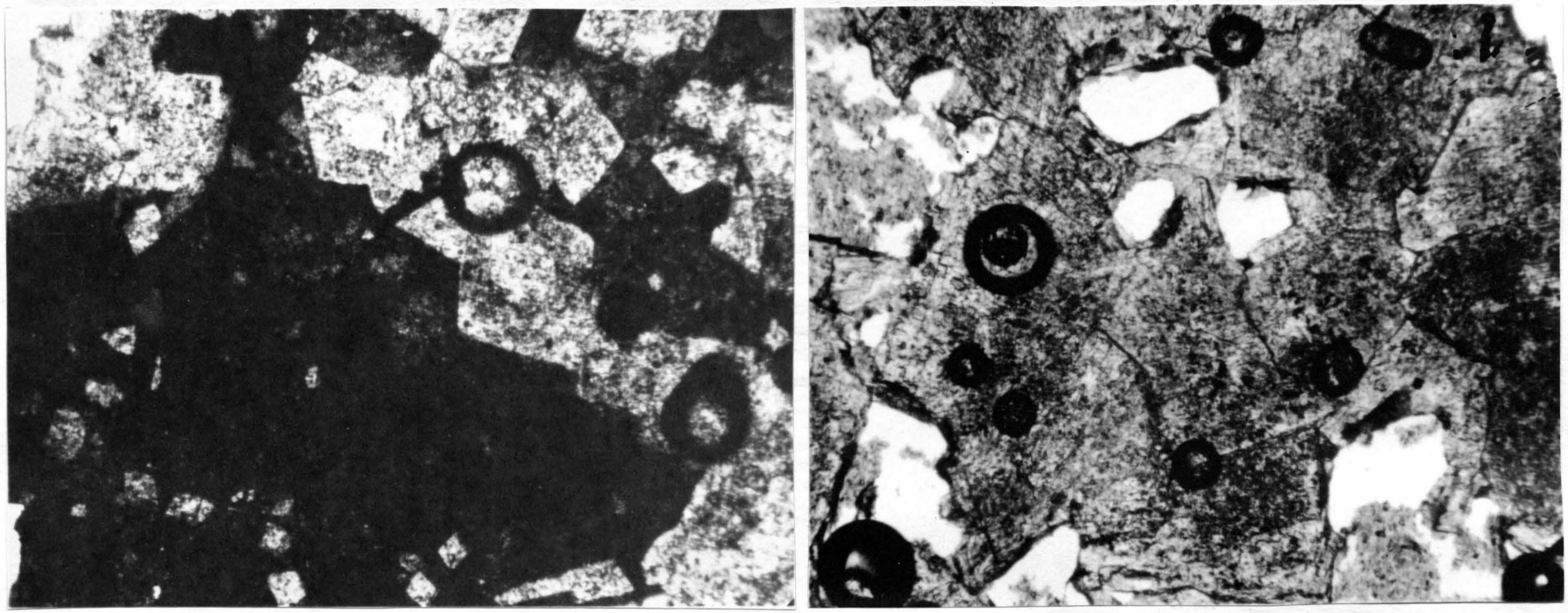

A B

Plate VIII: Upper L 1, thin sections (plane light, x85), stained by K_2CrO_4.

A, euhedral dolomite rhombs (light) in partially dolomitized limestone (dark).

B, anhedral dolomite crystals in completely dolomitized limestone: clear areas are vugs; note calcite (black) outlining interlocking dolomite crystals. Black circles are bubbles that develop when cover glass is applied to stained surface.

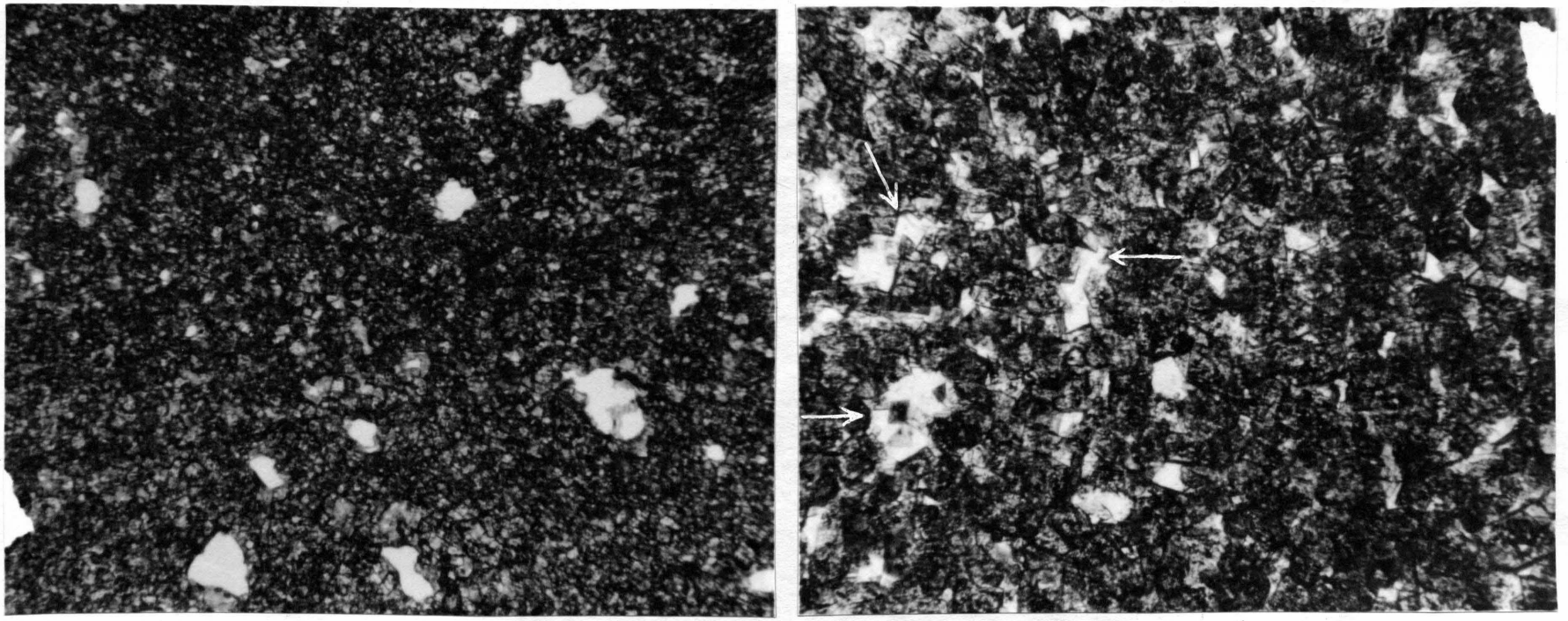

A B

Plate IX: Member MC 3, thin sections (plane light, x85) stained by K_2CrO_4.

A, dolomitic limestone: large clear areas are voids; small gray particles are dolomite; dark gray to black areas are interstitial calcite "flour".

B, silicified calcite dolomite: clear areas are crystalline quartz; note modified quartz by arrows; gray areas are dolomite crystals with interstitial (black) calcite. Micro particle sizes are characteristic of this member.

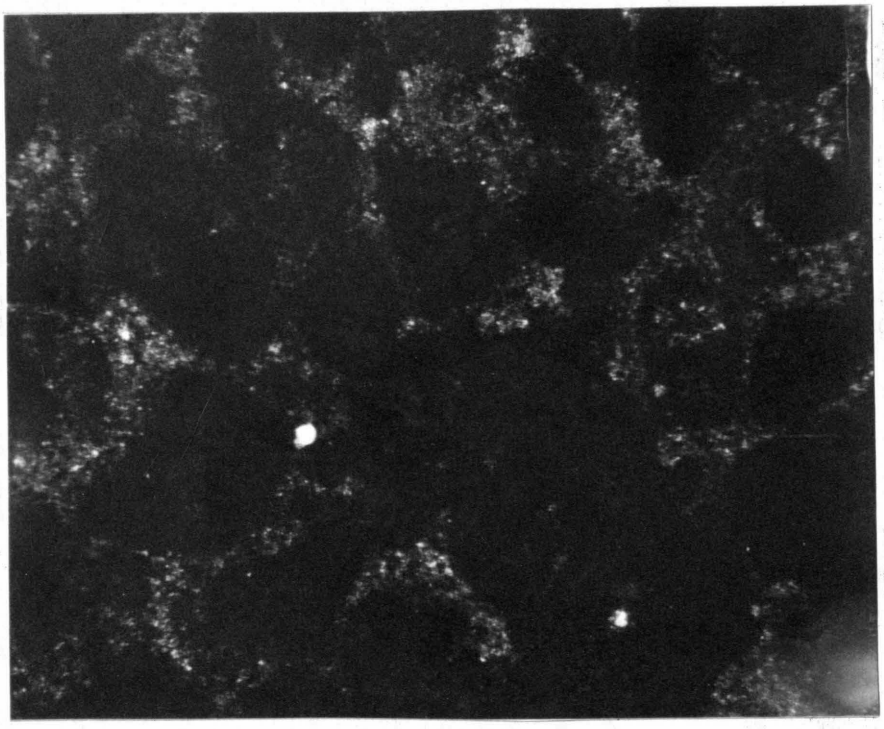

Plate X: Member MC 2, thin section (plane light, x85) stained by K_2CrO_4.

Fragmental (calcarenitic) limestone: black areas are limestone grains; gray areas are partially dolomitized matrix embodying minor quartz silt. No oolitic structure is found in limestone grains (note irregularity of shapes).

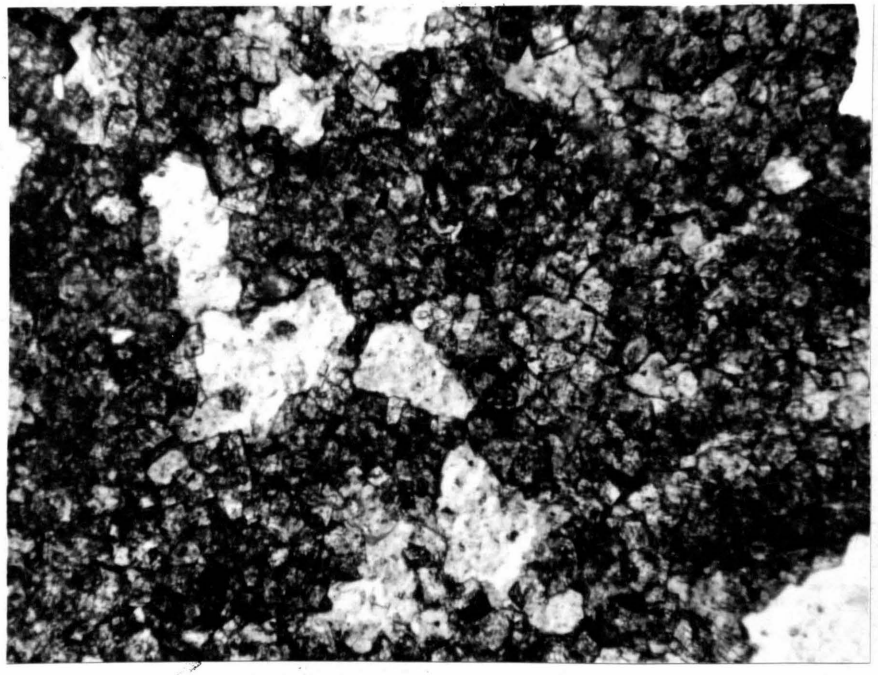

A

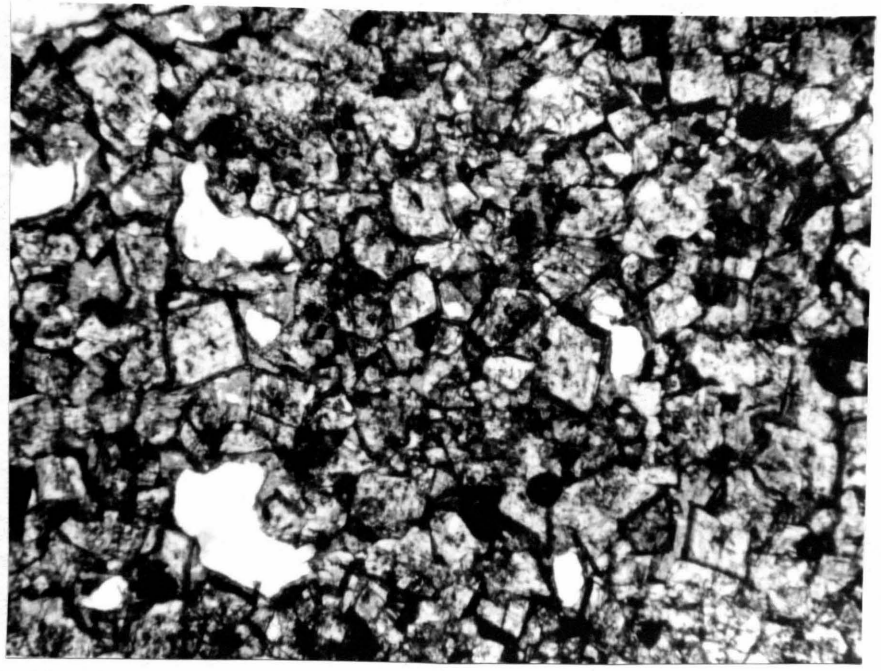

B

Plate XI: Member L 2, thin sections (plane light, x85).

A, euhedral to anhedral dolomite crystals (gray): large, light gray areas are partially leached vugs; smaller gray areas are partially leached vugs and dolomite crystals (note crystal size variation); black areas are calcitic.

B, euhedral to subhedral dolomite crystals (gray) from banded sequence: clear areas are leached vugs (note intercrystal calcite, black).

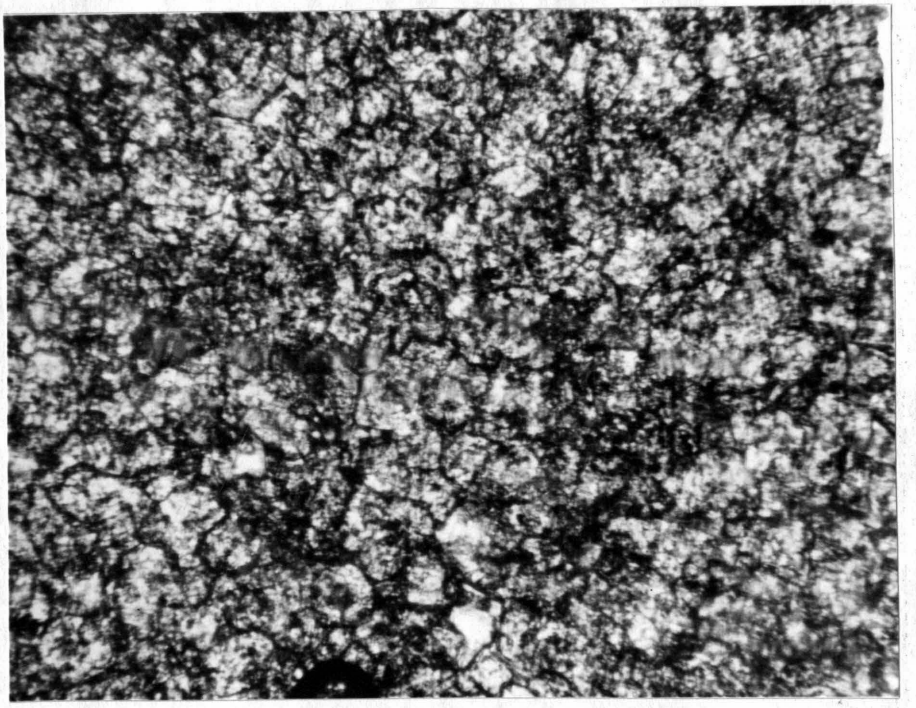

Plate XII: Member L 1, thin section (plane light, x85).

Cross-bedded clastic dolomite: note rounded and anhedral character of grains (gray), high degree of packing, and intergrain calcite "flour" (black).

A B

Plate XIII: Shoshone Canyon, pseudo-boulders. "Boulders" are calcitic dolomite concretions embedded in highly fractured, calcarenitic limestone.

A, dolomitic portions are outlined in black ink. The occurrence suggests that dolomitization proceeded upward from below. Note man (arrow) who is sitting on fluorite-bearing dolomite.

B, pseudo-boulder: vertical dimension of "boulder" about five feet; note bedded character.

BIBLIOGRAPHY

Berry, G. W. (1943) "Stratigraphy and Structure at Three Forks, Montana," Geol. Soc. Amer., Bull., Vol. 54.

Blackwelder, E. (1913) "Origin of the Bighorn Dolomite," Geol. Soc. Amer., Bull., Vol. 24.

(1918) "New Geological Formations in Western Wyoming," Jour. Washington Acad. Sci., Vol. 8, No. 13.

Branson, C. C. (1937) "Stratigraphy and Fauna of the Sacajawea Formation, Mississippian, of Wyoming," Jour. Paleon., Vol. 11.

Cheney, M. G. (1940) "Geology of North-Central Texas," Amer. Assoc. Petrol. Geol., Vol. 24, No. 1.

Cloud, P. E., Jr., & Barnes, V. E. (1948) "The Ellenburger Group of Central Texas," The Univ. of Texas, Pub. No. 4621.

Condit, D. D. (1916) "Relations of the Embar and Chugwater Formations in Central Wyoming," U. S. Geol. Survey, Prof. Paper 98-O.

Daly, R. A. (1909) "First Calcareous Fossils and the Evolution of the Limestones," Geol. Soc. Amer., Bull., Vol. 20.

Darton, N. H. (1904) "Comparison of the Stratigraphy of the Black Hills, Bighorn Mountains and Rocky Mountain Front Range," Geol. Soc. Am., Bull., Vol. 15.

(1906) "Geology of the Bighorn Mountains," U. S. Geol. Survey, Prof. Paper 51.

Deiss, C. F. (1938) "Cambrian Formations and Sections in Part of Cordilleran Trough," Geol. Soc. Amer., Bull., Vol. 49.

Goldich, S. S. & Parmelee, E. B. (1947) "Physical and Chemical Properties of Ellenburger Rocks, Llano County, Texas," Amer. Assoc. Petrol. Geol., Bull., Vol. 31, No. 11.

Grim, R. E., Lamar, J. E., & Bradley, W. F. (1937) "The Clay Minerals in Illinois Limestones and Dolomites," Jour. Geol., Vol. 45, No. 8.

Grim, R. E. (1947) "Relation of Clay Mineralogy to Origin and Recovery of Petroleum," Amer. Assoc. Petrol. Geol., Bull., Vol. 31, No. 8.

Grohskopf, J. G. & McCracken, E. (1949) "Insoluble Residues of Some Paleozoic Formations of Missouri, Their Preparation, Characteristics and Application," Missouri Geol. Survey and Water Res., Rept. Inves. No. 10.

Hewett, D. F. (1928) "Dolomitization and Ore Deposition," Econ. Geol., Vol. 23, No. 8.

(1931) "Geology and Ore Deposits of the Goodsprings Quadrangle, Nevada," U. S. Geol. Survey, Prof. Paper 162.

Holmes, A. (1921) Petrographic Methods and Calculations, Thomas Murby & Co., London.

Howell, J. V. (1931) "Silicified Shell Fragments as an Indication of Unconformity," Amer. Assoc. Petrol. Geol., Bull., Vol. 15, No. 9.

Ireland, H. A. et al (1947) "Terminology for Insoluble Residues," Amer. Assoc. Petrol. Geol., Bull., Vol. 31, No. 8.

King, P. B. (1948) "Geology of the Southern Guadalupe Mountains," U. S. Geol. Survey, Prof. Paper 215.

Kuenen, P. H. (1948) "Slumping in the Carboniferous Rocks of Pembrokeshire," Quar. Jour. Geol. Soc. London, Vol. 104, part 3.

Landes, K. K. (1946) "Porosity through Dolomitization," Amer. Assoc. Petrol. Geol., Bull., Vol. 15, No. 9.

Laudon, L. R. & Bowsher, A. L. (1941) "Mississippian Formations of Sacramento Mountains, New Mexico," Amer. Assoc. Petrol. Geol., Bull., Vol. 25, No. 12.

Lee, W. T. (1927) "Correlation of Geologic Formation between East-Central Colorado, Central Wyoming, and Southern Montana," U. S. Geol. Survey, Prof. Paper 149.

Love, J. D. (1939) "Geology along the Southern Margin of the Absaroka Range, Wyoming," Geol. Soc. Amer., Spec. Papers No. 20.

McKee, E. D. (1938) "Toroweap and Kaibab Formations of Arizona and Utah," Carnegie Inst. Washington, Pub. No. 492.

McQueen, H. S. (1931) "Insoluble Residues as a Guide in Stratigraphic Studies," Missouri Bur. Geol. and Mines, 56th Bien. Rept., App. I.

Miller, B. M. (1936) "Cambrian Stratigraphy of Northwestern Wyoming," Jour. Geol., Vol. 44.

Milner, H. B. (1940) Sedimentary Petrography, 3rd ed., Thomas Murby & Co., London

Miser, H. D. (1934) "Carboniferous Rocks of Ouachita Mountains," Amer. Assoc. Petrol. Geol., Bull., Vol. 18, No. 8.

Norton, W. H. (1917) "A Classification of Breccias," Jour. Geol., Vol. 25.

Peale, A. C. (1893) "The Paleozoic Section in the Vicinity of Three Forks, Montana," U. S. Geol. Survey, Bull. 110.

Pettijohn, F. J. (1949) Sedimentary Rocks, Harpers, New York.

Pierce, W. G. (1947) Extract p 35, "Field Conference in the Bighorn Basin," Guidebook, Univ. of Wyo., Wyo. Geol. Assoc., Yellowstone-Bighorn Res. Assoc.

Richards, R. W. & Mansfield, G. R. (1912) "The Bannock Overthrust," Jour. Geol., Vol. 20.

Richardson, G. B. (1913) "The Paleozoic Section in Northern Utah," Amer. Jour. Sci., 4th Ser., Vol. 36.

Scott, H. W. (1925) "Some Carboniferous Stratigraphy in Montana and Northwestern Wyoming," Jour. Geol., Vol. 43.

Shrock, R. R. (1948) Sequence in Layered Rocks, McGraw-Hill Book Co.

Sloss, L. L. (1947) "Environments of Limestone Deposition," Jour. Sed. Pet., Vol. 17, No. 3.

Sloss, L. L. & Hamblin, R. H. (1942) "Stratigraphy and Insoluble Residues of Madison Group (Mississippian) of Montana," Amer. Assoc. Petrol. Geol., Vol. 26, No. 3.

Sloss, L. L. & Laird, W. M. (1946) "Devonian Stratigraphy of Central and Northwestern Montana," U. S. Geol. Survey, Oil and Gas Inves., Prelim. Chart 25.

Steidtmann, E. (1911) "Evolution of Limestone and Dolomite," Jour. Geol., Vol. 19.

Stipp, T. F. (1947a) "Paleozoic Formations near Cody, Park County, Wyoming," Amer. Assoc. Petrol. Geol., Bull., Vol. 31, No. 2.

(1947b) "Paleozoic Formations of the Bighorn Basin," spec. paper, "Field Conference in the Bighorn Basin," Guidebook, Univ. of Wyo., Wyo. Geol. Assoc., Yellowstone-Bighorn Res. Assoc.

Thomas, H. D. (1934) "Phosphoria and Dinwoody Tongues in Lower Chugwater of Central and Southeastern Wyoming," Amer. Assoc. Petrol. Geol., Bull., Vol. 18, No. 12.

Tourtelot, H. A. & Thompson, R. M. (1948) "Geology of the Boysen Area, Central Wyoming," U. S. Geol. Survey, Oil and Gas Inves., Prelim. Map 91.

Van Tuyl, F. M. (1916a) "New Points on the Origin of Dolomite," Amer. Jour. Sci., Vol. 42, 4th Ser.

(1916b) "Brecciation Effects in the Saint Louis Limestone," abs. Geol. Soc. Amer., Bull., Vol. 27, p 122.

v Straaten, L. M. J. U. (1949) "Occurrence in Finland of Structures Due to Subaqueous Sliding of Sediments," 'Comptes Rendus de la Soc. Geol. de Finlande' N: oXXII.

Woodford, A. O. & Harriss, T. F. (1928) "Geology of Blackhawk Canyon, San Bernardino Mountains, California," Univ. Calif. Pub., Bull. Dept. Geol. Sci., Vol. 17, No. 8.